

Electronic Thesis and Dissertation Repository

9-16-2011 12:00 AM

Attitude Estimation and Control of VTOL UAVs

Andrew D. Roberts, *The University of Western Ontario*

Supervisor: Prof. Abdelhamid Tayebi, *The University of Western Ontario*

A thesis submitted in partial fulfillment of the requirements for the Doctor of Philosophy degree
in Electrical and Computer Engineering

© Andrew D. Roberts 2011

Follow this and additional works at: <https://ir.lib.uwo.ca/etd>



Part of the [Controls and Control Theory Commons](#)

Recommended Citation

Roberts, Andrew D., "Attitude Estimation and Control of VTOL UAVs" (2011). *Electronic Thesis and Dissertation Repository*. 303.

<https://ir.lib.uwo.ca/etd/303>

This Dissertation/Thesis is brought to you for free and open access by Scholarship@Western. It has been accepted for inclusion in Electronic Thesis and Dissertation Repository by an authorized administrator of Scholarship@Western. For more information, please contact wlsadmin@uwo.ca.

Attitude Estimation and Control of VTOL UAVs

(Spine title: Attitude Estimation and Control of VTOL UAVs)

(Thesis format: Monograph)

by

Andrew David Roberts

Graduate Program
in
Robotics and Control Engineering
Electrical and Computer Engineering

A thesis submitted in partial fulfillment
of the requirements for the degree of
Doctor of Philosophy

School of Graduate and Postdoctoral Studies
The University of Western Ontario
London, Ontario, Canada

© Andrew David Roberts, 2011

Certificate of Examination

THE UNIVERSITY OF WESTERN ONTARIO
SCHOOL OF GRADUATE AND POSTDOCTORAL STUDIES
CERTIFICATE OF EXAMINATION

Chief Advisor:

Dr. Abdelhamid Tayebi

Examining Board:

Dr. Samuel Asokanthan

Advisory Committee:

Dr. Mehrdad Kermani

Dr. Manfredi Maggiore

Dr. Ilia Polushin

The thesis by

Andrew David Roberts

entitled:

Attitude Estimation and Control of VTOL UAVs

is accepted in partial fulfillment of the
requirements for the degree of

Doctor of Philosophy

Date: _____

Chair of Examining Board
Dr. Charles G. Trick

Abstract

The theoretical challenge involved in the operation of VTOL UAVs is often divided into two main problems. The first problem involves the development of an estimation scheme which can accurately recover the orientation, or angular position, of the aircraft. The second problem involves the development of algorithms which can be used to reliably control the orientation and/or the position of the vehicle. These two problems are the primary focus of this thesis.

We first consider the problem of attitude estimation. To solve this problem we use vector measurements, and in many cases, a gyroscope (to measure the angular velocity of the system) in order to develop the estimation scheme. In the case where an accelerometer is used to provide a measurement of the apparent acceleration, we consider a special class of attitude observer, known as a *velocity-aided* attitude observer, which additionally use the system linear velocity to improve the estimation performance when the system is subject to high linear accelerations.

Secondly, we develop a number of algorithms which can be used to control the orientation and/or the position of the system. Two adaptive position tracking control laws are proposed which are able to compensate for exogenous disturbance forces. However, this control strategy (like other existing position control strategies) assumes that the system orientation is directly measured, where in reality only an estimate of the system orientation is available, which is obtained using some attitude estimation scheme. Therefore, we also propose an attitude stabilization control law, and two position control laws which do not assume that the system orientation is directly measured. To develop these control laws, we use vector measurements (that would normally be used by the attitude observer) directly in the control algorithms, which eliminates the requirement for an attitude observer. We also consider a special type of the vector-measurement-based position control laws which uses the accelerometer to measure the body-referenced apparent acceleration (rather than assuming only the gravity vector is measured). Therefore, this proposed control strategy may be better suited for VTOL UAVs, which are likely to be subjected to linear accelerations.

Acknowledgements

Throughout my six years as a graduate student, I have had the honor and unique privilege of having Prof. Abdelhamid Tayebi as my academic supervisor. As his student, I have immensely benefited from his guidance, motivation, creativity and the great wealth of knowledge and experience which he possesses. It is because of these qualities, first and foremost above all other factors, that I have been able to reach this point in my academic career. For this reason, I am forever indebted to him.

The list of all the people who have helped me during my time at UWO (either academically, administratively or personally) is quite a long list, and consequently I am unable to name them all; yet this omission does not in any way indicate my lack of appreciation for each one of them. I do, however, wish to make note of a special few who deserve special thanks.

I would like to thank Dr. Ilia Polushin for the many interesting conversations we have had in the areas of robotics and mathematics. I have enjoyed these conversations, which have proven to be very enlightening and helpful in solving some of the problems which I have faced.

I would also like thank Dr. Abdelkader Abdessameud, who I have had countless talks with about VTOL UAVs, and who has served as a valued test-audience for any ideas that may have come to my mind (whether they were good or bad!).

I would also like to thank my co-supervisor Dr. Abdallah Shami, who has helped me on numerous occasions.

Another person to whom I would like to thank is Sandra Vilovski, who served as the Graduate Coordinator in the Department of Electrical Engineering, up until recently this year.

I would also like to offer my sincere appreciation to Dr. Samuel Asokanthan, Dr. Mehrdad Kermani, Dr. Manfredi Maggiore and Dr. Ilia Polushin, for taking the time to serve as my thesis Examiners, and for their comments and constructive criticism.

Finally, I would like to thank those people who are closest to me: my parents Winston and Marion, who have always been extremely supportive, loving and encouraging. And of course, to Erin, who's patience, love and understanding is so dear to me, I cannot find words which accurately describes my own love and appreciation for her in return.

Table of Contents

Certificate of Examination	ii
Abstract	iii
Acknowledgements	iv
Table of Contents	v
List of Tables	viii
List of Figures	ix
Nomenclature	xi
1 Introduction	1
1.1 Vertical Take-Off and Landing Unmanned Airborne Vehicles	1
1.2 Attitude Parameterization	3
1.3 Rigid-Body-Attitude Estimation	7
1.4 Control of VTOL UAVs	11
1.5 Contributions of the Thesis	18
1.6 List of Publications	21
1.7 Thesis Outline	22
2 Background	24
2.1 Attitude Representation	24
2.1.1 Coordinate Frames	24
2.1.2 Direct Cosine (Rotation) Matrices	25
2.1.3 Unit Quaternion	26
2.1.4 Attitude Dynamics	30
2.2 Equations of Motion (Dynamic Model)	31
2.3 Mathematical Preliminary	32
2.3.1 Skew-Symmetric Matrix	32
2.3.2 Bounded Functions	33
2.3.3 Stability Definitions	35

3	Attitude Reconstruction and Estimation	38
3.1	Attitude Reconstruction	39
3.1.1	Attitude Reconstruction Using a Single Vector Measurement	39
3.1.2	Attitude Reconstruction Using Two or More Vector Measurements	41
3.2	Complementary Filtering	42
3.3	Vector Measurement Based Attitude Estimation	46
3.3.1	Attitude Error	47
3.3.2	Vector Measurements	48
3.3.3	Vector-Measurement Based Attitude Observer	50
3.3.4	Attitude Observer Using Filtered Vector Measurements	52
3.3.5	Attitude Estimation Using GPS and IMU Measurements	54
3.4	Simulations	60
3.4.1	Complementary Filter	60
3.4.2	Vector Measurement Based Attitude Observer	60
3.4.3	Attitude Observer Using IMU and GPS Measurements	63
3.4.4	Comparison of Attitude Observers	63
3.5	Concluding Remarks	71
4	VTOL UAV Control Design	75
4.1	Introduction	75
4.2	Vector Measurement Based Attitude Stabilization	79
4.3	Position Control of VTOL UAVs	81
4.3.1	Problem Formulation	81
4.3.2	Adaptive Position Tracking	86
4.3.3	Position Control Using Vector Measurements	101
4.3.4	Position Regulation Using GPS and IMU Measurements	108
4.4	Simulations	116
4.4.1	Adaptive position Controllers	116
4.4.2	Vector Measurement Based Position Control	123
4.4.3	Position Control Using IMU and GPS Measurements	125
4.5	Concluding Remarks	127
5	Thesis Summary and Future Work	134

Appendices

A	Proof for Lemmas and Propositions	147
A.1	Proofs for Lemmas	147
A.1.1	Proof for Lemma 3 (Single-Measurement Attitude Reconstruction)	147
A.1.2	Proof for Lemma 4 (Properties of z_γ and W)	148
A.2	Proofs for Propositions	149
A.2.1	Proof for Proposition 1 (Complementary Filtering)	149
A.2.2	Proof for Proposition 2 (Vector-Measurement Based Attitude Observer)	150
A.2.3	Proof for Proposition 3 (Attitude Observer Using Filtered Vector-Measurements)	151
B	Proof for Theorems	155
B.1	Proof for Theorem 3.1	155
B.2	Proof for Theorem 3.2	159
B.3	Proof for Theorem 4.1	164
B.4	Proof for Theorem 4.2	167
B.4.1	Bounded Control	167
B.4.2	Translational and Quaternion Dynamics	168
B.4.3	Angular Velocity Error Dynamics - Controller 1	171
B.4.4	Proof of Theorem 4.3	173
B.4.5	Derivatives of Angular Velocity Virtual Control Laws, β_2 and β_1	177
B.5	Proof of Theorem 4.4	181
B.6	Proof for Theorem 4.5	187
	Curriculum Vitae	196

List of Tables

3.1	Sensor Noise Standard Deviation Values	68
3.2	Comparison of Estimation Strategies	73
4.1	Simulation Parameters - Adaptive Position Control	130
4.2	Simulation Parameters - Vector Measurement Based Position Control	131
4.3	Simulation Parameters - Position Control Using IMU and GPS Measurements	132
4.4	Comparison of Control Strategies	133

List of Figures

1.1	The Ducted Fan and Quad-Rotor VTOL UAVs	2
3.1	Simulation Results for Complementary Filter	61
3.2	Simulation Results for Vector-Measurement-Based Attitude Observer	61
3.3	Simulation Results for Filtered-Vector-Measurement-Based Attitude Observer	62
3.4	Translational Dynamics and Angular Velocity Used For Simulation for IMU and GPS Based Attitude Observer	64
3.5	Simulation Results for Second Order IMU/GPS Based Attitude Observer	65
3.6	Simulation Results for Third Order IMU/GPS Based Attitude Observer	66
3.7	Rigid-body position for comparison simulation.	67
3.8	Inertial-referenced apparent acceleration of rigid-body.	67
3.9	Plots for Sensor Outputs (including noise and disturbances)	69
3.10	Comparison Simulation Results for Complementary Filter and Vector- Measurement Based Observers	70
3.11	Comparison Simulation Results for Filtered-Vector-Measurement Based Observer and IMU/GPS Based Observers	71
4.1	Attitude Extraction Algorithm for Position Control	83
4.2	Ducted Fan Exogenous Forces	87
4.3	Block Diagram of the Position Tracking Controllers	92
4.4	Torque-Generating Aerodynamic Forces As a Result of Airflow in Body- Fixed Frame	118
4.5	Simulation Results for First Adaptive Position Controller	119
4.5	Simulation Results for First Adaptive Position Controller (continued)	120
4.6	Simulation Results for Second Adaptive Position Controller	121
4.6	Simulation Results for Second Adaptive Position Controller (contin- ued)	122
4.7	Simulation Results for Vector Measurement Based Position Controller	124
4.8	Simulation Results for IMU/GPS Measurement Based Position Control	126

Nomenclature

NED	<i>Ortho-normal coordinate system where the x-axis is directed towards the Earth's magnetic North pole, the y-axis directed towards the East, and the z-axis is directed downwards.</i>
\mathcal{I}	<i>Inertial (Fixed) Coordinate Frame rigidly attached to a position on the Earth (assumed flat) expressed in NED coordinates.</i>
\mathcal{B}	<i>Body Coordinate Frame rigidly attached to the rigid-body center of gravity, where the x-axis is directed towards the front of the rigid-body, the y-axis is directed towards the right-hand-side of the rigid-body, and the z-axis is directed towards the bottom of the rigid-body.</i>
r_i	<i>A vector in \mathbb{R}^3 whose coordinates are expressed in \mathcal{I}.</i>
b_i	<i>Vector measurement of r_i in the body-frame \mathcal{B}.</i>
\hat{k}	<i>Unit-length vector in \mathbb{R}^3 which defines an axis of rotation.</i>
θ	<i>Angle of rotation about the unit-vector \hat{k}.</i>
\mathbb{Q}	<i>The set of unit-quaternion, or equivalently, the set of unit-length-vectors in \mathbb{R}^4, or equivalently the set of vectors contained in S^3 (4-dimensional unit-sphere)</i>
Q	<i>The unit-quaternion belonging to the set \mathbb{Q} which describes the relative orientation of \mathcal{B} taken with respect to \mathcal{I}.</i>
\hat{Q}	<i>Unit-quaternion which defines an adaptive estimate of Q.</i>
\bar{Q}	<i>Reconstruction or calculation of the unit-quaternion Q based upon the inertial vectors r_i and their measurements b_i.</i>
$SO(3)$	<i>The special orthogonal group in 3-dimensions (set of rotation matrices).</i>
R	<i>The rotation matrix belonging to $SO(3)$ which describes the relative orientation of \mathcal{B} taken with respect to \mathcal{I}.</i>
$R(Q)$	<i>Rotation matrix in $SO(3)$ which corresponds to the unit-quaternion Q.</i>
\hat{R}	<i>Rotation matrix which defines an adaptive estimate of R and corresponds to the unit-quaternion \hat{Q}.</i>
\bar{R}	<i>Reconstruction or calculation of the rotation matrix R based upon the inertial vectors r_i and their measurements b_i.</i>
p	<i>Position of the frame \mathcal{B} expressed in the frame \mathcal{I}.</i>
v	<i>Velocity of the frame \mathcal{B} expressed in the frame \mathcal{I}.</i>
ω	<i>Angular velocity of the frame \mathcal{B} expressed in the frame \mathcal{B}.</i>
ω_g	<i>Output of gyroscope sensor (measurement of ω).</i>
ω_b	<i>Gyroscope sensor bias.</i>
m_b	<i>Rigid-body mass.</i>
I_b	<i>Rigid-body inertia tensor expressed in the frame \mathcal{B}.</i>
g	<i>Acceleration due to gravity (9.81m/s^2).</i>
e_3	<i>The unit vector $[0, 0, 1]^T$.</i>

Chapter 1

Introduction

1.1 Vertical Take-Off and Landing Unmanned Airborne Vehicles

In the recent past the use of vertical take-off and landing (VTOL) unmanned airborne vehicles (UAVs) has seen a significant increase in popularity. This type of aircraft is often desired due to its hovering capabilities as well as the fact that they can take-off and land in a relatively much smaller footprint than other fixed-wing type aircraft. Due to these capabilities, these aircraft are suitable for a variety of applications such as visual inspection of structures (buildings, bridges, etc), search and recovery, defence, recreational use, or a variety of other applications where human presence is either hazardous or difficult to achieve. Two of the most common VTOL UAV aircraft are the ducted-fan and the quad-rotor helicopters, which are shown in Figures 1.1a and 1.1b, respectively.

As its name suggests, the quad-rotor uses four rotors to collectively generate thrust necessary for flight. The quad-rotor is controlled by regulating the value of each rotor thrust independently, which is used to generate a moment (control torque input) about the system center of gravity (COG). Alternatively, the ducted fan uses one or two rotors which operate within a shroud or duct in a coaxial/series arrangement. In the case where two rotors are used, they are rotated in opposite directions in order to eliminate the torque due to rotor aerodynamic drag, which could otherwise



Figure 1.1: The Ducted Fan and Quad-Rotor VTOL UAVs

cause the system to spin about its vertical axis. The ducted fan uses a set of control surfaces (ailerons or wings) located at the exit of the duct which are actuated to generate aerodynamic forces due to the duct airflow, thereby generating a torque which is proportional to the distance from the control surfaces to the system COG. This control strategy is sometimes referred to as *vectored thrust*. Since the rotors are contained within a shroud the ducted fan offers a higher degree of safety than the quad-rotor. As a result it is more common to see ducted fan aircraft possessing more powerful motors and rotors which results in higher payload capabilities.

Piloting these types of aircraft has been proven to be quite challenging, and was typically only suitable for operators with a high degree of training or experience. This fact has motivated a number of researchers to study and develop flight control systems which reduce the complexity of the task presented to the operator. In the development of these flight control systems there are two main theoretical challenges which researchers face: obtaining accurate knowledge about the system's attitude (orientation or angular position), and developing the necessary control and estimation algorithms needed to ensure reliable performance of the system while in autonomous flight. These are the two main challenges addressed in this thesis.

1.2 Attitude Parameterization

The use of an attitude observer or position controller, requires that the orientation of the rigid-body is represented using one of a few mathematical parameterizations, such as Euler angles, direct cosine (rotation) matrices, modified Rodriguez parameters and unit-quaternion (see, for instance, Murray et al. (1994), Shuster (1993) and Hughes (1986) for more details). By orientation, we mean the relative angular position of a body-fixed frame (rigidly attached to the system COG), and an inertial frame rigidly attached to the Earth. Choosing a particular type of attitude parameterization is not necessarily straightforward, since each representation has unique advantages and disadvantages. However, the key deciding factors one faces when deciding on the choice of attitude parameterization generally involve three criteria: whether the parameterization is a *global representation* (globally non-singular), the *uniqueness* of the representation, and the *mathematical complexity* involved in the use of the parameterization.

Perhaps the most familiar form of attitude parameterizations (at least for those not involved in the study of attitude parameterizations) are the Euler angles. The Euler angle representation takes advantage of the fact that the relative orientation of two frames of reference can always be described by three separate rotations. There are twelve different types of Euler angle representations, which differ by the axes of rotation which are used for the three individual rotations. Using one of the twelve sets of rotation vectors, the Euler angle parameterizations uses three elements to represent the value of the *angle of rotation* about each axis. Among the twelve different parameterizations, the most common convention used is the one where the three angles are taken consecutively as: a rotation about the body-referenced *z-axis*, followed by a rotation about the body-referenced *y-axis*, followed by a rotation

about the body-referenced x -axis. The angles which correspond to these three axes of rotation are referred to as the *yaw*, *pitch* and *roll* angles, respectively. One of the useful characteristics of the yaw-pitch-roll representation, is that given a value of these angles, one can almost immediately visualize the corresponding orientation of a vehicle. The use of other parameterizations, however, are more ambiguous and do not immediately offer insight on the physical orientation of a vehicle. Unfortunately, the Euler angle parameterization is not a global representation. In fact, at a particular value of one of the three Euler angles, there exist an infinite number of solutions for the other two angles, which describes the relative orientation of two frames of reference. In terms of the yaw-pitch-roll representation, this *singularity* corresponds to when the cosine of the pitch angle becomes zero. Some authors suggest that this is not a likely operating mode of certain aircraft, and subsequently continue with the control design by assuming the singularity is never encountered. However, those who desire a global representation of orientation are therefore forced to use a different form of attitude parameterization.

Although Euler angles use three-separate rotations to define the relative orientation between two frames of reference, we know from Euler's rotation theorem, that it is always possible to represent orientation in three-dimensional space using a single axis about a single vector of rotation (for example, see Hughes (1986), page 10). This convention is usually referred to as the *axis-angle* parameterization. Although this is a global attitude parameterization, it is not unique (for example, the same orientation could be achieved by simultaneously taking the negative value for both the angle and axis of rotation). However, it seems the axis-angle parameterization has not been very widely used in the literature. Alternatively, a very commonly used attitude parameterization which also uses four elements is the *unit-quaternion*. Similar to the axis-angle representation, the unit-quaternion offers a global attitude representation,

which is not unique. In fact, the unit quaternion parameterization is a double-cover, or two-to-one map, over the real space. As discussed in Bhat (2000), this presents a topological obstruction since for every equilibrium solution which exists in the real space (Euclidean space in three-dimensions), two antipodal equilibrium solutions exist in the quaternion space S^3 . Note that although this pair of equilibrium solutions correspond to the same physical point in the real space, this does not necessarily mean that both points share the same characteristics in terms of stability. In fact, in some cases, the pair of equilibrium points can have completely different behaviors (for example one point is an attractor, and one is a repeller). In this case, the stable and unstable manifolds overlap in the real space, and the equilibrium point is a *homoclinic* point, Guckenheimer and Holmes (1983). This can result in some strange behavior of the system (as viewed in the real space), since trajectories which start near the desired equilibrium solution, can diverge and travel a large distance before coming back to the same equilibrium solution, since both the stable and unstable equilibrium points (in the quaternion space) map to the same point in the real space. Trajectories of this nature are referred to as *homoclinic orbits*, however, in the study of the literature involving unit-quaternion based attitude parameterization, this characteristic is typically referred to as *unwinding*. In other cases, both antipodal equilibrium points in the quaternion space are shown to be stable (and therefore the problem of unwinding is avoided). However, in this case, the quaternion space contains an unstable invariant manifold which divides the quaternion space into two halves (each containing a stable equilibrium). This manifold is usually unstable, yet trajectories starting on the manifold remain there indefinitely and therefore do not converge to one of the two stable equilibrium points. Due to these problems, when the unit-quaternion is used to represent the attitude of a rigid-body, it is impossible to achieve global asymptotic stability using strictly continuous feedback. In the case where the equilibrium point

in the real space is homoclinic, asymptotic stability cannot be achieved due to the nonlinear behavior of the homoclinic orbits. When both antipodal equilibrium points are stable, and an invariant manifold exists, in Koditschek (1988) the authors use the term *almost global stability*, which refers to the asymptotic stability of a system for all initial conditions except for those contained in a set of Lebesgue measure zero, (for example, the unstable manifold). For more information on this topological obstruction, the reader is referred to Koditschek (1988) and Chaturvedi et al. (2011). In some cases, discontinuous feedback has been used to avoid the problems associated with the undesired equilibrium solutions and unwinding, for example see Mayhew et al. (2009b) and Mayhew et al. (2009a).

Another attitude parameterization, which is just as popular as than the unit-quaternion, is the rotation matrix. The rotation matrix has some clear advantages since it is a global bijective map (one-to-one) from the rotation-space $SO(3)$ to the real-space (Euclidean space in three-dimensions). Therefore, it is not affected by the unwinding phenomena that are sometimes attributed to the quaternion parameterization. However, the invariant manifold (previously mentioned in the discussion of unit-quaternion) may still exist. In these cases, systems are said to exhibit almost-global stability (asymptotically stable for all initial conditions except for the invariant manifold, which is a set of Lebesgue measure zero). However, despite the advantages of the rotation matrix, researchers sometimes prefer the use of the unit-quaternion. This choice is partly attributed to the fact that quaternions are represented using a vector, rather than the more cumbersome matrix representation. Also, in many cases, the mathematical analysis of systems which use unit-quaternion seems to be greatly simplified when compared to those which use rotation matrices. For this reason, in this thesis we typically use unit-quaternion for attitude parameterization. However, in the case where a rotation matrix is desired, we can apply straightfor-

ward transformations which can yield a rotation matrix corresponding to a particular unit-quaternion.

1.3 Rigid-Body-Attitude Estimation

In the absence of a pilot, it is essential for the operation of UAVs to utilize sensors in order to recover the orientation of the aircraft. Unfortunately, there does not exist a sensor (to our knowledge) which directly measures the orientation of a rigid-body with respect to an inertial frame. To address this limitation, researchers and practitioners have sought the use of sensors which give the body-frame coordinates of an inertial-referenced vector. Examples of such a sensor often include accelerometers and magnetometers, which are attached to the rigid-body in order to provide body-referenced coordinates of the gravity vector and the Earth's magnetic field, respectively. However, although these *vector measurements* contain very useful information about the rigid-body orientation, they do not directly yield the orientation of the system, and therefore some attitude estimation scheme must be used based upon these measurements. It should be noted that there does exist some commercially available so-called "orientation sensors". However, these devices typically include an inertial measurement unit (usually a set of vector-measurement sensors and a gyroscope), with some type of attitude estimation scheme, all of which are contained in a complete package.

The attitude estimation problem has been the focus of several research groups who have subsequently produced some very promising results in this area. To solve this problem, researchers have typically used vector measurements and sometimes a gyroscope (which measures the angular velocity of the rigid-body) to develop an estimation scheme. In theory, using gyroscopes one can obtain the attitude of a rigid-

body by integration of the rigid-body angular velocity. However, due to problems associated with accuracy of estimator initial conditions, gyroscope bias, sensor gain and axis misalignments, it is well-known that this approach leads to errors, and potentially to the particularly disastrous effect of gyroscope drift; a well known problem which causes the attitude estimates to continuously diverge over time. These problems have led to the development of highly-accurate gyroscopes, which are usually very expensive and heavy devices, and are typically considered only for commercial applications. For other applications where size, weight and cost are important factors (such as in the area of small scale VTOL UAVs), control engineers prefer low-cost sensors, for example the Integrated Micro-Electro-Mechanical systems (IMEMs), which are cheap, small and lightweight (since they are contained within an integrated circuit). In this case, rigorous design of robust attitude observers is required to deal with sensor inaccuracies.

Attitude reconstruction is one estimation scheme where the vector measurements are used to calculate (without the use of a filter/observer) the orientation of a rigid body. In several cases, this problem has been addressed as an optimization problem (for example, see Shuster and Oh (1981) and Shuster (2006)), which seeks a value for the rigid-body attitude that is a *best-fit* for the vector-measurement data. This is typically referred to as *Wahba's problem*, named after Grace Wahba who originally formulated this problem. However, some are not attracted to these solutions, due to delay and the high computational complexity required in the solution of optimization problems. However, other closed-form reconstruction methods have also been proposed (which do not require the minimization of a cost function), for example see Wahba (1965), Shuster and Oh (1981), Fisher et al. (1993), Reynolds (1998) and Metni et al. (2006).

Some researchers have worked to develop observers which combine the use of

these attitude reconstructions with a gyroscope. This is particularly desirable when the rigid-body is in a rotating frame, since the gyroscopes are more accurate at higher frequencies (gyroscope drift occurs due to errors at low frequencies), and the reconstructions are generally more accurate at low frequencies (for example, when the system is not moving). The combination of the attitude reconstructions with the gyroscope signal are commonly referred to as *complementary filters*. Examples of linear complementary filters can be found in Tayebi and McGillvray (2006) and Baerveldt and Klang (1997). Other nonlinear complementary filters which have used the rotation matrix and unit-quaternion can be found in Hamel and Mahony (2006), Mahony et al. (2005), Mahony et al. (2008), Tayebi and McGillvray (2006) and Tayebi et al. (2007). In some other cases, vector-measurement based attitude observers have been proposed which do not require the use of the so-called attitude reconstruction algorithms. Instead, the vector measurements are used directly with an observer, where the error signal used to correct the attitude is usually calculated using the vector or cross-product. Examples of these attitude observers can be found in Hamel and Mahony (2006), Mahony et al. (2008), Martin and Salaun (2007), Martin and Salaun (2010) and Tayebi et al. (2011). Another attractive feature of these results, is that the authors are also able to estimate the gyroscope sensor bias, which is normally assumed to be constant or slowly varying. In many practical situations, in the presence of sensor noise (which can be excessive in applications involving VTOL UAVs), control engineers are forced to pre-filter the sensor data before applying it to the attitude observer, which is normally not considered during the design of the observers. Therefore, it would be beneficial if one could design an observer which considers filtering of the sensor data with accompanying proofs for stability.

In addition to complementary filtering, and the more *classic* filters that have been developed using traditional nonlinear control design tools, the use of Extended

Kalman filters for the vector-measurement-based attitude estimation problem has received a great deal of attention, such as Rehbinder (2004) and Rehbinder (2000), Choukroun et al. (2006b), Choukroun et al. (2006a), Markley (2004) and Crassidis (2006). For more details on Kalman filtering based attitude estimation the reader is also referred to the survey paper Crassidis et al. (2007) and the references therein.

As indicated by the references mentioned above, due to the efforts of the research community the area of vector-measurement-based attitude estimation has experienced significant breakthroughs. However, these estimation schemes (including Kalman filtering) can face a problem when they require the vectors to be known in the inertial frame (which is a common assumption). Unfortunately, this condition is usually not satisfied by the sensors typically used for these applications. Indeed, the magnetometer is one sensor which does satisfy this requirement (provided that the ambient magnetic field is known). However, perhaps the most common sensor used in this manner is the accelerometer, which is used in many (if not most) cases, to measure the gravity vector in the body-fixed frame. In this case, in order to satisfy the requirement that the inertial vector is known and constant in the inertial frame, one must assume that the body-fixed frame must be non-accelerating (such that the gravity measurement is not contaminated with forces due to linear acceleration). It is clear that this condition is not guaranteed to be satisfied for the particular case involving VTOL UAVs. Therefore many of the results for the attitude estimation and control of VTOL UAVs require that the system is in a near-hover configuration in order to avoid significant linear accelerations which can affect the accelerometer.

Fortunately, this limitation of the existing vector-measurement-based attitude observers has led to the development of a new class of attitude observer which uses the accelerometer (and magnetometer) to provide vector-measurements. This type of observer acknowledges the fact that the accelerometer measures the forces due to

acceleration of the rigid-body in addition to the gravity vector, in the body-fixed frame. The corresponding inertial vector which is measured is commonly referred to as the *apparent acceleration*, which unlike the requirements needed for previous observers, is not assumed to be known or constant. In order to deal with the fact that the inertial vector is unknown, this type of attitude observer uses the linear velocity of the rigid-body (assumed to be measurable using, for instance, a GPS) in addition to the signals obtained from an IMU, which includes an accelerometer, magnetometer and a gyroscope. These attitude observers, which are often referred to as *velocity-aided attitude observers*, can be found in Bonnabel et al. (2008) and Martin and Salaun (2008) with proofs for local stability. In Hua (2010) the author extends these results to show that the domain of convergence can be arbitrarily increased using the observer gains (semi-global). As expected, these observers are shown to offer superior performance when the rigid body is subjected to significant linear accelerations, and are therefore better suited for applications involving VTOL UAVs. However, the proofs for these observers are quite complicated, and the mechanisms behind how the velocity observer aids in the estimation of the system attitude is not clear. Therefore, future study into these observers may provide further insight and new developments in this area.

1.4 Control of VTOL UAVs

The study of control systems for unmanned aircraft has received considerable attention over the past two decades. One main focus for the control of VTOL UAVs has been to develop control laws which stabilize the attitude of the system to a certain desired attitude (attitude stabilization/regulation), or possibly to track a time-varying attitude-trajectory (attitude tracking). Traditionally, these attitude controllers as-

sume that the system attitude and angular velocity are accurately known, and are used to provide a proportional-derivative (PD) type of feedback, for example see Joshi et al. (1995) and Wen and Kreutz-Delgado (1991). A number of authors were also able to provide solutions for the attitude control problem without the use of the system angular-velocity measurements, for example see Caccavale (1999), Egeland and Godhavn (1994), Lizarralde and Wen (1996), Salcudean (1991), Tayebi (2008) and Tsiotras (1998). The non-requirement of the angular velocity vector is an important result since it reduces complexity of the closed loop system (one less sensor required). For systems which are equipped with a gyroscope sensor, this control scheme can also be used as a redundant back-up control scheme in the case where a fault is detected on the gyroscope measurements. To deal with the absence of angular velocity measurements, the authors mentioned above typically use an auxiliary system, or lead filter, in order to generate the necessary damping to stabilize the system, using only system attitude measurements. However, as discussed in the description of the attitude estimation schemes, the system attitude is not directly known. Rather, it is obtained using some attitude estimation scheme, which typically involves the measurement of the system angular velocity. Therefore, the knowledge of the system attitude usually requires the measurement of the system angular velocity, and consequently, one may question whether the results obtained above are truly angular-velocity-free. Therefore, there seems to be some room for improvement in this regard.

Another main objective for the autonomous operation of VTOL UAVs is to develop algorithms which control the position of the vehicle. This objective has been the focus of several groups in the research community, which has resulted in significant and interesting breakthroughs in this field, for example see Abdessameud and Tayebi (2010), Aguiar and Hespanha (2007), Frazzoli et al. (2000), Hamel et al. (2002), Hauser et al. (1992), Hua et al. (2009) and Pflimlin et al. (2007). Due to the

underactuated nature of VTOL UAVs, the system attitude must be used in order to control the position and velocity of the system. However, this presents some difficulty due to the fundamental differences between Euclidean space (used to model the position and velocity) and the rotational space (unit-quaternion or rotation matrix). In many cases, the authors first derive an expression for a desired system acceleration, which corresponds to the ideal acceleration required to force the position and velocity error signals to zero. Subsequently, a control law is derived to force the actual system acceleration to the desired value. Although this is a straightforward concept, the manner in which the rotational dynamics are controlled is not necessarily straightforward. In some cases, for example Pflimlin et al. (2007) and Hua et al. (2009), the authors attempt to control the *thrust vector* (a function of the attitude and system thrust which is associated to the system acceleration). In other cases, for example Abdessameud and Tayebi (2010) and Frazzoli et al. (2000), based upon the value of the desired acceleration, a *desired system attitude* is derived, and the control laws are designed to force the actual system attitude to the desired value. These are just two examples, and as a result of the complexity, there have been a number of different methods which have been proposed in the literature in order to accomplish this task. Despite the differences in these procedures, they all are affected by a common problem involving the magnitude of the system thrust (the vertical thrust force that is generated to achieve the VTOL capabilities). A critical design requirement for these aircraft is to ensure that the value of the thrust is non-vanishing (different from zero), since the system may not be controllable in this state. Also, there are often inherent singularities associated with the control laws which occur when the system thrust vanishes. For example, when the desired acceleration is the acceleration due to gravity, a desired attitude cannot be extracted (since there exists an infinite number of solutions for the desired attitude which can achieve the free-fall state). In some

cases, position controllers have been developed based upon an assumption that the system thrust is non-vanishing since it corresponds to an undesirable and/or unlikely free-fall operating condition. As a result, these controllers contain an inherent singularity which can be reached for certain values of system initial-conditions and choice of gains. Therefore, it is desired to seek position controllers which, in some manner, ensure that the system thrust is non-vanishing.

The design of position control laws are complicated for a number of reasons, for example, handling of external disturbances, coupling between system dynamics, singularities as well as achieving global stability results. Some examples of position controllers which deal with unknown disturbances include Hua et al. (2009) and Pflimlin et al. (2007). In most cases, the disturbance force is required to satisfy some assumptions in order to develop the control laws (for example, the disturbance is constant in the inertial frame of reference). However, for VTOL UAVS, the external disturbances are most likely caused by aerodynamic forces which can change due to the motion and/or orientation of the vehicle. Therefore, there may be some room for improvement concerning the design of control laws which consider time varying disturbances.

A second problem is related to which system inputs are used to specify the control law. Usually it is desired to obtain the control torque that is applied to the rotational dynamics of the system (that is generated by the vectored thrust in the case of the ducted fan, or in the case of the quad-rotor the difference in the thrust of the four-rotors). This goal can be challenging, especially in the presence of external disturbances, and as a result, the control law is sometimes specified in terms of the desired system angular velocity (one integrator away from the control torque), for example see Hua et al. (2009). The desired angular velocity must then be implemented using high-gain feedback. There are few examples of controllers in the literature that

use the control torque as a system input while considering external disturbances. In Pflimlin et al. (2007), a result is achieved for the position regulation problem; however this result only guarantees local stability and does not consider position tracking. In Johnson and Turbe (2006), a Neural Network adaptive controller has been proposed; however, it is not accompanied with proofs of stability, either locally or globally.

For the ducted-fan type of VTOL UAV, in the process of generating a torque used to control the system orientation, a translational force is also generated due to the vectored thrust action. Due to this system characteristic, another well known problem is due to this coupling between the rotational and translational dynamics. This coupling is usually in the form of a perturbing term (given as a function of the control torque or angular velocity) that affects the translational acceleration of the system. This problem is discussed in more detail in Hauser et al. (1992) and Olfati-Saber (2002). In most cases, it is assumed that the coupling term is negligible and is thus omitted in the control design. However, as discussed in Hauser et al. (1992) and Olfati-Saber (2002), depending on the strength of the coupling and the choice of control gains, this can lead to unexpected oscillations in the system states. There are some examples of controllers in the literature which address the coupling problem. For instance, in Olfati-Saber (2002) a nice change of coordinates is presented, however, only for a planar system. In Pflimlin et al. (2007), a change of coordinates is also presented that removes the coupling due to the control torque. A consequence of this change of coordinates is that a new coupling is introduced in terms of the system angular velocity. Although this new coupling vanishes when the yaw rate is zero (angular velocity about the body-referenced z-axis), in practice this would likely not be the case. Therefore, there still seems to be some potential for improvement regarding this coupling term in future work. Note that this coupling term is system dependant, and is not always present in certain VTOL systems, for example the quad-

rotor aircraft. In Hamel et al. (2002) a position tracking controller is proposed for the quad-rotor aircraft achieving practical stability. Also, an attitude controller for the quad-rotor aircraft is proposed in Tayebi and McGillvray (2006). Position tracking control laws, that do not address disturbance forces, can be found in Frazzoli et al. (2000) for the case of a helicopter, and in Abdessameud and Tayebi (2010) for the case of a general VTOL UAV system. Also, in Hua et al. (2009) a result is obtained for a VTOL UAV system achieving almost-global stability using a simple control law which is given in terms of the system angular velocity. However, although there have been significant breakthroughs in addressing the problems discussed above, to the best of our knowledge, there are no results in the available literature which simultaneously address the position tracking problem in the presence of disturbance forces which use the system control torque as the system input while providing almost-global asymptotic stability. Therefore, one of the objectives of this thesis is the development of a position tracking controller which satisfies these objectives.

Existing position controllers all require that a number of system states are accurately known or measured, including the position, velocity, angular velocity in addition to the orientation of the system. However, as discussed in the previous section (attitude estimation), there does not exist a sensor which directly provides a measurement of the system attitude. Consequently, in practice a vector-measurement-based attitude observer is used to feed attitude estimates to the position controller. However, due to errors and observer dynamics (which are not considered by the control design), this may lead to undesirable performance. In this case, one relies on the robustness of the position controller, however, there are no stability guarantees for the coupled observer-controller. Therefore, there is some room for improvement in this regard. For example, this problem could be addressed by designing position control laws which do not require direct measurement of the system attitude. Instead, it may

be possible to design a position controller which utilizes the vector measurements directly (that would otherwise be used by the attitude estimation scheme). In this case, an attitude observer would no longer be required for the overall closed-loop system, which would reduce complexity (as well as cost and weight) of the overall system.

If we were to obtain a position controller which utilized the vector measurements instead of the system attitude, we may be faced with the problem regarding the availability of sensors which provide ideal vector measurements (for example sensors which provide the measurements of vectors which are known in an inertial frame). For example, similar to the attitude observers previously discussed, the two most commonly used sensors which are used to provide vector measurements are the accelerometer and the magnetometer, which are used to measure the body-referenced coordinates of the gravity-vector and Earth's magnetic field, respectively. However, the accelerometer measures forces due to linear acceleration in addition to the gravity vector. Therefore, existing position controllers which depend on accelerometer measurements must assume that the system is near hover. Clearly, this assumption may be easily violated in the case of VTOL UAVs, and especially in the context of position control. However, one may recall that this problem was addressed for the attitude estimation problem, by additionally using a GPS to obtain linear velocity measurements, in order to deal with the fact that the accelerometer actually measures the system *apparent acceleration*, which includes both the gravity forces and the forces due to linear motion. In light of these results, one may be able to develop vector-measurement-based position controllers which use the accelerometer signal with linear velocity measurements in a similar manner. This would likely result in a position controller which is much more suitable to be used in the presence of linear accelerations, thus making it more suitable for VTOL UAVs.

1.5 Contributions of the Thesis

First, we propose a new vector-measurement based attitude observer. This observer is unique since we consider pre-filtering of the sensor data as part of the observer design. We show that the observer, which is driven by filtered measurements, guarantees convergence of the attitude estimates to the actual system attitude for almost all initial conditions. Therefore, this observer may offer improved performance when the vector measurements are affected by noise and disturbances. The results for this work has been reported in Tayebi et al. (2011).

Two new *velocity-aided* attitude observers are also proposed which use a GPS in addition to vector measurements obtained using an accelerometer and magnetometer contained within an IMU. However, in this case it is not assumed that the accelerometer provides an ideal vector measurement (measurement of only the gravity vector). Instead, the accelerometer is used to provide the body-referenced system apparent acceleration, which is used with a new filter (which is driven by measurements of the system velocity obtained using the GPS) in order to successfully estimate the system attitude. As a result, this observer is better suited when the rigid-body is accelerating, and is therefore better suited for VTOL UAVs. The observer estimates are shown to converge to the actual attitude as long as the trajectories are initialized within a certain domain of attraction, which can be arbitrarily increased through an adequate choice of the gains. Although these stability results are similar to the work of Hua (2010), the structure of our observer which uses the unit-quaternion leads to a much simpler stability analysis which provides important insight on the mechanisms involved in the operation of the observer. The results for this work have been reported in Roberts and Tayebi (2011b).

We propose two new adaptive position tracking control laws for VTOL UAVs.

To develop the control laws, we first propose a new attitude extraction algorithm (which extracts the desired attitude corresponding to a desired translational acceleration) in terms of the unit-quaternion that has almost no restrictions on the demanded acceleration, except for a mild singularity that can be avoided. Relying on this quaternion extraction method, we present two adaptive tracking controllers using the torque (that is applied to the system rotation dynamics) as a control input. Both controllers depend on an adaptive estimation method, which uses a projection mechanism Ioannou and Sun (1996), Cai et al. (2006). The projection mechanism is required to avoid the singularity associated with the value of the system thrust, which as a result, is guaranteed to be non-vanishing. The first proposed controller achieves the position-tracking objective for any initial condition of the state, whereas the second controller achieves the position-tracking objective for a set of initial conditions which are dependant on the control gains. The latter controller is included since it is less complicated than the prior case and may be more suitable to use in practice. During the process of developing the two control laws, the disturbance forces are assumed to be constant in the inertial frame. In this case, both control laws are proven to achieve the position tracking objective provided that an upper bound of the disturbance force is known a-priori (although the actual magnitude of this disturbance force may be less than this limit). The results for this work have been reported in Roberts and Tayebi (2011a).

The proposed controller described above and the existing attitude and position controllers in the literature, share a limitation since they assume that the system attitude is known, where in reality it is likely obtained using an attitude observer. To address this problem, we propose a new vector-measurement-based control law which no longer assumes the system attitude is directly measured. Instead, first we propose an angular-velocity-free attitude stabilization controller which uses the vec-

tor measurements (that would normally be applied to the attitude observer) directly in the control design, and therefore does not require an attitude observer in order to be implemented on the system. Furthermore, in light of the fact that existing angular-velocity-free attitude controllers require the measurement of the system attitude (which is obtained by an attitude observer which typically requires the use of the angular-velocity measurements), this result may be the first attitude controller which is truly angular-velocity free. The results for this work have been reported in Tayebi et al. (2011).

We also extend the results of the vector-measurement-based attitude controller described above to the position control problem. Relying on the attitude extraction algorithm used with the adaptive position tracking controller, we propose a new position control law which uses the vector measurements instead of assuming the system attitude is known. We show that for an appropriate choice of control gains, the system states are uniformly bounded and converge to some predefined trajectory for almost all initial conditions. The results for this work have been reported in Roberts and Tayebi (2011e).

In the case where an accelerometer is used to provide a vector measurement (usually to obtain body-frame coordinates of the gravity vector), the vector-measurement-based position controller described above may yield unexpected performance when the accelerometer is affected by forces due to the linear acceleration of the system (which is to be expected for the position control problem). To address this problem, we extend the results of the velocity-aided attitude observers to the case of position control. We propose a new vector-measurement based attitude controller which uses a filter (which is driven by the accelerometer and system velocity measurements obtained by a GPS), in order to obtain information about the system attitude. We show that for an appropriate choice of control gains, the system states are bounded and the

system position converges to a constant target in the presence of disturbances that are assumed to be due to aerodynamic forces. The results for this work have been reported in Roberts and Tayebi (2011b).

In addition to these main points, there are several other minor contributions which are offered as Lemmas or Propositions throughout the thesis.

1.6 List of Publications

The following list contains the publications obtained throughout the completion of this work, including submitted articles:

Journal publications:

- Andrew Roberts and Abdelhamid Tayebi (2011b), "*Attitude Estimation and Position Control of VTOL UAVs using IMU and GPS Measurements*", Submitted to Automatica (2011), (document can be viewed in arXiv database: <http://arxiv.org/> document number:1106.0016).
- Andrew Roberts and Abdelhamid Tayebi (2011a), "*Adaptive Position Tracking of VTOL UAVs*", IEEE Transactions on Robotics, Vol.27, No.1, pages 129-142.

Refereed conference proceedings:

- Andrew Roberts and Abdelhamid Tayebi (2011c), "*On the Attitude Estimation of Accelerating Rigid-Bodies Using GPS and IMU Measurements*", Accepted as regular paper for the 50th IEEE Conference on Decision and Control and European Control Conference, Orlando, FL, USA, 2011.
- Andrew Roberts and Abdelhamid Tayebi (2011d), "*Position Control of VTOL UAVs Using IMU and GPS Measurements*", Accepted as regular paper for the

50th IEEE Conference on Decision and Control and European Control Conference, Orlando, FL, USA, 2011.

- Abdelhamid Tayebi, Andrew Roberts and Abdelaziz Benallegue (2011), "*Inertial Measurements Based Dynamic Attitude Estimation and Velocity-Free Attitude Stabilization*", In proc. of the 2011 IEEE American Control Conference, San Francisco, CA, USA, 2011, pp. 1027-1032.
- Andrew Roberts and Abdelhamid Tayebi (2011e), "*Position Control of VTOL UAVs using Inertial Vector Measurements*", In proc. of the 18th IFAC World Congress, Milan, Italy, 2011, pp. 2614-2619.
- Andrew Roberts and Abdelhamid Tayebi (2009), "*Adaptive Position Tracking of VTOL UAVs*", In proc. of the 48th IEEE Conference on Decision and Control, Shanghai, China, 2009, pp. 5233-5238.
- A. Tayebi, S. McGilvray, A. Roberts and M. Moallem (2007), "*Attitude estimation and stabilization of a rigid body using low-cost sensors*", In proc. of the 46th IEEE Conference on Decision and Control, New Orleans, LA, USA, 2007, 6424-6429.

1.7 Thesis Outline

The following is a general overview of how the main sections of the thesis are organized:

- **Chapter 2** provides an overview of the mathematical background used in the development and analysis of the estimation and control laws. This includes

mathematical details regarding the unit-quaternion and rotation matrix attitude parameterizations which are used, and definitions for the system dynamic equations (system model). In this chapter we also introduce a class of bounded functions, which are useful later in the thesis, and discuss the skew-symmetric matrix and some of its properties which are frequently used.

- **Chapter 3** contains the contributions to the thesis in the area of attitude estimation. In this chapter we discuss several types of attitude estimation schemes. These methods include attitude reconstruction (closed form solutions which do not use an observer), complementary filtering and vector-measurement-based attitude estimation.
- **Chapter 4** contains the contributions to the thesis in the area of the control of VTOL UAVs. In this chapter we propose a velocity-free attitude stabilization control law using vector measurements, and a number of position control strategies. The position control strategies include adaptive position tracking (which includes the estimation of disturbance forces), as well as two types of vector-measurement based position control laws.
- **Chapter 5** provides a summary of the work presented in the thesis, and discusses new potential areas for improvement and future research.

Chapter 2

Background

In this chapter we review some of the mathematical background that is used in the development and analysis of the control and estimation laws. A major component of this background involves the definitions of the attitude parameterizations used to describe the orientation of the system (rigid-body). A description of these attitude parameterizations and some of these properties are provided in Section 2.1. However, for a more complete description of these parameterizations the reader is referred to Shuster (1993), Hughes (1986) and Murray et al. (1994). Section 2.2 defines the equations which govern the vehicle dynamics (system model), and Section 2.3 reviews some preliminary mathematical details that will be helpful during the discussion of the estimation and control algorithms.

2.1 Attitude Representation

2.1.1 Coordinate Frames

To represent the orientation (angular position) of the aircraft (rigid-body), we introduce two reference frames:

- **Inertial Frame \mathcal{I} :** A frame rigidly attached to a position on the Earth (assumed flat) in NED coordinates¹.
- **Body Frame \mathcal{B} :** A frame which is rigidly attached to the aircraft COG. The orthonormal basis of \mathcal{B} is taken such that the x axis is directed towards the front of the aircraft, the y axis is taken towards the right side, and the z axis is directed downwards (opposite the direction of the system thrust).

Throughout the paper we often refer to the *orientation* of the rigid-body, by which we mean the relative orientation of \mathcal{B} with respect to \mathcal{I} . The goal of the attitude representation is to mathematically describe the orientation of the rigid-body.

2.1.2 Direct Cosine (Rotation) Matrices

The direct-cosine, or rotation matrix, is a three-dimensional orthogonal matrix. A matrix $R \in \mathbb{R}^{3 \times 3}$ is considered a rotation matrix if it is contained within the set

$$SO(3) := \left\{ R \in \mathbb{R}^{3 \times 3} \mid \det(R) = 1 \mid R^T R = R R^T = I_{3 \times 3} \right\}. \quad (2.1)$$

The set $SO(3)$ forms a group with the linear matrix multiplication with identity element $I = I_{3 \times 3}$ and inverse $R^{-1} = R^T$. This set is often used since it offers a global and unique representation of the orientation of a frame of reference, and therefore we refer to this set as the *rotation space*. The rotation matrix $R \in SO(3)$ can be used to map vector coordinates from one frame to another. For example, let x_1 denote the coordinates of a vector in frame \mathcal{I}_1 , and x_2 denote the coordinates

1. North-East-Down coordinate system: Refers to the right-handed frame where the x axis is directed towards (magnetic) North, y axis is directed towards the East, and the z axis is directed downwards towards the Earth.

of x_1 expressed in frame \mathcal{I}_2 . Let R denote the rotation matrix which describes the rotation from \mathcal{I}_1 to \mathcal{I}_2 . Then, a well known property of the rotation matrix is

$$x_2 = Rx_1 \quad (2.2)$$

The rotation matrix can also be expressed in terms of the axis-angle representation. For example, if we let $\hat{k} \in \mathbb{R}^3$ denote a unit-length vector of rotation and $\theta \in \mathbb{R}$ denote the corresponding angle of rotation, then the corresponding rotation matrix $R(\theta, \hat{k}) \in SO(3)$ is given by the following transformation

$$R(\theta, \hat{k}) = I - \sin(\theta)S(\hat{k}) + (1 - \cos(\theta))S(\hat{k})^2 \quad (2.3)$$

where, in general $S(u)$, $u = [u_1, u_2, u_3]^T \in \mathbb{R}^3$, is the skew-symmetric matrix associated with the vector u given by

$$S(u) = \begin{bmatrix} 0 & -u_3 & u_2 \\ u_3 & 0 & -u_1 \\ -u_2 & u_1 & 0 \end{bmatrix} \quad (2.4)$$

A more thorough description of the skew-symmetric matrix is provided later in section 2.3.1.

2.1.3 Unit Quaternion

To denote the unit-quaternion, we use $Q = (\eta, q) \in \mathbb{Q}$, where $\eta \in \mathbb{R}$ and $q \in \mathbb{R}^3$, and \mathbb{Q} is the set of unit-quaternion defined by

$$\mathbb{Q} := \left\{ Q \in \mathbb{R} \times \mathbb{R}^3 \mid \|Q\| = 1 \right\}. \quad (2.5)$$

The unit-quaternion is often considered as an *axis-angle* representation due to the fact the relative orientation of two reference frames can always be expressed by a single rotation by some angle θ about some axis (of unit length) \hat{k} , where in this case the unit-quaternion can be written as

$$Q = \left(\cos(\theta/2), \sin(\theta/2)\hat{k} \right). \quad (2.6)$$

The axis-angle representation can be used to reveal some interesting facts about the unit-quaternion. For example, the particular case $Q = (0, q)$, such that $\eta = 0$ and $\|q\| = 1$, suggests that $\theta = \pi(2n + 1)$ where $n \in \mathbb{Z}$. In this case, the unit-quaternion Q physically describes a rotation of 180 degrees about the unit-length axis of rotation $\hat{k} = q$. This condition will be of particular interest in the analysis of the attitude estimation and control laws, due to some unique challenges which are attributed to this condition.

Due to the use of four elements, the unit-quaternion is an over-parameterization of the rotation space $SO(3)$. That is, the transformation from $\mathbb{Q} \rightarrow SO(3)$ is a two-to-one map. This characteristic results in some difficulties due to the multiplicity of equilibrium solutions (which relate to the same point in the rotation space) when using this representation. This is due to the fact that a coordinate frame whose orientation is described by the unit-quaternion Q is physically equivalent to the coordinate frame whose orientation is defined by the unit-quaternion $-Q$. This can easily be seen from the definition of the axis-angle representation (2.6) since

$$-Q = \left(-\cos(\theta/2), -\sin(\theta/2)\hat{k} \right) = \left(\cos((\theta + 2\pi)/2), \sin((\theta + 2\pi)/2)\hat{k} \right). \quad (2.7)$$

In terms of the axis-angle representation, we see that the unit-quaternion $-Q$ differs

from Q in that the angle θ is increased by a value of 2π (or a multiple thereof). Therefore, if the orientation of two different frames of reference (each taken with respect to the inertial frame) are described by the unit-quaternion Q and $-Q$, the orientation of the two coordinate frames are physically equivalent and actually share the same value for the rotation matrix using the $SO(3)$ parameterization. In fact, a well known transformation which provides a rotation matrix $R(Q)$ which corresponds to the unit quaternion Q is known as the *Rodrigues* formula, and is given by

$$R(Q) = I_{3 \times 3} + 2S(q)^2 - 2\eta S(q), \quad (2.8)$$

from which one can easily confirm $R(Q) = R(-Q)$. Throughout this thesis we make use of this transformation frequently when it is convenient to use a rotation matrix instead of the unit-quaternion. Regardless of the physical equivalence of two points in the quaternion space, as discussed in the introduction, if a system has an equilibrium solution which corresponds to a value of the rotation matrix given by $R \in SO(3)$, there exists two antipodal equilibrium solutions when using the quaternion parameterization given by $\pm Q \in \mathbb{Q}$. As previously discussed, the multiplicity of equilibrium solutions presents a topological obstruction to making claims such as global stability (for more details see Bhat (2000) and Koditschek (1988)).

When unit-quaternion are used, it is often necessary to employ the use of the well-known *quaternion product* operation. To define this operation, we let $Q_1 = (\eta_1, q_1) \in \mathbb{Q}$, $Q_2 = (\eta_2, q_2) \in \mathbb{Q}$ denote two unit-quaternion. Then the *quaternion product* of Q_1 and Q_2 , denoted by $Q_3 = (\eta_3, q_3) \in \mathbb{Q}$ is defined by

$$Q_3 = Q_1 \odot Q_2 = \left(\eta_1 \eta_2 - q_1^T q_2, \eta_1 q_2 + \eta_2 q_1 + S(q_1) q_2 \right). \quad (2.9)$$

The set \mathbb{Q} forms a group with the quaternion multiplication operation \odot , with quaternion inverse $Q^{-1} = (\eta, -q)$, and identity element $Q \odot Q^{-1} = Q^{-1} \odot Q = (1, \mathbf{0})$. Using this operation, the unit-quaternion can also be used to give the coordinates of a vector in multiple frames of reference. For example, using the vector-transformation property described by 2.2, where we denote an arbitrary vector $x_1 \in \mathbb{R}^3$ and denote the vector expressed in a rotated coordinated frame given by $x_2 = R(Q)x_1$, then the vector x_2 can also be obtained using the quaternion product by the following operation

$$(0, x_2) = Q^{-1} \odot (0, x_1) \odot Q. \quad (2.10)$$

Although the aforementioned topological obstruction can be avoided by using the set $SO(3)$, many researchers have still relied on the quaternion representation due to some significant advantages it offers over $SO(3)$ representation. One advantage can be attributed to the unique mathematical properties of the quaternion, which often yields greatly simplified proofs when compared to works which rely solely on $SO(3)$. Another advantage of the unit quaternion stems from the fact it is represented using a vector (of four elements) instead of a 3×3 orthogonal matrix, which can be useful, especially in the development of computer simulations. For example, when implementing a particular unit-quaternion-based estimation or control algorithm (or when performing computer simulations), preserving the properties of the attitude representation becomes important. To ensure a vector preserves the properties of a unit-quaternion, one can simply normalize the vector (divide by the norm). Preserving $SO(3)$ properties of a 3×3 matrix involves more complicated algorithms, such as the *Gram-Schmidt* orthonormalization algorithm (see, for instance, Nicholson (1995)).

2.1.4 Attitude Dynamics

Since the $SO(3)$ and quaternion parameterizations will be used to describe the orientation of frames which are moving with respect to time, it is necessary to describe the time-derivatives of these attitude parameterizations. Consider the two reference frames \mathcal{I} and \mathcal{B} as described in Section 2.1.1, and let $\omega \in \mathbb{R}^3$ denote the angular velocity of \mathcal{B} with respect to \mathcal{I} , expressed in \mathcal{B} (*body-referenced angular velocity*). Let $Q \in \mathbb{Q}$ denote a unit quaternion which describes the orientation of \mathcal{B} , and let $R = R(Q)$ denote the corresponding rotation matrix. The time-derivatives of the unit quaternion and the corresponding rotation matrix are described as follows

$$\dot{Q} = \frac{1}{2}Q \odot (0, \omega) = \frac{1}{2}A(Q)\omega \quad (2.11)$$

$$\dot{R} = -S(\omega)R \quad (2.12)$$

where $A(Q) \in \mathbb{R}^{4 \times 3}$ is given by

$$A(Q) = \begin{bmatrix} -q^\top \\ \eta I + S(q) \end{bmatrix} \quad (2.13)$$

In the case where \dot{Q} is known, the angular velocity can be obtained using

$$\omega = 2A(Q)^\top \dot{Q} \quad (2.14)$$

where we use the fact that $A(Q)^\top A(Q) = qq^\top + \eta^2 I - S(q)^2 = (\eta^2 + q^\top q)I = I$.

2.2 Equations of Motion (Dynamic Model)

In this section we present the dynamic model for the VTOL that is used to develop the attitude estimation and control algorithms. Recall from Section 2.1.1 the definitions of the inertial and body-fixed frames, denoted as \mathcal{I} and \mathcal{B} , respectively, and let $Q \in \mathbb{Q}$ and $R \in SO(3)$ denote the unit-quaternion and rotation matrix, respectively, which describes the orientation of \mathcal{B} with respect to \mathcal{I} . Let p and v denote the inertial referenced position and linear velocity of \mathcal{B} with respect to \mathcal{I} , expressed in \mathcal{I} . The system thrust is denoted as $T \in \mathbb{R}$, which is assumed to be directed along the body-referenced z-axis which we denote as $e_3 = [0, 0, 1]^\top$. Finally, let g denote the acceleration due to gravity, m_b denote the system mass, and $\delta_t \in \mathbb{R}^3$ denote a disturbance input caused by exogenous aerodynamic forces. Let $I_b \in \mathbb{R}^{3 \times 3}$ denote the moment of inertia of the rigid-body, and recall $\omega \in \mathbb{R}^3$ is the body-referenced angular velocity of \mathcal{B} . Using this framework we can now present the model for the system translational and rotational dynamics.

Translational dynamics:

$$\dot{p} = v \quad (2.15)$$

$$\dot{v} = ge_3 - \frac{T}{m_b} R^\top e_3 + \delta_t \quad (2.16)$$

Rotational dynamics:

$$\dot{Q} = \frac{1}{2} \begin{bmatrix} -q^\top \\ \eta I_{3 \times 3} + S(q) \end{bmatrix} \omega \quad (2.17)$$

$$I_b \dot{\omega} = -\omega \times I_b \omega + \delta_r + u \quad (2.18)$$

where $u \in \mathbb{R}^3$ is the exogenous torque applied to the rigid-body (control torque input),

and $\delta_r \in \mathbb{R}^3$ is a disturbance torque expressed in \mathcal{B} .

2.3 Mathematical Preliminary

In this section we review some mathematical preliminaries which are necessary to describe the estimation and control algorithms. The skew-symmetric matrix, which is extensively used throughout this work, is defined in Section 2.3.1 in addition to some commonly used properties of this matrix. We also define a class of bounded functions in Section 2.3.2, and in Section 2.3.3 we define some tools frequently used in the stability analysis of the proposed estimation and control algorithms.

2.3.1 Skew-Symmetric Matrix

Throughout this work we extensively use the skew-symmetric matrix. In fact, to quote M.D. Shuster, "it could be said with no little justification that the theoretical study of attitude is the study of the skew-symmetric matrix." Shuster (1993).

Let $x = [x_1, x_2, x_3]^T \in \mathbb{R}^3$ and $y = [y_1, y_2, y_3]^T \in \mathbb{R}^3$ denote two arbitrary vectors. The skew-symmetric matrix $S(x) : \mathbb{R}^3 \rightarrow \mathbb{R}^3 \times \mathbb{R}^3$ is given by

$$S(x) = \begin{bmatrix} 0 & -x_3 & x_2 \\ x_3 & 0 & -x_1 \\ -x_2 & x_1 & 0 \end{bmatrix}. \quad (2.19)$$

Some useful properties of this matrix are given below (for a more complete list the

reader is referred to Shuster (1993), page 446):

$$S(x)x = \mathbf{0}_{3 \times 1} \quad (2.20)$$

$$S(x)^\top = -S(x) \quad (2.21)$$

$$S(x)^2 = xx^\top - x^\top x I_{3 \times 3} \quad (2.22)$$

$$S(Rx) = RS(x)R^\top, \quad R \in SO(3) \quad (2.23)$$

$$S(x)y = -S(y)x = x \times y \quad (2.24)$$

$$\lambda(S(x)^2) = \begin{bmatrix} 0, & -\|x\|^2, & -\|x\|^2 \end{bmatrix} \quad (2.25)$$

where $x \times y$ is the (right-handed) vector product of the vectors x and y , and $\lambda(M)$ denotes the eigenvalues of the matrix $M \in \mathbb{R}^{3 \times 3}$.

2.3.2 Bounded Functions

The use of bounded functions is sometimes required, especially in the development of control laws which are required to be bounded *a priori*. We consider a bounded, (at least) twice-differentiable function, denoted as $h(\cdot) : \mathbb{R}^3 \rightarrow \mathbb{R}^3$, where we also denote $\phi(u) := \frac{\partial}{\partial u} h(u)$, and $f_\phi(u, v) := \frac{\partial}{\partial u} \phi(u)v$, satisfying the following properties:

$$\left. \begin{aligned} h(\mathbf{0}) &= \mathbf{0} \\ u^\top h(u) &> 0 & \forall u \in \mathbb{R}^3, \|u\| \in (0, \infty) \\ 0 < \|h(u)\| &< 1 \\ 0 < \|\phi(u)\| &\leq 1 \\ \|f_\phi(u, v)\| &\leq c_f \|v\| \end{aligned} \right\} \forall u \in \mathbb{R}^3, \|u\| \in (0, \infty) \quad (2.26)$$

Throughout the thesis we make use of one example of this type of function which is given by

$$h(u) = \left(1 + u^\top u\right)^{-1/2} u. \quad (2.27)$$

Using this definition for $h(u)$ one can derive the expressions for $\phi(u)$ and $f_\phi(u, v)$ to obtain

$$\phi(u) = \left(1 + u^\top u\right)^{-3/2} \left(I_{3 \times 3} - S(u)^2\right) \quad (2.28)$$

$$\begin{aligned} f_\phi(u, v) &= \left(1 + u^\top u\right)^{-5/2} \left(3(S(u)^2 - I)vu^\top\right. \\ &\quad \left.+ (1 + u^\top u)(2S(u)S(v) - S(v)S(u))\right) \end{aligned} \quad (2.29)$$

from which one can find the bound

$$\begin{aligned} \|f_\phi(u, v)\| &\leq \left(1 + \|u\|^2\right)^{-5/2} \left(6(1 + \|u\|^2)\|u\|\|v\|\right) \\ &\leq 6(1 + \|u\|^2)^{-3/2}\|u\|\|v\| \end{aligned} \quad (2.30)$$

To find an upper bound for $f_\phi(u, v)$ (in terms of u), we construct the cost function $J = (1 + u^\top u)^{-3}u^\top u$, which we differentiate with respect to u to obtain

$$\frac{\partial}{\partial u} J = -6u^\top u(1 + u^\top u)^{-4}u^\top + 2(1 + u^\top u)^{-3}u^\top \quad (2.31)$$

Setting this result to zero yields two results given by $\|u\| = 0$ (minimum value for J) and $\|u\| = 1/\sqrt{2}$ (maximum value for J), which implies $\sup \left\{ (1 + \|u\|)^{-3/2}\|u\| \right\} = (2/3)^{3/2}/\sqrt{2}$. Consequently, we find the bound $f_\phi(u, v) \leq c_f\|v\|$ where $c_f = 4/\sqrt{3}$.

2.3.3 Stability Definitions

Throughout this work, based upon a proposed estimation or control law, we seek to describe the qualitative behavior of the system equilibrium solutions. We say that an equilibrium point is stable if for initial conditions sufficiently close to the equilibrium point, the system states remain in a neighborhood of the equilibrium point for all time. An equilibrium point is said to be asymptotically stable if the system states remain in a neighborhood of the equilibrium point, and converge to the equilibrium point for all initial conditions contained within a set defined as the domain of attraction. In the case where the domain of attraction is the entire space, the equilibrium point is said to be globally asymptotically stable. In the case where the domain of attraction is the entire set except for a subset of Lebesgue measure zero, the equilibrium point is said to be almost globally asymptotically stable. If the domain of attraction can be arbitrarily increased to contain any subset of the entire space, the equilibrium point is said to be semi-globally stable. For more formal stability definitions the reader is referred to Khalil (2002).

Throughout the thesis, we study the performance of closed loop systems (using the proposed estimation and control laws) using Lyapunov based techniques. In general, let $x \in \mathbb{R}^n$ denote the state of a given system, and $D \subset \mathbb{R}^n$ denote a subset of the space. We assume that x is continuously differentiable, where in general $\dot{x} = f(t, x)$ where we assume the function $f(t, x)$ is Lipschitz in D . We denote $\mathcal{V}(t, x) : D \rightarrow \mathbb{R}$ as a continuously differentiable positive-definite function on the domain D which contains the origin $x = 0$, which is referred to as a *Lyapunov* function. Also, in many cases we may denote $\mathcal{V} := \mathcal{V}(t) := \mathcal{V}(t, x)$, where the arguments t and x may be intentionally removed, unless they are specifically required. Using Lyapunov functions, in general we analyze the stability of the particular equilibrium point $x = 0$

by differentiating \mathcal{V} with respect to time. To identify this operation we often denote the time-derivative of a function using the *dot* notation, for example $\dot{x} := dx/dt$ and $\ddot{x} := d^2x/dt^2$. Furthermore, when we require derivatives of a higher-order, we use the notation $x^{(n)} := d^n x/dt^n$. Fortunately, there are a variety of mathematical tools which are available in the literature which assist us in the stability analysis of equilibrium solutions. One of these tools, is known as *Barbalat's Lemma*, which is restated below for convenience.

Lemma 1 (Barbalat's Lemma Khalil (2002), page 323). *Let $\phi : \mathbb{R} \rightarrow \mathbb{R}$ be a uniformly continuous function on $[0, \infty)$. Suppose that $\lim_{t \rightarrow \infty} \int_0^t \phi(\tau) d\tau$ exists and is finite. Then $\phi(t) \rightarrow 0$ as $t \rightarrow \infty$.*

In most cases it can be very difficult to show the time-derivative of Lyapunov functions are negative definite, especially in the case of non-autonomous systems. In these cases, one cannot use invariance set theorems (such as Lasalle's theorem, Khalil (2002)), and therefore one often relies on the use of Barbalat's Lemma. In particular, we make frequent use of the following Lemma (which is actually a corollary of Barbalat's Lemma) which involves the study of non-autonomous systems.

Lemma 2 (Lyapunov-Like Lemma, Slotine and Li (1991), page 125). *If a scalar function $\mathcal{V}(t, x)$ satisfies the following conditions*

- $\mathcal{V}(t, x)$ is lower bounded,
- $\dot{\mathcal{V}}(t, x)$ is negative semi-definite,
- $\dot{\mathcal{V}}(t, x)$ is uniformly continuous in time,

then $\dot{\mathcal{V}}(t, x) \rightarrow 0$ as $t \rightarrow \infty$.

In some situations it may not be straightforward to show $\dot{\mathcal{V}}(t, x)$ is uniformly continuous. In these situations, a sufficient (yet conservative) condition for the uniform continuity of $\dot{\mathcal{V}}(t, x)$ is to show that $\ddot{\mathcal{V}}(t, x)$ is uniformly bounded.

In the case where a system has multiple equilibria, it is sometimes helpful to show that a particular undesired equilibrium point is unstable. One useful Lemma which can be used to demonstrate the instability of a particular equilibrium point is known as Chetaev's Theorem, which is also restated for convenience.

Theorem 2.1 (Chetaev's Theorem Khalil (2002)). *Let $x = 0$ be an equilibrium point for $\dot{x} = f(x)$. Let $V_c : D \rightarrow \mathbb{R}$ be a continuously differentiable function on a domain $D \subset \mathbb{R}^n$ that contains the origin $x = 0$, such that $V_c(0) = 0$ and for any $\epsilon > 0$ there exists $x_0 \in B(\epsilon, 0) \cap D$ such that $V_c(x_0) > 0$. Let $B_r = \{x \in \mathbb{R}^n \mid \|x\| \leq r\}$ denote a ball of radius $r > 0$ and define the set $U = \{x \in B_r \mid V_c(x) > 0\}$, and suppose that $\dot{V}_c(x) > 0$ in U . Then, $x = 0$ is unstable.*

Chapter 3

Attitude Reconstruction and Estimation

In this chapter we explore the challenge of determining the orientation of a rigid-body. We recall the inertial frame \mathcal{I} and body frame \mathcal{B} (defined in Section 2.1.1), where our primary objective is to determine the rotation matrix $R \in SO(3)$ or unit-quaternion $Q \in \mathbb{Q}$ which describes the orientation of \mathcal{B} .

To solve our problem we make use of vector-measurements, which refers to the body-frame measurements of vectors which are known in the inertial frame. In some situations, we also require the knowledge of the system angular velocity (measured using a gyroscope which is rigidly attached to \mathcal{B}).

In Section 3.1 we describe the so-called attitude reconstruction algorithms, which seek to recover a closed-form solution for the attitude of a rigid-body, without the use of an observer or filter. In the case where the rigid-body is rotating, other estimation schemes have been proposed which combine these attitude reconstructions with the gyroscope measurement, and are known as complementary filters. In Section 3.2, one example of a nonlinear complementary filter is discussed.

Other observers have eliminated the requirement of the reconstruction algorithms by applying the vector measurements directly to the estimation laws, which is described in Section 3.3.3. Also, in Section 3.3.4 we describe a similar vector-measurement based observer (that does not require the attitude reconstructions) which also considers low-pass filtering of the vector measurements, and therefore

may be better suited in the case where the measurements are affected by noise or other disturbances.

For the type of observers listed above, the vector measurements are assumed to be constant and known in the inertial frame. However, in many practical situations, two vector measurements most commonly used are obtained using a magnetometer and accelerometer which are rigidly attached to \mathcal{B} . The magnetometer is used to measure the ambient magnetic field which is assumed to be known in \mathcal{I} , and the accelerometer is used to measure the apparent acceleration of \mathcal{B} . However, since the apparent acceleration is not known in \mathcal{I} , the previous attitude observer is no longer applicable. This problem is addressed by using an additional filter which uses linear-velocity measurements which are obtained using a GPS. The filtered version of the system velocity can be used to obtain information about the (unknown) system apparent acceleration, and can therefore be used to aid in the estimation of the rigid-body attitude. Two observers of this type are proposed in Section 3.3.5.

3.1 Attitude Reconstruction

3.1.1 Attitude Reconstruction Using a Single Vector Measurement

In the case where only one vector measurement is available we seek to determine an expression for the rotation matrix $R \in SO(3)$ which satisfies

$$b_1 = Rr_1. \tag{3.1}$$

where $r_1 \in \mathbb{R}^3$ is a known vector whose coordinates are given in the inertial frame \mathcal{I} and $b_1 \in \mathbb{R}^3$ is its resulting measurement in the body-frame \mathcal{B} . Note that (3.1) can also be expressed using the unit quaternion

$$(0, b_1) = Q^{-1} \odot (0, r_1) \odot Q, \quad (3.2)$$

where $R = R(Q)$ as defined by (2.8). One solution to this problem is proposed by the following Lemma.

Lemma 3. *Roberts and Tayebi (2011a) Given two vectors r and b where $\|r\| = \|b\| \neq 0$, and where $r \neq -b$, then a solution for $R = R(Q) \in SO(3)$ (as defined by (2.8)) where $Q = (\eta, q) \in \mathbb{Q}$, that satisfies $b = Rr$ exists and is given by*

$$\eta = \frac{1}{\|r\|} \sqrt{\frac{\|r\|^2 + r^\top b}{2}}, \quad (3.3)$$

$$q = \frac{1}{\|r\|} \sqrt{\frac{1}{2(\|r\|^2 + r^\top b)}} S(b)r. \quad (3.4)$$

The proof for this lemma is given in Appendix A.1.1 on page 147.

Remark 1. *The solution for $R = R(Q)$ given in Lemma 3 is not unique, since there exists an infinite number of solutions to the problem when using only a single vector measurement. This is due to the fact that (3.1) is equivalent to $b = RR(\theta, \hat{r})r = Rr$ where $R(\theta, \hat{r})$ is the rotation matrix which corresponds to the rotation axis $\hat{r} = r/\|r\|$ and θ is the corresponding angle of rotation as defined by (2.3). Note that $R(\theta, \hat{r})r = r$ for any value of θ . In order to extract a rotation matrix (or unit-quaternion) which describes the orientation of a frame of reference (in three-dimensional Euclidean space),*

in most cases two non-collinear vector measurements are required. This problem is considered in the next section.

3.1.2 Attitude Reconstruction Using Two or More Vector Measurements

In the previous section we considered the problem of finding a suitable value for a unit-quaternion and rotation matrix using a single vector measurement. Since there exists an infinite number of solutions for this particular problem, a single vector measurement is usually not sufficient to find a unique value. In the sequel, we use multiple vector measurements to find a unique solution for the rotation matrix R , which satisfies

$$b_i = Rr_i, \quad i = 1, 2, \dots, n, \quad (3.5)$$

where r_i is a vector known in frame \mathcal{I} which is measured in the frame \mathcal{B} , R is the rotation matrix which describes the orientation of \mathcal{B} with respect to \mathcal{I} , and n is the number of available vector measurements. We assume that $n > 1$, and that at least two of the vectors are not collinear.

Attitude Reconstruction Using Two Vector Measurements: When only two non-collinear vector measurements are available, it is possible to construct a third vector $r_3 = r_1 \times r_2$ and $b_3 = b_1 \times b_2 = Rr_3$. Using the three vector pairs we construct the following matrices

$$U = [r_1, r_2, r_3], \quad Y = [b_1, b_2, b_3], \quad (3.6)$$

which are full-rank provided r_1 and r_2 are not collinear. In this case it is obvious that $Y = RU$ and therefore a unique solution for the rotation matrix R exists which

is given by

$$R = YU^{-1}. \quad (3.7)$$

This solution is very similar to the TRIAD algorithm defined in Shuster and Oh (1981). In fact, a nice feature of the TRIAD algorithm is attributed to the fact it guarantees solutions to be $SO(3)$ even in the presence of noise, which is not necessarily the case with the method proposed above.

Attitude Reconstruction Using More Than Three Vector Measurements: In the more general case where $n > 3$ vectors are measured, we construct the matrices $U, Y \in \mathbb{R}^{3 \times n}$ such that

$$U = [r_1, r_2, \dots, r_n], \quad Y = [b_1, b_2, \dots, b_n], \quad (3.8)$$

where we know $Y = RU$. In this more general case, if the matrix UU^T has full rank, a unique solution for R can be found using the *pseudo-inverse* which is given by

$$R = YU^T(UU^T)^{-1}. \quad (3.9)$$

The condition that UU^T has a rank of three requires we have three vectors which are not collinear. In the case where only two of the vectors are linearly independent, we can always construct a third non-collinear vector $r_3 = r_1 \times r_2$ and the corresponding measurement $b_3 = b_1 \times b_2$, and the above method is repeated with $n + 1$ vectors.

3.2 Complementary Filtering

In the previous section we demonstrate how the orientation of a rigid-body can be calculated (without a filter or observer) using two or more vector inertial vectors and

their corresponding measurements. In ideal situations, the attitude extraction algorithms would be sufficient for obtaining attitude estimates for a rigid-body. However, when the inertial vectors and their measurements are not ideal, it is useful to use an observer (or filter) in order to improve the accuracy of the estimates.

One common method incorporates the use of the attitude reconstruction methods, for example the ones discussed in the previous section, together with a gyroscope in a filter, which is commonly referred to as *complementary filtering*. In this section we present a complementary filter which has been previously proposed by Tayebi et al. (2007). However other examples of complementary filtering are proposed in Hamel and Mahony (2006), Mahony et al. (2005), Mahony et al. (2008) and Tayebi and McGillvray (2006).

Let $R \in SO(3)$ denote the orientation of the body-fixed frame \mathcal{B} with respect to \mathcal{I} , and let \bar{R} denote an estimate of R which is obtained using an attitude reconstruction algorithm, for example the one defined in Section 3.1.2. Furthermore, let $\bar{Q} \in \mathbb{Q}$ denote the unit-quaternion which corresponds to the rotation matrix \bar{R} (for algorithms which give a unit-quaternion based upon a rotation matrix see Shuster (1993)). If we assume for the time being that the vector measurements are not perturbed by noise or other disturbances, using the model given by (2.17), the rotational dynamics are governed by

$$\dot{\bar{Q}} = \frac{1}{2}\bar{Q} \odot (0, \omega) = \frac{1}{2}A(\bar{Q})\omega, \quad (3.10)$$

where ω is the body-referenced angular velocity of \mathcal{B} . Let ω_g denote a biased measurement of ω , for example, as measured using a gyroscope, such that

$$\omega_g = \omega + \omega_b, \quad (3.11)$$

where $\omega_b \in \mathbb{R}^3$ is the unknown gyroscope sensor bias, which is assumed to be constant. In some cases, an attitude observer is proposed which also estimates this unknown gyroscope bias in order to improve the performance of the overall observer. Let $\hat{Q} \in \mathbb{Q}$ denote an estimate of Q , and let $\hat{\omega}_b \in \mathbb{R}^3$ denote an estimate of ω_b , and consider the following observer/complementary filter:

$$\dot{\hat{Q}} = \frac{1}{2}\hat{Q} \odot (0, \beta), \quad (3.12)$$

$$\beta = \omega_g - \hat{\omega}_b + \Gamma_1 \tilde{q}, \quad (3.13)$$

$$\dot{\hat{\omega}}_b = -\Gamma_2 \tilde{q}, \quad (3.14)$$

where Γ_1 and Γ_2 are positive definite matrices, and \tilde{q} is the vector part of the quaternion defined by

$$\tilde{Q} = (\tilde{\eta}, \tilde{q}) = \hat{Q}^{-1} \odot \bar{Q}, \quad (3.15)$$

and denote the *gyroscope bias error* as $\tilde{\omega}_b = \hat{\omega}_b - \omega_b$.

Proposition 1 (Tayebi et al. (2007)). *Consider the system given by (3.10) and the observer (3.12)-(3.14). Assume that the bias ω_b is constant, and assume that ω and $\dot{\omega}$ are bounded. Then, all observer signals are bounded and $\lim_{t \rightarrow \infty} \tilde{q}(t) = \lim_{t \rightarrow \infty} \tilde{\omega}_b(t) = \mathbf{0}$.*

Sketch of Proof:

(For a complete proof please see Appendix A.2.1 on page 149)

We first find the time-derivative of the attitude error $\tilde{Q} = (\tilde{\eta}, \tilde{q})$ is governed by

$$\dot{\tilde{Q}} = \frac{1}{2}\tilde{Q} \odot (0, \omega - \tilde{R}\beta), \quad (3.16)$$

from which we find $\dot{\tilde{\eta}} = -\tilde{q}^\top(\omega - \beta)$ since $\tilde{q}^\top \tilde{R}\beta = \tilde{q}^\top \beta$. We consider the following Lyapunov function

$$\mathcal{V} = \tilde{q}^\top \tilde{q} + (1 - \tilde{\eta})^2 + \frac{1}{2} \tilde{\omega}_b^\top \Gamma_2^{-1} \tilde{\omega}_b = 2(1 - \tilde{\eta}) + \frac{1}{2} \tilde{\omega}_b^\top \Gamma_2^{-1} \tilde{\omega}_b, \quad (3.17)$$

which, in light of the control and estimation laws, has the time derivative given by $\dot{\mathcal{V}} = -\tilde{q}^\top \Gamma_1 \tilde{q}$. Due to the boundedness of ω , Barbalat's Lemma implies $\tilde{q} \rightarrow 0$. Similarly, the bound of $\dot{\omega}$ also implies $\dot{\tilde{Q}} \rightarrow 0$ and therefore $\beta \rightarrow \omega$, which in turn implies $\hat{\omega}_b \rightarrow \omega_b$. \square

Remark 2. *The fact that $\tilde{q} \rightarrow 0$ implies that $\hat{Q} \rightarrow \pm \bar{Q}$, which is not necessarily the true orientation defined by Q . Consequently, the performance of the complementary filter is dependant on the accuracy of reconstructed attitude \tilde{R} .*

Remark 3. *Note that when using the unit-quaternion, there are two antipodal equilibrium solutions in the space $\mathbb{Q} \times \mathbb{R}^3$ which are given by $(\tilde{\eta} = \pm 1, \tilde{q} = 0, \tilde{\omega}_b = 0)$. In terms of the rotation matrix representation, both of these equilibria correspond to the single equilibrium solution in the space $SO(3) \times \mathbb{R}^3$ given by $(\tilde{R} = I_{3 \times 3}, \tilde{b} = 0)$. Note that the equilibrium solution corresponding to $\tilde{\eta} = 1$ is a stable equilibrium, where the solution corresponding to $\tilde{\eta} = -1$ is a repeller. In this case the equilibrium point $(\tilde{R} = I_{3 \times 3}, \tilde{b} = 0)$ is a homoclinic point and therefore the unwinding phenomenon exists.*

3.3 Vector Measurement Based Attitude

Estimation

As discussed in the previous sections, the attitude reconstruction algorithms are a crucial part of the complementary filters. However, in many cases attitude observers have been designed which do not depend on the attitude reconstructions. Instead, the vector measurements, which would normally be applied to the attitude reconstruction algorithms, are now applied directly to the estimation laws. Similar to the previous observers, we use the frames \mathcal{B} and \mathcal{I} (as defined in Section 2.1.1), and let $Q \in \mathbb{Q}$ denote the unit-quaternion which defines the relative orientation of the frame \mathcal{B} with respect to \mathcal{I} , and $R = R(Q) \in SO(3)$ the corresponding rotation matrix as defined by (2.8), which are unknown. As previously defined by (2.17), the attitude dynamics are governed by

$$\dot{Q} = \frac{1}{2}Q \odot (0, \omega) = \frac{1}{2} \begin{bmatrix} -q^\top \\ \eta I_{3 \times 3} + S(q) \end{bmatrix} \omega, \quad \dot{R} = -S(\omega)R, \quad (3.18)$$

where $\omega \in \mathbb{R}^3$ is the body-referenced angular velocity. For the purposes of the estimator design, we now assume the gyroscope measurement is unbiased, or $\omega_b \approx 0$, and therefore the gyroscope provides the ideal measurement $\omega_g = \omega$. In many cases, we also require that the system angular velocity is bounded, which we state more formally by the following assumption. This assumption is a realistic constraint for a physical system, and therefore does not limit the applicability of the proposed observers.

Assumption 3.1. *The body-referenced angular velocity $\omega = \omega(t)$ is bounded for all $t \geq t_0$.*

Let $\hat{Q} = (\hat{\eta}, \hat{q}) \in \mathbb{Q}$, $\hat{\eta} \in \mathbb{R}$, $\hat{q} \in \mathbb{R}^3$, denote the unit quaternion which is an

estimate of Q , and $\hat{R} = R(\hat{Q})$ denote the corresponding rotation matrix as defined by (2.8). To preserve the properties of the attitude parameterizations, we consider observer laws which are governed by

$$\dot{\hat{Q}} = \frac{1}{2} \hat{Q} \odot (0, \omega + \sigma) = \frac{1}{2} \begin{bmatrix} -\hat{q}^\top \\ \hat{\eta} I_{3 \times 3} + S(\hat{q}) \end{bmatrix} (\omega + \sigma), \quad (3.19)$$

where $\sigma \in \mathbb{R}^3$ is an observer law which is defined later. Based upon this definition, the dynamic equation of the corresponding rotation matrix is given by

$$\dot{\hat{R}} = -S(\omega + \sigma) \hat{R}. \quad (3.20)$$

To study the performance of the proposed observers we require a measure of the relative orientation between the attitude estimates and the actual attitude. This is the goal of the next section.

3.3.1 Attitude Error

To define the attitude error, we use the unit-quaternion $\tilde{Q} = (\tilde{\eta}, \tilde{q}) \in \mathbb{Q}$, and rotation matrix $\tilde{R} \in SO(3)$ which are defined by

$$\tilde{Q} = Q \odot \hat{Q}^{-1}, \quad \tilde{R} = R(\tilde{Q}) = \hat{R}^\top R. \quad (3.21)$$

To obtain the time-derivative of the unit-quaternion \tilde{Q} , we first note that $Q = \tilde{Q} \odot \hat{Q}$, from which one can find $\dot{Q} = \dot{\tilde{Q}} \odot \hat{Q} + \tilde{Q} \odot \dot{\hat{Q}}$, which leads to $\dot{\tilde{Q}} = \dot{Q} \odot \hat{Q}^{-1} - \tilde{Q} \odot \dot{\hat{Q}} \odot \hat{Q}^{-1}$. Applying the definitions (3.18) and (3.19) we find

$$\dot{\tilde{Q}} = \frac{1}{2} \tilde{Q} \odot \hat{Q} \odot (0, -\sigma) \odot \hat{Q}^{-1}. \quad (3.22)$$

Using the property (2.10) the result for the derivative of \tilde{Q} can be written in the desired form (quaternion-derivative)

$$\dot{\tilde{Q}} = \frac{1}{2} \tilde{Q} \odot (0, \tilde{\omega}) = \frac{1}{2} \begin{bmatrix} -\tilde{q} \\ \tilde{\eta} I_{3 \times 3} + S(\tilde{q}) \end{bmatrix} \tilde{\omega}, \quad (3.23)$$

$$\tilde{\omega} = -\hat{R}^\top \sigma. \quad (3.24)$$

A similar result can also be achieved using the rotation matrix \tilde{R} . In fact, in light of (3.18) and (3.20), we find $\dot{\tilde{R}} = \hat{R}^\top S(\sigma) \tilde{R} \tilde{R}$. Applying the property (2.23), we find

$$\dot{\tilde{R}} = -S(\tilde{\omega}) \tilde{R}. \quad (3.25)$$

Clearly, using $SO(3)$ representation, the goal of the attitude observers is to force $\hat{R} \rightarrow R$, which is equivalent to $\tilde{R} \rightarrow I$. In terms of the unit-quaternion, as discussed in Section 2.1.3, this objective has two (antipodal) solutions $\tilde{Q} = (\pm 1, \mathbf{0})$. The fact that $\tilde{Q} = (1, \mathbf{0})$ implies $\hat{Q} = Q$ which is clearly desired. The fact that $\tilde{Q} = (-1, \mathbf{0})$ implies $\hat{Q} = -Q$, which implies the relative orientation of \mathcal{B} with respect to \mathcal{I} differs by an angle of rotation equal to 2π , and therefore also satisfies the objectives.

3.3.2 Vector Measurements

Let r_i , $i = 1, 2, \dots, n$, denote a set of inertial vectors and let $b_i = Rr_i$ denote the measurement of the vector r_i . Using the attitude estimate $\hat{R} = R(\hat{Q})$, we define the *measurement estimate* as $\hat{b}_i = \hat{R}r_i$, and the *measurement error* as $\tilde{b}_i = \hat{b}_i - b_i$. We also define two particularly useful functions which are given by

$$z_\gamma := \sum_{i=1}^n \gamma_i S(\hat{b}_i) b_i, \quad (3.26)$$

$$W := - \sum_{i=1}^n \gamma_i S(r_i)^2, \quad (3.27)$$

where γ_i are strictly positive constants. The vector z_γ provides a useful corrective term in the estimator feedback since this vector is comprised by the cross-products of the actual and estimated vector measurements, or b_i and \hat{b}_i , respectively. This is intuitive since a straightforward choice for the axis of rotation to force $\hat{b}_i \rightarrow b_i$ is the vector which is orthogonal to both vectors.

In some cases we require that the inertial vectors r_i satisfy some requirements which are stated in the following assumption.

Assumption 3.2. *The vectors r_i , $i = 1, 2, \dots, n$, are known and constant in an inertial frame \mathcal{I} , and contain at least two non-collinear vectors.*

We now propose the following Lemma which identifies some useful characteristics of the functions given by (3.26) and (3.27).

Lemma 4 (Tayebi et al. (2011)). *Consider a set of vectors b_i , $i = 1, 2, \dots, n$, which are measured in the body-frame \mathcal{B} , corresponding to n inertial vectors r_i , which satisfy Assumption 3.2. Assume the parameters γ_i are strictly positive. Then,*

(a) *The matrix W defined by (3.27) is positive-definite.*

(b) *The following property holds*

$$z_\gamma := \sum_{i=1}^n \gamma_i S(\hat{b}_i) b_i = -2\hat{R}(\tilde{\eta}I - S(\tilde{q}))W\tilde{q}, \quad (3.28)$$

(c) *$z_\gamma = 0$ is equivalent to $(\tilde{\eta} = 0, \tilde{q} = \pm v)$ or $(\tilde{\eta} = \pm 1, \tilde{q} = 0)$, where v is a unit-eigenvector of the matrix W defined by (3.27).*

The proof for this Lemma is given in Appendix A.1.2 on page 148.

Based upon this framework, we propose two types of attitude observers. The first observer, given in Section 3.3.3, uses the vector measurements directly, where the observer discussed in Section 3.3.4 uses a filtered version of the vector measurements. The latter observer may be better suited in practical situations, for example when the vector measurements are contaminated with noise.

3.3.3 Vector-Measurement Based Attitude Observer

Using the framework previously defined, we now propose an observer based upon the vector measurements. The estimation laws are given as follows:

$$\dot{\hat{Q}} = \frac{1}{2} \begin{bmatrix} \hat{q}^\top \\ \hat{\eta}I + S(\hat{q}) \end{bmatrix} \beta, \quad (3.29)$$

$$\beta = \omega - z_\gamma, \quad (3.30)$$

where z_γ is given by (3.26). Let $\tilde{Q} = (\tilde{\eta}, \tilde{q})$ denote the attitude error as defined by (3.21), and consider the following proposition.

Proposition 2 (Tayebi et al. (2011)). *Consider the system defined by (3.18) where we apply the observer (3.29)-(3.30), with $n \geq 2$ vector measurements b_i , corresponding to n inertial vectors r_i , $i = 1, 2, \dots, n$. Let Assumptions 3.1 and 3.2 be satisfied. Then,*

(a) $\lim_{t \rightarrow \infty} \tilde{Q}(t) = (\text{sgn}(\tilde{\eta}(t_0)), \mathbf{0})$, (or equivalently $\lim_{t \rightarrow \infty} \tilde{R}(t) = I$), for almost any initial condition except for a set of Lebesgue measure zero described by $\Psi = \left\{ \tilde{Q} = (\tilde{\eta}, \tilde{q}) \in \mathbb{Q} \mid \tilde{\eta} = 0 \right\}$.

(b) The manifold Ψ is invariant and non-attractive.

(c) If $\tilde{Q}(t_0) \in \Psi$, then $\tilde{Q}(t) \in \Psi$ for all $t \geq t_0$ and $\lim_{t \rightarrow \infty} \tilde{Q}(t) = (0, \pm v)$, where v are the unit eigenvectors of W .

Sketch of Proof

(For a complete proof please see Appendix A.2.2 on page 150)

Using the vector measurement error $\tilde{b}_i = \hat{b}_i - b_i$ we construct the Lyapunov function candidate

$$\mathcal{V} = \frac{1}{2} \sum_{i=1}^n \gamma_i \tilde{b}_i^T \tilde{b}_i, \quad (3.31)$$

which yields the negative semi-definite result for the time-derivative $\dot{\mathcal{V}} = -z_\gamma^T z_\gamma$. Since ω and β are bounded, $\ddot{\mathcal{V}}$ is bounded, and therefore Barbalat's Lemma implies $z_\gamma \rightarrow 0$. Invoking Lemma 4 we find this corresponds to the desired equilibria ($\tilde{\eta} = \pm 1, \tilde{q} = 0$) and the undesired equilibria ($\tilde{\eta} = 0, \tilde{q} = \pm v$). To show that Ψ is invariant, and the undesired equilibria are unstable, we study the dynamics of $\tilde{\eta}^2$. In fact, we show that for all $\tilde{\eta}(t_0) \neq 0$, $|\tilde{\eta}|$ is always increasing and therefore $\tilde{\eta}(t)$ converges to $\text{sgn}(\tilde{\eta}(t_0))$. In the case where $\tilde{\eta} = 0$, we show $\dot{\tilde{\eta}} = 0$ which shows the invariance of Ψ . Therefore, in the case where $\tilde{\eta}(t_0) = 0$, Lemma 4 implies $\lim_{t \rightarrow \infty} \tilde{\eta}(t) = 0$ and $\lim_{t \rightarrow \infty} \tilde{q}(t) = \pm v$. \square

Remark 4. As discussed in the proof, there are two antipodal equilibrium solutions given by ($\tilde{\eta} = \pm 1, \tilde{q} = 0$), which both correspond (in terms of the $SO(3)$ parameterization) to $\tilde{R} = R(\tilde{Q}) = I_{3 \times 3}$. However, since both antipodal equilibrium solutions are asymptotically stable, the equilibrium point $\tilde{R} = I_{3 \times 3}$ is not homoclinic and the unwinding phenomenon is avoided. However, the invariant manifold Ψ exists which divides the quaternion space into two halves, with each half containing one of the two stable equilibria. All trajectories which start on this manifold stay there for all time, and converge to one of the hyperbolic equilibria which are contained in Ψ . Despite this

disadvantage, this observer offers superior performance when compared to the complementary filter since the unwinding problem is avoided, and the attitude reconstruction is no longer required.

3.3.4 Attitude Observer Using Filtered Vector

Measurements

In practical situations the vector measurements b_i are likely to be contaminated with noise. A well known practice is to use low-pass filtering of the sensor data before applying the signals to the attitude observer, which is done without rigorous proofs of stability. In this section we extend the results given in Section 3.3.3 by including a low-pass filter which is applied to the sensor data as part of the attitude observer. We let $\psi \in \mathbb{R}^3$ denote the filter state-variable, and consider the following observer

$$\dot{\hat{Q}} = \frac{1}{2}A(\hat{Q})\beta, \quad (3.32)$$

$$\beta = \omega - \alpha\psi, \quad (3.33)$$

$$\dot{\psi} = -\alpha\psi + \alpha z_\gamma, \quad (3.34)$$

where $\alpha \in \mathbb{R}$ is chosen to be strictly positive and z_γ is defined in Lemma 4. Let $\tilde{Q} = (\tilde{\eta}, \tilde{q}) \in \mathbb{Q}$ denote the attitude error as defined by (3.21).

Proposition 3 (Tayebi et al. (2011)). *Consider the system (3.18) with the observer (3.32)-(3.34). Let Assumptions 3.1 and 3.2 be satisfied. Then,*

- (a) *The estimator has the following equilibria: $(\tilde{\eta} = \pm 1, \tilde{q} = 0, \psi = 0)$ and $(\tilde{\eta} = 0, \tilde{q} = \pm v, \psi = 0)$.*

(b) There exists $\bar{\gamma}_i$, such that for all $\gamma_i > \bar{\gamma}_i$, the equilibria $(\tilde{\eta} = \pm 1, \tilde{q} = 0, \psi = 0)$ are almost globally asymptotically stable and the equilibria $(\tilde{\eta} = 0, \tilde{q} = \pm v, \psi = 0)$ are unstable.

Sketch of Proof:

(For a complete proof please see Appendix A.2.3 on page 151)

Using the vector measurement error $\tilde{b}_i = \hat{b}_i - b_i$ we construct the Lyapunov function candidate

$$\mathcal{V} = \frac{1}{2} \sum_{i=1}^n \gamma_i \tilde{b}_i^\top \tilde{b}_i, \quad (3.35)$$

which in light of (3.32) and (3.34) has the time-derivative $\dot{\mathcal{V}} = -\alpha \psi^\top \psi$. Due to the boundedness of $\dot{\psi}$, Barbalats lemma implies $\psi \rightarrow 0$ and $z_\gamma \rightarrow 0$. Invoking Lemma 4, we find this corresponds to the desired equilibria $(\tilde{\eta} = \pm 1, \tilde{q} = 0, \psi = 0)$ and the undesired equilibria $(\tilde{\eta} = 0, \tilde{q} = \pm v, \psi = 0)$. To show that the undesired equilibria are unstable we use the Chetaev function candidate $\mathcal{V}_c = \tilde{\eta} \delta$ where $\delta = \tilde{q}^\top \hat{R}^\top \psi$. We show that there exists a neighborhood U (which contains the undesired equilibria characterized by $\mathcal{V}_c = 0$) where $\mathcal{V}_c > 0$ and $\dot{\mathcal{V}}_c > 0$, and therefore the undesired equilibria are unstable. \square

Remark 5. *The use of the low-pass filter, in addition to improving the performance of the observer in the presence of noise, can also be used to destroy the invariance of the manifold $\Psi = \{\tilde{Q} = (\tilde{\eta}, \tilde{q}) \in \mathbb{Q} \mid \tilde{\eta} = 0\}$. In fact, if $\delta(t_0) = \tilde{q}(t_0)^\top \hat{R}(t_0)^\top \psi(t_0) \neq 0$, the manifold Ψ is non invariant, which causes trajectories which start on this set to converge to one of the two desired equilibria.*

3.3.5 Attitude Estimation Using GPS and IMU

Measurements

In the previous section we described an observer which uses a set of vector measurements, which were assumed to be constant and known in an inertial frame of reference. The applicability of this type of observer may be questioned in situations where there are a limited number of sensors that offer measurements which satisfy these criteria.

To address this problem, we now focus on observers which use the accelerometer to measure the acceleration of the body-fixed frame (and not only the gravity vector). This type of observer utilizes measurements from an IMU (containing a magnetometer, accelerometer and a gyroscope) in addition to a GPS which is used to obtain measurements of the linear velocity of a body-fixed frame.

Let $v \in \mathbb{R}^3$ denote the linear velocity of \mathcal{B} with respect to \mathcal{I} , whose coordinates are known in frame \mathcal{I} (or measured with a GPS), and let $Q \in \mathbb{Q}$ and $R = R(Q) \in SO(3)$ describe the orientation of \mathcal{B} with respect to \mathcal{I} . We extend our dynamical model to include the dynamics of v . Therefore, our system is now governed by

$$\dot{v} = ge_3 + r_2, \quad (3.36)$$

$$\dot{Q} = \frac{1}{2} \begin{bmatrix} -q^\top \\ \eta I_{3 \times 3} + S(q) \end{bmatrix} \omega, \quad (3.37)$$

where ω is the body-referenced angular velocity of \mathcal{B} , and $r_2 \in \mathbb{R}^3$ is the *inertial-referenced apparent acceleration* of \mathcal{B} with respect to \mathcal{I} . Let $b_1 = Rr_1 \in \mathbb{R}^3$ denote the output of a magnetometer which is rigidly attached to \mathcal{B} , where $r_1 \in \mathbb{R}^3$ is the known magnetic-field of the surrounding environment. We also make use of an accelerometer

which is rigidly attached to \mathcal{B} which provides the measurement

$$b_2 = R(\dot{v} - ge_3) = Rr_2. \quad (3.38)$$

The previous observers (given in Sections 3.3.3 and 3.3.4) can not be used since the inertial vector r_2 is not known. To address this problem, both observers make use of the additional adaptive state vector $\hat{v} \in \mathbb{R}^3$. Furthermore, we also define the following error function

$$\tilde{v} = v - \hat{v}. \quad (3.39)$$

The adaptive state \hat{v} and error function \tilde{v} are very useful since, for an appropriate choice of the estimation law $\dot{\hat{v}}$, the error signal \tilde{v} can be viewed as a filtered version of the system acceleration, and therefore contains information about the unknown signal r_2 . Consequently, the signal \tilde{v} can be used by the observer (in some manner) instead of the vector r_2 . This point will be discussed later in more detail. The difficulty of our objective can be somewhat simplified by placing some realistic constraints on the value of r_2 , which are stated in the following assumptions.

Assumption 3.3. *There exists positive constants c_1 and c_2 such that $\|r_2\| \leq c_1$, and $\|\dot{r}_2\| \leq c_2$.*

Assumption 3.4. *Given two positive constants, γ_1 and γ_2 , there exists a positive constant $c_w = c_w(\gamma_1, \gamma_2)$ such that $c_w < \lambda_{\min}(W)$ where*

$$W = -\gamma_1 S(r_1)^2 - \gamma_2 S(r_2)^2. \quad (3.40)$$

The second assumption is satisfied if r_2 is non-vanishing and is not collinear to

the magnetic field vector r_1 . In the case where $r_2 = 0$, the system velocity dynamics become $\dot{v} = ge_3$ (which corresponds to the rigid body being in a free-fall state) which is not likely in normal circumstances. When this assumption is satisfied, it follows that W is positive definite (for justification of this point, the reader is referred to Lemma 4 and the corresponding proof). Furthermore, if this assumption is satisfied, the value of $c_w > 0$ can be arbitrarily increased by increasing the values of γ_1 and γ_2 .

In addition to these assumptions, we place the following constraint on the system linear velocity signal.

Assumption 3.5. *The system linear velocity v is bounded.*

Although the third assumption is not needed to show convergence of the attitude estimates, we include this requirement in order to ensure all signals involved with the attitude observers remain bounded (internal stability).

3.3.5.1 Second Order Observer Using GPS and IMU Measurements

We propose the following second-order observer:

$$\dot{\hat{Q}} = \frac{1}{2} \begin{bmatrix} -\hat{q}^\top \\ \hat{\eta}I + S(\hat{q}) \end{bmatrix} (\omega + \sigma), \quad (3.41)$$

$$\sigma = -\gamma_1 S(\hat{R}r_1)b_1 - \gamma_2 k_1 S(\hat{R}\tilde{v})b_2, \quad (3.42)$$

$$\dot{\hat{v}} = k_1 \tilde{v} + ge_3 + \hat{R}^\top b_2 + \frac{1}{k_1} \hat{R}^\top S(\sigma) b_2, \quad (3.43)$$

where $k_1, \gamma_1, \gamma_2 > 0$, $\tilde{v} = v - \hat{v}$, $\hat{R} = R(\hat{\eta}, \hat{q})$ is defined using (2.8) and $S(\cdot)$ is the skew-symmetric matrix defined by (2.19). Let $\tilde{Q} = (\tilde{\eta}, \tilde{q})$ define the unit-quaternion which describes the attitude error as defined by (3.23).

Theorem 3.1 (Roberts and Tayebi (2011b)). *Consider the observer (3.41) - (3.43) used with the system defined by (3.36)-(3.37), where Assumptions 3.1, 3.3, 3.4, and 3.5 are satisfied. Then for all initial conditions $\tilde{\eta}(t_0) \neq 0$ (or equivalently $\|\tilde{q}(t_0)\| \neq 1$), there exists a strictly positive constant $\kappa_1 > 0$ such that for all $k_1 > \kappa_1$, all associated observer signals are bounded, and $(\tilde{v}(t), q(t), \tilde{\eta}(t))$ converges exponentially to $(0, 0, \text{sgn}(\eta(t_0)))$.*

Sketch of Proof:

(For a complete version of the proof please see Appendix B.1 on page 155)

We first define the error function $\tilde{r}_2 = k_1 \tilde{v} - (I - \tilde{R})r_2$. In order to show that the error signals \tilde{r}_2 and \tilde{q} converge to zero, we construct the Lyapunov function

$$\mathcal{V} = \frac{\gamma}{2} \tilde{r}_2^T \tilde{r}_2 + \gamma_q \tilde{q}^T \tilde{q} = \frac{\gamma}{2} \tilde{r}_2^T \tilde{r}_2 + \gamma_q (1 - \tilde{\eta}^2), \quad (3.44)$$

which we differentiate with respect to time along the trajectories of the system. We then show that, based upon a suitable choice for the estimator gain k_1 , there exists a set D such that $\dot{\mathcal{V}} \leq 0$ if $\tilde{q} \in D$. Using the set D and the fact that $\sqrt{\mathcal{V}/\gamma_q} \geq \|\tilde{q}\|$, we find an estimate of the domain of attraction, which we denote as U , where all the estimator trajectories are guaranteed to converge to the equilibrium ($\tilde{\eta} = \pm 1, \tilde{q} = 0, \tilde{r}_2 = 0$). Using these results we show that there exists an upper bound for the error function $\|\tilde{q}(t)\| < 1$ for all $t \geq t_0$. Consequently, we find that $\dot{\mathcal{V}} \leq -\epsilon_v \mathcal{V}$, where ϵ_v is a strictly positive constant that depends on the estimator parameters and initial conditions, and therefore the estimator trajectories converge exponentially. \square

3.3.5.2 Third-Order Observer Using IMU and GPS Measurements

For the second observer we introduce another adaptive state denoted by $\psi \in \mathbb{R}^3$. The observer laws are chosen as follows:

$$\dot{\hat{Q}} = \frac{1}{2} \begin{bmatrix} -\hat{q}^\top \\ \hat{\eta}I + S(\hat{q}) \end{bmatrix} (\omega + \sigma), \quad (3.45)$$

$$\sigma = -\gamma_1 S(\hat{R}r_1)b_1 - \gamma_2 S(\hat{R}r_2)b_2, \quad (3.46)$$

$$\hat{r}_2 = k_2\psi + k_3\tilde{v}, \quad (3.47)$$

$$\dot{\psi} = -k_4\psi + \frac{1}{k_2}\hat{R}^\top S(b_2)\sigma - k_5\tilde{v}, \quad (3.48)$$

$$\dot{\hat{v}} = k_1\tilde{v} + ge_3 + \hat{R}^\top b_2 + k_6\psi, \quad (3.49)$$

where $k_1, k_3, \gamma_1, \gamma_2 > 0$, $\tilde{v} = v - \hat{v}$, $\hat{R} = R(\hat{Q})$ as defined by (2.8) and $S(\cdot)$ is the skew-symmetric matrix defined by (2.19). Let $\tilde{Q} = (\tilde{\eta}, \tilde{q})$ as defined by (3.21).

Theorem 3.2 (Roberts and Tayebi (2011b)). *Consider the system (3.36)-(3.37), with the observer given by (3.45)-(3.49), where we choose the following values for the gains k_5 and k_6*

$$k_5 = \frac{k_3(k_3 - k_1)}{k_2} + \frac{k_4 - k_3}{k_2 k_3 \gamma_r}, \quad k_6 = \frac{k_2(k_3 - k_4)}{k_3}, \quad (3.50)$$

where $\gamma_r > 0$. Let Assumptions 3.1, 3.3, 3.4, and 3.5 be satisfied. Then for all initial conditions $\tilde{\eta}(t_0) \neq 0$ (or equivalently $\|\tilde{q}(t_0)\| \neq 1$), there exists strictly positive constants $\kappa_3 > 0$ and $\kappa_1 > \kappa_3 - k_4 > 0$, such that for all $k_1 > \kappa_1$ and $k_3 > \kappa_3$, all associated observer signals are bounded, and $(\tilde{v}(t), \tilde{q}(t), \tilde{\eta}(t))$ converges exponentially to $(0, 0, \text{sgn}(\tilde{\eta}(t_0)))$.

Sketch of Proof:

(For a complete version of the proof please see Appendix B.2 on page 159)

We first consider the error function $\tilde{r}_2 = k_2\psi + k_3\tilde{v} + (\tilde{R} - I)r_2$, and propose the following Lyapunov function candidate

$$\mathcal{V} = \frac{\gamma}{2} \left(\tilde{v}^T \tilde{v} + \gamma_r \tilde{r}_2^T \tilde{r}_2 \right) + \gamma_q (1 - \tilde{\eta}^2) = \frac{\gamma}{2} \left(\tilde{v}^T \tilde{v} + \gamma_r \tilde{r}_2^T \tilde{r}_2 \right) + \gamma_q \tilde{q}^T \tilde{q}, \quad (3.51)$$

which we differentiate with respect to time along the trajectories of the system. Using this new Lyapunov function, the remaining steps of the proof are the same as the previous observer, except in this case, we also require a condition on the gain k_3 (in addition to k_1). \square

Remark 6. For both observers we show that there exists an upper bound $\|\tilde{q}(t)\| < 1$ for all $t \geq t_0$, and therefore $\tilde{\eta}$ is guaranteed to never cross zero (due to the unit-norm constraint of the unit-quaternion). Consequently, we find $\tilde{\eta}(t) \rightarrow \text{sgn}(\tilde{\eta}(t_0))$ as $t \rightarrow \infty$, and therefore the two equilibrium solutions ($\tilde{\eta} = \pm 1, \tilde{q} = 0, \tilde{r}_2 = 0$) are both asymptotically stable. Therefore, the problem of unwinding is avoided. However, unlike the results we obtained for observers given in Sections 3.3.3 and 3.3.4, we can no longer state that the observer dynamics are almost globally stable, since there exists a set (of finite Lebesgue measure) from which the system trajectories are not guaranteed to converge to one of the desired equilibria. Instead, we show that the domain of attraction can be arbitrarily increased to contain **almost** any initial condition. Although this is similar to semi-global stability, we refrain from the use of this term, since there does exist a set $\Phi = \{(\tilde{r}_2, \tilde{v}, \tilde{q}) \in \mathbb{R}^3 \times \mathbb{R}^3 \times \mathbb{R}^3 \mid \|\tilde{q}\| = 1\}$ which cannot be reached by arbitrarily increasing the domain of attraction, which violates the definition of semi-global stability.

3.4 Simulations

3.4.1 Complementary Filter

Simulation results were performed for the complementary filter given by (3.12)-(3.14) with the system (3.18). The gyroscope was used to measure $\omega_g = \omega + \omega_b$ where the bias was specified as $\omega_b = [0.01, -0.01, 0.005]^T rad/s$ and the angular velocity was chosen as $\omega = (\sin(0.1t), 0.2 \sin(0.2t + \pi), 0.1 \sin(0.3t + \pi/3)) rad/s$. The estimator gains were chosen as $\Gamma_1 = \Gamma_2 = 10I_{3 \times 3}$. The attitude estimate was initialized with $\hat{Q}(t_0) = [1, 0, 0, 0]^T$, with the system initial attitude was specified as $Q(t_0) = [0.5, 0.5, 0.5, 0.5]^T$. The simulations results are shown by Figure 3.1.

3.4.2 Vector Measurement Based Attitude Observer

Simulation results are provided for the two observers specified by (3.29)-(3.30) (vector-measurement-based) and (3.32)-(3.34) (filtered-vector-measurement based) with the system specified by (3.18). The body-referenced angular velocity was specified as $\omega = (\sin(0.1t), 0.2 \sin(0.2t + \pi), 0.1 \sin(0.3t + \pi/3))^T$ which was assumed to be ideally measured using a gyroscope (no bias). Two non-collinear vector measurements were used, which were assigned the values $r_1 = [1, 0, 1]^T$ and $r_2 = [0, 0, 1]^T$. For both simulations the observer gains were chosen as $\gamma_1 = \gamma_2 = 5$, and the observers were initialized with $\hat{Q}(t_0) = [1, 0, 0, 0]^T$, with the system initial attitude was specified as $Q(t_0) = [0.5, 0.5, 0.5, 0.5]^T$. For the filtered-vector-measurement based observer, we used the value $\alpha = 3$ and initialized the filter state vector as $\psi(t_0) = [0, 0, 1]^T$. The plots for these simulations are provided by Figure (3.2) for the vector-measurement based attitude observer, and by Figure (3.3) for the filtered-vector measurements.

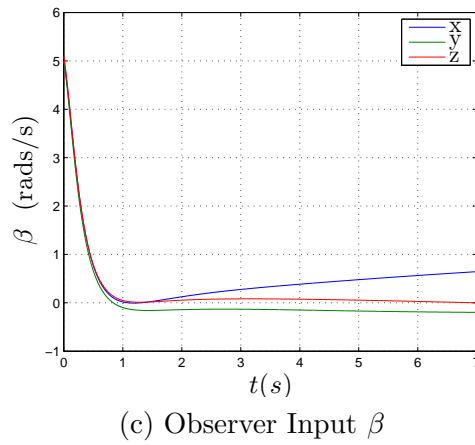
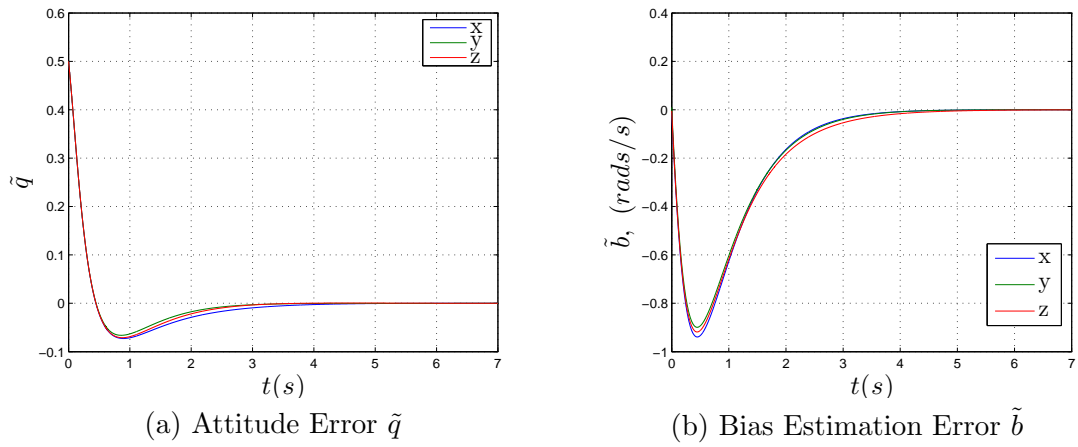


Figure 3.1: Simulation Results for Complementary Filter

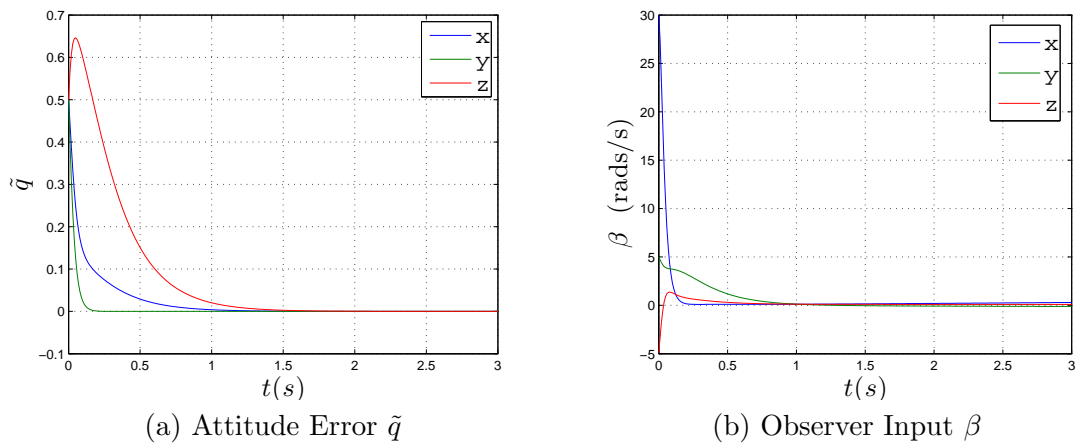


Figure 3.2: Simulation Results for Vector-Measurement-Based Attitude Observer

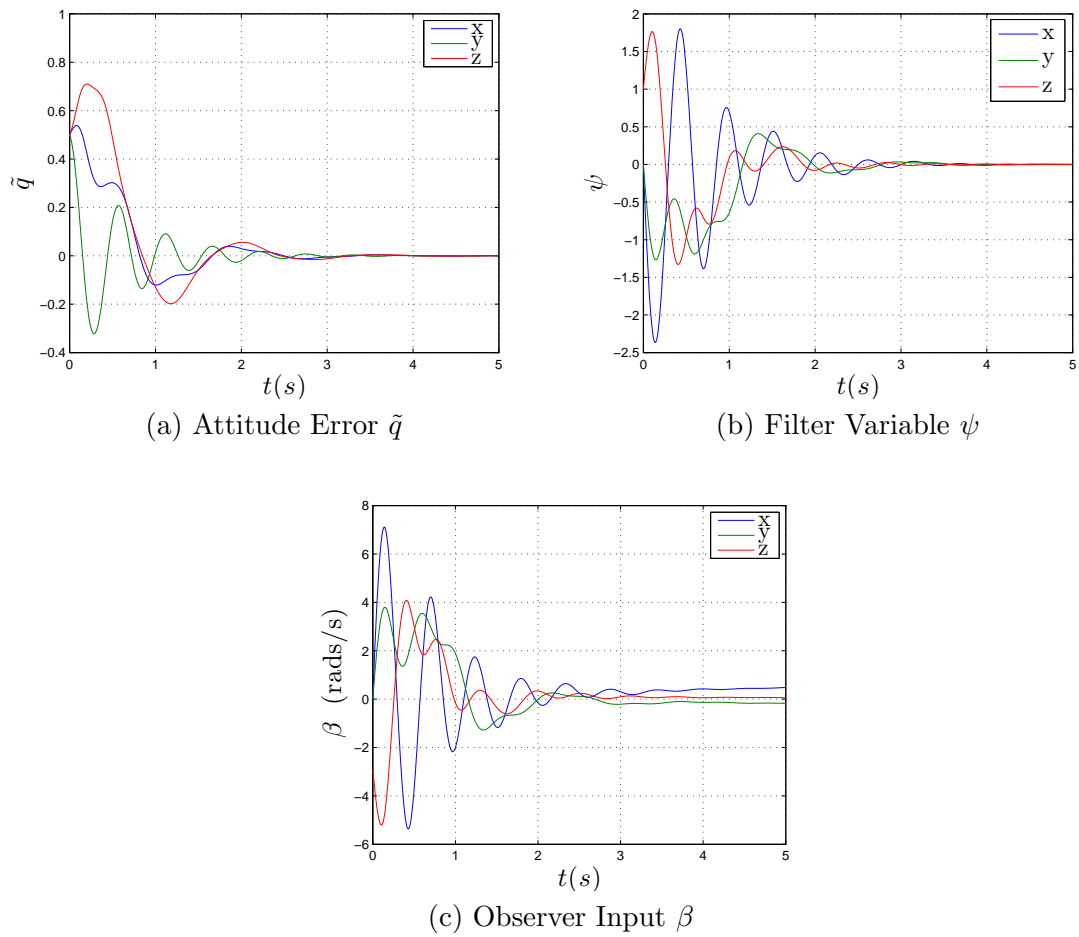


Figure 3.3: Simulation Results for Filtered-Vector-Measurement-Based Attitude Observer

3.4.3 Attitude Observer Using IMU and GPS Measurements

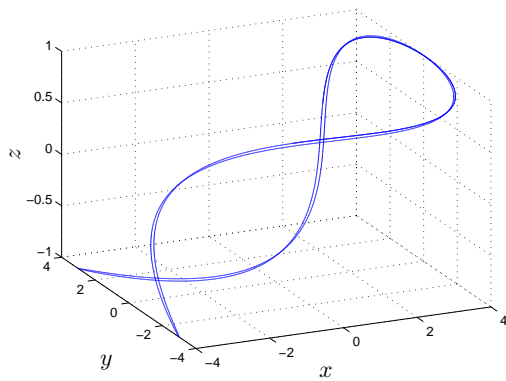
Simulations were performed to test the performance of the two proposed attitude observers. For both simulations the trajectory of the rigid-body position was specified as $p(t) = (4 \sin(0.5t + 0.5), 3 \sin(1.25t + 0.5), \sin(0.5t + 0.5)) m$, from which the rigid-body velocity v and apparent acceleration r_2 were obtained. The angular velocity of the rigid body was chosen as $\omega = (\sin(0.1t), 0.2 \sin(0.2t + \pi), 0.1 \sin(0.3t + \pi/3)) rad/s$. The inertial-referenced ambient magnetic field vector was chosen as $r_1 = [0.05, 0, 0.5]^T$. Figures (3.5a)-(3.5c) give the simulation results for the first observer, and (3.6a)-(3.6d) give the results for the second observer.

The following initial conditions were used for both simulations: $\hat{v}(t_0) = [0, 1, 0]^T$, $\hat{\eta}(t_0) = 1$, $\hat{q} = [0, 0, 0]^T$, $\eta(t_0) = 0$ and $q(t_0) = [1, 0, 0]^T$. This choice corresponds to a value of the attitude error $\tilde{\eta} = 0$ and $\tilde{q} = [1, 0, 0]^T$, which is the worst case scenario where the stability of the proposed observers is not guaranteed according to our proof. This initial conditions have been selected on purpose to show that the proposed observers did not fail even in this extreme case.

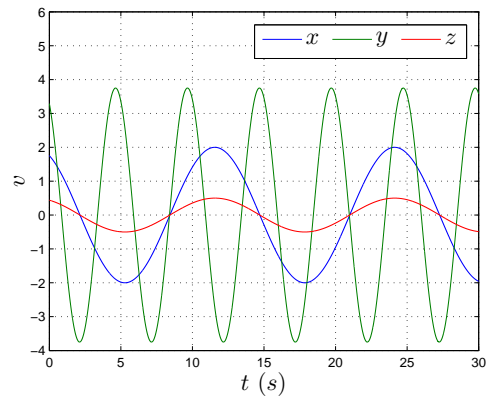
The following gains were used for observer 1: $k_1 = \gamma_1 = \gamma_2 = 10$. For the second observer the following gains were used: $k_1 = \gamma_1 = \gamma_2 = 10$, $k_2 = k_3 = 2$ and $k_4 = 1$. The gains k_5 and k_6 were chosen to satisfy (3.50).

3.4.4 Comparison of Attitude Observers

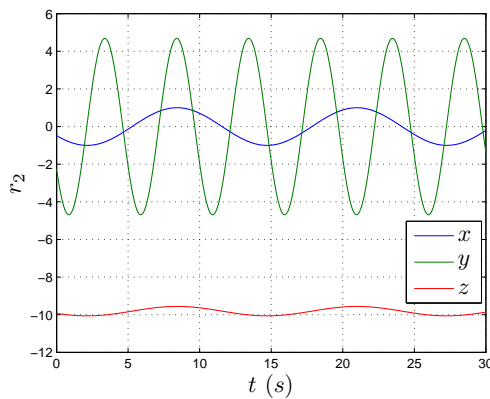
In addition to the simulations previously presented, additional simulations have also been performed in order to determine the performance of the proposed attitude observers in the presence of noise and disturbances. For each simulation it is assumed that a magnetometer and an accelerometer are used to provide the only two vector



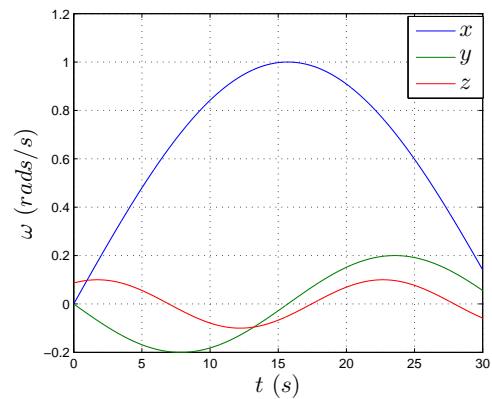
(a) 3D Trajectory Plot of Rigid-Body Position



(b) System Velocity $v(t)$ (m/s)



(c) System Apparent Accel. $r_2(t)$ (m/s^2)



(d) System Angular Velocity $\omega(t)$ ($rads/s$)

Figure 3.4: Translational Dynamics and Angular Velocity Used For Simulation for IMU and GPS Based Attitude Observer

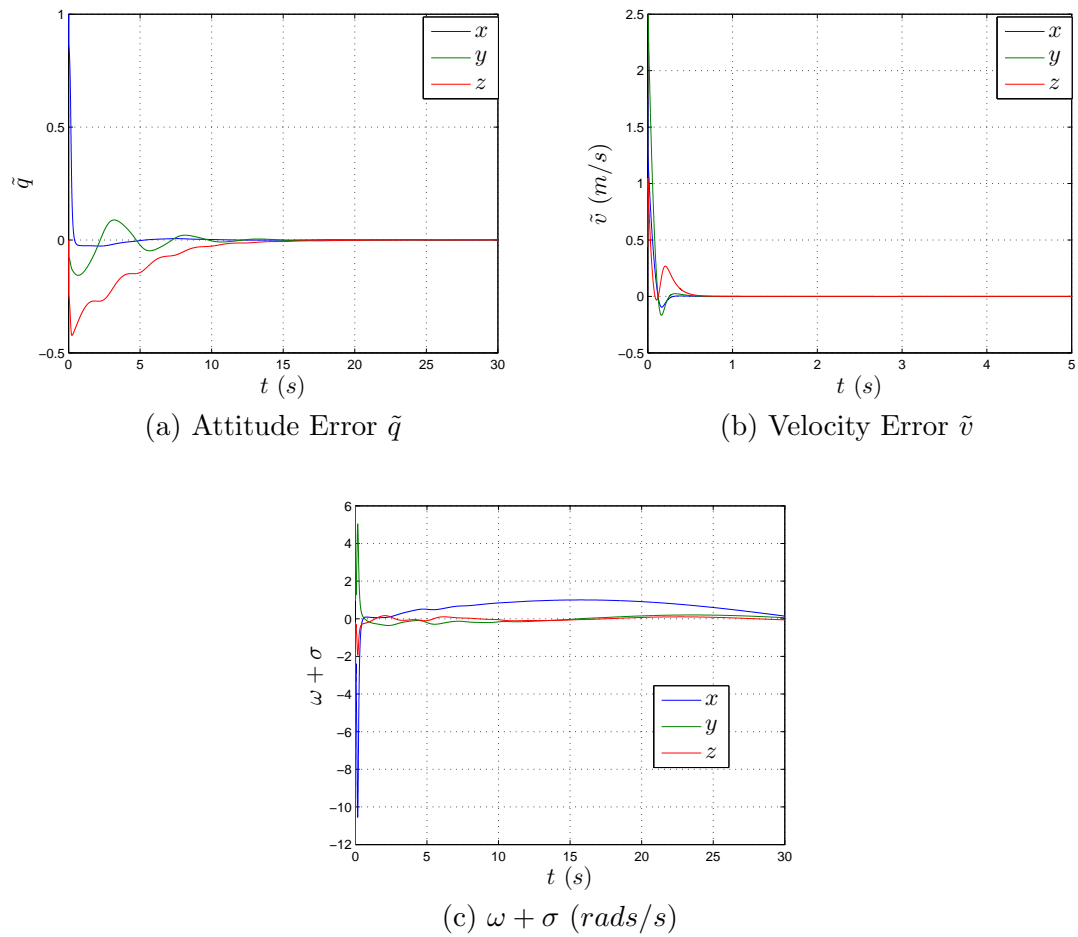


Figure 3.5: Simulation Results for Second Order IMU/GPS Based Attitude Observer

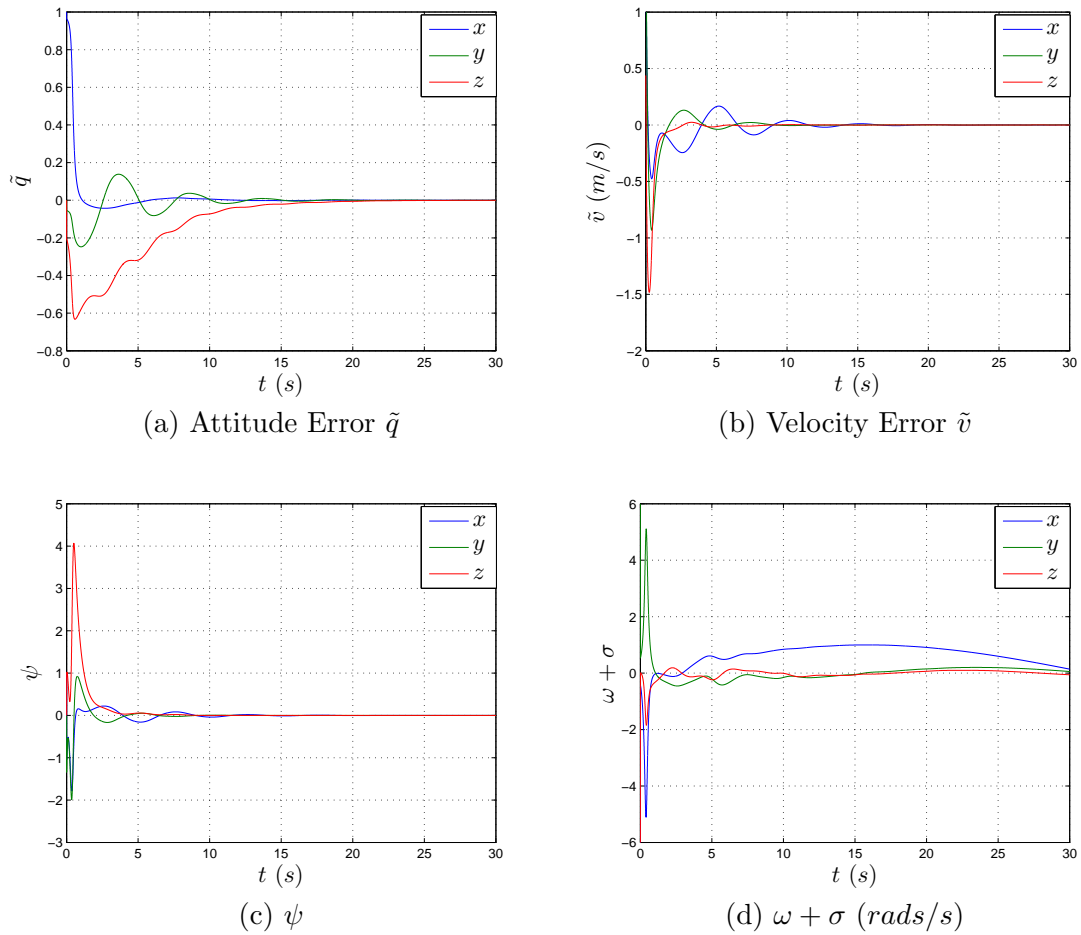


Figure 3.6: Simulation Results for Third Order IMU/GPS Based Attitude Observer

measurements (which is often the case). In order to determine the effect of rigid-body accelerations on the performance of attitude estimates (since the accelerometer is used), the simulation also considered accelerations of the rigid-body. A plot of the rigid-body position trajectory which was used in the simulation is given by Figure 3.7. The rigid-body position was chosen in such a manner that the rigid-body experienced a time-interval of zero-acceleration, followed by a short period of significant accelerations (for instance, when the rigid-body makes a turn). The resulting inertial-referenced apparent acceleration vector r_2 is shown in Figure 3.8.

The angular velocity for the rigid-body used for the simulation was chosen to be $\omega = [\sin(0.1t), 0.2 \sin(0.2t + \pi), 0.1 \sin(0.3t + \pi/3)]^\top$.

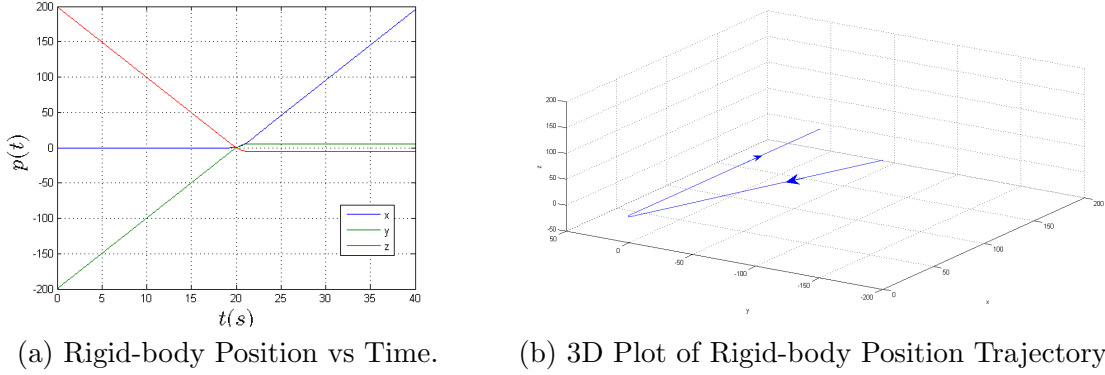


Figure 3.7: Rigid-body position for comparison simulation.

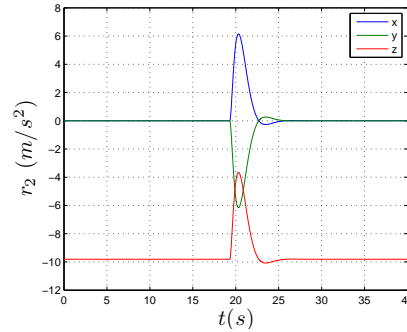


Figure 3.8: Inertial-referenced apparent acceleration of rigid-body.

To further demonstrate the effectiveness of the proposed observers, noise and other sensor inaccuracies were included in the comparison simulation. We assumed the gyroscope sensor has a constant bias of $\omega_b = [0.1, 0.05, -0.2] \text{ deg/s}$. Zero-mean Gaussian noise was also injected into the accelerometer, magnetometer, gyroscope and GPS velocity measurements. Since GPS sensors can often have low-sampling rates, we also assumed that the GPS sensor operated with a sampling rate of $5Hz$ and had a time-delay of $0.1s$. These values for sampling rate and time-delay are quite conservative and there does exist sensors which offer superior performance, for exam-

ple the NovAtel OEM615 GPS receiver. However, we chose these non-ideal values in order to demonstrate the robustness of the proposed observers. Table 3.1 lists the standard deviation values used to model the noise on each sensor, and Figure 3.9 shows examples of the sensor outputs including the effect of noise and disturbances.

Sensor Noise Standard Deviation			
Accelerometer	Magnetometer	Gyroscope	GPS
1 m/s^2	0.1 G	0.05 rad/s	0.1 m/s

Table 3.1: Sensor Noise Standard Deviation Values

In order to compare the results associated with the different observers, for each simulation the observers were initialized with the initial condition $\hat{Q}(t_0) = [1, 0, 0, 0]^T$, and the same initial condition for the actual attitude was used, which was specified to be $Q(t_0) = [0.5, 0.6124, 0.6124, 0]^T$. For the complementary filter the bias estimate was initialized using $\hat{\omega}_b = [0, 0, 0]^T$. For the two IMU/GPS based observers the initial condition $\hat{v}(t_0) = [0, 1, 0]^T$ was used, and for the third-order IMU/GPS based observer the initial condition $\psi(t_0) = [1, 0, 0]^T$ was used.

When tuning each observer, in general the gains were chosen to be as low as possible in order to avoid amplifying the sensor noise. The gains used for the complementary filter were chosen to be $\Gamma_1 = \Gamma_2 = 30I_{3 \times 3}$ where the gains for the vector measurement based observer were chosen as $\gamma_1 = \gamma_2 = 0.01$. The wide range of gains between these two observers was due to the slow convergence of the complementary filter. For the filtered-vector measurement based observer the gain $\alpha = 20$ was used. For the second order IMU/GPS based observer the gains were chosen as $k_1 = 2$ and $\gamma_1 = \gamma_2 = 0.01$. For the third order IMU/GPS based observer the gains were chosen to be $\gamma_r = 1$, $k_1 = 2$, $k_2 = 0.02$, $k_3 = 0.02$, $k_4 = 0.01$ and the gains k_5 and k_6 were chosen to satisfy (3.50).

Figure 3.10 shows the norm of the attitude error (vector part of the quaternion

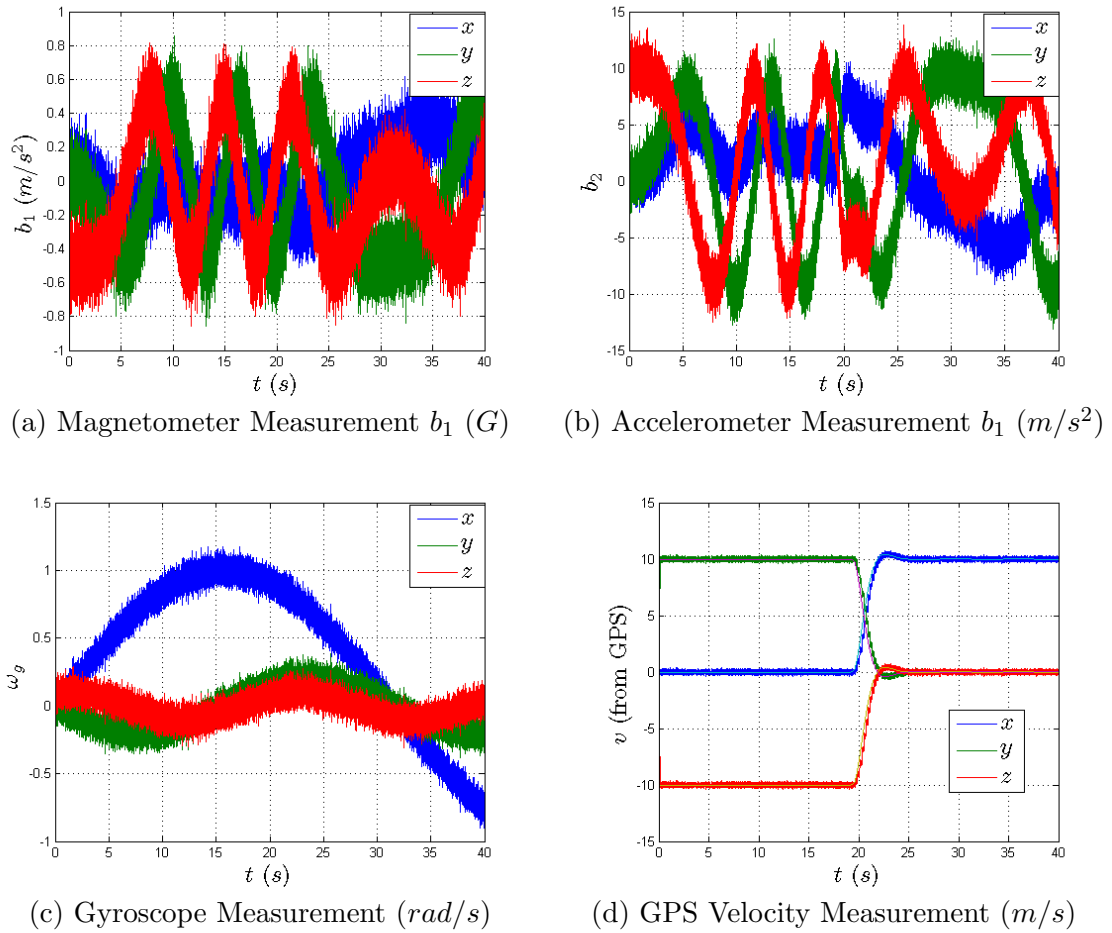


Figure 3.9: Plots for Sensor Outputs (including noise and disturbances)

\tilde{Q}) for the complementary filter, vector measurement based observer, and the filtered-vector-measurement based observer. The plots suggests that the performance of the complementary filter is dramatically affected by the noise and other disturbances, while the two vector-measurement based observers performed quite well in recovering an accurate estimate of the rigid-body attitude. The plots also demonstrate the ability of the two vector-measurement based observers to attenuate or reject noise. However, the vector-measurement based observers experienced a significant increase in the attitude error at the approximate time $t = 20s$, which we can see from Figure 3.8

is the time when the rigid-body is accelerating. In this case, the observer estimation error is increased significantly since the accelerometer is assumed to measure only the forces due to gravity and not forces due to linear acceleration.

Figure 3.11 shows the norm of the attitude error (vector part of the quaternion \tilde{Q}) for the filtered-vector-measurement based observer (also included in previous plot) and the two IMU/GPS Based Observers. As expected, the plots show the two IMU/GPS based observers demonstrate a significant improvement in performance during the time interval where the rigid-body is accelerating. The plots show a small increase in the attitude error for the IMU/Based observers during the period of accelerations, which is due to the simulated values for time-delay and sampling time for the GPS sensor. In fact, by decreasing the values for sampling time and time-delay, the attitude error associated with the GPS/IMU observers would improve considerably.

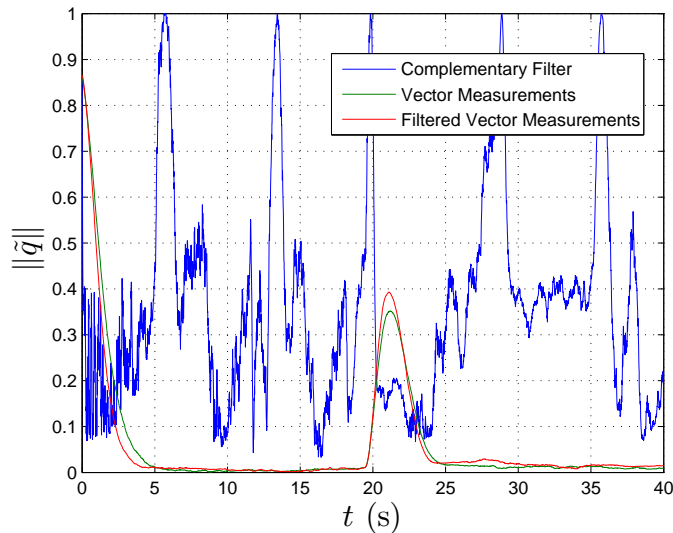


Figure 3.10: Comparison Simulation Results for Complementary Filter and Vector-Measurement Based Observers

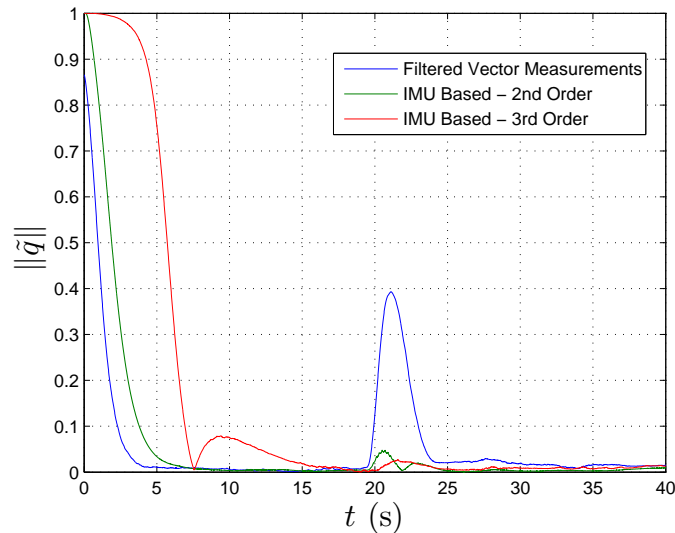


Figure 3.11: Comparison Simulation Results for Filtered-Vector-Measurement Based Observer and IMU/GPS Based Observers

3.5 Concluding Remarks

In this chapter we proposed several attitude estimation and reconstruction strategies. In one way or another, all of the proposed methods require the use of vector measurements. The attitude reconstruction algorithms offer closed form-solutions for the orientation of a rigid-body by using one or more vector measurements. In the case where a single vector measurement is available, to the best of our knowledge it is not possible to reconstruct (in closed-form) the orientation of a rigid-body¹. Therefore, the solution provided in Section 3.1.1 does not necessarily fully describe the orientation of a rigid-body. However, this result is still useful, especially in the position control of VTOL UAVs, which is discussed later in Section 4.3.

1. Although we are currently unaware of any solutions for the single-vector attitude reconstruction problem (closed-form solutions), there does exist attitude *observers* which can yield estimates of rigid-body attitude using only a single vector measurement. This problem has been solved, for example see Mahony et al. (2009), by assuming the system body-referenced angular velocity is *persistently excited* in order to fully recover the attitude of the rigid-body.

In most situations involving the attitude estimation of mobile robotics, the magnetometer and accelerometer sensors have been used to provide vector measurements, in order to provide body-frame coordinates of the Earth's magnetic field and gravity vectors, respectively. However, since the accelerometer also measures forces due to linear accelerations, that attitude reconstruction algorithms are thought to be more accurate at low frequencies (*i.e.*, when the system is not moving). Alternatively, the gyroscopes are considered to be accurate at higher frequencies, since problems associated with gyroscopic drift occurs due to a constant sensor bias (low frequency). This motivated the research community to combine the use of the attitude reconstructions and the integration of the gyroscope, in order to take advantage of the characteristics of each method (*i.e.*, frequency versus accuracy), which led to the introduction of the complementary filter, for example the observer (or filter) given in Section 3.2. However, in theory, the attitude estimates obtained from a complementary filter are shown to converge to the value obtained from the attitude reconstructions, and not necessarily to the actual attitude. Therefore, when using complementary filters, one must assume the system eventually comes to rest in order to guarantee asymptotic convergence of the estimates to the actual attitude.

Subsequently, new observers were also proposed which did not require the use of the attitude reconstruction algorithms. Instead, these new observers use the vector measurements directly in the attitude estimation laws, for example the observer given in Section 3.3.3. This observer was able to avoid the problem of unwinding, which negatively affected the complementary filter proposed in Section 3.2. However, the new vector measurement based observer is affected by an invariant manifold, which contains a set of trajectories which do not converge to one of the two desired equilibria. Fortunately, the invariance of this manifold can be broken, by increasing the order of the observer, for example the observer given in Section 3.3.4. Another

attractive characteristic of this result is that the vector measurements are applied to a low-pass filter as a part of the observer design, which is desirable in practice (*i.e.*, when the vector measurements are perturbed by noise). Unfortunately, these vector-measurement based attitude observers still depend on an assumption that the inertial vectors are known and constant in the inertial frame, which may be violated especially in the case where the accelerometer is used.

Control Scheme	Advantages	Disadvantages
Complementary Filter	<ul style="list-style-type: none"> • Gyroscope bias estimation. 	<ul style="list-style-type: none"> • Susceptible to unwinding. • Requires high gains. • Sensitive to disturbances and noise.
Observers using vector measurements	<ul style="list-style-type: none"> • Avoids unwinding. • Does not require reconstruction of attitude. 	<ul style="list-style-type: none"> • Affected by rigid-body linear accelerations.
Observer using filtered vector measurement	<ul style="list-style-type: none"> • Proves performance of observers which filter sensor data. 	<ul style="list-style-type: none"> • Higher order. • Trade off between noise rejection and rate of convergence. • Affected by rigid-body linear accelerations.
IMU/GPS Based Observers	<ul style="list-style-type: none"> • Greatly simplified proofs of performance (with respect to existing observers). • Allows the use of accelerometer in the presence of linear accelerations. 	<ul style="list-style-type: none"> • Dependant on linear velocity measurement.

Table 3.2: Comparison of Estimation Strategies

This problem has motivated the research community to use the accelerometer in a more realistic manner: to measure the body-referenced system apparent acceleration, which is a combination of gravity forces and forces due to linear acceleration of the rigid-body. This problem is complicated by the fact that we don't know the inertial-frame coordinates of the apparent acceleration vector (we only know body-

referenced coordinates as obtained by the accelerometer measurement). Instead, we rely on measurements of the system linear velocity which is intrinsically related to the apparent acceleration (*i.e.*, through an integral). Therefore, using the linear velocity measurements with a special filter, we obtain information about the apparent acceleration vector, which can be used with the accelerometer measurement to obtain information about the system attitude. In theory, we show these velocity-aided attitude observers given in Section 3.3.5 ensure that the attitude estimates converge asymptotically to the actual rigid-body attitude in a specified domain of attraction. This domain of attraction can be arbitrarily increased to contain almost any set, except in the case where the attitude estimates are rotated 180 degrees away from the actual system attitude. However, despite this limitation, simulation results show that the attitude estimates converge even for this worst case scenario and for any choice of the observer gains. Therefore, future work may involve showing stronger stability results for these observers.

Chapter 4

VTOL UAV Control Design

4.1 Introduction

In this chapter we consider the design and analysis of various control strategies which can be applied to the VTOL UAV system. Although there are a number of objectives that the research community has addressed in this area, they all can be divided into two categories: those which are designed to control only the rotational dynamics, and those designed to control the system translational dynamics (position, velocity). In the former case, this problem is more generally referred to as *rigid-body* attitude control, and can refer to several control objectives, for example forcing the system attitude to achieve the hover-configuration (*attitude stabilization*), forcing the system attitude to a desired orientation (*attitude regulation*), or forcing the rigid-body attitude to converge to a desired attitude trajectory (*attitude tracking*). To accomplish these objectives the system attitude is always assumed to be known, and in many cases the system angular velocity is required, although a number of researchers have been able to remove the requirement of the angular velocity. The attitude control laws typically assume that the orientation of the rigid-body is fully actuated by three orthogonal moments which are applied to the rotational system dynamics. Together these moments are commonly referred to as the *torque control-input*.

In Section 4.2 we propose a control strategy for the attitude stabilization problem. This control strategy is noteworthy since it does not require the knowledge

of the system angular velocity, and also does not require direct measurement of the system orientation. Rather, it uses vector measurements (which would normally be applied to an attitude estimation scheme) in order to develop the control laws. Previous angular-velocity-free attitude control strategies required the knowledge of the system attitude, which in practice is typically obtained using an attitude estimation scheme (for example the observers discussed in Section 3.3), which require the measurement of the system angular velocity. Therefore, this strategy may be the first *truly* angular-velocity-free attitude control law.

When considering the control of the system translational dynamics, typically, only a single additional control input is assumed to be available: the system thrust (generated by the system rotors or propellers), which is normally assumed to be directed along the body-referenced vertical axis. As a consequence of the limited number of available control inputs, the system translational dynamics are highly underactuated, and must be controlled by using the system orientation to manipulate the direction and magnitude of the *thrust-vector* (the body-referenced vertical thrust vector expressed inertial frame coordinates). Therefore, the control of the translational dynamics also require some form of attitude control in order to satisfy the objectives. There are a number of objectives involving the control of VTOL UAV translational dynamics, perhaps the most common being position regulation or position tracking, which aim to force the system position to a constant desired position, or to a desired position trajectory, respectively. This is the focus of Section 4.3.

A necessary step for the position control problem is to obtain a method to extract the magnitude and direction of the thrust from a given desired linear acceleration (which achieves the position control objectives). Since this desired orientation is dependant on a single vector (*i.e.*, the vector which describes the desired acceleration), we extend the results obtained for the extraction algorithm proposed in Section

3.1.1 for the position control problem, which is given in Section 4.3.1.1. The attitude extraction algorithm that is presented requires some mild assumptions on the desired acceleration. In order to ensure that these assumptions are satisfied, we specify the virtual control law for the desired acceleration using expressions which are bounded *a priori*. This is the purpose of the bounded functions defined in Section 2.3.2. Relying on the thrust and attitude extraction method, we derive two adaptive position tracking controllers in Section 4.3.2, which are shown to satisfy the position tracking objective, even in the presence of constant disturbance forces and torques which are applied to the system. Both controllers use a projection based adaptive mechanism to avoid the singularity in the attitude extraction. The first proposed controller, given in Section 4.3.2.4, achieves the position-tracking objective for any initial condition of the state, whereas the second controller, given in Section 4.3.2.5, achieves the position-tracking objective for a set of initial conditions which are dependant on the control gains. The latter controller is included, since it is less complicated than the prior case and may be more suitable to use in practice. During the process of developing the control laws, the disturbance forces are assumed to be constant in the inertial frame. In this case, both control laws are proven to achieve the position-tracking objective provided that an upper bound of the disturbance force is known a priori (although the actual magnitude of this disturbance force may be less than this limit). To evaluate the robustness the proposed controller when the disturbance force is not constant, simulation results are provided, which considers a model of the aerodynamic forces that are exerted on the system in the presence of a uniform external wind, which is assumed to have a constant velocity.

The adaptive position tracking controllers which are discussed require that several system states are measured or known (for example, the system position, velocity and angular velocity), in addition to the system attitude. However, the system ori-

entation is likely provided using some attitude estimation scheme which is dependant on a set of vector measurements. Unfortunately, the existing position control laws (including the ones mentioned above) do not consider the estimation scheme as a component of the system, which may lead to unexpected system performance due to unmodeled dynamics and other errors associated with the estimation scheme. To address this problem, in Section 4.3.3 we propose a new type of position tracking control law which does not require direct measurement of the system attitude. Instead (similar to the attitude stabilization controller described above), we use the vector measurements directly in the control scheme, and therefore an attitude observer is no longer required.

In the case where a vector measurement is provided using the accelerometer, the above position controller may not be applicable since the accelerometer also measures forces due to system linear acceleration (in addition to the gravity vector). However, in Section 4.3.4 we discuss a new type of position controller which uses the accelerometer to measure the system apparent acceleration instead of only the gravity vector. Consequently, this position controller may be better suited for position control of VTOL UAVs, which are likely to be subjected to linear accelerations.

To aid in the development of the control laws, we first recall the two frames \mathcal{I} and \mathcal{B} , and let Q and $R = R(Q)$ denote the unit-quaternion and rotation matrix, respectively, which describes the orientation of \mathcal{B} with respect to \mathcal{I} (orientation of aircraft). In the case where the control laws are derived using vector measurements (where we assume that R and Q are unknown), we denote the inertial vectors r_i , $i = 1, 2, \dots, n$, which are measured in \mathcal{B} to yield $b_i = Rr_i$. In the case where the magnetometer and accelerometer are specifically used, we let r_1 denote the ambient magnetic field, and let r_2 denote the apparent acceleration of \mathcal{B} expressed in \mathcal{I} .

4.2 Vector Measurement Based Attitude Stabilization

In this section we consider an attitude stabilization control law which uses vector measurements. We assume that only vector measurements are available for feedback, and therefore the control law does not depend on the direct measurement of the system attitude or the body-referenced angular velocity. In terms of the attitude parameterizations, our objectives are satisfied by forcing the system orientation $R \rightarrow I_{3 \times 3}$, or in terms of unit-quaternion $Q \rightarrow (\pm 1, \mathbf{0})$. Recall the model given by (2.17)-(2.18), where we assume that the disturbance torque $\delta_r = 0$, which we restate again as follows

$$\dot{Q} = \frac{1}{2}Q \odot (0, \omega), \quad (4.1)$$

$$I_b \dot{\omega} = u - S(\omega)I_b \omega. \quad (4.2)$$

We assume there are $n \geq 2$ inertial vectors $r_i, i = 1, 2, \dots, n$, which provide the body-frame measurements $b_i = Rr_i$, where R is the rotation matrix which describes the orientation of \mathcal{B} . We let $\hat{Q} \in \mathbb{Q}$ denote an estimate of Q and define $\hat{R} = R(\hat{Q})$ as defined by (2.8). We define the *measurement estimates* $\hat{b}_i = \hat{R}r_i$, which are used to define the two functions $z_\gamma \in \mathbb{R}^3$ and $z_\rho \in \mathbb{R}^3$ given by

$$z_\gamma := \sum_{i=1}^n \gamma_i S(\hat{b}_i) b_i, \quad z_\rho := \sum_{i=1}^n \rho_i S(\hat{b}_i) r_i, \quad (4.3)$$

and we also define the two matrices

$$W := - \sum_{i=1}^n \gamma_i S(r_i)^2, \quad W_c := - \sum_{i=1}^n \rho_i S(r_i)^2. \quad (4.4)$$

Note that in the case where at least two vector measurements are non-collinear, the matrices W and W_c are positive definite, and their eigenvalues can be arbitrarily increased by increasing the parameters γ_i and ρ_i , respectively.

We consider the following control and estimation laws

$$\dot{\hat{Q}} = \frac{1}{2}\hat{Q} \odot (0, \beta), \quad (4.5)$$

$$\beta = -z_\gamma, \quad (4.6)$$

$$u = z_\gamma - z_\rho. \quad (4.7)$$

To represent the attitude error and vector measurement error functions, respectively, we use $\tilde{Q} \in \mathbb{Q}$ and $\tilde{b} \in \mathbb{R}^3$ where $\tilde{Q} = (\tilde{\eta}, \tilde{q}) = Q \odot \hat{Q}^{-1}$ and $\tilde{b}_i = \hat{b}_i - b_i$.

Theorem 4.1 (Tayebi et al. (2011)). *Consider the system defined by (4.1) where the control input u is defined by (4.7). Assume that there are at least two non-collinear vectors amongst the set of n vectors r_i . Then, all signals are bounded and $\lim_{t \rightarrow \infty} \omega = 0$. Furthermore, there exists k_c such that for all $\lambda_{\min}(W_c) > k_c$, $\lim_{t \rightarrow \infty} Q(t) = (\pm 1, \mathbf{0})$ for almost any initial conditions.*

Sketch of Proof (For a complete proof please see appendix B.3):

We consider the error function $\tilde{b}_i = \hat{b}_i - b_i$ and define the Lyapunov function candidate

$$\mathcal{V} = \frac{1}{2}\omega^\top I_b \omega + \frac{1}{2} \sum_{i=1}^n \left(\gamma_i \tilde{b}_i^\top \tilde{b}_i + \rho_i (b_i - r_i)^\top (b_i - r_i) \right), \quad (4.8)$$

which in light of the system dynamics and control laws has the time-derivative $\dot{\mathcal{V}} = -z_\gamma^\top z_\gamma \leq 0$. Using these facts, one can show $\lim_{t \rightarrow \infty} z_\rho = 0$, which corresponds to a set of equilibrium solutions characterized by $Q = (\pm 1, \mathbf{0})$ (desired equilibria) or $\tilde{Q} = (0, \pm v_c)$ where v_c are the unit-eigenvectors of the matrix W_c . To show that the

undesired equilibrium are unstable, we use the Chetaev function $\mathcal{V}_c = -\eta\delta$ where $\delta = q^\top I_b \omega$. Note that $\mathcal{V}_c = 0$ at the undesired equilibria. For an appropriate choice of the gains ρ_i , we show that $\mathcal{V}_c > 0$ and $\dot{\mathcal{V}}_c > 0$ in a neighborhood of $\mathcal{V}_c = 0$, which proves the undesired equilibria are unstable. \square

Remark 7. *This controller provides almost global stability since there exists a potentially invariant manifold $\Psi = \{(\tilde{\eta}, \delta) \in [-1, 1] \times \mathbb{R} \mid \tilde{\eta} = 0, \delta = 0\}$ which contains the undesired hyperbolic equilibria. However, the invariance of the manifold Ψ can be destroyed if there exists a time $t_1 \geq t_0$ such that $\delta(t_1) = q^\top(t_1)I_b\omega(t_1) \neq 0$, at which time the system trajectories diverge from this manifold and converge to the desired equilibria.*

4.3 Position Control of VTOL UAVs

4.3.1 Problem Formulation

In this section we consider objectives which involve the position control of VTOL UAVs. In this case, we recall from Section 2.2 the full VTOL UAV model, given by

$$\dot{p} = v, \quad (4.9)$$

$$\dot{v} = ge_3 - \frac{T}{m_b} R^\top e_3 + \delta_t, \quad (4.10)$$

$$\dot{Q} = \begin{bmatrix} -q^\top \\ \eta I_{3 \times 3} + S(q) \end{bmatrix} \omega, \quad (4.11)$$

$$I_b \dot{\omega} = -\omega \times I_b \omega + \delta_r + u, \quad (4.12)$$

where the thrust control input u_t is given by

$$u_t = T/m_b. \quad (4.13)$$

Using the model given by (4.9) through (4.12) our objective is to determine control laws for the system thrust control input u_t and control torque u to force the position p to track some desired reference trajectory, which we denote as $p_d \in \mathbb{R}^3$. We place some mild conditions on the desired trajectory p_d which is stated in the following assumption.

Assumption 4.1. *The second, third and fourth derivatives (with respect to time) of the reference trajectory p_d are uniformly continuous. Furthermore, there exists positive constants δ_r and δ_{rz} such that $\|\ddot{p}_d\| \leq \delta_r$ and $e_3^\top \ddot{p}_d < \delta_{rz} < g$.*

Given the reference trajectory p_d we define the following error signals

$$\tilde{p} = p - p_d, \quad \text{position error}, \quad (4.14)$$

$$\tilde{v} = v - \dot{p}_d, \quad \text{velocity error}. \quad (4.15)$$

As shown by (4.9)-(4.12), the system is underactuated, since there are only four control inputs (u_t, u). As expected for this type of system, the dynamics of the linear velocity v are actuated by system thrust input u_t and system attitude R . To clearly define this relationship we define the function

$$\mu = ge_3 - u_t R^\top e_3, \quad (4.16)$$

which is the acceleration of the system due to gravity and the system thrust expressed in the inertial frame, where we note that $\dot{v} = \mu + \delta_t$. In order to achieve the objectives

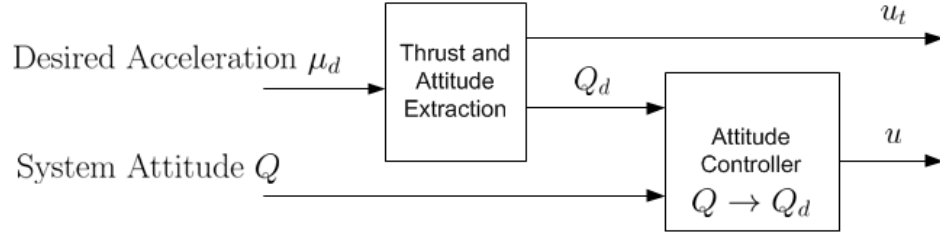


Figure 4.1: Attitude Extraction Algorithm for Position Control

of the position control law, we are forced to use the system attitude R , or Q , in order to control the system translational dynamics. Let $Q_d = (\eta_d, q_d) \in \mathbb{Q}$ denote the *desired orientation* (given in terms of the unit-quaternion) which satisfies the desired translational dynamics, and let $R_d = R(Q_d) \in SO(3)$ denote the corresponding rotation matrix as defined by (2.8). Then the desired value of μ , which we denote as μ_d , is defined as

$$\mu_d = ge_3 - u_t R_d^T e_3, \quad (4.17)$$

where we also define the error function

$$\tilde{\mu} = \mu - \mu_d. \quad (4.18)$$

The control strategy is based upon the following steps:

- (i) Find the expression for the virtual control law μ_d which satisfies the translational dynamics.
- (ii) Find the required system thrust u_t and desired system attitude R_d which satisfies (4.17).
- (iii) Develop a control law for the torque input u which forces $R \rightarrow R_d$.

Figure 4.1 provides a block-diagram for this procedure. The solution for the

desired attitude R_d which satisfies (4.17) is similar to the problem of the single-vector attitude extraction algorithm defined in Section 3.1.1. In the next section, we extend the previous results to the particular case involving the position control of a VTOL UAV system.

4.3.1.1 Attitude and Thrust Extraction

Given the virtual control law μ_d , we seek an expression for the unit-quaternion $Q_d = (\eta_d, q_d) \in \mathbb{Q}$, and the rotation matrix $R_d = R(Q_d) \in SO(3)$ which satisfies (4.17). Provided that some mild-conditions are satisfied regarding the virtual control input μ_d , a solution to this problem is proposed by the following lemma.

Lemma 5 (Roberts and Tayebi (2011a)). *Let $\mu_d = [\mu_{d1}, \mu_{d2}, \mu_{d3}] \in \mathbb{R}^3$, $Q_d = (\eta_d, q_d) \in \mathbb{Q}$ and $R_d = R(Q_d)$ as defined by (2.8). Then a solution for $u_t \in \mathbb{R}$ and Q_d which satisfies $\mu_d = ge_3 - u_t R_d^\top e_3$ is given by*

$$u_t = \|\mu_d - ge_3\|, \quad (4.19)$$

$$\eta_d = \left(\frac{1}{2} \left(1 + \frac{g - \mu_{d3}}{\|\mu_d - ge_3\|} \right) \right)^{1/2}, \quad (4.20)$$

$$q_d = \frac{1}{2\|\mu_d - ge_3\|\eta_d} S(\mu_d)e_3, \quad (4.21)$$

for all $\mu_d \in U$ where

$$U := \{\mu_d \in \mathbb{R}^3 \mid \mu_d = [0, 0, \mu_{d3}]^\top, \mu_{d3} < g\}. \quad (4.22)$$

Proof: Note that for all $\mu_d \in U$ the thrust control input is non-vanishing ($u_t > 0$). Therefore, in light (4.19), the expression for μ_d given by (4.17) is equivalent to $e_3 = R_d(ge_3 - \mu_d)/\|ge_3 - \mu_d\|$. This is equivalent to the problem addressed by Lemma 3 with $b = e_3$ and $r = (ge_3 - \mu_d)/\|ge_3 - \mu_d\|$, where we note that

$\|r\| = \|b\| = 1$. Provided that $\mu_d \in U$ it follows that $r \neq -b$ and therefore Lemma 3 can always be applied. Applying the expressions for r and b in (3.3) (3.4) leads to (4.20) and (4.21). \square

Remark 8. *The singularity associated with $\mu_d \notin U$ corresponds to the desired attitude being perfectly inverted (upside-down) such that the vertical acceleration of the vehicle is greater than or equal to the acceleration due to gravity. Note that the singularity only applies to the desired attitude Q_d , and the actual attitude of the system can take any value without ever encountering a singularity. Since the singularity corresponds to an un-desirable operating mode of the aircraft, avoiding this singularity does not significantly limit the normal operating mode of the system. Avoiding this singularity can be achieved by using a bounded law for the desired virtual acceleration μ_d .*

During the development of the control laws, it is necessary to find the *desired angular velocity* $\omega_d \in \mathbb{R}^3$ of the desired attitude Q_d and R_d , where

$$\dot{Q}_d = \frac{1}{2}Q_d \odot (0, \omega_d), \quad \dot{R}_d = -S(\omega_d)R_d. \quad (4.23)$$

To obtain an expression for ω_d in terms of the virtual control law μ_d and its time-derivative, in light of (2.14), we obtain

$$\omega_d = 2A(Q_d)^T \frac{d}{dt} \begin{bmatrix} \eta_d \\ q_d \end{bmatrix}. \quad (4.24)$$

By differentiating the expressions for η_d and q_d from (4.20) and (4.21), respectively, after some tedious albeit straightforward manipulations we eventually obtain

$$\omega_d = M(\mu_d)\dot{\mu}_d, \quad (4.25)$$

$$M(\mu_d) = \frac{1}{4\eta_d^2 u_t^4} \left(-4S(\mu_d)e_3e_3^\top + 4\eta_d^2 u_t S(e_3) \right. \\ \left. + 2S(\mu_d) - 2e_3^\top \mu_d S(e_3) \right) S(\mu_d - ge_3)^2. \quad (4.26)$$

In some cases we also require the time-derivative of the desired angular velocity ω_d . Therefore, we wish to obtain an expression for the partial-derivative of the matrix $M(\mu_d)$. Note that for $\mu_d \in U$, the function $M(\mu_d)$ is differentiable. To this end, we define the function $Z(\mu_d, v) : \mathbb{R}^3 \rightarrow \mathbb{R}^3$ where $v \in \mathbb{R}^3$ is an arbitrary vector, which is defined as

$$Z(\mu_d, v) := \frac{\partial}{\partial \mu_d} M(\mu_d) v = \gamma_m \left(\mu_d^\top v S(e_3) + S(e_3) \mu_d v^\top - e_3^\top v S(e_3) (2\mu_d \mu_d^\top / u_t \right. \\ \left. + (g + 2u_t) I - 2g\mu_d e_3^\top / u_t) + S(e_3) v e_3^\top (2u_t I_{3 \times 3} + (\mu_d - ge_3) (\mu_d - ge_3)^\top / u_t \right. \\ \left. + \mu_d (\mu_d - ge_3)^\top / u_t) - 2S(e_3) v (\mu_d - ge_3)^\top + S(v) \mu_d (\mu_d - ge_3)^\top / u_t + u_t S(v) \right) \\ - \gamma_m^2 \left(S(e_3) \mu_d \mu_d^\top + (g + 2u_t) S(\mu_d) e_3 e_3^\top - u_t S(\mu_d) \right. \\ \left. + \left(e_3^\top \mu_d u_t - 2\eta_d^2 u_t^2 \right) S(e_3) \right) v \left(-3u_t^2 e_3^\top + 3u_t (\mu_d - ge_3)^\top - 2e_3^\top S(\mu_d - ge_3)^2 \right),$$

where $\gamma_m = 1 / \left((u_t + e_3^\top (g - \mu_d)) u_t^2 \right)$.

Therefore, given a desired virtual control law for μ_d , the dynamics of extracted desired attitude can be specified using the functions given above.

4.3.2 Adaptive Position Tracking

In this section we propose an adaptive position tracking control law for VTOL UAVs, which requires that several system states are known or measured, including the linear position and velocity, system attitude, and angular velocity. In this case, we are able to estimate unknown disturbance forces and torques which are applied to the system.

The controller designed in this section is tailored for the ducted-fan VTOL

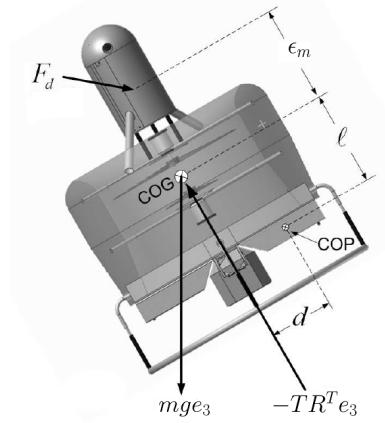


Figure 4.2: Ducted Fan Exogenous Forces

UAV. Although this control scheme can be applied for other VTOL UAV systems, we design this controller based upon a disturbance model which is more closely associated with the ducted fan system due to its geometrical properties. Recall the ducted fan uses a set of control surfaces located at the duct-exit in order to generate (body-referenced) horizontal forces, resulting in a torque-moment which is proportional to the distance from control surface center-of-pressure (COP) and the system COG. Figure 4.2 illustrates the ducted fan VTOL UAV which shows the horizontal and vertical distances, denoted as d and ℓ , respectively, from the control surface COP to the system COG. This figure also shows an external inertial-referenced force $F_d \in \mathbb{R}^3$ acting on the system. Due to the cylindrical symmetry of the ducted fan system, we assume F_d is applied at a point on the body-referenced z -axis which (denoted by $e_3 = [0, 0, 1]^T$), which is located at a distance of ϵ_m away from the system COG. Note that the force F_d and the lever-arm ϵ_m creates a disturbance torque about the system center of gravity.

The proposed adaptive control laws attempt to achieve the position tracking objective by estimating the external disturbance forces and torques which are applied to the system. For the case of the ducted fan VTOL UAV described above, the

disturbances δ_t and δ_r which are used with the model (4.10) and (4.12) are now given in terms of the disturbance force F_d by

$$\delta_t = 1/m_b F_d - 1/(m_b \ell) R^\top S(e_3)u, \quad \delta_r = \epsilon_m S(e_3) R F_d. \quad (4.27)$$

The term involving the control torque u in the new expression for δ_t is due to the horizontal-forces caused by the torque-generating control surfaces. These forces are an undesired side-effect of generating the control torque, and has been the focus of several researchers. For example, in Pflimlin et al. (2007) the authors use a change of coordinates which removes this coupling term provided that the system yaw-rate (angular velocity about the z-axis) is zero, which is not likely in the case of VTOL UAVs. In Olfati-Saber (2002) the authors propose another change of coordinates which removes the coupling term, but is only considered for a planar system. In light of the limitations of the proposed solutions this is still an open-problem, and therefore we place some restrictions on the strength of the coupling term.

Assumption 4.2. *The control torque lever arm ℓ is sufficiently large such that $m_b \ell \gg 1$, and therefore the coupling term $(m_b \ell)^{-1} R^\top S(e_3)u \approx 0$.*

To simplify notation we denote two unknown parameters $\theta_a, \theta_b \in \mathbb{R}^3$ which we define as

$$\theta_a := \frac{1}{m_b} F_d, \quad \theta_b := \epsilon_m F_d, \quad (4.28)$$

and therefore in light of Assumption (4.2) we find $\delta_t = \theta_a = 1/m_b F_d$ and $\delta_r = S(e_3) R \theta_b$. Although in general the disturbance force F_d exerted on the aircraft can be time-varying, for the purposes of developing the control laws we consider (for the time-being) that the disturbance force is constant in the inertial frame of reference

(for example this may be valid if the system is moving with a constant velocity in the presence of a constant and uniform wind).

Assumption 4.3. *The disturbances θ_a and θ_b are constant and there exists positive constants $\delta_a < g$ and δ_b such that the disturbances are contained, respectively, in the sets $B_a := \{\theta_a \in \mathbb{R}^3 \mid \|\theta_a\| < \delta_a < g\}$ and $B_b := \{\theta_b \in \mathbb{R}^3 \mid \|\theta_b\| < \delta_b\}$.*

The control design is based upon the attitude extraction algorithm given in Section 4.3.1.1. Using an expression for the virtual control law μ_d (to be defined later), we extract the desired attitude Q_d and system thrust u_t which satisfies the desired translational objectives. Since the control law is designed to force the actual attitude Q to the desired attitude Q_d , we require a description of the attitude error, which is given in Section 4.3.2.1. In Section 4.3.2.2 we give the time-derivatives of the error functions involved in the control design. Section (4.3.2.3) describes a projection algorithm proposed by Cai et al. (2006). This projection algorithm is required to ensure the virtual control law μ_d is bounded *a priori*, and therefore always satisfies $\mu_d \in U$ where the set U is given by (4.22). Finally, in Sections 4.3.2.4 and 4.3.2.5 we propose two adaptive position tracking control laws. The first position controller exhibits almost global stability when applied to the system. Although the second position control law is shown to have a smaller domain of attraction, we include this result since the expression for the torque control input is less complicated, and therefore may be more suitable for practical applications.

4.3.2.1 Attitude Error

Let $Q_d = (\eta_d, q_d) \in \mathbb{Q}$ denote the desired attitude which is obtained using the virtual control law μ_d using the attitude extraction algorithm defined by (4.20)-(4.21). To

define the *attitude error*, we let $\tilde{Q} = (\tilde{\eta}, \tilde{q}) \in \mathbb{Q}$, and let $\tilde{R} = R(\tilde{Q}) \in SO(3)$ denote the corresponding rotation matrix, which are given by

$$\tilde{Q} = Q_d^{-1} \odot Q, \quad \tilde{R} = R\hat{R}^\top, \quad \text{attitude error.} \quad (4.29)$$

To obtain the dynamics which govern the attitude error \tilde{Q} , we use a procedure similar to the one used in the proof of Proposition 1, to obtain

$$\dot{\tilde{Q}} = \frac{1}{2} \begin{bmatrix} -\tilde{q}^\top \\ \tilde{\eta}I + S(\tilde{q}) \end{bmatrix} (\omega - \tilde{R}\omega_d), \quad \dot{\tilde{R}} = -S(\omega - \tilde{R}\omega_d)\tilde{R} \quad (4.30)$$

In terms of the attitude error, forcing the system attitude to the desired value $R \rightarrow R_d$, is equivalent to forcing $\tilde{Q} \rightarrow (\pm 1, \mathbf{0})$.

4.3.2.2 Control Strategy

As a result of the above formulation the system error dynamics are given by

$$\dot{\tilde{p}} = \tilde{v}, \quad (4.31)$$

$$\dot{\tilde{v}} = \mu_d + \tilde{\mu} + \theta_a - \ddot{p}_d, \quad (4.32)$$

$$\dot{\tilde{Q}} = \frac{1}{2} \begin{bmatrix} -\tilde{q}^\top \\ \tilde{\eta}I + S(\tilde{q}) \end{bmatrix} (\beta - \tilde{R}\omega_d + \tilde{\omega}), \quad (4.33)$$

$$I_b \dot{\tilde{\omega}} = -S(\omega)I_b\omega + S(e_3)R\theta_b - I_b\dot{\beta} + u, \quad (4.34)$$

with $\tilde{\omega} = \omega - \beta$, where β is a virtual control law for the angular velocity that is defined later in the control design. More specifically, we find two virtual control laws $\beta = \beta_1$ for the first control law, and $\beta = \beta_2$ for the second control law. Based on this formulation our control strategy can be separated into four tasks:

1. Specify the virtual control law for the desired virtual acceleration μ_d that satisfies the position and velocity tracking objectives ($\tilde{p} \rightarrow 0, \tilde{v} \rightarrow 0$).
2. Using the expression for μ_d as defined by step 1, obtain the desired system thrust u_t and desired attitude Q_d and $R_d = R(Q_d)$ using the thrust and attitude extraction algorithm defined in Section 4.3.1.1.
3. Specify the virtual control law for the angular velocity β that forces the system attitude Q to track the desired system attitude Q_d specified in step 2, or equivalently to force $\tilde{Q} \rightarrow (\pm 1, \mathbf{0})$.
4. Specify the system control torque u to force the system angular velocity ω to track the desired angular velocity β , or equivalently to force $\tilde{\omega} \rightarrow 0$.

The first step of the control design is to choose the desired virtual acceleration μ_d . Based on the above formulation there are some requirements for this control law that must be considered:

- To ensure a solution always exists for the desired orientation, Q_d , the desired virtual acceleration μ_d must be bounded such that it is always contained within the set U defined by (4.22).
- From (4.32), one can see that in order to satisfy the tracking objective ($\tilde{p} \rightarrow 0, \tilde{v} \rightarrow 0$), the expression for the desired virtual acceleration μ_d must contain an (adaptive) estimate of the disturbance force. Let $\hat{\theta}_1 \in \mathbb{R}^3$ denote this estimate of the disturbance θ_a .
- Due to the use of backstepping, the expression for μ_d must be twice-differentiable.

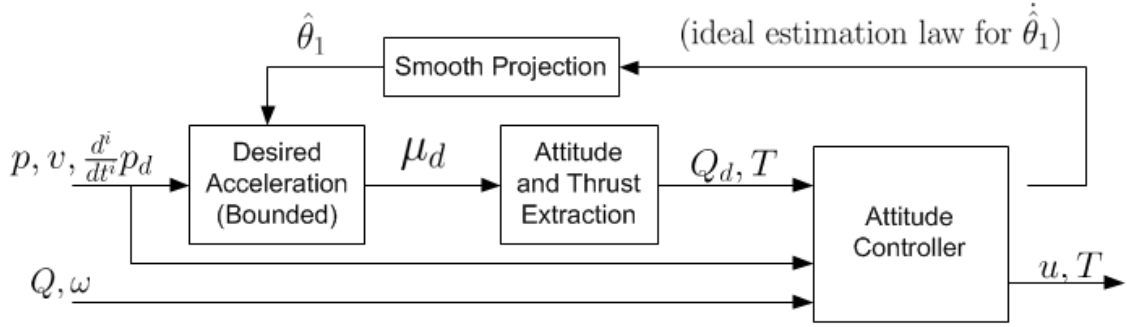


Figure 4.3: Block Diagram of the Position Tracking Controllers

In order to satisfy the first two requirements, the adaptive estimate $\hat{\theta}_1$ must be guaranteed to be bounded *a priori*. To meet this criteria, we use a *projection-based* estimation algorithm. The use of projection takes advantage of the known upper bound for the disturbance (*i.e.* $\|\theta_a\| \leq \delta_a$ as stated by Assumption 4.3), and subsequently ensures the adaptive estimate $\hat{\theta}_1$ remains bounded and close to this set. Furthermore, in order to satisfy the third requirement, the solution for the disturbance estimates obtained using the projection-based adaptation law must be twice differentiable. This motivates us to use the *sufficiently smooth projection* algorithm described by Cai et al. (2006). The use of other existing projection-based algorithms (for example see Ioannou and Sun (1996), Marino and Tomei (1998)) is not directly applicable since they are not always differentiable.

As shown in Cai et al. (2006), when utilizing projection, over-parameterization is required when the system is of a sufficiently high-order. For this reason we use two adaptive estimates $\hat{\theta}_1$ and $\hat{\theta}_2$, which are both estimates of the disturbance force θ_a . We use a third adaptive estimate $\hat{\theta}_3$ which is an estimate of the disturbance torque θ_b .

Figure 4.3 shows a block-diagram which highlights some of the key points involved in this control strategy.

4.3.2.3 Adaptive Estimation Using Projection

In this section we restate the projection algorithm described by Cai et al. (2006), which yields adaptive estimates whose trajectories are sufficiently smooth. The use of the projection algorithm allows us to use an adaptive estimate of the disturbance force in the expression of the desired virtual acceleration, μ_d , while ensuring μ_d remains in the set U defined by (4.22).

Consider a constant unknown parameter θ_p which belongs to the set $B_p := \{\theta_p \in \mathbb{R}^3 \mid \|\theta_p\| < \delta_p\}$, where the parameter δ_p is known *a priori*. Let $\hat{\theta}_p$ be the corresponding adaptive estimate of θ_p , and define the error $\tilde{\theta}_p = \theta_p - \hat{\theta}_p$. In general, the ideal adaptive estimation law is given by $\dot{\hat{\theta}}_p = \tau$, which does not necessarily guarantee that $\hat{\theta}_p \in B_p$. Based on the ideal adaptive estimation law, a projection-based adaptation law which guarantees the bound of $\hat{\theta}_p$ is given for our particular case by

$$\dot{\hat{\theta}}_p = \tau + \alpha(\hat{\theta}_p, \delta_p, \tau), \quad (4.35)$$

$$\alpha(\hat{\theta}_p, \delta_p, \tau) = -k_\alpha \eta_1 \eta_2 \hat{\theta}_p, \quad (4.36)$$

$$k_\alpha = \left(2 \left(\epsilon_\alpha^2 + 2\epsilon_\alpha \delta_p \right)^2 \delta_p^2 \right)^{-1}, \quad (4.37)$$

$$\eta_1 = \begin{cases} \left(\hat{\theta}_p^\top \hat{\theta}_p - \delta_p^2 \right)^2 & \text{if } \hat{\theta}_p^\top \hat{\theta}_p > \delta_p^2 \\ 0 & \text{otherwise} \end{cases}, \quad (4.38)$$

$$\eta_2 = \hat{\theta}_p^\top \tau + \left(\left(\hat{\theta}_p^\top \tau \right)^2 + \delta_\alpha^2 \right)^{1/2}, \quad (4.39)$$

where $\epsilon_\alpha > 0$, $\delta_\alpha > 0$, and has the properties

$$\|\hat{\theta}_p\| < \delta_p + \epsilon_\alpha, \quad \tilde{\theta}_p^\top \alpha \geq 0, \quad \dot{\hat{\theta}}_p \in C^1. \quad (4.40)$$

4.3.2.4 Controller 1

The next step in the control design is to specify a virtual control law for the desired acceleration μ_d which is guaranteed to be bounded *a priori* such that μ_d is guaranteed to be in the set U defined by (4.22). Using the bounded function $h(u)$ defined in section (2.3.2) we propose the following law for the desired virtual acceleration

$$\mu_d = \ddot{p}_d - \hat{\theta}_1 - k_p \Gamma_v^{-1} h(\tilde{p}) - (k_v + k_\theta) h(\tilde{v}), \quad (4.41)$$

where $k_p, k_\theta, k_v > 0$, $\Gamma_v = \Gamma_v^\top > 0$ and $e_3 = \text{col}[0, 0, 1]$. Using the parameters δ_{rz} and δ_a defined in Assumptions 4.1 and 4.3 we place the restriction

$$k_p \|e_3^\top \Gamma_v^{-1}\| + 2k_\theta + k_v + \epsilon_\alpha < g - \delta_{rz} - \delta_a, \quad (4.42)$$

where $\epsilon_\alpha > 0$ is a control gain used in the projection algorithm. Applying the value of the desired virtual acceleration (4.41) to the thrust and attitude extraction algorithm specified by (4.19)-(4.21) we extract the system thrust u_t and desired attitude Q_d from which we obtain $R_d = R(Q_d)$. Using the desired attitude Q_d , we obtain the attitude error $\tilde{Q} = (\tilde{\eta}, \tilde{q})$ as defined by (4.29). Using projection, we propose the

following estimation law for the first adaptive estimate:

$$\dot{\hat{\theta}}_1 = \gamma_{\theta_1} \left(\tau_2 + \alpha \left(\hat{\theta}_1, \delta_a + k_\theta, \tau_2 \right) \right), \quad (4.43)$$

$$\begin{aligned} \tau_2 = & \Gamma_v \tilde{v} + \frac{k_\theta}{\gamma_{\theta_1}} k_p \phi_h(\tilde{v}) \Gamma_v^{-1} h(\tilde{p}) + \frac{k_\theta k_v}{\gamma_{\theta_1}} \phi_h(\tilde{v}) h(\tilde{v}) \\ & + \left(\gamma_q (k_\theta + k_v) \phi_h(\tilde{v}) M(\mu_d)^\top - \frac{2u_t k_\theta}{\gamma_{\theta_1}} \phi_h(\tilde{v}) R^\top S(\bar{q}) \right) \tilde{q}, \end{aligned} \quad (4.44)$$

$$\bar{q} = (\tilde{\eta} I_{3 \times 3} - S(\tilde{q})) e_3, \quad (4.45)$$

where $\gamma_{\theta_1} > 0$, $\gamma_q > 0$, $\phi_h(u)$ is the partial derivative of $h(u)$ as defined by (2.28), and α is the projection function defined by (4.36). Let $\tilde{\omega} = \omega - \beta_1$, where we propose the following desired angular velocity virtual control law for β_1 :

$$\beta_1 = M(\mu_d) \left(p_d^{(3)} + w_\beta \right) - \frac{1}{\gamma_q} \Phi \tilde{v} - K_q \tilde{q}, \quad (4.46)$$

$$w_\beta = k_p k_v \phi_h(\tilde{v}) \Gamma_v^{-1} h(\tilde{p}) - \gamma_{\theta_1} \alpha \left(\hat{\theta}_1, \delta_a + k_\theta, \tau_2 \right) \quad (4.47)$$

$$\Phi = \left(\gamma_{\theta_1} \gamma_q M(\mu_d) - 2u_t S(\bar{q}) R \right) \Gamma_v + \gamma_q k_p M(\mu_d) \Gamma_v^{-1} \phi_h(\tilde{p}), \quad (4.48)$$

where $K_q = K_q^\top > 0$ and the matrix $M(\mu_d)$ is given by (4.26). In general, the derivative of (4.46) is given by

$$\dot{\beta}_1 = f_{\beta_1} + \bar{f}_{\beta_1} \theta_a, \quad (4.49)$$

where the actual expressions for f_{β_1} and \bar{f}_{β_1} are given in Appendix B.4.5. We propose the following control law for the system torque control input:

$$u = -\gamma_q \tilde{q} + S(\omega) I_b \omega - S(e_3) R \hat{\theta}_3 + I_b f_{\beta_1} + I_b \bar{f}_{\beta_1} \hat{\theta}_2 - K_\omega \tilde{\omega}, \quad (4.50)$$

where $K_\omega = K_\omega^\top > 0$, in addition to the following adaptation laws

$$\dot{\hat{\theta}}_2 = \gamma_{\theta_2} \left(-\bar{f}_{\beta_1}^\top I_b \tilde{\omega} + \alpha \left(\hat{\theta}_2, \delta_a, -\bar{f}_{\beta_1}^\top I_b \tilde{\omega} \right) \right), \quad (4.51)$$

$$\dot{\hat{\theta}}_3 = \gamma_{\theta_3} \left(-R^\top S(e_3) \tilde{\omega} + \alpha \left(\hat{\theta}_3, \delta_b, -R^\top S(e_3) \tilde{\omega} \right) \right), \quad (4.52)$$

where $\gamma_{\theta_{2,3}} > 0$ and $\delta_b > 0$ is the upper bound for $\|\theta_b\|$ as defined by Assumption (4.3).

Theorem 4.2 (Roberts and Tayebi (2011a)). *Consider the system described (4.31)-(4.34) using the control and estimation laws defined by (4.43) and (4.50)-(4.52), where we choose the control gains to satisfy (4.42) and*

$$\lambda_{\min}(K_q) > \frac{2\sqrt{2}k_v \bar{c}_t \underline{c}_t + 2\gamma_{\theta_1} \gamma_q (k_v + k_\theta)}{\underline{c}_t^2} + \frac{k_v^2}{2\epsilon_1}, \quad (4.53)$$

$$\lambda_{\min}(\Gamma_v) > \frac{\gamma_q k_v \epsilon_1}{\underline{c}_t}, \quad (4.54)$$

where $\epsilon_1 > 0$, $\bar{c}_t = g + \delta_r + \delta_a + k_p \|\Gamma_v^{-1}\| + k_v + 2k_\theta + \epsilon_\alpha$, and $\underline{c}_t = g - \delta_{rz} - \delta_a - k_p \|e_3^\top \Gamma_v^{-1}\| - k_v - 2k_\theta - \epsilon_\alpha$. Let Assumptions 4.1, 4.2 and 4.3 be satisfied. Then the system thrust input u_t is bounded and non-vanishing such that $0 < \underline{c}_t < u_t < \bar{c}_t$, the system states (p, v, ω) are bounded for all time and

$$\lim_{t \rightarrow \infty} [p(t) - p_d(t), v(t) - \dot{p}_d(t), \tilde{q}(t), \tilde{\omega}(t)] = \mathbf{0}, \quad (4.55)$$

for any initial condition. Furthermore, the adaptive estimates $\hat{\theta}_1, \hat{\theta}_2, \hat{\theta}_3$ are bounded, and in particular the estimate $\hat{\theta}_1$ converges asymptotically to the constant unknown disturbance θ_a .

Sketch of proof:

(For a complete proof please see appendix B.4 on page 167)

Note that the expression for μ_d is bounded *a priori*, due to the use of the function $h(\cdot)$, the bound of \ddot{p}_d given in Assumption 4.1, and the bound of $\hat{\theta}_1$ due to the use of the projection mechanism. Also, due to the gain restriction (4.42), we ensure $\mu_d \in U$ where U is the set defined by (4.22), which also ensures that the thrust is bounded and non-vanishing. We consider the following Lyapunov function candidate

$$\mathcal{V} = k_p \left(\sqrt{1 + \tilde{p}^\top \tilde{p}} - 1 \right) + \frac{1}{2} X^\top C X \quad (4.56)$$

where $X = \text{col}[\tilde{v}, 1 - \tilde{\eta}, \tilde{q}, \tilde{\omega}, \theta_a - k_\theta h(\tilde{v}) - \hat{\theta}_1, \theta_a - \hat{\theta}_2, \theta_b - \hat{\theta}_3]$, $C = \text{diag}[\Gamma_v, 4\gamma_q I_{4 \times 4}, I_b, \gamma_{\theta_1}^{-1} I, \gamma_{\theta_2}^{-1} I, \gamma_{\theta_3}^{-1} I]$, where $I = I_{3 \times 3}$ unless otherwise noted. In light of the control and estimation laws we find the time derivative of \mathcal{V} is bounded by

$$\dot{\mathcal{V}} \leq -\tilde{v}^\top \Delta_v h(\tilde{v}) - \gamma_q \tilde{q}^\top \Delta_q \tilde{q} - \frac{k_\theta}{\gamma_{\theta_1}} \tilde{\theta}_1^\top \phi_h(\tilde{v}) \tilde{\theta}_1 - \tilde{\omega}^\top K_\omega \tilde{\omega}, \quad (4.57)$$

where $\Delta_v = k_v(\Gamma_v - (\gamma_q k_v \epsilon_1)/\underline{c}_t^2 I_{3 \times 3})$ and $\Delta_q = K_q - (2\sqrt{2}k_v \bar{c}_t \underline{c}_t + 2\gamma_{\theta_1} \gamma_q (k_v + k_\theta))/\underline{c}_t^2 + k_v^2/(2\epsilon_1)$. Due to (4.54), the matrices Δ_v and Δ_q are positive definite. Due to the boundedness of $\ddot{\mathcal{V}}$ and $\ddot{\tilde{v}}$, one can show that the states are bounded and $(\tilde{v}, \tilde{q}, \tilde{\theta}_1, \tilde{\omega}) \rightarrow 0$, and since $\dot{\tilde{v}} \rightarrow 0$ then $\tilde{p} \rightarrow 0$. \square

4.3.2.5 Controller 2

In this section we propose a similar albeit simpler version of the control law described in Section 4.3.2.4. The motivation to simplify the previous result is largely due to the complexity of the virtual control law for the angular velocity, β_1 , from (4.46), and its derivative (4.49). It is possible to simplify this virtual control law, if an additional constraint is satisfied that is based on the initial conditions of the state and the control gains. This simplified version, which may be more suitable from a practical

perspective, is described below.

Using the previous law for the desired virtual acceleration from (4.41) under the restriction (4.42), and the extraction of the thrust control input u_t and desired attitude Q_d from (4.19)-(4.21), we obtain the attitude error $\tilde{Q} = (\tilde{\eta}, \tilde{q}) = Q_d^{-1} \odot Q$. Let $\hat{\theta}_1$ denote the first estimate of θ_a where we use the estimation law (4.43). We propose the following virtual control law for the angular velocity:

$$\beta_2 = M(\mu_d) \left(p_d^{(3)} + w_\beta \right) - K_q \tilde{q}, \quad (4.58)$$

where $K_q = K_q^\top > 0$, and w_β is given by (4.47). The derivative of β_2 can be written as

$$\dot{\beta}_2 = f_{\beta_2} + \bar{f}_{\beta_2} \theta_a, \quad (4.59)$$

where the actual expressions for f_{β_2} and \bar{f}_{β_2} are given in Appendix B.4.5. Using the angular velocity error $\tilde{\omega} = \omega - \beta_2$ we propose the following control law for the system control torque input:

$$u = -\gamma_q \tilde{q} + S(\omega) I_b \omega - S(e_3) R \hat{\theta}_3 + I_b f_{\beta_2} + I_b \bar{f}_{\beta_2} \hat{\theta}_2 - K_\omega \tilde{\omega} \quad (4.60)$$

where $K_\omega = K_\omega^\top > 0$. Using the new expression for angular velocity error $\tilde{\omega}$, we apply the adaptive estimation laws (4.51)-(4.52).

Theorem 4.3 (Roberts and Tayebi (2011a)). *Consider the system described (4.31)-(4.34) where we apply the control and estimation laws (4.43) and (4.60). Using the angular velocity error $\tilde{\omega} = \omega - \beta_2$ where β_2 is obtained using (4.58), we apply the estimation laws (4.51) and (4.52). Let Assumptions 4.1, 4.2 and 4.3 be satisfied, and*

assume the control gains are chosen to satisfy (4.42) in addition to

$$\lambda_{\min}(K_q) > \frac{2\sqrt{2}k_v\bar{c}_t\underline{c}_t + 2\gamma\theta_1\gamma_q(k_v + k_\theta)}{\underline{c}_t^2} + \frac{k_v^2}{2\epsilon_1} + \frac{\delta_1^2}{2\gamma_q\epsilon_2}, \quad (4.61)$$

$$\lambda_{\min}(\Gamma_v) > \frac{\gamma_q k_v \epsilon_1}{\underline{c}_t^2}, \quad (4.62)$$

$$\delta_1 = \left(2\bar{c}_t + \frac{\sqrt{2}\gamma_q\gamma\theta_1}{\underline{c}_t} \right) \|\Gamma_v\| + \frac{\sqrt{2}\gamma_q k_p}{\underline{c}_t} \|\Gamma_v^{-1}\|, \quad (4.63)$$

where $\bar{c}_t = g + \delta_r + \delta_a + k_p \|\Gamma_v^{-1}\| + k_v + 2k_\theta + \epsilon_\alpha$, and $\underline{c}_t = g - \delta_{rz} - \delta_a - k_p \|e_3^\top \Gamma_v^{-1}\| - k_v - 2k_\theta - \epsilon_\alpha$, $\epsilon_2 > 0$, then the system thrust input u_t is bounded and non-vanishing such that $0 < \underline{c}_t < u_t < \bar{c}_t$, the system states (p, v, ω) are bounded and

$$\lim_{t \rightarrow \infty} [p(t) - p_d(t), v(t) - \dot{p}_d(t), \tilde{q}(t), \tilde{\omega}(t)] = \mathbf{0}, \quad (4.64)$$

for all system initial conditions that satisfy

$$k_p \left(\sqrt{1 + \tilde{p}(0)^\top \tilde{p}(0)} - 1 \right) + \frac{1}{2} X(0)^\top \bar{C} X(0) < \lambda_{\min}(\Gamma_v) \left(\frac{2\|\Delta_v\|}{\epsilon_2} - \frac{1}{2} \right), \quad (4.65)$$

$$\Delta_v = k_v \left(\Gamma_v - \frac{\gamma_q k_v \epsilon_1}{\underline{c}_t^2} I \right), \quad (4.66)$$

$$X = \text{col} \left[\tilde{v}, 1 - \tilde{\eta}, \tilde{q}, \tilde{\omega}, \theta_a - k_\theta h(\tilde{v}) - \hat{\theta}_1, \theta_a - \hat{\theta}_2, \theta_b - \hat{\theta}_3 \right], \quad (4.67)$$

$$\bar{C} = \text{diag} \left[\|\Gamma_v\| I, 4\gamma_q I_{4 \times 4}, \|I_b\| I, \gamma_{\theta_1}^{-1} I, \gamma_{\theta_2}^{-1} I, \gamma_{\theta_3}^{-1} I \right]. \quad (4.68)$$

where $I = I_{3 \times 3}$ unless otherwise noted. Furthermore, the adaptive estimates $\hat{\theta}_1, \hat{\theta}_2, \hat{\theta}_3$ are bounded, and in particular the estimate $\hat{\theta}_1$ converges asymptotically to the constant unknown disturbance θ_a .

Sketch of Proof:

(For a complete version of the proof please see Appendix B.4.4 on page 173).

Similar to the proof of theorem 4.2, we first show that $\mu_d \in U$, and the thrust control input is bounded and non-vanishing. Using the same Lyapunov function candidate (4.56), we now find the time-derivative of \mathcal{V} to be given by

$$\dot{\mathcal{V}} \leq -\tilde{v}^\top \bar{\Delta}_v h(\tilde{v}) - \gamma_q \tilde{q}^\top \bar{\Delta}_q \tilde{q} - \frac{k_\theta}{\gamma_{\theta_1}} \tilde{\theta}_1^\top \phi_h(\tilde{v}) \tilde{\theta}_1 - \tilde{\omega}^\top K_\omega \tilde{\omega} \quad (4.69)$$

where $\bar{\Delta}_q = \gamma_q \Delta_q - \delta_1^2 / (2\epsilon_2) I_{3 \times 3}$ and $\bar{\Delta}_v = 1 / \sqrt{1 + \tilde{v}^\top \tilde{v}} \Delta_v - \epsilon_2 / 2 I_{3 \times 3}$. Therefore, we find $\bar{\Delta}_v > 0$ and $\dot{\mathcal{V}} \leq 0$ if $\|\tilde{v}\|^2 < 4/\epsilon_2^2 \|\Delta_v\|^2 - 1$. Since $\|\tilde{v}\|^2 \leq 2\mathcal{V} \lambda_{\min}(\Gamma_v)^{-1}$, we find for all initial conditions which satisfy (4.65), $\dot{\mathcal{V}}(t) \leq 0$ for all $t \geq t_0$. Barbalat's Lemma is then invoked to show $\dot{\mathcal{V}} \rightarrow 0$, $\dot{\tilde{v}} \rightarrow 0$ and therefore $\tilde{p} \rightarrow 0$. \square

Remark 9. For both adaptive controllers, there are two antipodal equilibrium solutions given by $(\tilde{p} = 0, \tilde{v} = 0, \tilde{\eta} = \pm 1, \tilde{q} = 0)$. The equilibrium solution characterized by $\tilde{\eta} = 1$ is stable, while the one characterized by $\tilde{\eta} = -1$ is unstable (repeller equilibrium), and therefore the equilibrium solution characterized by $(\tilde{p} = 0, \tilde{v} = 0, \tilde{\omega} = 0, \tilde{R} = 0)$ is homoclinic, and the unwinding phenomenon exists.

4.3.2.6 Implementation

To implement the controllers given in Sections (4.3.2.4) and (4.3.2.5) consider the following iterative procedure:

1. Obtain the signals p, v, Q, ω , and the desired reference trajectory p_d and $\frac{d^{(i)}}{dt^{(i)}} p_d$, $i = 2, 3, 4$, and calculate the error signals \tilde{p}, \tilde{v} .
2. Calculate the virtual control law μ_d using (4.41), which is used to obtain the system thrust input u_t from (4.19), desired attitude Q_d using (4.20) and (4.21), and the matrix $M(\mu_d)$ from (4.26).

3. Calculate the error signals \tilde{Q} and $\tilde{\mu}$ from (4.29) and (4.18), respectively, which is used to obtain τ_2 from (4.44) and $\dot{\hat{\theta}}_1$ from (4.43).
4. Using the virtual control law for the desired angular velocity (4.46) (or (4.58) for controller 2) calculate the angular velocity error $\tilde{\omega} = \omega - \beta_1$ ($\tilde{\omega} = \omega - \beta_2$ for controller 2).
5. Using the expression for the derivative $\dot{\beta}_1$ ($\dot{\beta}_2$ for the second control law) given by (B.88)-(B.89) ((B.86)-(B.87) for controller 2), apply the control law u from (4.50) (or (4.60) for controller 2), and the estimation laws $\dot{\hat{\theta}}_2$ and $\dot{\hat{\theta}}_3$ from (4.51) and (4.52), respectively.

4.3.3 Position Control Using Vector Measurements

Most of the existing position control laws described in the literature (including the control law described in the previous section) require that several system states are accurately known, including the system attitude. However, there does not exist a sensor (to our knowledge) that can directly measure the orientation of a rigid body¹. In reality, an attitude estimation scheme is typically used in order to obtain an estimate of the system attitude (for example the attitude estimation schemes described in Chapter 3). This may present a problem since, currently, there are no guarantees for the closed-loop system that couples an observer with a control law.

In light of this problem we are motivated to design a control scheme which does not assume that the system attitude is known, and also does not require the use of

1. There are sensor systems which use cameras and visual feedback in order to measure the orientation of a rigid-body. However, we exclude these solutions since they require the rigid-body, or VTOL UAV, to operate in a region viewed by the camera. We refer to the lack of a sensor which can measure the system orientation in environments where visual feedback is not available.

an attitude observer to provide estimates of the system attitude. One might recall from Chapter 3, that the attitude estimation schemes typically depend upon a set of vector measurements in order to recover the attitude of a rigid body. Instead of using these vector measurements with an attitude observer, we now incorporate the vector measurements directly in the control design, thereby eliminating the requirement for the measurement of the system attitude. For this particular problem, we assume that there are no external disturbances (forces or torques) that are exerted on the system. Therefore, considering the model defined by (4.10) and (4.12), we assume that the disturbances $\delta_t = 0$ and $\delta_r = 0$.

We consider a set of n inertial vectors r_i , $i = 1, 2, \dots, n$, which are known in the inertial frame \mathcal{I} , and are measured in the frame \mathcal{B} (which is rigidly attached to the system COG) to give $b_i = Rr_i$. In the design of the control laws we place some restrictions on the inertial vectors which are stated by the following assumption.

Assumption 4.4. *There are at least two non-collinear vectors r_i which are known and constant in the inertial frame \mathcal{I} .*

Since the vector measurements provide information (in some way) about the system attitude, they are involved later in the control design when we consider the system rotational dynamics. Before this step, we first must consider the desired translational dynamics of the system. Recall from Section 4.3.1 the virtual control law μ_d (desired linear acceleration), used to extract the system thrust u_t and desired system attitude Q_d , which we now choose as follows

$$\mu_d = \ddot{p}_d - \Gamma_v (k_p h(\tilde{p}) + k_v h(\tilde{v})), \quad (4.70)$$

where $\Gamma_v = \Gamma_v^T > 0$, $k_p, k_v > 0$ and $h(\cdot)$ is the bounded function defined by (2.27). Provided that the acceleration of the reference trajectory is bounded, (4.70)

is bounded *a priori*. To ensure that μ_d is contained within the set U (and therefore the extraction for the desired attitude exists) we wish to choose the gains such that $\|e_3^\top \mu_d\| < g$. In light of Assumption 4.1, we can place the following restriction

$$\delta_{pz} + (k_p + k_v) \|e_3^\top \Gamma_v\| < g, \quad (4.71)$$

which guarantees $\mu_d \in U$ and therefore the system thrust u_t and attitude Q_d can be obtained using (4.19)-(4.21). In light of (4.9)-(4.12), (4.14), (4.15) and (4.70) the dynamics of the position and velocity error are given by

$$\dot{\tilde{p}} = \tilde{v}, \quad \dot{\tilde{v}} = -k_p \Gamma_v h(\tilde{p}) - k_v \Gamma_v h(\tilde{v}) + \tilde{\mu}, \quad (4.72)$$

where $\tilde{\mu} = \mu - \mu_d$. Using the extraction method provided in Section 4.3.1.1 and the value of μ_d from (4.70) we obtain the required system thrust u_t and the desired attitude Q_d . Since Assumption 4.1 is satisfied, there exists a positive constant δ_p such that $\|\ddot{p}_d\| < \delta_p$. Furthermore, (4.19) and (4.71) ensures that the thrust is positive and bounded such that

$$0 < \underline{c}_t < u_t < \bar{c}_t, \quad (4.73)$$

where $\bar{c}_t = g + \delta_p + (k_p + k_v) \|\Gamma_v\|$ and $\underline{c}_t = g - \delta_{pz} - (k_p + k_v) \|e_3^\top \Gamma_v\|$. Also, due to the lower bound of the thrust specified by (4.73), the matrix $M(\mu_d)$ (which is used to calculate the desired angular velocity ω_d from (4.25)) has an upper-bound defined by

$$\|M(\mu_d)\| \leq \sqrt{2}/\underline{c}_t. \quad (4.74)$$

To obtain details on how to find this bound, the reader is referred to the proof of Theorem 4.2. Using the desired quaternion Q_d obtained using (4.20)-(4.21) we

obtain the corresponding desired rotation matrix $R_d = R(Q_d)$ from (2.8). Using the rotation matrix R_d and the n known inertial vectors r_i we define the *desired vector measurements* as

$$b_i^d = R_d r_i \quad i = 1, 2, \dots, n. \quad (4.75)$$

The *attitude error*, or the error between the actual and desired orientation, is defined using the unit-quaternion $\tilde{Q} = (\tilde{\eta}, \tilde{q})$ and rotation matrix \tilde{R} by $\tilde{Q} = Q \odot Q_d^{-1}$ and $\tilde{R} = R_d^T R$, which have the time derivatives

$$\begin{aligned} \dot{\tilde{Q}} &= \frac{1}{2} \begin{bmatrix} -\tilde{q}^T \\ \eta_e I_{3 \times 3} + S(\tilde{q}) \end{bmatrix} \omega_e, \quad \dot{\tilde{R}} = -S(\omega_e) \tilde{R}, \\ \omega_e &= R_d^T (\omega - \omega_d), \end{aligned} \quad (4.76)$$

where $\omega_d = M(\mu_d) \dot{\mu}_d$ is obtained using (4.25) and differentiating (4.70) (which is not exactly known since it depends on the system attitude (Q, R)). At this stage in the procedure, our objective is to force the actual system attitude to the desired attitude $R \rightarrow R_d$ using ω , which is equivalent to $\tilde{R} \rightarrow I_{3 \times 3}$ or $\tilde{Q} \rightarrow (\pm 1, 0)$. However, since ω is a state we define the virtual control law $\bar{\omega}$ that forces $R \rightarrow R_d$ and define the error $\tilde{\omega} = \omega - \bar{\omega}$ where we choose $\bar{\omega}$ to be

$$\bar{\omega} = M(\mu_d) f_{\mu_d} + \sum_{i=1}^n \gamma_i S(b_i^d) b_i, \quad (4.77)$$

where $f_{\mu_d} = p_d^{(3)} + k_p k_v \Gamma_v \phi_h(\tilde{v}) \Gamma_v h(\tilde{p}) - k_p \Gamma_v \phi_h(\tilde{p}) \tilde{v}$. The time derivative of $\bar{\omega}$ is

given by $\dot{\tilde{\omega}} = f_{\tilde{\omega}} + g_{\tilde{\omega}}e_{\mu}$ where

$$\begin{aligned}
f_{\tilde{\omega}} = & Z(\mu_d, f_{\mu_d}) \left(f_{\mu_d} + k_v^2 \Gamma_v \phi_h(\tilde{v}) \Gamma_v h(\tilde{v}) \right) + M(\mu_d) \left(p_d^{(4)} \right. \\
& + k_p k_v \Gamma_v \phi_h(\tilde{v}) \Gamma_v \phi_h(\tilde{p}) \tilde{v} - k_p k_v \Gamma_v f_{\phi}(\tilde{v}, \Gamma_v h(\tilde{p})) \Gamma_v (k_p h(\tilde{p}) + k_v h(\tilde{v})) \\
& \left. - k_p \Gamma_v f_{\phi}(\tilde{p}, \tilde{v}) \tilde{v} + k_p^2 \Gamma_v \phi_h(\tilde{p}) \Gamma_v h(\tilde{p}) + k_p k_v \Gamma_v \phi_h(\tilde{p}) \Gamma_v h(\tilde{v}) \right) \\
& + \left(\sum_{i=1}^n \gamma_i S(b_i^d) S(b_i) \right) \omega - \left(\sum_{i=1}^n \gamma_i S(b_i) S(b_i^d) \right) \left(M(\mu_d) f_{\mu_d} \right. \\
& \left. + k_v^2 M(\mu_d) \Gamma_v \phi_h(\tilde{v}) \Gamma_v h(\tilde{v}) \right), \tag{4.78}
\end{aligned}$$

$$\begin{aligned}
g_{\tilde{\omega}} = & -k_v Z(\mu_d, f_{\mu_d}) \Gamma_v \phi_h(\tilde{v}) + k_v \left(\sum_{i=1}^n \gamma_i S(b_i) S(b_i^d) \right) M(\mu_d) \Gamma_v \phi_h(\tilde{v}) \\
& - k_p M(\mu_d) \Gamma_v \phi_h(\tilde{p}) + k_p k_v M(\mu_d) \Gamma_v f_{\phi}(\tilde{v}, \Gamma_v h(\tilde{p})), \tag{4.79}
\end{aligned}$$

where $Z(\mu_d, v)$ is the function defined by (4.27). Finally, the proposed control torque input is defined as

$$u = S(\omega) I_b \omega + I_b f_{\tilde{\omega}} - K_{\omega} \tilde{\omega}, \tag{4.80}$$

where $K_{\omega} = K_{\omega}^{\top} > 0$.

Theorem 4.4 (Roberts and Tayebi (2011e)). *Consider the system defined by (4.9)-(4.12) where $\delta_t = \delta_r = 0$, the system thrust u_t is defined by (4.19) using the virtual control law (4.70) under the restriction (4.71), and the torque control input u is defined by (4.80). Let Assumptions 4.1 and 4.4 be satisfied. Then, for any initial condition $\tilde{\eta}(t_0) \neq 0^2$ there exists positive constants $\bar{\gamma}_i$, $i = 1, 2, \dots, n$, such that for $\gamma_i > \bar{\gamma}_i$ the system states \tilde{p} , \tilde{v} and $\tilde{\omega}$ are bounded and $\lim_{t \rightarrow \infty} [\tilde{p}(t), \tilde{v}(t), \tilde{\omega}(t)] = \mathbf{0}$.*

Sketch of Proof: (For a detailed proof the reader is referred to Appendix B.5)

2. This condition can be easily satisfied if the system is at rest at the time t_0 , i.e. $R(t_0) = I_{3 \times 3}$, since in this case $q = \mathbf{0}_{3 \times 1}$, $\eta = \pm 1$, and therefore $\tilde{\eta} = \pm \eta_d$. In this case, from (4.20) one can see that for any value of μ_d , $\inf_{\mu_d \in U} \{|\tilde{\eta}(t_0)|\} = \inf_{\mu_d \in U} \{|\eta_d(t_0)|\} = 1/\sqrt{2} > 0$.

Consider the Lyapunov function candidate

$$\mathcal{V} = k_p \left(\sqrt{1 + \|\tilde{p}\|^2} - 1 \right) + \frac{1}{2} \tilde{v}^\top \Gamma_v^{-1} \tilde{v} + \gamma_q \left(1 - \tilde{\eta}^2 \right) + \frac{1}{2} \tilde{\omega}^\top I_b \tilde{\omega}. \quad (4.81)$$

In light of the control law, we eventually find an upper-bound for the time derivative of \mathcal{V} . In order to show that $\dot{\mathcal{V}}(t) \leq 0$ for all $t \geq t_0$, we must show that there exists a positive constant $\tilde{\eta}^*$ such that $\tilde{\eta}(t) \geq \tilde{\eta}^*$ for all $t \geq t_0$ ($\tilde{\eta}$ does not vanish). To show that this fact is true, we define the function $J = \tilde{\eta}^2/2$. In light of the control law, we find the time-derivative of J is guaranteed to be non-decreasing (and therefore $|\tilde{\eta}|$ is non-decreasing) if $\tilde{\eta}$ is contained within the open-set $D := (\tilde{\eta}_\ell, \tilde{\eta}_u)$. We show that the upper and lower limits of D can be arbitrarily increased using the control gains such that $D \rightarrow (0, 1)$. Therefore, for all $\tilde{\eta}(t_0) \neq 0$, the control gains can be increased to ensure $\tilde{\eta}_\ell < \tilde{\eta}(t_0)$ and therefore $|\tilde{\eta}(t)|$ is always non-decreasing for all $t \geq t_0$, and $\tilde{\eta}^* = \inf |\tilde{\eta}(t)| > 0$ exists. Using this fact we then show that $\dot{\mathcal{V}}(t) \leq 0$ for all $t \geq t_0$. Applying Barbalat's Lemma we show that $(\tilde{p}, \tilde{v}, \tilde{q}, \tilde{\omega}) \rightarrow \mathbf{0}$ and $\tilde{\eta} \rightarrow \text{sgn}(\tilde{\eta}(t_0))$.

Remark 10. *This proposed control law has two clear advantages. First, since the vector measurements are used directly in the control law, it does not require the direct knowledge of the system attitude, and therefore does not require an attitude observer or other estimation scheme when implemented on a VTOL UAV. Second, we show that the quaternion scalar does not cross zero (i.e. $|\tilde{\eta}(t)| > 0$ for all $t \geq t_0$), and there are two asymptotically stable antipodal equilibria given by $(\tilde{p} = 0, \tilde{v} = 0, \tilde{\omega} = 0, \tilde{\eta} = \text{sgn}(\tilde{\eta}(t_0)), \tilde{q} = 0)$. Therefore, the problem of unwinding is avoided.*

Practical considerations for vector-measurement-based position controller: In many cases, two vector measurements are available which are obtained using a magnetometer (measures the earth's magnetic field in \mathcal{B}), and an accelerometer which is intended to measure the direction of the gravity vector in \mathcal{B} . However,

since the accelerometer measures forces due to system accelerations (in addition to the gravity force), this approximation is valid for *low-acceleration* conditions. Let b_2 denote the accelerometer output (we reserve the use of b_1 for the measurement of the magnetometer). A well-known model for the accelerometer is given by

$$b_2 = R(\dot{v} - ge_3). \quad (4.82)$$

In order to use the accelerometer to measure the gravity vector in \mathcal{B} we must assume $\|\dot{v}\| \leq \epsilon$ for some sufficiently small $\epsilon > 0$, and therefore

$$b_2 = Rr_2, \quad (4.83)$$

where r_2 is the approximated (inverted) gravity vector in the inertial frame, $r_2 \approx -ge_3$. Therefore, for the proposed controller to be applicable, the acceleration of the reference trajectory $\ddot{p}_d(t)$ and the desired acceleration μ_d (bounded a priori) should be chosen to satisfy the low-acceleration condition. Therefore, in light of (4.70), in the case where an accelerometer is used as a vector measurement we place the additional constraint

$$\delta_p + (k_p + k_v) \|\Gamma_v\| < \epsilon. \quad (4.84)$$

Therefore, for certain slowly-accelerating reference trajectories, by choosing sufficiently small control gains for k_p , k_v and Γ_v the proposed controller can be implemented in the case where an accelerometer is used as one of the vector measurements.

However, in practice it can be difficult to determine ϵ quantitatively. Therefore, in the case where the accelerometer is used, a better solution may involve using the accelerometer to measure the system apparent acceleration (rather than just the gravity vector). In fact, a vector-measurement based position control law, which uses

the accelerometer similar to the velocity-aided attitude observer discussed in Section 3.3.5, has been proposed which is discussed in the following section.

4.3.4 Position Regulation Using GPS and IMU

Measurements

In Section 4.3.3 we described a position control scheme which assumes that the system attitude cannot be measured. By using vector measurements directly in the control design procedure, this control scheme also eliminates the need for an attitude observer, thus reducing the complexity of the closed-loop system. However, the development of the control laws required that the inertial vectors r_i were constant and known in the inertial frame \mathcal{I} . In reality, it is difficult to find sensors that provide a measurement of vectors which meet these criteria. The most commonly used sensor set, typically referred to as an inertial measurement unit (IMU), contain an accelerometer and magnetometer, which are rigidly attached to the vehicle (body-frame \mathcal{B}). The magnetometer is used to provide a measurement of the ambient magnetic field (for example the Earth's magnetic field) which we assume is constant and known. In most applications, the accelerometer is used to measure the direction of the gravity vector in the body-frame. However, since the accelerometer actually measures the body-referenced *apparent acceleration* (which includes the gravity forces and forces due to linear accelerations), in these cases we must assume that the body-frame is non-accelerating, which may be an unrealistic assumption, especially for VTOL UAVs. The same can also be said for position-controllers which use attitude estimates from an attitude observer which assumes the accelerometer measures only the gravity vector.

One may recall, that this was also the motivation for the development of the

velocity-aided attitude observers (for example, the observers defined in Section 3.3.5), which use the accelerometer to measure the system apparent acceleration and therefore are better suited for applications where the system is subjected to significant linear accelerations. To achieve this result for the attitude estimation case, a special filter was derived which used the system linear velocity. This filter proved to be useful since the filtered version of the system velocity can be used to provide some information about the system attitude.

In the following sections, using the techniques described in the development of the attitude observers, we extend these concepts to the problem of position control of VTOL UAVs. Using an accelerometer to measure the system apparent acceleration, we design a position controller which uses the vector measurements directly, rather than using the orientation (which cannot be directly measured). The resulting position controller therefore does not require the use of an attitude observer when implemented on a VTOL UAV. Furthermore, the position controller is likely to yield improved performance when the system experiences forces due to linear acceleration, when compared with other position controllers which use estimates of the orientation that are obtained by assuming the accelerometer only measures the gravity vector.

Due to the complexity involved in the stability analysis, one drawback associated with the proposed control scheme, is that we assume the system angular velocity ω is available as a control input (and not the control torque u). Note that some other works have also used the angular velocity as a control input, for example Hua et al. (2009), where in this case we use a high-gain feedback for the control torque u in order to achieve the desired value of ω specified by the control law. In this case, the

truncated model is given by

$$\dot{p} = v, \quad (4.85)$$

$$\dot{v} = \mu + \delta_t, \quad \mu = ge_3 - u_t R^\top e_3, \quad (4.86)$$

$$\dot{Q} = \frac{1}{2} \begin{bmatrix} -q^\top \\ \eta I_{3 \times 3} + S(q) \end{bmatrix} \omega, \quad (4.87)$$

The system output is defined as $y = [p, v, b_1, b_2]^\top$ where b_2 is the signal obtained using an accelerometer, $b_1 = Rr_1$ is a signal obtained using a magnetometer, and r_1 is the magnetic field of the surrounding environment which is assumed to be known and constant. Note that the system attitude R (or Q) is not assumed to be a known output of the system. Due to the use of the VTOL UAV model, the description of the dynamics \dot{v} are no longer specified as a function of the apparent acceleration vector r_2 . However, using the definition of the accelerometer model given by

$$b_2 = R(\dot{v} - ge_3) = -u_t e_3 + R\delta_t = R(-u_t R^\top e_3 + \delta_t) = Rr_2, \quad (4.88)$$

one can find the expressions for the system velocity, and apparent acceleration also satisfy

$$\dot{v} = ge_3 + r_2, \quad r_2 = -u_t R^\top e_3 + \delta_t. \quad (4.89)$$

Note the proposed control strategy is not adaptive in nature. Therefore, one may question why we include the aerodynamic disturbance force δ_t in our system model. In fact, it is interesting to note this aerodynamic disturbance force is actually important in recovering the attitude of the system using the accelerometer and the linear velocity measurements. In situations where the VTOL UAV model (4.86) is used, and where the aerodynamic disturbance vector δ_t is assumed to be negligible

($\delta_t \approx 0$), then the accelerometer provides the measurement $b_2 = -u_t e_3$, which is the constant vector e_3 multiplied by the system thrust. In this case the use of the accelerometer seems trivial since its measurement is known a priori and does not contain any information about the system attitude. This fact is counter-intuitive, especially since the accelerometer has been typically used to provide the measurement of the gravity vector, or $b_2 = g R e_3$ in the case where $\dot{v} \approx 0$. Therefore, we see that for the VTOL UAV system, the assumption that the accelerometer measures only the gravity vector may be a dangerous assumption which may lead to unexpected performance, even in the case where $\dot{v} \approx 0$. In fact, it seems that the utility of the accelerometer measurements is related to the measurement of the vector δ_t since the accelerometer in reality measures $b_2 = -u_t e_3 + R \delta_t$, which is likely the reason why the use of the accelerometer has been effective in practice. For this reason we believe that it is important to include a model of the aerodynamic disturbances. Furthermore, these facts highlight some serious concerns for the use of the accelerometer to measure only the gravity vector, in applications involving VTOL UAVs.

Since we do not employ adaptive control for this problem, in light of the disturbance force δ_t we consider only the position regulation problem (and not position tracking). Therefore, we require that the desired position p_d is constant (or slowly varying). We also require some mild restrictions on the apparent acceleration vector r_2 .

Assumption 4.5. *There exists positive constants c_1 and c_2 such that $\|r_2\| \leq c_1$ and $\|\dot{r}_2\| \leq c_2$.*

Assumption 4.6. *Given two positive constants, γ_1 and γ_2 , there exists a positive*

constant $c_w(\gamma_1, \gamma_2)$ such that $c_w < \lambda_{\min}(W)$ where

$$W = -\gamma_1 S(r_1)^2 - \gamma_2 S(r_2)^2. \quad (4.90)$$

The second assumption is true if the apparent acceleration vector r_2 is non-vanishing and is not-collinear to the magnetic field vector r_1 . Note the case where $r_2 = \mathbf{0}$ implies that the system is in free-fall which is not a likely operating mode for this system. In addition to this assumption, we also require some conditions on the aerodynamic force vector δ_t .

Assumption 4.7 (Aerodynamic Forces). *In light of the fact that the disturbance force δ_t is due to aerodynamic forces exerted on the vehicle we make the following simplifying assumptions:*

- (a) *The aerodynamic disturbance δ_t is dissipative with respect to the system translational kinetic energy and satisfies $\delta_t^\top v \leq 0$.*
- (b) *The aerodynamic disturbance force δ_t is only dependant on the system translational velocity, and there exists a positive constant c_1 such that $\|\delta_t\| \leq c_1 \|v\|^2$.*
- (c) *There exists positive constants c_2 and c_3 such that $\|\dot{\delta}_t\| < c_2 + c_3 \|v\|^3$.*

To help justify Assumptions 4.7(a) and 4.7(b) we normally assume the system is operating in an environment where the exogenous airflow is negligible (no wind). Assumption 4.7(c) can be satisfied when the system geometry is sufficiently symmetrical such that the system aerodynamic forces do not significantly depend on the system orientation. Although this assumption may be reasonable for certain VTOL type

aircraft, for example the ducted-fan, this assumption may not be the case with certain systems, for example fixed wing aircraft, where the system aerodynamics depend largely on the orientation of the vehicle.

4.3.4.1 Position Controller

Similar to the design of the previous controllers, we rely on the thrust and attitude extraction algorithm defined in Section 4.3.1.1, which provides an expression for the system thrust u_t and desired attitude $Q_d \in \mathbb{Q}$ which corresponds to the desired linear acceleration μ_d . Given the desired position p_d we define the position error $\tilde{p} = p - p_d$. Using the position error and measurement of the system linear velocity, we specify the virtual control law for the desired acceleration μ_d as

$$\mu_d = -k_p h(\tilde{p}) - k_v h(v) \quad (4.91)$$

which is used to obtain the system thrust u_t and desired attitude $Q_d = (\eta_d, q_d) \in \mathbb{Q}$ using (4.19)-(4.21). The desired attitude given in the $SO(3)$ parametrization, denoted as $R_d = R(Q_d)$, is subsequently obtained using (2.8). To represent the relative orientation of the desired attitude Q_d with respect to the actual attitude Q , we let $\tilde{Q} = (\tilde{\eta}, \tilde{q}) \in \mathbb{Q}$ and $\tilde{R} = R(\tilde{Q}) \in SO(3)$ denote the *attitude error* which is defined by

$$\tilde{Q} = Q \odot Q_d^{-1}, \quad \tilde{R} = R(\tilde{Q}) = R_d^T R, \quad (4.92)$$

where Q_d is the unit quaternion obtained using (4.20) and (4.21). In light of \dot{Q} and \dot{Q}_d , as defined by (4.87) and (4.23), respectively, the time derivative of the attitude

error is found to be

$$\dot{\tilde{Q}} = \frac{1}{2} \begin{bmatrix} -\tilde{q}^\top \\ \tilde{\eta}I + S(\tilde{q}) \end{bmatrix} \tilde{\omega}, \quad \dot{\tilde{R}} = -S(\tilde{\omega})\tilde{R}, \quad (4.93)$$

$$\tilde{\omega} = R_d^\top (\omega - \omega_d), \quad (4.94)$$

where ω_d is the *desired angular velocity* of the desired attitude (R_d and Q_d) as defined by (4.25). One of the objectives of the control design is to force the system orientation to the desired attitude, or in terms of the rotation matrices, to force $R \rightarrow R_d$ (and therefore $\mu \rightarrow \mu_d$), in order to obtain the desired translational dynamics. As mentioned in Section 2.1, this corresponds to two possible solutions for the unit-quaternion which are given by $\tilde{Q} = (\pm 1, \mathbf{0})$.

Since the system attitude is not known, similar to the design of the velocity-aided attitude observers in Section 3.3.5, we use a new adaptive state vector $\hat{v} \in \mathbb{R}^3$ and define the error function $\tilde{v} = v - \hat{v}$. As demonstrated by the previous attitude observers, based upon a suitable adaptation law for \hat{v} , the use of the error function \tilde{v} can provide some information relating to the system unknown apparent acceleration vector r_2 . Since this vector is known in the body fixed frame (measured using an accelerometer to obtain $b_2 = Rr_2$), the error function \tilde{v} can be used with the accelerometer measurement to provide information related to the system attitude. After these steps, the remaining control design is focused on forcing the actual system attitude to the desired attitude using the control input ω .

The proposed control law is given as follows:

$$\omega = M(\mu_d) \left(f_{\mu_d} - k_v \phi(v) R_d^\top (b_2 + u_t e_3) \right) + \psi, \quad (4.95)$$

$$f_{\mu_d} = -k_p \phi(\tilde{p}) v + k_v \phi(v) (k_p h(\tilde{p}) + k_v h(v)), \quad (4.96)$$

$$\psi = \gamma_1 S(R_d r_1) b_1 + \gamma_2 k_1 S(R_d (v - \hat{v})) b_2, \quad (4.97)$$

$$\dot{\hat{v}} = g e_3 + R_d^\top b_2 + k_1 (v - \hat{v}) + \frac{1}{k_1} R_d^\top S(b_2) \psi, \quad (4.98)$$

where $k_1, \gamma_1, \gamma_2 > 0$, $M(\mu_d)$ is the function defined by (4.26), $\phi(\cdot)$ is the bounded function defined by (2.28), $u_t = \|\mu_d - g e_3\|$, $R_d = R(Q_d)$ and $Q_d = (\eta_d, q_d)$ is obtained from the value of μ_d using the attitude extraction algorithm defined in Section 4.3.1.1.

Theorem 4.5 (Roberts and Tayebi (2011b)). *Consider the system given by (4.85)-(4.87), where we apply the control laws $u_t = \|\mu_d - g e_3\|$, ω as defined by (4.95), and μ_d as defined by (4.91) where $k_p > 0$ and $k_v > 0$ are chosen such that $k_p + k_v < g$. Let Assumptions 4.6 and 4.7 be satisfied. Then the system thrust u_t is bounded and non-vanishing such that*

$$0 < \underline{c}_t \leq u_t(t) \leq \bar{c}_t, \quad \underline{c}_t = g - k_p - k_v, \quad \bar{c}_t = g + k_p + k_v, \quad (4.99)$$

and for all initial conditions $\tilde{\eta}(t_0) \neq 0$ (or equivalently $\|\tilde{q}(t_0)\| \neq 1$), there exists strictly positive constants $\bar{\gamma}_1, \bar{\gamma}_2, \kappa_1 > 0$ such that for $\gamma_1 > \bar{\gamma}_1$, $\gamma_2 > \bar{\gamma}_2$, $k_1 > \kappa_1$, the system states \tilde{p} and v are bounded and $\lim_{t \rightarrow \infty} \tilde{p}(t) = \lim_{t \rightarrow \infty} v(t) = \mathbf{0}$.

Sketch of Proof: (For a detailed proof the reader is referred to B.6 on page 187)

First, we show that due to the bound of the function $h(\cdot)$, one can arrive at the upper and lower bounds of the thrust input u_t using straightforward arguments.

We then define the error function $\tilde{r}_2 = k_1 \tilde{v} - (I - \tilde{R})r_2$, and consider the following Lyapunov function candidate:

$$\mathcal{V} = \gamma k_p \left(\sqrt{1 + \tilde{p}^\top \tilde{p}} - 1 \right) + \frac{\gamma}{2} v^\top v + \frac{\gamma k_r}{2} \tilde{r}_2^\top \tilde{r}_2 + \gamma_q (1 - \tilde{\eta}^2), \quad (4.100)$$

where k_r , γ , and γ_q are strictly positive constants. We subsequently find the time derivative of \mathcal{V} along the system trajectories. By making appropriate choices on the controller parameters and gains, we first show that $\dot{\mathcal{V}}(t_0) \leq 0$ and further show that $\dot{\mathcal{V}}(t) \leq 0$ provided that the quaternion scalar satisfies $\tilde{\eta}(t) \geq \rho$, where ρ is a strictly positive constant which is assumed to be chosen such that $0 < \rho < \tilde{\eta}(t_0)$. Subsequently, we show that $\tilde{\eta}(t) \geq \rho$ for all $t \geq t_0$ by using a contradiction argument. Therefore, this implies $\dot{\mathcal{V}}(t) \leq 0$ for all $t \geq t_0$. This fact is used with Barbalat's Lemma to show that the states $(\tilde{v}, \tilde{r}_2, \tilde{q}) \rightarrow 0$ and $\tilde{\eta} \rightarrow \text{sgn}(\tilde{\eta}(t_0))$. \square

4.4 Simulations

4.4.1 Adaptive position Controllers

Simulation results have been performed for the two adaptive position tracking control laws. To test the performance of the adaptive disturbance estimation, an approximate aerodynamic model for the ducted fan VTOL UAV is used, which considers aerodynamic drag forces in addition to other aerodynamic effects due to the airflow created by the duct-enclosed propellers. Both proposed control laws are applied to the full system model (including the control-torque coupling term) defined by (2.15)-(2.18), where we use the (translational) disturbance model

$$\delta_t = \frac{1}{m_b} F_d - \frac{1}{m_b \ell} R^\top S(e_3) u, \quad (4.101)$$

where F_d are aerodynamic forces created due to external airflow. Recall from Assumption 4.2 we previously assumed that this coupling term (due to the control torque input u) was assumed to be negligible, which may not always be the case, and therefore is included in the simulation to test the robustness of the proposed control strategy. Furthermore, to aid in the development of the adaptive control laws, Assumption 4.3 stated that the disturbance forces were assumed to be constant in the inertial frame. However, these may be unlikely and/or unrealistic assumptions since the disturbance forces are dependant on system aerodynamic forces caused by wind and the motion of the system. Therefore, we consider a disturbance model which includes aerodynamic drag forces applied to the vehicle. We consider that the system is operating in the presence of a constant and uniform wind, where the wind velocity is denoted by $v_w \in \mathbb{R}^3$. We consider the following aerodynamic drag model:

$$\begin{aligned} F_d &= F_{drag} + F_{ram}, \\ F_{drag} &= \|v_w - v\| R^\top C_d R (v_w - v), \\ F_{ram} &= \sqrt{\frac{T \rho A}{2}} R^\top I_{xy} R (v_w - v), \end{aligned}$$

where F_{drag} are frictional drag forces that are proportional to the square of the external airflow, F_{ram} is the *ram-drag* force³, $I_{xy} = \text{diag}(1, 1, 0)$, ρ is the air density, A is the duct cross-sectional area and $C_d \in \mathbb{R}^3$ is a matrix that consists of system-dependant aerodynamic constants expressed in the body-fixed frame. Assuming that

3. For the ducted-fan VTOL UAV, in addition to generating the thrust T along the body-referenced vertical axis e_3 , the change in momentum of the airflow (due to the system rotors/propellers) can cause an additional force when the external duct airflow velocity has a component which is orthogonal to the thrust vector $T e_3$. This force (which is also orthogonal to the thrust vector) is caused due to the deceleration of the horizontal component of the airflow, and is known as the *ram-drag*. For further information the reader is referred to Ko et al. (2007).

the external airflow is uniform, due to the cylindrical symmetry of the system the net aerodynamic force is assumed to be applied at a point on the body-referenced z -axis, located at a constant distance of ϵ_M from the system center of gravity, which is often referred to as the aerodynamic center-of-pressure (see Figure 4.4).

Also, to simulate uncertainty in the system inertia tensor (which can be difficult to measure), the controllers were implemented using an expected value of the inertial tensor I_b , where the actual value was chosen to be a different value. To obtain these expected and actual values for the inertial tensor, in addition to the system parameters, control gains and initial conditions used in the simulation, please see Table 4.1.

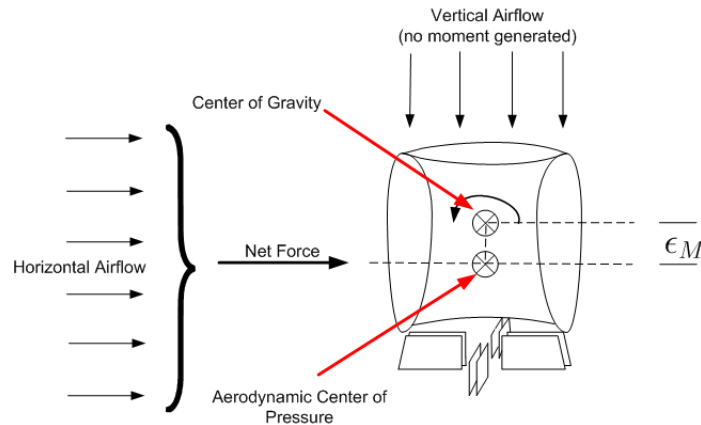
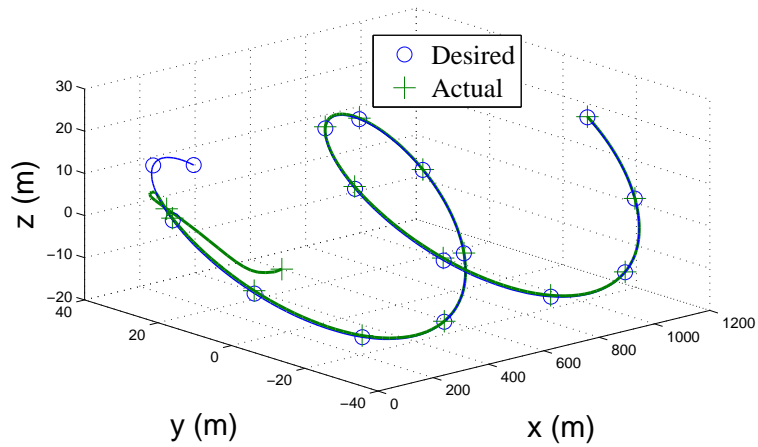
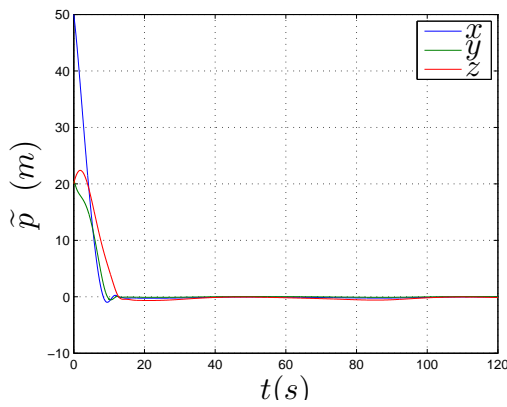


Figure 4.4: Torque-Generating Aerodynamic Forces As a Result of Airflow in Body-Fixed Frame

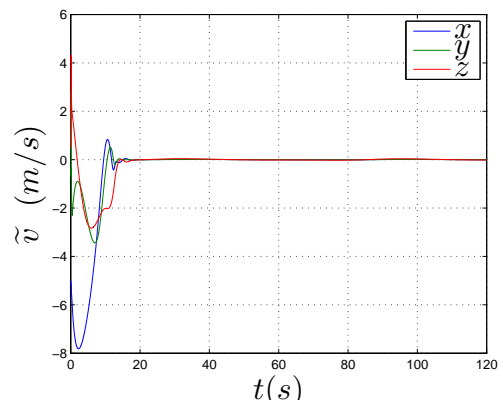
The simulation results are given by Figures 4.5 and 4.6 for the first and second adaptive control laws, respectively. Although the second controller is easier to implement, in situations where the system initial conditions are sufficiently far from the desired trajectory, some control gains are required to have extremely large values (as specified by requirements (4.61)-(4.65)). These requirements are likely conservative, and simulations suggest that the domain of attraction is actually larger than the



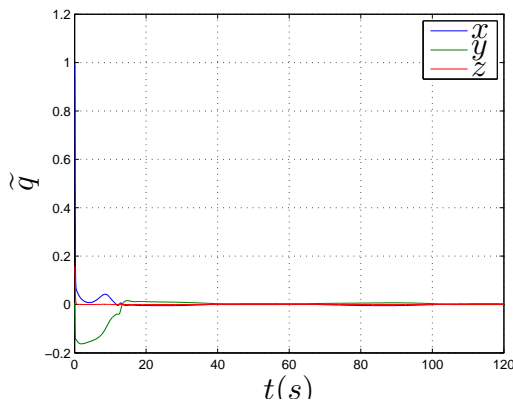
(a) Desired vs Actual Trajectory



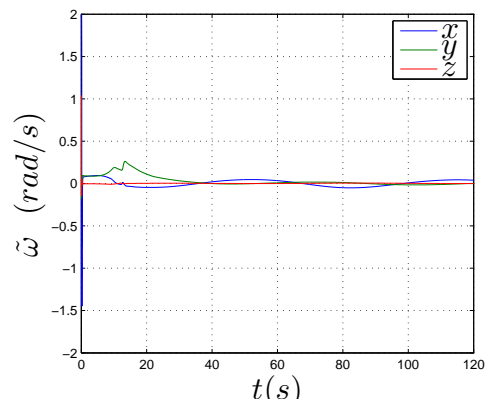
(b) Position Error \tilde{p}



(c) Velocity Error \tilde{v}



(d) Attitude Error \tilde{q}



(e) Angular Velocity Error $\tilde{\omega}$

Figure 4.5: Simulation Results for First Adaptive Position Controller

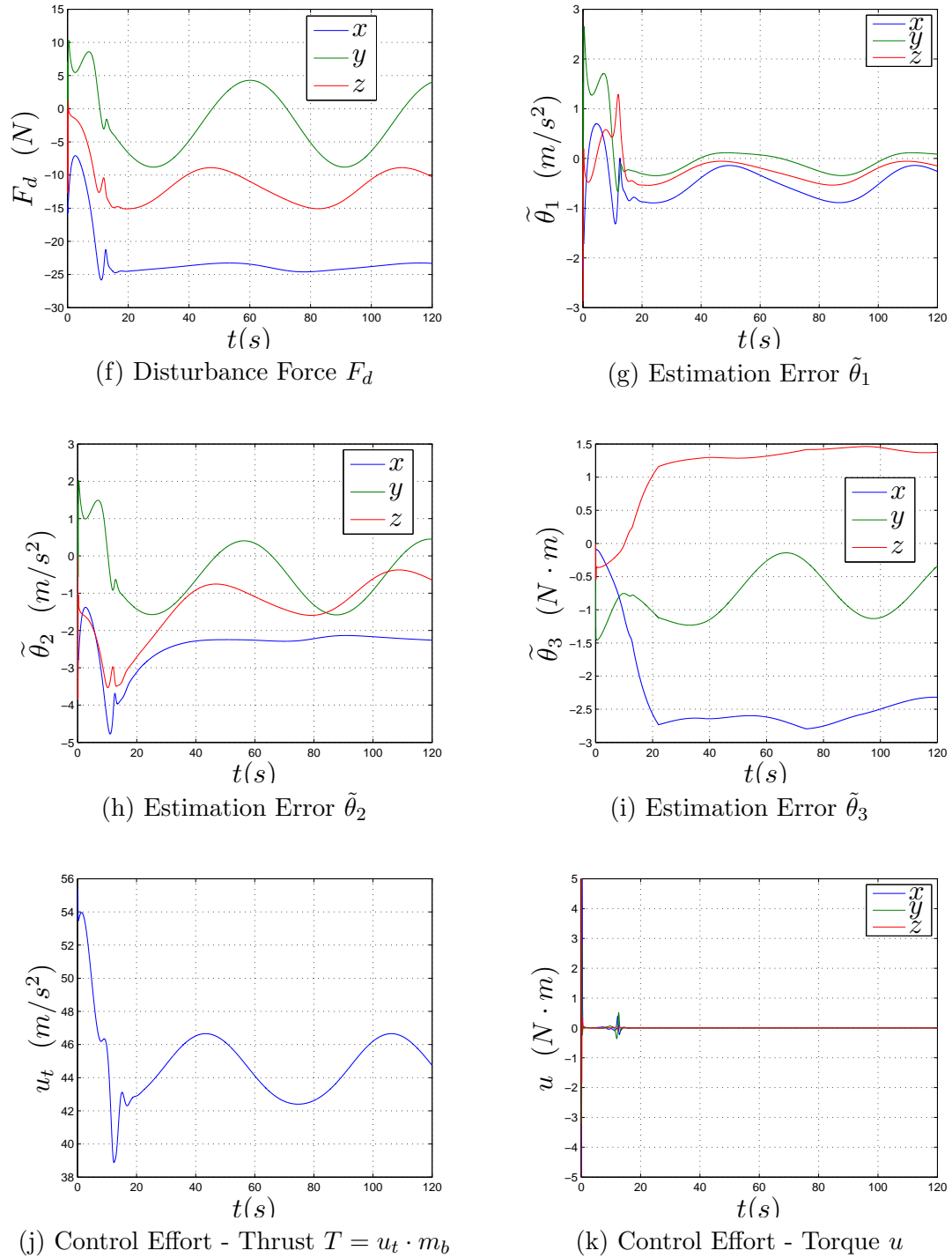
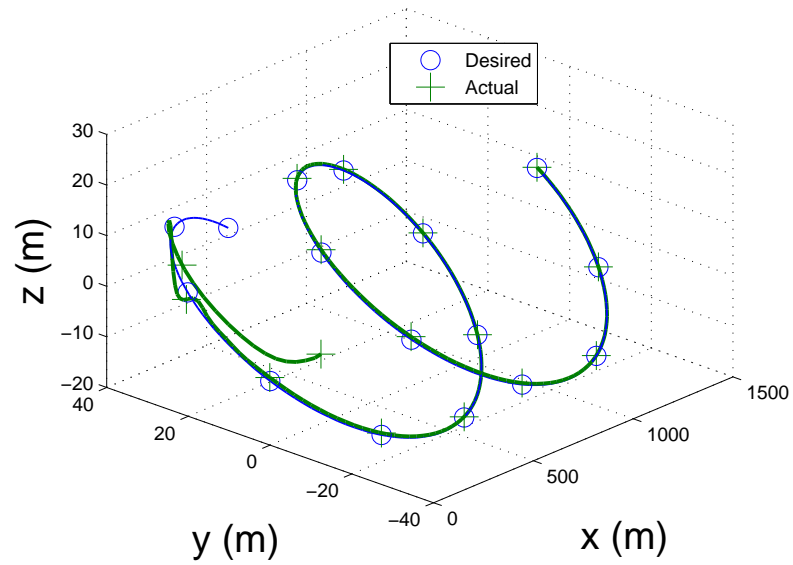
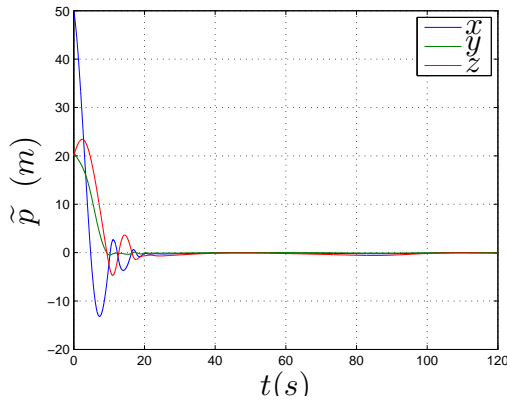


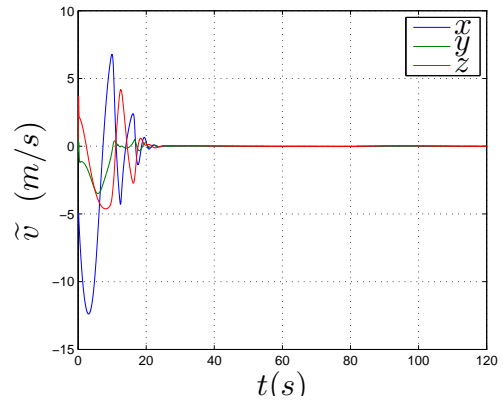
Figure 4.5: Simulation Results for First Adaptive Position Controller (continued)



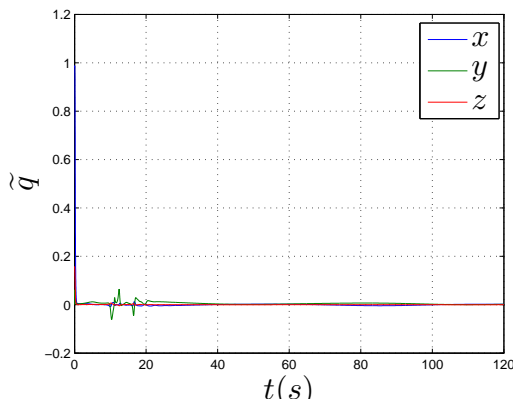
(a) Desired vs Actual Trajectory



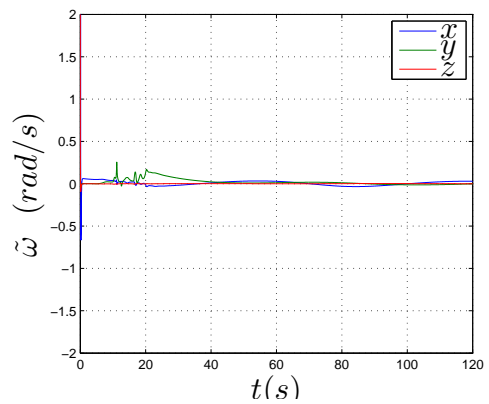
(b) Position Error \tilde{p}



(c) Velocity Error \tilde{v}



(d) Attitude Error \tilde{q}



(e) Angular Velocity Error $\tilde{\omega}$

Figure 4.6: Simulation Results for Second Adaptive Position Controller

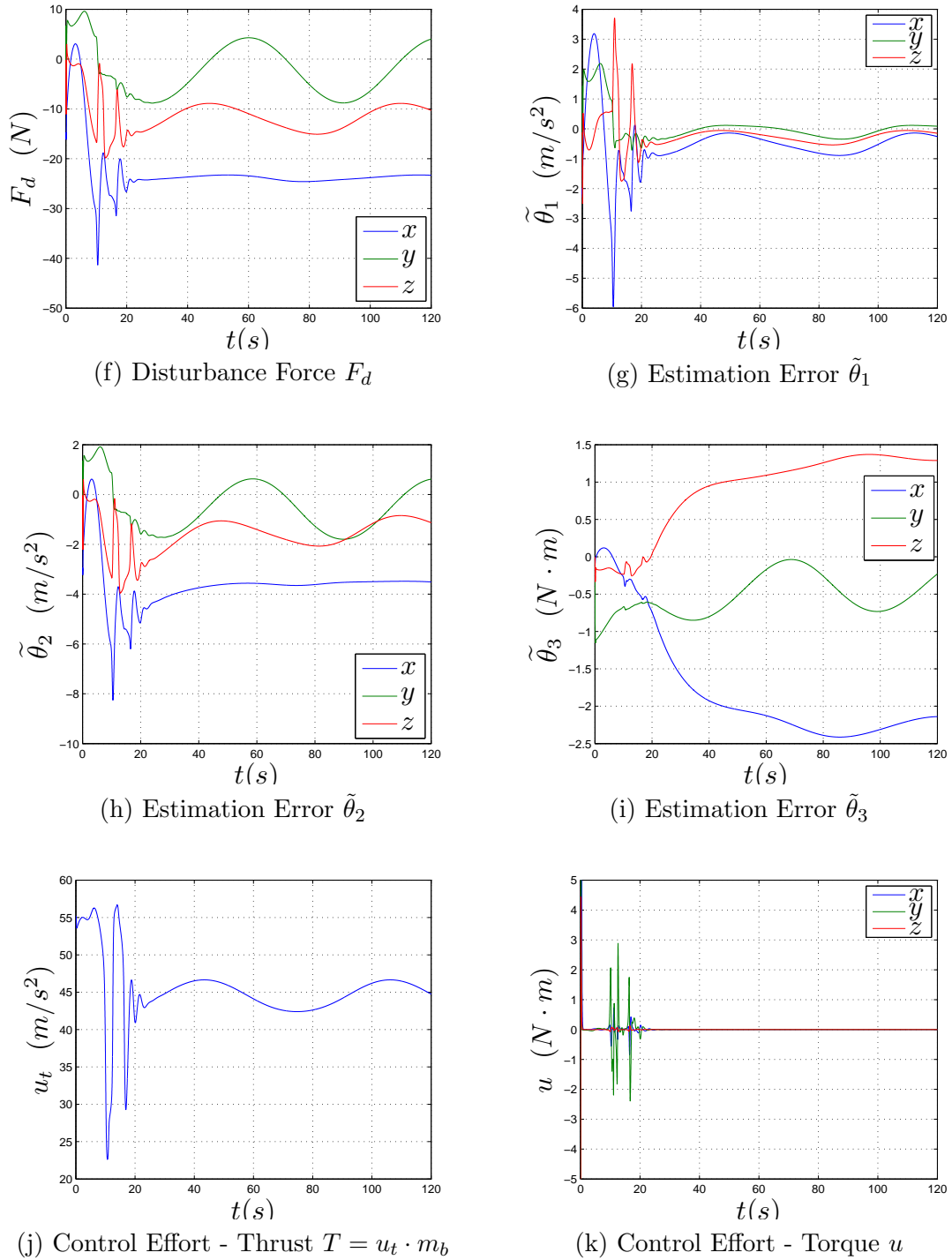


Figure 4.6: Simulation Results for Second Adaptive Position Controller (continued)

region specified by (4.65).

The simulations show that both controllers are successful in forcing the system to the desired trajectory. For each case the system attitude was initialized at $Q = (0, 1, 0, 0)$, which corresponds to the system being completely inverted. This is done to demonstrate the effectiveness of the control laws for extreme deviations in the system attitude. The control laws were effective despite the time-varying disturbance due to aerodynamic drag, the coupling term which was omitted during the control design, and uncertainty in the inertia tensor.

4.4.2 Vector Measurement Based Position Control

Simulations were performed to test the proposed vector-measurement-based position controller applied to the system (4.9) -(4.12). Unlike the adaptive position tracking control law, the vector-measurement-based position control strategy does not attempt to compensate for disturbances which are applied to the vehicle. Instead, this simulation attempts to show how the closed loop system performs (in an ideal environment) in the case where vector measurements are used instead of the direct measurement of the system attitude (given in terms of the unit-quaternion Q of rotation matrix R). Therefore, no aerodynamic model was used for this simulation, and therefore we have $\delta_t = \delta_r = 0$.

A desired position trajectory was chosen similar to the one shown in the previous simulation by Figure 4.5a. To obtain the system parameters, control gains, initial conditions, and the three inertial vectors that were used please see Table 4.2. The simulation results are given by Figure (4.7).

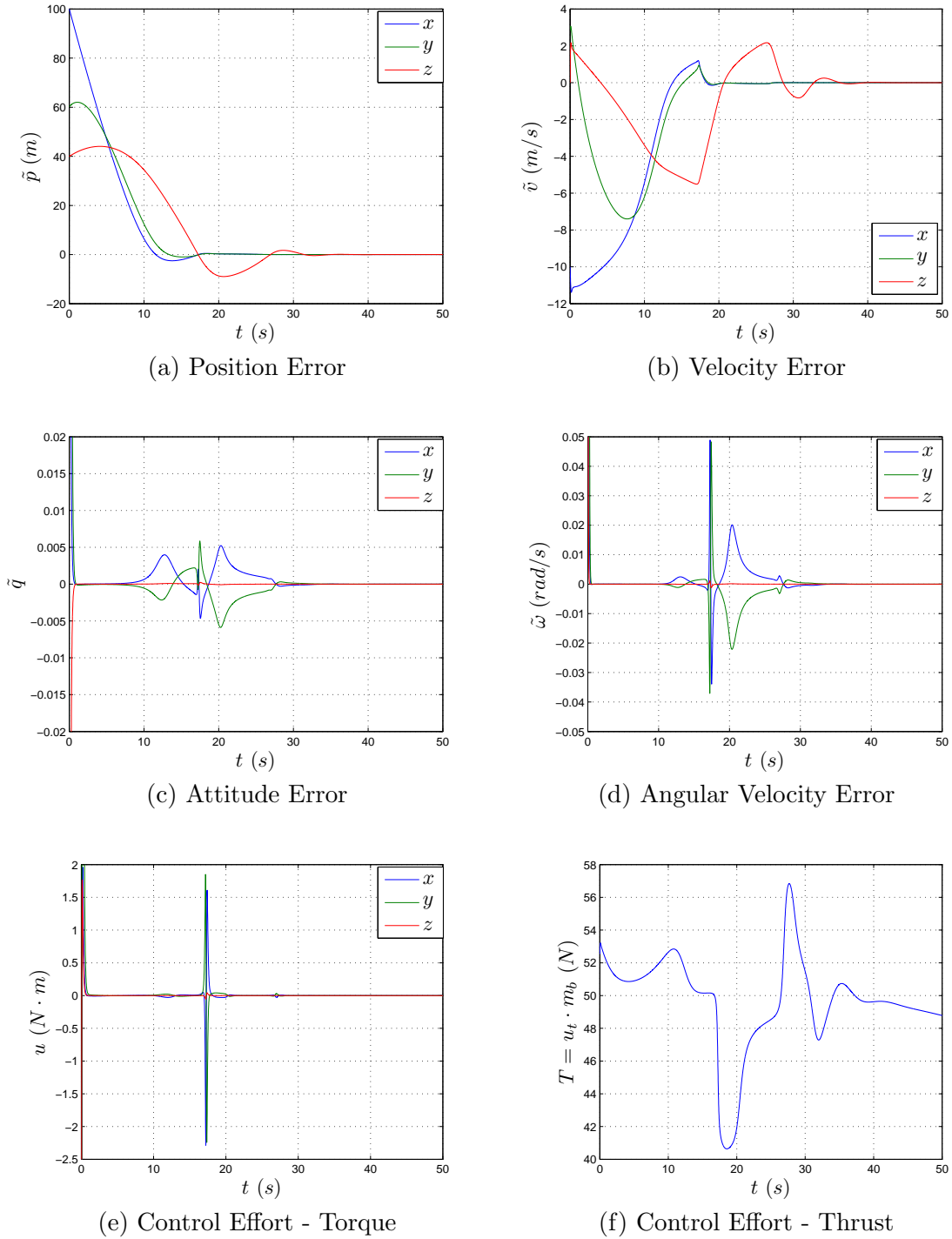


Figure 4.7: Simulation Results for Vector Measurement Based Position Controller

4.4.3 Position Control Using IMU and GPS Measurements

Simulation results have been provided for the system defined by (4.9)-(4.12) using the proposed control law (4.95). Recall in the development of this control law we assumed the angular velocity ω was an available control input. However, since ω is a state, we let ω_d denote the desired angular velocity as defined by (4.95) and use the control law $u = -K_w(\omega - \omega_d)$, where u is the control torque input used in the dynamic equation (4.12). During the design of this control strategy, Assumption 4.7(b) stated that $\dot{\delta}$ was only dependant on the system linear velocity. However, when the system geometry is not exactly symmetrical the time-derivative of the aerodynamic forces may depend on other states, such as the angular velocity. In order to test the robustness of the proposed control method we use an aerodynamic disturbance model (similar to the drag model used by the adaptive position controller) which is dependant on the orientation of the system, and therefore may violate some of the assumptions. The following disturbance model was used:

$$\delta_t = -\frac{1}{m_b} \|v\| R^T C_d R v \quad (4.102)$$

where m_b is the system mass and $C_d = C_d^T > 0$ is a constant positive definite matrix that represents body-referenced aerodynamic drag coefficients that are dependant on the system geometry. We assumed that no disturbance torque was applied to the vehicle and therefore we set $\delta_r = 0$. To obtain the system parameters, control gains and initial conditions please see Table 4.3 simulation results are given by Figure 4.8.

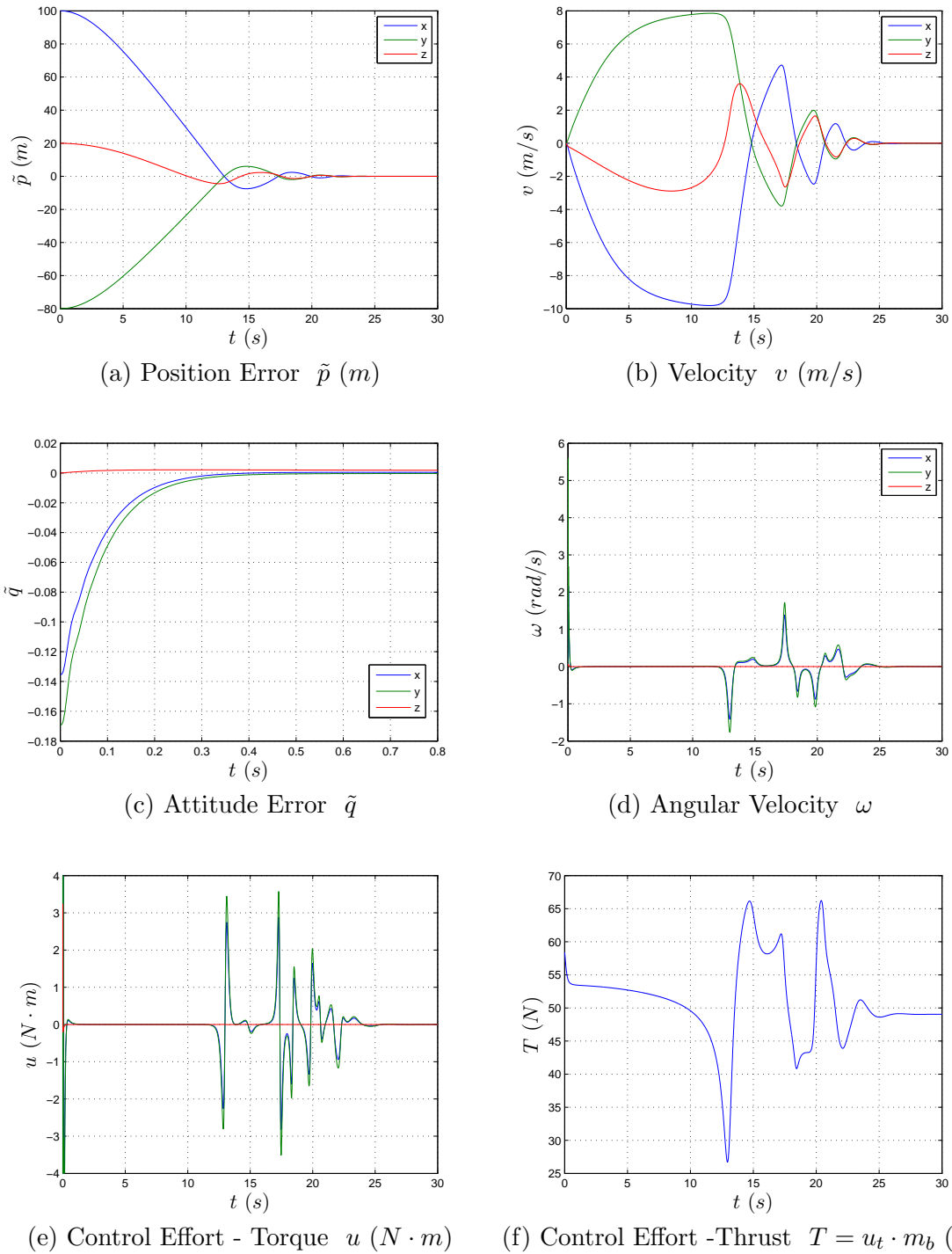


Figure 4.8: Simulation Results for IMU/GPS Measurement Based Position Control

4.5 Concluding Remarks

In this chapter we proposed a vector-measurement-based velocity-free attitude stabilization controller, two adaptive position controllers, and two vector-measurement-based position control laws for VTOL UAVs. All of the proposed position control strategies are dependant on a thrust and attitude extraction method, which provides an expression for the system thrust and desired attitude in terms of the ideal linear acceleration which satisfies the control objectives. The attitude extraction algorithm provides an expression for the desired attitude in terms of the unit-quaternion parameterization, which always exists provided that the desired acceleration meets some mild criteria. These criteria are met by using bounded expressions in the virtual control law for the desired linear acceleration.

The requirement of the bounded expression for the desired linear acceleration is somewhat more complicated for the case of the adaptive controllers, since the desired acceleration has to include some estimate of the disturbance force which is applied to the vehicle. This fact presented a problem since we had to ensure that the disturbance estimates were bounded *a priori* in order to meet specific requirements regarding the bound of the desired linear acceleration. Thus, the projection mechanism was adopted which modifies the adaptive estimation law (which is obtained using standard adaptive control) in such a way that the adaptive estimate is guaranteed to remain within a user-defined set (bounded), and has convenient properties which helps to ensure the Lyapunov function derivatives remain negative semi-definite (despite the perturbation involved in the projection mechanism). A consequence of the projection mechanism is that we require some knowledge of the disturbance force (*i.e.* the upper-bound for the magnitude of the disturbance). To arrive at the control law (in terms of the torque applied to the rotational system dynamics), we required that the expression

for the desired linear velocity was differentiable twice (with respect to time). This required that the projection-based estimation law was required to be (once) differentiable, which is not always possible with the projection-based algorithms available in the literature. Fortunately, a sufficiently-smooth projection algorithm was available which satisfied all of our requirements Cai et al. (2006).

Unfortunately, the two adaptive position tracking controllers have some disadvantages. First, they are by far the most complicated of all the position control laws proposed in this thesis (largely due to the estimation of the disturbance forces and torques). Second, they both assume that the system orientation is known or directly measured. Of course, the system attitude is typically obtained using a vector-measurement-based attitude estimation scheme, which is not considered in the design of the adaptive position control laws. Therefore, we have no choice but to rely on the robustness of the control system in order to deal with unmodeled dynamics or other unexpected errors due to the observers. This disadvantage has led us to study the vector measurement based control law in Section 4.3.3. This control strategy allows the use of vector measurements directly in the position control laws, and therefore does not require the system orientation explicitly, nor the use of an attitude observer when implemented on the system. However, this control strategy does not take into consideration disturbance forces (or torques) which are applied to the vehicle. Yet this disadvantage may be off-set by the resulting simplicity of the (disturbance-estimate-free) vector measurement based control scheme (when compared to the adaptive position control system).

Another problem associated with the vector-measurement-based control strategy, is due to the assumption that the inertial vectors are known and constant in the inertial frame of reference. Unfortunately, there are limited sensors which provide measurements of inertial vectors which satisfy these criteria. This is especially true

when the popular accelerometer sensor is used (in most cases to measure the gravity vector). Since the accurate measurement of the gravity vector requires the system to be non-accelerating (or weakly-accelerating), this vector measurement based position control scheme may not be ideal when an accelerometer is used to provide a vector measurement. This motivated the research community to use the accelerometer in a more realistic manner: to measure the body-reference system apparent acceleration. Similar to the design of the velocity-aided attitude observers, we developed a vector-measurement-based position control law which uses the accelerometer in this manner. Since the system linear velocity is intrinsically related to the apparent acceleration (*i.e.* through an integration), by using a filtered version of the linear velocity we are able to obtain information about the system attitude. Also, rather than estimating a disturbance force, this position control scheme is shown to be effective in the presence of aerodynamic forces, where we take advantage of the fact that aerodynamic forces are dissipative with respect to the linear velocity (kinetic energy) of the system, which is realistic in the case where there is no wind. Unfortunately, this position control scheme also has some disadvantages. First, due to the aerodynamic disturbances, we can only guarantee that the system position converges to a constant (or slowly moving) desired position, instead of converging to a desired trajectory. Second, due to the complexity involved in the stability analysis, we provide the control laws in terms of the system angular velocity (one integrator away from the control input). In this case, a high-gain feedback law is required (for the torque control-input) to force the actual system attitude to the desired value. Despite this limitation, we are still confident that the performance of this position control law may be superior to the previous control laws due to the effect of linear accelerations on the accelerometer measurement.

Description	Parameter	Value
Reference Trajectory	p_d	$\begin{pmatrix} 10t \\ 30 \sin(0.1t + 3.49) \\ 20 \sin(0.1t + 4.71) \end{pmatrix} m$
System Inertia Tensor (expected)	I_b	$\text{diag}(0.5, 0.5, 0.25) kg \cdot m^2$
System Inertial Tensor (actual)	I_b	$\text{diag}(0.6, 0.6, 0.3) kg \cdot m^2$
System Mass	m_b	$5 kg$
Control Torque Moment Lever arm	ℓ	$0.5 m$
Disturbance Moment Lever Arm	ϵ_M	$0.1 m$
Upper bound for $\theta_a = F_d/m$	δ_a	$5 m \cdot s^{-2}$
Upper bound for $\theta_b = \epsilon_M F_d$	δ_b	$3 m \cdot s^{-2}$
Duct cross-sectional area	A	$0.114 m^2$
Gravitational acceleration	g	$9.81 m/s^2$
Air density	ρ	$1.2 kg/m^3$
Wind vector	v_w	$[-1, -1, 0] m/s$
Aero. drag coefficient matrix	C_d	$\text{diag}(0.1, 0.1, 0.05) kg/m$
Initial Conditions	$p(t_0)$	$\text{col}[50, 10, 0] m$
	$v(t_0)$	$\text{col}[5, 0, 0.5] m/s$
	$Q(t_0)$	$\text{col}[0, 1, 0, 0]$
	$\omega(t_0)$	$\text{col}[0, 0, 0] \text{ rad/s}$
Control Gains	k_p	1
	k_v	0.1
	Γ_v	$\text{diag}[0.2, 0.2, 0.8]$
	k_θ	1
	γ_q	10
	K_q	$20 I_{3 \times 3}$
	K_w	$20 I_{3 \times 3}$
Adaptation Gains	γ_{θ_1}	0.2
	γ_{θ_1}	1
	γ_{θ_1}	1

Table 4.1: Simulation Parameters - Adaptive Position Control

Description	Parameter	Value
Reference Trajectory	p_d	$\begin{pmatrix} 10t \\ 30 \sin(0.1t + 3.49) \\ 20 \sin(0.1t + 4.71) \end{pmatrix} m$
System Inertia Tensor	I_b	$\text{diag}(0.5, 0.5, 0.25) \text{ kg} \cdot \text{m}^2$
System Mass	m_b	5 kg
Gravitational acceleration	g	9.81 m/s^2
Initial Conditions	$p(t_0)$	$\text{col}[100, 50, 20] \text{ m}$
	$v(t_0)$	$\text{col}[0, 0, 0] \text{ m/s}$
	$Q(t_0)$	$\text{col}[0.71, 0, 0.71, 0]$
	$\omega(t_0)$	$\text{col}[0, 0, 0] \text{ rad/s}$
Control Gains	k_p	1
	k_v	0.8
	Γ_v	$\text{diag}[5, 5, 1]$
	γ_1	5
	γ_2	5
	γ_3	5
	K_w	$10I_{3 \times 3}$
Inertial Vectors	r_1	$[0, 0, 1]$
	r_2	$[0, 1, 0]$
	r_3	$[1, 0, 0]$

Table 4.2: Simulation Parameters - Vector Measurement Based Position Control

Description	Parameter	Value
Desired Position	p_d	$[0, 0, 0] m$
System Inertia Tensor	I_b	$\text{diag}(0.5, 0.5, 0.25) kg \cdot m^2$
Aerodynamic Coefficients	C_d	$\text{diag}(0.1, 0.1, 0.05) kg/m$
System Mass	m_b	$5 kg$
Gravitational acceleration	g	$9.81 m/s^2$
Initial Conditions	$p(t_0)$	$\text{col}[100, -80, 20] m$
	$v(t_0)$	$\text{col}[0, 0, 0] m/s$
	$Q(t_0)$	$\text{col}[1, 0, 0, 0]$
	$\omega(t_0)$	$\text{col}[0, 0, 0] \text{ rad/s}$
Control Gains	k_p	5
	k_v	2
	γ_1	10
	γ_2	3
	k_1	15
	K_w	$50I_{3 \times 3}$
Magnetic Field Vector	r_1	$[0.1, 0, 0.5]G$

Table 4.3: Simulation Parameters - Position Control Using IMU and GPS Measurements

Control Scheme	Advantages	Disadvantages
Velocity free attitude stabilization	<ul style="list-style-type: none"> • Does not require measurement of attitude (or attitude observer). • Does not require angular velocity. 	<ul style="list-style-type: none"> • Does not offer attitude tracking. • Can be affected by rigid-body accelerations.
Adaptive Position Tracking Controllers	<ul style="list-style-type: none"> • Can estimate constant disturbance forces and torques. 	<ul style="list-style-type: none"> • Requires attitude observer (no proofs for stability when coupled with observer). • Affected by unwinding. • Complicated control laws. • Can result in slower rates of convergence.
Vector Measurement Based Position Tracking Controller	<ul style="list-style-type: none"> • No attitude observer required. • Simplified control laws. 	<ul style="list-style-type: none"> • No disturbance estimation. • Affected by rigid-body accelerations.
IMU/GPS Based Position Controller	<ul style="list-style-type: none"> • No attitude observer required. • Simplified control laws. 	<ul style="list-style-type: none"> • Does not offer position tracking. • Gives control law in terms of angular velocity (high gain controller required for torque).

Table 4.4: Comparison of Control Strategies

Chapter 5

Thesis Summary and Future Work

In this thesis we have studied two of the fundamental problems associated with the autonomous control of VTOL UAVs: rigid-body attitude estimation, and the development of algorithms to control the orientation and/or position of the vehicle. These two problems have been studied separately in the literature. Yet, practitioners and control engineers are faced with these two problems simultaneously when developing these systems.

The study of attitude estimation has resulted in the development of several strategies which use vector measurements, for example, the attitude reconstruction algorithms given in Section 3.1, the complementary filter given in Section 3.2, and the vector-measurement based attitude observers given in Section 3.3.3 and 3.3.4. There have also been a variety of numerical iterative-based algorithms based upon optimization techniques, and substantial efforts to apply Extended Kalman Filtering to solve this problem. Yet all of these methods have a common downfall associated with the use of the accelerometer. Since, in most cases, the accelerometer is used to obtain body-referenced coordinates of the gravity vector, these vector-measurement-based estimation strategies listed above will exhibit degraded performance in proportion to the magnitude of the linear inertial-acceleration experienced by the rigid body. This downfall has led the research community to the development of the velocity-aided attitude observers, which use the accelerometer in a more realistic manner: to

measure the body-referenced apparent acceleration (which contain forces due to the gravity vector and linear acceleration). For a period of time, this type of observer was only known to be locally stable. Fortunately, further investigations revealed that this type of observer exhibited performance which was close to semi-global stability (semi-global stability in a domain which is almost the entire space, except for a set of Lebesgue measure zero). However, the required proofs were very complicated and did not intuitively reveal how the linear velocity measurement aided in the estimation of the system attitude. This difficulty led us to the development of the velocity-aided attitude observers proposed in Section 3.3.5. These proposed observers, through the use of a new estimation law, in our opinion offer greatly simplified proofs when compared to the existing literature, and offer new insights into the mechanism which allows the use of the linear velocity measurement to obtain information about the system attitude.

Until quite recently, the state-of-the-art in control systems for these vehicles required that at least the system attitude was known. Yet, due to the unavailability of sensors which can directly measure the attitude of a rigid-body, one is left with no choice but to couple an attitude observer (such as the ones describe above) with the desired controller, in order to successfully achieve the desired autonomous capabilities. This is also the case with the adaptive position tracking control laws proposed in Section 4.3.2. Due to this disconnect between these two fundamental system objectives (estimation and control), we were motivated to develop new control strategies which considered these two problems together. This led to the development of the vector-measurement based attitude stabilization and position control laws given in Sections 4.2 and 4.3.3, respectively. By utilizing the vector measurements, these control laws can be implemented without the use of an attitude estimation scheme, which as an added benefit, also reduces the complexity of the overall system. This proposed

strategy addresses the concern of using an attitude observer with a control system which assumes the system orientation is directly measured. However, similar to the vector-based attitude observers, the vector based control strategies can be negatively affected when the accelerometer is used to measure the gravity vector. Fortunately, in light of the insight we obtained through the development of the velocity-aided attitude observer, we were able to extend these concepts to develop the control strategy proposed in Section 4.3.4.1. Since this new vector-measurement based position controller uses the accelerometer to measure the system apparent acceleration (instead of the gravity vector), we feel that this control strategy is better suited for VTOL UAVs, for flights requiring high linear accelerations.

In light of these contributions, most of the proposed control strategies assume the aircraft are equipped with a common sensor set which includes a GPS, in order to measure the system inertial-referenced position and velocity. Consequently, the estimation and control strategies proposed in this thesis are best suited for applications where the system is assumed to operate in an external (outdoor) environment, where GPS signals are available. With this characteristic in mind, aircraft which utilize the proposed control strategies may be best suited for applications which involve distant locations or operation in regions which are difficult to reach (for example, the side of a building). Although the quality of the data obtained using a GPS has been improving as a result of technological advancements, in general these measurements can be affected by a variety of problems (*i.e.*, delay, low sampling-time, noise, atmospheric disturbances, multi-path, indoor operation, etc.). One way to address the problems associated with the GPS is to use robust control techniques in order to demonstrate the performance of the proposed estimation and control strategies in the presence of these disturbances. However, another interesting area of future research may involve the use of other sensors to provide information about the position and velocity of the

system. For example, there are a variety of Doppler-based radar sensors which are becoming increasingly small, lightweight and inexpensive (such as the sensors used for collision avoidance in automobiles). These sensors can successfully measure relative linear velocity and may be used for applications where the system is operated inside (for example, by measuring the relative velocity with respect to the floor and surrounding walls). Therefore, future work may consider the use of these sensors to reduce the dependence on the data from a GPS. In addition to the Doppler-based velocity sensors, other technologies have also been studied to measure the system position and velocity (*i.e.*, proximity sensors, RF based positioning, motion capture, etc.). Many motion capture systems use a set of cameras which are mounted on the surrounding walls and ceiling in order to observe the vehicle. Usually, reflective surfaces are placed on the vehicle which can easily be recognized by the computer programs which process the camera data. Furthermore, the use of motion capture has also been used to remove the requirement of the IMU, by calculating (or estimating) the orientation of the vehicle using multiple reflective surfaces which are strategically positioned on the vehicle. However, when using technology such as motion capture, the aircraft is confined to a relatively small workspace which is observed by the motion-capture-enabling cameras, and are not necessarily equipped for operation outside of these regions. Despite this limitation, this is still a very interesting area of research which we may consider in future endeavors.

In other applications where cameras have been placed on the system, typically colored or patterned targets have been used which are intended to be viewed by the cameras, and thus the usefulness of the proposed strategies depends upon the close proximity of the vehicle to the target. In light of these advancements, an interesting problem is to develop vision-based strategies which, unlike previous work, does not depend on a classic or well-defined target. Instead, it may be possible to use the

camera to detect features which appear naturally in the aircraft environment. In fact, a relatively new research area involves the study of *optical flow*, where a camera is used to detect the apparent motion of the system due to linear motion. In most cases, this strategy also uses a gyroscope in order to compensate for the motion of the camera due to rotational motion of the vehicle. Using this strategy, it is possible to obtain measurements of the system linear velocity using only visual feedback. Therefore, one possible contribution may involve the use of optical flow with the velocity-aided attitude observers and/or position controller, where the velocity data is retrieved from a camera using optical flow data, rather than from the GPS. Consequently, in this case the system may be able to operate in environments where GPS data is unavailable.

References

- Abdessameud, A. and Tayebi, A. (2010). Global trajectory tracking control of VTOL-UAVs without linear velocity measurements. *Automatica*, 46(6):1053–1059.
- Aguiar, a. P. and Hespanha, J. A. P. (2007). Trajectory-Tracking and Path-Following of Underactuated Autonomous Vehicles With Parametric Modeling Uncertainty. *IEEE Transactions on Automatic Control*, 52(8):1362–1379.
- Baerveldt, A. and Klang, R. (1997). A low-cost and low-weight attitude estimation system for an autonomous helicopter. In *proceedings of the 1997 IEEE International Conference on Intelligent Engineering Systems, INES'97*, pages 391–395.
- Bhat, S. (2000). A topological obstruction to continuous global stabilization of rotational motion and the unwinding phenomenon. *Systems & Control Letters*, 39(1):63–70.
- Bonnabel, S., Martin, P., and Rouchon, P. (2008). Symmetry-Preserving Observers. *IEEE Transactions on Automatic Control*, 53(11):2514–2526.
- Caccavale, F. (1999). Output feedback control for attitude tracking. *Systems & Control Letters*, 38(2):91–98.
- Cai, Z., de Queiroz, M., and Dawson, D. (2006). A sufficiently smooth projection operator. *IEEE Transactions on Automatic Control*, 51(1):135–139.
- Chaturvedi, N., Sanyal, A., and McClamroch, N. H. (2011). Rigid-Body Attitude Control. *IEEE Control Systems Magazine*, pages 30–51.

- Choukroun, D., Bar-itzhack, I., and Oshman, Y. (2006a). Novel quaternion Kalman filter. *IEEE Transactions on Aerospace and Electronic Systems*, 42(1):174–190.
- Choukroun, D., Weiss, H., Bar-itzhack, I., and Oshman, Y. (2006b). Kalman filtering for matrix estimation. *IEEE Transactions on Aerospace and Electronic Systems*, 42(1):147–159.
- Crassidis, J. (2006). Sigma-point Kalman filtering for integrated GPS and inertial navigation. *IEEE Transactions on Aerospace and Electronic Systems*, 42(2):750–756.
- Crassidis, J. L., Markley, F. L., and Cheng, Y. (2007). Survey of Nonlinear Attitude Estimation Methods. *Journal of Guidance, Control, and Dynamics*, 30(1):12–28.
- Egeland, O. and Godhavn, J. (1994). Passivity-based adaptive attitude control of a rigid spacecraft. *IEEE Transactions on Automatic Control*, 39(4):842–846.
- Fisher, H., Musser, K., and Shuster, M. (1993). Coarse attitude determination from Earth albedo measurements. *IEEE Transactions on Aerospace and Electronic Systems*, 29(1):22–26.
- Frazzoli, E., Dahleh, M., and Feron, E. (2000). Trajectory tracking control design for autonomous helicopters using a backstepping algorithm. In *proceedings of the 2000 IEEE American Control Conference*, pages 4102–4107.
- Guckenheimer, J. and Holmes, P. (1983). *Nonlinear oscillations, dynamical systems and bifurcations of vector fields*. Springer-Verlag.
- Hamel, T. and Mahony, R. (2006). Attitude estimation on $SO[3]$ based on direct inertial measurements. In *proceedings of the 2006 IEEE International Conference on Robotics and Automation, ICRA 2006.*, pages 2170–2175.

- Hamel, T., Mahony, R., Lozano, R., and Ostrowski, J. (2002). Dynamic Modelling and Configuration Stabilization for a X4-Flyer. In *proceedings of the 2002 IFAC World Congress*.
- Hauser, J., Sastry, S., and Meyer, G. (1992). Nonlinear control design for slightly non-minimum phase systems: Applications to v/stol aircraft. *Automatica*, 28(4):665–679.
- Hua, M.-D. (2010). Attitude estimation for accelerated vehicles using GPS/INS measurements. *Control Engineering Practice*, 18(7):723–732.
- Hua, M.-D., Hamel, T., Morin, P., and Samson, C. (2009). A Control Approach for Thrust-Propelled Underactuated Vehicles and its Application to VTOL Drones. *IEEE Transactions on Automatic Control*, 54(8):1837–1853.
- Hughes, P. C. (1986). *Spacecraft Attitude Dynamics (Dover Books on Engineering)*. Dover Publications.
- Ioannou, P. and Sun, J. (1996). *Robust adaptive control*. Prentice Hall.
- Johnson, E. and Turbe, M. (2006). Modeling, Control, and Flight Testing of a Small-Ducted Fan Aircraft. *Journal of Guidance, Control, and Dynamics*, 29(4):769–779.
- Joshi, S., Kelkar, A., and Wen, J. (1995). Robust attitude stabilization of spacecraft using nonlinear quaternion feedback. *IEEE Transactions on Automatic Control*, 40(10):1800–1803.
- Khalil, H. K. (2002). *Nonlinear Systems, Third Edition*. Prentice Hall.
- Ko, A., Ohanian, O., and Gelhausen, P. (2007). Ducted fan UAV modeling and simulation in preliminary design. In *proceedings of the 2007 AIAA Model, Simulation and Technology Conference*.

- Koditschek, D. (1988). Application of a new Lyapunov function to global adaptive attitude tracking. In *proceedings of the 27th IEEE Conference on Decision and Control, 1988*.
- Lizarralde, F. and Wen, J. (1996). Attitude control without angular velocity measurement: a passivity approach. *IEEE Transactions on Automatic Control*, 41(3):468–472.
- Mahony, R., Hamel, T., and Pflimlin, J.-M. (2005). Complementary filter design on the special orthogonal group $SO(3)$. In *proceedings of the 44th IEEE Conference on Decision and Control*, pages 1477–1484.
- Mahony, R., Hamel, T., and Pflimlin, J.-M. (2008). Nonlinear Complementary Filters on the Special Orthogonal Group. *IEEE Transactions on Automatic Control*, 53(5):1203–1218.
- Mahony, R., Hamel, T., Trumpf, J., and Lageman, C. (2009). Nonlinear attitude observers on $SO(3)$ for complementary and compatible measurements: A theoretical study. In *proceedings of the 48th IEEE Conference on Decision and Control, 2009 held jointly with the 2009 28th Chinese Control Conference, CDC/CCC 2009*, pages 6407–6412.
- Marino, R. and Tomei, P. (1998). Robust adaptive state-feedback tracking for nonlinear systems. *IEEE Transactions on Automatic Control*, 43(1):84–89.
- Markley, F. (2004). Attitude Estimation or Quaternion Estimation? *Journal of Astronautical Sciences*, 52(1):221–238.
- Martin, P. and Salaun, E. (2007). Invariant observers for attitude and heading esti-

- mation from low-cost inertial and magnetic sensors. *Proceedings of the 46th IEEE Conference on Decision and Control*, pages 1039–1045.
- Martin, P. and Salaun, E. (2008). An invariant observer for earth-velocity-aided attitude heading reference systems. In *proceedings of the 2008 IFAC World Congress*, pages 9857–9864.
- Martin, P. and Salaun, E. (2010). Design and implementation of a low-cost observer-based attitude and heading reference system. *Control Engineering Practice*, 18(7):712–722.
- Mayhew, C. G., Sanfelice, R. G., and Teel, A. R. (2009a). Robust global asymptotic attitude stabilization of a rigid body by quaternion-based hybrid feedback. In *proceedings of the 48th IEEE Conference on Decision and Control (CDC) held jointly with 2009 28th Chinese Control Conference*, pages 2522–2527.
- Mayhew, C. G., Sanfelice, R. G., and Teel, A. R. (2009b). Robust global asymptotic stabilization of a 6-DOF rigid body by quaternion-based hybrid feedback. In *proceedings of the 48th IEEE Conference on Decision and Control (CDC) held jointly with 2009 28th Chinese Control Conference*, pages 1094–1099. Ieee.
- Metni, N., Pfimlin, J., Hamel, T., and Soueres, P. (2006). Attitude and gyro bias estimation for a VTOL UAV. *Control Engineering Practice*, 14(12):1511–1520.
- Murray, R. M., Sastry, S. S., and Zexiang, L. (1994). *A Mathematical Introduction to Robotic Manipulation*. CRC press.
- Nicholson, W. (1995). *Linear Algebra with Applications*. PWS Pub. Co. (Boston).
- Olfati-Saber, R. (2002). Global configuration stabilization for the VTOL aircraft with

- strong input coupling. *IEEE Transactions on Automatic Control*, 47(11):1949–1952.
- Pfifflin, J. M., Soueres, P., and Hamel, T. (2007). Position control of a ducted fan VTOL UAV in crosswind. *International Journal of Control*, 80(5):666–683.
- Rehbinder, H. (2000). Nonlinear state estimation for rigid-body motion with low-pass sensors. *Systems & Control Letters*, 40(3):183–190.
- Rehbinder, H. (2004). Drift-free attitude estimation for accelerated rigid bodies. *Automatica*, 40(4):653–659.
- Reynolds, R. (1998). Quaternion parametrization and a simple algorithm for global attitude estimation. *Journal of guidance, control, and dynamics*, 21(4):669–671.
- Roberts, A. and Tayebi, A. (2009). Adaptive position tracking of VTOL UAVs. In *proceedings of the Joint 48th IEEE Conference on Decision and Control and 28th Chinese Control Conference, Shanghai, China, 2009*, pages 5233–5238. IEEE.
- Roberts, A. and Tayebi, A. (2011a). Adaptive position tracking of VTOL UAVs. *IEEE Transactions on Robotics*, 27(1):129–142.
- Roberts, A. and Tayebi, A. (2011b). Attitude Estimation and Position Control of VTOL UAVs using IMU and GPS Measurements. *Submitted to Automatica, Document available as Arxiv preprint arXiv:1106.0016*.
- Roberts, A. and Tayebi, A. (2011c). On the attitude estimation of VTOL UAVs using GPS and IMU Measurements. *Accepted as regular paper for the 50th IEEE Conference on Decision and Control and European Control Conference, December 12-15, 2011, Orlando, FL, USA*.

- Roberts, A. and Tayebi, A. (2011d). Position Control of VTOL UAVs using GPS and IMU Measurements. *Accepted as regular paper for the 50th IEEE Conference on Decision and Control and European Control Conference, December 12-15, 2011, Orlando, FL, USA.*
- Roberts, A. and Tayebi, A. (2011e). Position Control of VTOL UAVs Using Inertial Vector Measurements. In *proceedings of the 18th World Congress of the International Federation of Automatic Control (IFAC), Milano, Italy, 2011*, pages 2614–2619.
- Salcudean, S. (1991). A globally convergent angular velocity observer for rigid body motion. *IEEE Transactions on Automatic Control*, 36(12):1493–1497.
- Shuster, M. (1993). A survey of attitude representations. *The Journal of Astronautical Sciences*, 41(4):439–517.
- Shuster, M. (2006). The generalized Wahba problem. *Journal of the Astronautical Sciences*, 54(2):245.
- Shuster, M. D. and Oh, S. D. (1981). Three-axis attitude determination from vector observations. *Journal of Guidance, Control, and Dynamics*, 4(1):70–77.
- Slotine, J. and Li, W. (1991). *Applied Nonlinear Control*. Prentice hall.
- Tayebi, A. (2008). Unit quaternion-based output feedback for the attitude tracking problem. *IEEE Transactions on Automatic Control*, 53(6):1516–1520.
- Tayebi, A. and McGilvray, S. (2006). Attitude stabilization of a VTOL quadrotor aircraft. *IEEE Transactions on Control Systems Technology*, 14(3):562–571.

- Tayebi, A., McGilvray, S., Roberts, A., and Moallem, M. (2007). Attitude estimation and stabilization of a rigid body using low-cost sensors. In *proceedings of the 46th IEEE Conference on Decision and Control*, pages 6424–6429.
- Tayebi, A., Roberts, A., and Benallegue, A. (2011). Inertial measurements based dynamic attitude estimation and velocity-free attitude stabilization. In *proceedings of the 2011 IEEE American Control Conference, San Francisco, CA, USA*, pages 1027–1032.
- Tsiotras, P. (1998). Further passivity results for the attitude control problem. *IEEE Transactions on Automatic Control*, 43(11):1597–1600.
- Wahba, G. (1965). A least squares estimate of spacecraft attitude. *Siam Review*, 7(3):409.
- Wen, J.-Y. and Kreutz-Delgado, K. (1991). The attitude control problem. *IEEE Transactions on Automatic Control*, 36(10):1148–1162.

Appendix A

Proof for Lemmas and Propositions

A.1 Proofs for Lemmas

A.1.1 Proof for Lemma 3 (Single-Measurement Attitude Reconstruction)

One definition of a unit-quaternion as it pertains to a rotational transformation is given by $Q = \left(\cos(\delta/2), \sin(\delta/2) \hat{k} \right)$, where δ is an angle of rotation about the normalized axis of rotation \hat{k} . One possible solution for the angle and axis of rotation can be found by using the scalar and vector products, *i.e.* $r^T b = \|r\| \|b\| \cos(\delta)$ and $S(b)r = \|r\| \|b\| \sin(\delta) \hat{k}$. From the definition of the scalar product, we find $\cos(\delta) = \frac{r^T b}{\|r\|^2}$, where we assume $\|r\| = \|b\|$. The result $\sin(\delta) = \frac{1}{\|r\|^2} \sqrt{(\|r\|^2 + r^T b)(\|r\|^2 - r^T b)}$ follows from the fact that $\sin^2(\delta) = 1 - \cos^2(\delta)$. Applying the double angle formula $\cos(\delta) = 1 - 2\sin^2(\delta/2)$, we obtain $\sin(\delta/2) = \frac{1}{\|r\|} \sqrt{\frac{\|r\|^2 - r^T b}{2}}$. Subsequently, the normalized axis of rotation is given by $\hat{k} = \left((\|r\|^2 + r^T b)(\|r\|^2 - r^T b) \right)^{-1/2} S(b)r$. Therefore, the solution for the vector and scalar parts of the quaternion are given by

$$\hat{k} \sin(\delta/2) = \frac{1}{\|r\|} \sqrt{\frac{1}{2(\|r\|^2 + r^T b)}} S(b)r,$$

$$\cos(\delta/2) = \frac{\sin(\delta)}{2 \sin(\delta/2)} = \frac{1}{\|r\|} \sqrt{\frac{\|r\|^2 + r^T b}{2}}.$$

□

A.1.2 Proof for Lemma 4 (Properties of z_γ and W)

First, let us show that the matrix $W := -\sum_{i=1}^n \gamma_i S(r_i)^2$ is positive definite. Due to the property 2.21, it is clear $W = W^\top$. Let us define $\alpha(x) = x^\top W x$, where $x \in \mathbb{R}^3$, and let $\alpha_i(x) = -\gamma_i x^\top S(r_i)^2 x$ such that $\alpha(x) = \sum_{i=1}^n \alpha_i(x)$. Then, due to property 2.25, it is clear that $\alpha_i(x) \geq 0$ for any $x \in \mathbb{R}^3$, and $\alpha_i(x) = 0$ implies that x is collinear to the vector r_i (null-space of $S(r_i)^2$). In light of Assumption 3.2, let r_1 and r_2 denote two non-collinear vectors. Then, if $\alpha_1(x) = 0$ it is true that $\alpha_2(x) \neq 0$ since the vector x cannot be collinear to both r_1 and r_2 . It follows that the condition $\alpha(x) = 0$ is only possible if and only if $x = 0$, and therefore W is positive definite.

To prove (b), we use the fact $b_i = R r_i$, $\hat{b}_i = \hat{R} r_i$, and the definition of the attitude error $\tilde{R} = \hat{R}^\top R$, then applying the property (2.23) to z_γ yields

$$z_\gamma = \sum_{i=1}^n \gamma_i S(\hat{b}_i) b_i = \hat{R} \sum_{i=1}^n \gamma_i S(r_i) \tilde{R} r_i. \quad (\text{A.1})$$

Using (2.8) and the property (2.22) with \tilde{R} , we find

$$z_\gamma = 2\hat{R} \sum_{i=1}^n \gamma_i S(r_i) (\tilde{q}\tilde{q}^\top - \tilde{\eta}S(\tilde{q})) r_i = -2\hat{R}(S(\tilde{q})M + \tilde{\eta}W), \quad (\text{A.2})$$

where $M = \sum_{i=1}^n \gamma_i r_i r_i^\top$. Due to the property (2.22), we find $M = \mu I - W$, $\mu = \sum_{i=1}^n \gamma_i r_i^\top r_i$. Substituting this expression for M we arrive at (3.28).

To prove (c) we first note $z_\gamma = 0$ is equivalent to

$$(\tilde{\eta}I - S(\tilde{q}))W\tilde{q} = 0. \quad (\text{A.3})$$

From this result it is clear that $\tilde{q} = 0$ is a trivial solution, where due to the unity-norm constraint further implies $\tilde{\eta} = \pm 1$. For the case where $\tilde{q} \neq 0$, let us pre-multiply the result (A.3) by $\tilde{q}^\top \neq 0$ to obtain $\tilde{\eta}\tilde{q}^\top W\tilde{q} = 0$, from which it is clear that $\tilde{\eta} = 0$ is the only solution since W is a positive definite matrix. In the case where $\tilde{\eta} = 0$ (and therefore $\|\tilde{q}\| = 1$), (A.3) becomes $S(\tilde{q})W\tilde{q} = 0$, which implies that $W\tilde{q}$ (which is non-zero) is collinear to \tilde{q} . Therefore \tilde{q} must be collinear to v , where v is unit-eigenvector of W . \square

A.2 Proofs for Propositions

A.2.1 Proof for Proposition 1 (Complementary Filtering)

In light of the attitude error defined by (3.15), since $\bar{Q} = \hat{Q} \odot \tilde{Q}$, we obtain the time derivative $\dot{\hat{Q}} \odot \tilde{Q} = \dot{\bar{Q}} - \dot{\hat{Q}} \odot \tilde{Q}$. Using the quaternion multiplication operation \odot , we multiply by \hat{Q} to obtain

$$\dot{\hat{Q}} = \frac{1}{2}\hat{Q}^{-1} \odot \bar{Q} \odot (0, \omega) - \frac{1}{2}(0, \beta) \odot \tilde{Q} \quad (\text{A.4})$$

$$= \frac{1}{2}\tilde{Q} \odot (0, \omega - \tilde{R}\beta) \quad (\text{A.5})$$

Let us consider the following Lyapunov function candidate:

$$\mathcal{V} = \tilde{q}^\top \tilde{q} + (1 - \tilde{\eta})^2 + \frac{1}{2}\tilde{\omega}_b^\top \Gamma_2^{-1} \tilde{\omega}_b = 2(1 - \tilde{\eta}) + \frac{1}{2}\tilde{\omega}_b^\top \Gamma_2^{-1} \tilde{\omega}_b, \quad (\text{A.6})$$

where we note \mathcal{V} can be expressed using only the quaternion scalar $\tilde{\eta}$ due to the unit-norm constraint $\tilde{\eta}^2 + \tilde{q}^\top \tilde{q} = 1$. In light of (A.5) the time-derivative of the quaternion scalar is given by $\dot{\tilde{\eta}} = -1/2\tilde{q}^\top(\omega - \tilde{R}\beta)$. Using the fact that $\tilde{q}^\top \tilde{R}\beta = \tilde{q}^\top \beta$ and

$\omega_b = \hat{\omega}_b - \tilde{\omega}_b$, the time-derivative of \mathcal{V} is given by

$$\dot{\mathcal{V}} = -\tilde{q}^\top(\beta - \omega_g + \hat{\omega}_b - \tilde{\omega}_b) + \tilde{\omega}_b^\top \Gamma_2^{-1} \dot{\tilde{\omega}}_b \quad (\text{A.7})$$

Applying the observer estimation laws (3.13) and (3.14) we obtain

$$\dot{\mathcal{V}} = -\tilde{q}^\top \Gamma_1 \tilde{q}. \quad (\text{A.8})$$

Due to the boundedness of $\dot{\tilde{q}}$ (since we assume ω is bounded), Barbalat's Lemma can be applied to show that $\dot{\mathcal{V}} \rightarrow 0$ and therefore $\tilde{q} \rightarrow 0$. Also, due to the boundedness of $\dot{\omega}$ we have $\dot{\tilde{Q}} \rightarrow 0$ which implies $\beta \rightarrow \omega$, and therefore $\hat{\omega}_b \rightarrow \omega_b$. \square

A.2.2 Proof for Proposition 2 (Vector-Measurement Based Attitude Observer)

Let $\tilde{b}_i = \hat{b}_i - b_i$ and consider the following Lyapunov function candidate

$$\mathcal{V} = \frac{1}{2} \sum_{i=1}^n \gamma_i \tilde{b}_i^\top \tilde{b}_i \quad (\text{A.9})$$

In light of (3.18) and (3.20) the derivative of \mathcal{V} is given by

$$\dot{\mathcal{V}} = \sum_{i=1}^n \gamma_i \tilde{b}_i^\top (S(\omega)(\tilde{b}_i + \hat{b}_i) - S(\beta)\hat{b}_i) = -z_\gamma^\top z_\gamma \quad (\text{A.10})$$

Therefore, all signals involved in the control scheme are bounded, \mathcal{V} is non-increasing and converges to a constant as t goes to infinity. Since ω and β are bounded, $\ddot{\mathcal{V}}$ is also bounded which guarantees $\dot{\mathcal{V}}$ is uniformly continuous. Barbalat's lemma therefore

implies

$$\lim_{t \rightarrow \infty} z_\gamma(t) = 0 \quad (\text{A.11})$$

Invoking Lemma (4) we conclude that the observer dynamics has the following equilibria: $(\tilde{\eta} = 0, \tilde{q} = \pm v)$ and $(\tilde{\eta} = \pm 1, \tilde{q} = 0)$.

To show that the manifold Ψ is invariant, we study the dynamics of $\tilde{\eta}^2$. Using (3.23) we find

$$\frac{d}{dt} (\tilde{\eta}^2) = 2\tilde{\eta} \left(-\frac{1}{2} \tilde{q}^\top \hat{R}^\top (\omega - \beta) \right) = \tilde{\eta}^2 \tilde{q}^\top W \tilde{q} \quad (\text{A.12})$$

from which it is clear $\dot{\tilde{\eta}} = 0$ when $\tilde{\eta} = 0$, which shows the invariance of Ψ . The non-attractiveness of Ψ follows from the fact that for any $\tilde{\eta}(t_0) \neq 0$, $|\tilde{\eta}|$ is always increasing (since W is positive-definite) and therefore $|\tilde{\eta}|$ must converge to an upper limit. Since we know that $z_\gamma \rightarrow 0$, then this must imply that $\lim_{t \rightarrow \infty} \tilde{\eta}(t) = \text{sgn}(\tilde{\eta}(t_0))$. Therefore, for all initial conditions satisfying $\tilde{\eta}(t_0) = 0$, invoking Lemma 4 implies that $\lim_{t \rightarrow \infty} \tilde{\eta}(t) = 0$ and $\lim_{t \rightarrow \infty} \tilde{q}(t) = v$.

A.2.3 Proof for Proposition 3 (Attitude Observer Using Filtered Vector-Measurements)

Let $\tilde{b}_i = \hat{b}_i - b_i$ denote the vector-measurement error, and consider the following Lyapunov function candidate

$$\mathcal{V} = \frac{1}{2} \sum_{i=1}^n \gamma_i \tilde{b}_i^\top \tilde{b}_i + \frac{1}{2} \psi^\top \psi \quad (\text{A.13})$$

In light of (3.18) and (3.19) it follows that $\dot{\hat{b}}_i = -S(\beta)\hat{b}_i$ and $\dot{\tilde{b}}_i = -S(\omega)\tilde{b}_i = -S(\omega)(\hat{b}_i - \tilde{b}_i)$. Therefore, the time derivative of \mathcal{V} is given by

$$\dot{\mathcal{V}} = \sum_{i=1}^n \gamma_i \tilde{b}_i^T \left(S(\hat{b}_i)(\beta - \omega) \right) + \psi^T \dot{\psi} = z_\gamma^T (\beta - \omega) + \psi^T \dot{\psi} \quad (\text{A.14})$$

Applying the expressions for β and $\dot{\psi}$ from (3.33) and (3.34), respectively we obtain

$$\dot{\mathcal{V}} = -\alpha \psi^T \psi \quad (\text{A.15})$$

which implies that ψ is bounded, and therefore $\dot{\psi} = -\alpha\psi + \alpha z_\gamma$ is bounded since z_γ is bounded by definition (the vectors r_i and b_i are bounded). Therefore, since $\ddot{\mathcal{V}}$ is bounded, then $\dot{\mathcal{V}}$ is uniformly continuous and Barbalat's lemma implies $\dot{\mathcal{V}} \rightarrow 0$ and therefore $\psi \rightarrow 0$. Similarly, since $\ddot{\psi} = -\alpha\dot{\psi} + \alpha\dot{z}_\gamma$, and since \dot{z}_γ is a function of β and ω (which are bounded), then it follows that $\ddot{\psi}$ is also bounded. Then $\dot{\psi} \rightarrow 0$ and therefore $z_\gamma \rightarrow 0$. Invoking Lemma 4 we find the estimator has the equilibria $(\tilde{\eta} = \pm 1, \tilde{q} = 0, \psi = 0)$ or $(\tilde{\eta} = 0, \tilde{q} = \pm v, \psi = 0)$.

Now, let us show that the undesired equilibria $(\tilde{\eta} = 0, \tilde{q} = \pm v, \psi = 0)$ are unstable, which we will do using Chetaev's theorem (Khalil (2002)). First we define $\delta := \tilde{q}^T \hat{R}^T \psi$, and consider the dynamics of $\tilde{\eta}$ and δ around the undesired equilibria

$$\dot{\tilde{\eta}} = -\alpha\delta/2 \quad (\text{A.16})$$

$$\dot{\delta} = -\alpha\delta - 2\alpha\xi\tilde{\eta} + v^T \hat{R}^T S(\omega)\psi \quad (\text{A.17})$$

where $\xi := v^T W v$ and v is a unit-eigenvector of W which corresponds to the equilibrium point. Note that by definition, ξ is equal to one of the eigenvalues of W , and therefore must satisfy $\xi \geq \lambda_{\min}(W) > 0$. Now let us consider the following Chetaev

function candidate:

$$\mathcal{V}_c = -\tilde{\eta}\delta \quad (\text{A.18})$$

Let $0 < r < 1$ and define a ball

$$B_r = \{x := (\tilde{\eta}, \delta) \in [-1, 1] \times \mathbb{R}, \|x\| < r\} \quad (\text{A.19})$$

where $r > 0$ is chosen sufficiently small such that the linearized model given by (A.16) and (A.17) is valid, and also define a subset of B_r where $\mathcal{V}_c > 0$ given by

$$U = \{x \in B_r, \mathcal{V}_c(x) > 0\} \quad (\text{A.20})$$

Note that U_r is non-empty for all $0 < r < 1$. In light of (A.16) and (A.17), the time-derivative of \mathcal{V}_c is given by

$$\begin{aligned} \dot{\mathcal{V}}_c &= \alpha\delta^2/2 + 2\alpha\xi\tilde{\eta}^2 + \alpha\tilde{\eta}\delta - \tilde{\eta}v^\top \hat{R}^\top S(\omega)\psi \\ &\geq \alpha\delta^2/2 + 2\alpha\lambda_{\min}(W)\tilde{\eta}^2 - \alpha(\epsilon_1\tilde{\eta}^2 + \delta^2/(4\epsilon_1) - \|\omega\|(\epsilon_2\tilde{\eta}^2 + \kappa^2\delta^2/(4\epsilon_2))) \\ &\geq k_1\delta^2 + k_2\tilde{\eta}^2 \end{aligned} \quad (\text{A.21})$$

where $k_1 = \alpha/2 - \alpha/(4\epsilon_1) - k_\omega\kappa^2/(4\epsilon_2)$ and $k_2 = 2\alpha\lambda_{\min}(W) - \alpha\epsilon_1 - k_\omega\epsilon_2$, and k_ω is the upper bound of ω . We also used the fact that ψ and δ are bounded to guarantee that, for any $(\delta, \tilde{\eta}) \in U_r$, there exists a finite parameter $\kappa > 0$ such that $\|\psi\| \leq \kappa|\delta|$. Note that Young's inequality has been used, with arbitrary $\epsilon_1 > 0$ and $\epsilon_2 > 0$, to obtain the result (A.21). Note that the eigenvalues of W can be arbitrarily increased using the gains γ_i . Therefore, we choose $\alpha > 0$, $\epsilon_1 > 0$ and $\epsilon_2 > 0$ such that $k_1 > 0$, and choose the gains γ_i such that $\lambda_{\min}(W) > k_\xi := (\alpha\epsilon_1 + k_\omega\epsilon_2)/(2\alpha)$ to ensure $k_2 > 0$. Then, $\dot{\mathcal{V}}_c > 0$ for all $(\tilde{\eta}, \delta) \in B_r$.

If we choose initial conditions near the equilibrium point such that $x(0) \in U_r$ and $\mathcal{V}_c(x(0)) = \sigma > 0$, it is clear $x(t)$ must leave U_r since $\mathcal{V}_c(x)$ is bounded on U_r and $\dot{\mathcal{V}}_c(x) > 0$ everywhere in U_r . Since $\mathcal{V}_c(x(t)) \geq \sigma$, it is clear $x(t)$ must leave U_r through the radial boundary $\|x\| = r$ and not through the edges $\mathcal{V}_c(x) = 0$, (i.e. $\delta = 0$ or $\tilde{\eta} = 0$). Since this can happen for arbitrarily small r it is clear $(\tilde{\eta} = 0, \delta = 0)$ is an unstable equilibrium. \square

Appendix B

Proof for Theorems

B.1 Proof for Theorem 3.1

(Second Order Attitude Observer Using IMU and GPS Measurements)

Let us first define the following error function

$$\tilde{r}_2 = k_1 \tilde{v} - (I - \tilde{R})r_2. \quad (\text{B.1})$$

To find the time-derivative of this signal we recall the expressions (3.36), (3.21), (3.24), which are used to obtain $\dot{\tilde{r}}_2 = k_1(g e_3 + r_2 - \dot{v}) - S(-\hat{R}^\top \sigma) \hat{R}^\top b_2 - (I - \tilde{R})\dot{r}_2$. Applying the expression for \dot{v} from (3.43), and using the fact that $-k_1 \tilde{v} + r_2 - \hat{R}^\top b_2 = -\tilde{r}_2$, we obtain the result

$$\dot{\tilde{r}}_2 = -k_1 \tilde{r}_2 - (I - \tilde{R})\dot{r}_2. \quad (\text{B.2})$$

At this point it is obvious that if the signal r_2 was constant, the error signal \tilde{r}_2 would exponentially converge to zero, which is equivalent to \tilde{v} converging to $(I - \tilde{R})r_2$. This offers some insight on how the error function \tilde{v} aids in the attitude observer in the case where the signal r_2 is unknown. However, since the signal r_2 is not constant we must continue with the stability-analysis. Using these results, we now study the dynamics of the attitude error, by finding the time-derivative of the quaternion scalar

$\tilde{\eta}$. Using the expression of $\tilde{\omega}$ from (3.24), in addition to the expression for σ from (3.42), the definition of the error signal defined by (B.1), the property (2.23), and the fact that $S(\tilde{R}r_2)\tilde{R}r_2 = 0$, the time-derivative of the attitude error in terms of the quaternion scalar $\tilde{\eta}$ is given by

$$\dot{\tilde{\eta}} = -\frac{1}{2}\tilde{q}^T \left(\gamma_1 S(r_1)\tilde{R}r_1 + \gamma_2 S(r_2)\tilde{R}r_2 + \gamma_2 S(\tilde{r}_2)\tilde{R}r_2 \right). \quad (\text{B.3})$$

Using (2.8) and the property (2.22), one can further show that

$$\tilde{q}^T S(r_i)\tilde{R}r_i = 2\tilde{q}^T S(r_i)(\tilde{q}\tilde{q}^T - \tilde{\eta}S(\tilde{q}))r_i = 2\tilde{\eta}\tilde{q}^T S(r_i)^2\tilde{q}, \quad (\text{B.4})$$

where $r_i \in \mathbb{R}^3$. Therefore, the time-derivative of $\tilde{\eta}$ is found to be

$$\dot{\tilde{\eta}} = \tilde{\eta}\tilde{q}^T W\tilde{q} + \frac{\gamma_2}{2}\tilde{q}^T S(\tilde{R}r_2)\tilde{r}_2, \quad (\text{B.5})$$

where W is the matrix defined by (3.40). Using this framework, we now wish to show that \tilde{q} converges to zero (or equivalently $\tilde{\eta}^2$ converges to one), using Lyapunov arguments. With this goal in mind, let us consider the following Lyapunov function candidate:

$$\mathcal{V} = \frac{\gamma}{2}\tilde{r}_2^T\tilde{r}_2 + \gamma_q\tilde{q}^T\tilde{q} = \frac{\gamma}{2}\tilde{r}_2^T\tilde{r}_2 + \gamma_q(1 - \tilde{\eta}^2), \quad (\text{B.6})$$

where γ and γ_q are strictly positive constants. As shown by (B.6), \mathcal{V} can be expressed using either the quaternion vector \tilde{q} or the quaternion scalar $\tilde{\eta}$ due to the constraint $\tilde{\eta}^2 + \tilde{q}^T\tilde{q} = 1$. Using the expressions (B.2) and (B.5) the time-derivative of \mathcal{V} is found to be

$$\dot{\mathcal{V}} = -\gamma k_1\tilde{r}_2^T\tilde{r}_2 - 2\gamma_q\tilde{\eta}^2\tilde{q}^T W\tilde{q} - \gamma_2\gamma_q\tilde{\eta}\tilde{q}^T S(\tilde{R}r_2)\tilde{r}_2 - \gamma\tilde{r}_2^T(I - \tilde{R})\dot{r}_2. \quad (\text{B.7})$$

To determine the upper bound for $\dot{\mathcal{V}}$, in light of Assumption 3.3, using Young's inequality we find

$$\gamma_2 \gamma_q \tilde{\eta} \tilde{q}^\top S(\tilde{R}r_2) \tilde{r}_2 \leq \frac{\epsilon_1 \gamma_2 \gamma_q c_1^2}{2} \tilde{r}_2^\top \tilde{r}_2 + \frac{\gamma_2 \gamma_q}{2\epsilon_1} \tilde{\eta}^2 \tilde{q}^\top \tilde{q}, \quad (\text{B.8})$$

$$\gamma \tilde{r}_2^\top (I - \tilde{R}) \dot{r}_2 = 2\gamma \tilde{r}_2^\top (S(\tilde{q}) - \tilde{\eta}I) S(\dot{r}_2) \tilde{q} \leq \epsilon_2 \gamma c_2^2 \tilde{r}_2^\top \tilde{r}_2 + \frac{\gamma}{\epsilon_2} \tilde{q}^\top \tilde{q}, \quad (\text{B.9})$$

where ϵ_1 and ϵ_2 are strictly positive constants, and where we used the fact that $\|S(\tilde{q}) - \tilde{\eta}I_{3 \times 3}\|^2 = \|\tilde{\eta}^2 I_{3 \times 3} - S(\tilde{q})^2\| = 1$ due to (2.25) and the unity-norm constraint $\tilde{\eta}^2 + \tilde{q}^\top \tilde{q} = 1$. Using these results, one obtains

$$\dot{\mathcal{V}} \leq -\gamma \left(k_1 - \epsilon_1 \frac{\gamma_2 \gamma_q c_1^2}{2\gamma} - \epsilon_2 c_2^2 \right) \|\tilde{r}_2\|^2 - \|\tilde{q}\|^2 \left(\left(2\gamma_q c_w - \frac{\gamma_2 \gamma_q}{2\epsilon_1} \right) (1 - \|\tilde{q}\|^2) - \frac{\gamma}{\epsilon_2} \right), \quad (\text{B.10})$$

where $c_w > 0$ is the lower bound of the minimum eigenvalue of W as defined in assumption (3.4). Using this result we find $\dot{\mathcal{V}} \leq 0$ if

$$k_1 > \kappa_1(\epsilon_1, \epsilon_2) := \epsilon_1 \gamma_2 \gamma_q c_1^2 / (2\gamma) + \epsilon_2 c_2^2, \quad (\text{B.11})$$

and \tilde{q} is contained within the set $D := \{\tilde{q} \in \mathbb{R}^3, \|\tilde{q}\| < \sqrt{1 - \gamma/(\epsilon_2 \xi)}\}$, where $\xi = 2\gamma_q c_w - \gamma_2 \gamma_q / (2\epsilon_1)$ and we assume that ϵ_1 and ϵ_2 are taken sufficiently large to ensure $\xi > 0$, and $1 - \gamma/(\epsilon_2 \xi) > 0$, respectively. Since $\mathcal{V} \geq \gamma_q \|\tilde{q}\|^2$, it follows that the domain of attraction contains the set

$$U := \left\{ (\tilde{r}_2, \tilde{q}) \in \mathbb{R}^3 \times \mathbb{R}^3, \frac{\gamma}{2} \|\tilde{r}_2\|^2 + \gamma_q \|\tilde{q}\|^2 < \gamma_q \left(1 - \frac{\gamma}{\epsilon_2 \xi} \right) \right\}. \quad (\text{B.12})$$

Note that by decreasing the parameter γ , the set U can be arbitrarily increased to contain almost any initial condition for \tilde{r}_2 and \tilde{q} except for when $\|\tilde{q}\| = 1$. This choice for γ must be followed by a choice of k_1 to satisfy (B.11). For all $(\tilde{r}_2(t_0), \tilde{q}(t_0)) \in U$, then $\dot{\mathcal{V}} \leq 0$ for all $t > t_0$ which implies that \tilde{r}_2 is bounded. Since r_2 is bounded (due to Assumption 3.3), it follows from the definition of \tilde{r}_2 that the error function \tilde{v} is bounded, and therefore σ and \hat{v} are bounded. In light of Assumption 3.1, it follows that the observer input $(\omega + \sigma)$ is bounded. This proves that all associated observer signals are bounded.

The result $\dot{\mathcal{V}}(t) \leq 0$ also implies that a lower bound for $(1 - \|\tilde{q}\|^2) = \tilde{\eta}^2 > 0$ exists for all initial conditions in U . To show exponential convergence, we will now define this bound quantitatively. For the remainder of the proof, assume that $(\tilde{r}_2(t_0), \tilde{q}(t_0)) \in U$. Therefore, $\mathcal{V}(t_0)/\gamma_q < 1 - \gamma/(\epsilon_2\xi) < 1$, due to the choices for ϵ_1 and ϵ_2 . Also, since $\mathcal{V}/\gamma_q \geq \|\tilde{q}\|^2$, this further implies $1 - \|\tilde{q}\|^2 \geq 1 - \mathcal{V}/\gamma_q$. Since \mathcal{V} is a non-increasing function, it follows that the lower bound for the quaternion is given by

$$1 - \|\tilde{q}(t)\|^2 = \tilde{\eta}(t)^2 \geq 1 - \mathcal{V}(t_0)/\gamma_q > 0, \quad \forall t \geq t_0. \quad (\text{B.13})$$

Therefore, an upper-bound for $\dot{\mathcal{V}}$ is given by

$$\dot{\mathcal{V}} \leq -\delta_r \|\tilde{r}_2\|^2 - \delta_q \|\tilde{q}\|^2, \quad (\text{B.14})$$

$$\delta_r = \gamma \left(k_1 - \epsilon_1 \gamma_2 \gamma_q c_1^2 / (2\gamma) - \epsilon_2 c_2^2 \right), \quad (\text{B.15})$$

$$\delta_q = \xi \left(1 - \mathcal{V}(t_0)/\gamma_q \right) - \gamma/\epsilon_2, \quad (\text{B.16})$$

for all $t \geq t_0$. Therefore, since $\delta_q > 0$ for initial conditions starting in U , and $\delta_r > 0$

due to the choice for k_1 , we can further see that

$$\dot{\mathcal{V}} \leq -\epsilon_v \mathcal{V}, \quad \epsilon_v = \min(\delta_r, \delta_q) / \max(\gamma/2, \gamma_q), \quad (\text{B.17})$$

which implies that the states \tilde{r}_2 , \tilde{q} and therefore \tilde{v} converge exponentially to zero. Since \tilde{q} exponentially converges to zero, and since $\tilde{\eta}(t)$ never crosses zero, then this suggests that $\tilde{\eta}$ converges exponentially to $\text{sgn}(\tilde{\eta}(t_0))$, which concludes the proof. \square

B.2 Proof for Theorem 3.2

(Third Order Observer Using IMU and GPS Measurements)

From (3.46) we see that due to the choice for (3.47), the attitude observer is now updated using the error function \tilde{v} in addition to the dynamic state ψ . In this more general case, we define the error function \tilde{r}_2 as follows:

$$\tilde{r}_2 = k_2 \psi + k_3 \tilde{v} + (\tilde{R} - I)r_2. \quad (\text{B.18})$$

Using this error function, we now wish to write the time-derivative of the error function \tilde{v} in terms of \tilde{r}_2 . Using (3.36), (3.49), and substituting the value for ψ using (B.18) we find

$$\begin{aligned} \dot{\tilde{v}} &= -k_1 \tilde{v} + (I - \tilde{R})r_2 - \frac{k_6}{k_2} \left(\tilde{r}_2 - k_3 \tilde{v} - (\tilde{R} - I)r_2 \right) \\ &= \alpha_1 \tilde{v} + \alpha_2 \tilde{r}_2 + \alpha_3 (\tilde{R} - I)r_2, \end{aligned} \quad (\text{B.19})$$

where $\alpha_1 = -k_1 + k_3 k_6 / k_2$, $\alpha_2 = -k_6 / k_2$ and $\alpha_3 = k_6 / k_2 - 1$. Using the expressions for the time-derivatives of ψ , \tilde{v} and \tilde{R} from (3.48), (B.19) and (3.23), respectively, and the expression for $\tilde{\omega}$ from (3.24), we now find the time-derivative of \tilde{r}_2 to be given

by

$$\begin{aligned}
\dot{\tilde{r}}_2 &= -k_2 k_4 \psi + \hat{R}^\top S(b_2) \sigma - k_2 k_5 \tilde{v} + k_3 \left(\alpha_1 \tilde{v} + \alpha_2 \tilde{r}_2 \right. \\
&\quad \left. + \alpha_3 (\tilde{R} - I) r_2 \right) + S(\hat{R}^\top \sigma) \hat{R}^\top b_2 + (\tilde{R} - I) \dot{r}_2 \\
&= \alpha_4 \tilde{r}_2 + \alpha_5 \tilde{v} + \alpha_6 (\tilde{R} - I) r_2 + (\tilde{R} - I) \dot{r}_2,
\end{aligned} \tag{B.20}$$

where $\alpha_4 = -k_4 - k_3 k_6 / k_2$, $\alpha_5 = k_3 k_4 + k_3^2 k_6 / k_2 - k_2 k_5 - k_1 k_3$ and $\alpha_6 = k_4 - k_3 + k_3 k_6 / k_2$. Note that in light of the choices of k_5 and k_6 from (3.50), the coefficients α_i are subsequently found to be

$$\begin{aligned}
\alpha_1 &= -k_1 + k_3 - k_4, & \alpha_4 &= -k_3, \\
\alpha_2 &= k_4 / k_3 - 1, & \alpha_5 &= 1 / \gamma_r (1 - k_4 / k_3), \\
\alpha_3 &= -k_4 / k_3, & \alpha_6 &= 0.
\end{aligned} \tag{B.21}$$

Consequently, one can see that $\alpha_2 + \gamma_r \alpha_5 = 0$. Now, let us consider the dynamics of the quaternion scalar $\tilde{\eta}$. Using a similar procedure as in the proof for the first observer, in light of (3.23), (3.24), (3.46), (3.47) and the property (2.23) the time-derivative of $\tilde{\eta}$ is given by

$$\begin{aligned}
\dot{\tilde{\eta}} &= -\frac{1}{2} \tilde{q}^\top \left(\gamma_1 S(r_1) \tilde{R} r_1 + \gamma_2 S(\tilde{r}_2 + (I - \tilde{R}) r_2) \tilde{R} r_2 \right) \\
&= \tilde{\eta} \tilde{q}^\top W \tilde{q} + \frac{\gamma_2}{2} \tilde{q}^\top S(\tilde{R} r_2) \tilde{r}_2.
\end{aligned} \tag{B.22}$$

Now, let us consider the following Lyapunov function candidate:

$$\mathcal{V} = \frac{\gamma}{2} (\tilde{v}^\top \tilde{v} + \gamma_r \tilde{r}_2^\top \tilde{r}_2) + \gamma_q \tilde{q}^\top \tilde{q} = \frac{\gamma}{2} (\tilde{v}^\top \tilde{v} + \gamma_r \tilde{r}_2^\top \tilde{r}_2) + \gamma_q (1 - \tilde{\eta}^2), \tag{B.23}$$

where $\gamma, \gamma_q, \gamma_r > 0$. In light of the expressions for the time-derivatives of \tilde{v} , \tilde{r}_2 and $\tilde{\eta}$

from (B.19), (B.20) and (B.22), respectively, in addition to the fact that $\alpha_2 + \gamma_r \alpha_5 = 0$ and $\alpha_6 = 0$, the time-derivative of \mathcal{V} is given by

$$\dot{\mathcal{V}} = \gamma \alpha_1 \tilde{v}^\top \tilde{v} + \gamma \gamma_r \alpha_4 \tilde{r}_2^\top \tilde{r}_2 + \gamma \alpha_3 \tilde{v}^\top (\tilde{R} - I) r_2 - 2\gamma_q \tilde{\eta}^2 \tilde{q}^\top W \tilde{q} - \gamma_2 \gamma_q \tilde{\eta} \tilde{q}^\top S(\tilde{R} r_2) \tilde{r}_2. \quad (\text{B.24})$$

To find an upper bound for this result, in light of Assumption 3.3 and the expressions for the coefficients α_i given by (B.21), we use Young's inequality to find the bounds of the following cross terms:

$$\begin{aligned} \gamma \alpha_3 \tilde{v}^\top (\tilde{R} - I) r_2 &= 2\gamma \alpha_3 \tilde{v}^\top (\tilde{\eta} I - S(\tilde{q})) S(r_2) \tilde{q} \\ &\leq \epsilon_1 \frac{\gamma c_1^2 k_4^2}{k_3^2} \tilde{v}^\top \tilde{v} + \frac{\gamma}{\epsilon_1} \tilde{q}^\top \tilde{q}, \end{aligned} \quad (\text{B.25})$$

$$\gamma \gamma_r \tilde{r}_2^\top (\tilde{R} - I) r_2 \leq \epsilon_2 \gamma \gamma_r c_2^2 \tilde{r}_2^\top \tilde{r}_2 + \frac{\gamma \gamma_r}{\epsilon_2} \tilde{q}^\top \tilde{q}, \quad (\text{B.26})$$

$$\gamma_2 \gamma_q \tilde{\eta} \tilde{q}^\top S(\tilde{R} r_2) \tilde{r}_2 \leq \epsilon_3 \frac{\gamma_q c_1^2 \gamma_2^2}{2} \tilde{r}_2^\top \tilde{r}_2 + \frac{\gamma_q}{2\epsilon_3} \tilde{\eta}^2 \tilde{q}^\top \tilde{q}, \quad (\text{B.27})$$

where $\epsilon_{1,2,3} > 0$. Therefore, we have

$$\begin{aligned} \dot{\mathcal{V}} &\leq -\gamma (k_1 - \kappa_1(\epsilon_1)) \|\tilde{v}\|^2 - \gamma \gamma_r (k_3 - \kappa_3(\epsilon_2, \epsilon_3)) \|\tilde{r}_2\|^2 \\ &\quad - \gamma_q \left(\xi_1 (1 - \|\tilde{q}\|^2) - \gamma \xi_2 \right) \|\tilde{q}\|^2, \end{aligned} \quad (\text{B.28})$$

$$\kappa_1(\epsilon_1) := k_3 - k_4 + \epsilon_1 c_1^2 k_4^2 / k_3^2, \quad (\text{B.29})$$

$$\kappa_3(\epsilon_2, \epsilon_3) := \epsilon_2 c_2^2 + \epsilon_3 \gamma_q c_1^2 \gamma_2^2 / (2\gamma \gamma_r), \quad (\text{B.30})$$

$$\xi_1 = 2c_w - \frac{1}{2\epsilon_3}, \quad \xi_2 = \frac{1}{\gamma_q} \left(\frac{1}{\epsilon_1} + \frac{\gamma_r}{\epsilon_2} \right). \quad (\text{B.31})$$

Therefore, if $k_3 > \kappa_3(\epsilon_2, \epsilon_3)$ and $k_1 > \kappa_1(\epsilon_1)$, a sufficient condition for $\dot{\mathcal{V}} \leq 0$ is that \tilde{q} is contained within the set

$$D := \left\{ \tilde{q} \in \mathbb{R}^3, \|\tilde{q}\| < \sqrt{1 - \gamma\xi_2/\xi_1} \right\}, \quad (\text{B.32})$$

where we assume that ϵ_3 is chosen sufficiently large such that $\xi_1 > 0$, and ϵ_1 and ϵ_2 are chosen sufficiently large to ensure $\gamma\xi_2/\xi_1 < 1$. Since $\mathcal{V} \geq \gamma_q\|\tilde{q}\|^2$, it follows that the domain of attraction contains the set

$$U := \left\{ (\tilde{v}, \tilde{r}_2, \tilde{q}) \in \mathbb{R}^3 \times \mathbb{R}^3 \times \mathbb{R}^3; \gamma (\|\tilde{v}\|^2/2 + \gamma_r\|\tilde{r}_2\|^2) + \gamma_q\|\tilde{q}\|^2 < \gamma_q(1 - \gamma\xi_2/\xi_1) \right\}. \quad (\text{B.33})$$

Note that by decreasing the parameter γ , the set U can be arbitrarily increased to contain almost any initial condition for \tilde{v} , \tilde{r}_2 and \tilde{q} except when $\|\tilde{q}\| = 1$. This choice of γ is followed by a choice of k_3 and k_1 to ensure $k_3 > \kappa_3$ and $k_1 > \kappa_1$, and k_2 and k_4 can be arbitrarily chosen¹. Therefore, for all initial conditions $(\tilde{v}(t_0), \tilde{r}_2(t_0), \tilde{q}(t_0)) \in U$, it follows that $\dot{\mathcal{V}} \leq 0$ for all $t \geq t_0$. This implies that \tilde{v} and \tilde{r}_2 are bounded. Note that ω and v are bounded due to Assumption 3.1. Therefore, due to the bound of \tilde{v} then \hat{v} is also bounded. The bound of the signal ψ follows from the fact that \tilde{r}_2 and r_2 are bounded (due to Assumption 3.3). Therefore, the signal σ , and consequently the observer input $(\omega + \sigma)$, are bounded, thus proving that all associated observer signals are bounded.

To prove exponential convergence, we must first show that there exists a lower

1. Although the gain k_4 can be chosen to take any value, from a practical standpoint this gain should be chosen to be positive since this introduces a *leakage term* in the dynamics of ψ , and can improve the performance of the observer in the presence of noise and other disturbances. For more information on this leakage term, in addition to other practical tools in the area of adaptive control, the reader is referred to Ioannou and Sun (1996).

bound for the signal $\tilde{\eta}^2 = 1 - \|\tilde{q}\|^2$, which is strictly positive, for all initial conditions in U . For the remainder of the proof let us assume $(\tilde{v}(t_0), \tilde{r}_2(t_0), \tilde{q}(t_0)) \in U$. Recall the parameters ϵ_2 and ϵ_3 were chosen sufficiently large to ensure $1 - \gamma\xi_2/\xi_1 > 0$. If we start within the set U , then

$$\mathcal{V}(t_0) < \gamma_q(1 - \gamma\xi_2/\xi_1). \quad (\text{B.34})$$

Since $\mathcal{V} \geq \gamma_q\|\tilde{q}\|^2$, and due to the fact that \mathcal{V} is non-increasing in U , then the lower bound for the quaternion is given by $\tilde{\eta}^2 = 1 - \|\tilde{q}\|^2 \geq 1 - \mathcal{V}(t_0)/\gamma_q > \gamma\xi_2/\xi_1 > 0$ for all $t \geq t_0$. Therefore, one has

$$\dot{\mathcal{V}} \leq -\delta_r \tilde{r}_2^\top \tilde{r}_2 - \delta_v \tilde{v}^\top \tilde{v} - \delta_q \tilde{q}^\top \tilde{q}, \quad (\text{B.35})$$

$$\delta_r = \gamma\gamma_r(k_3 - \kappa_3(\epsilon_2, \epsilon_3)), \quad (\text{B.36})$$

$$\delta_v = \gamma(k_1 - \kappa_1(\epsilon_1)), \quad (\text{B.37})$$

$$\delta_q = \xi_1(\gamma_q - \mathcal{V}(t_0)) - \gamma\gamma_q\xi_2, \quad (\text{B.38})$$

for all $t \geq t_0$, where δ_q is positive for initial conditions in U , and δ_r and δ_v are positive constants due to the choices of the observer gains k_3 and k_1 , respectively. Also, in light of the definition of the Lyapunov function we obtain

$$\dot{\mathcal{V}} \leq -\epsilon_v \mathcal{V}, \quad (\text{B.39})$$

where $\epsilon_v = \min(\delta_v, \delta_r, \delta_q)/\max(\gamma/2, \gamma\gamma_r/2, \gamma_q)$, which implies that \mathcal{V} converges exponentially to zero. This implies that \tilde{r}_2 , \tilde{q} and \tilde{v} converge exponentially to zero. Since \tilde{q} converges exponentially to zero, and $\tilde{\eta}$ never crosses zero, then this implies that $\tilde{\eta}$ converges exponentially to $\text{sgn}(\tilde{\eta}(t_0))$, which concludes the proof. \square

B.3 Proof for Theorem 4.1

(Vector Measurement Based Attitude Stabilization)

Let $\tilde{b}_i = \hat{b}_i - b_i$ denote the *measurement error*, and consider the following candidate Lyapunov function:

$$\mathcal{V} = \frac{1}{2}\omega^\top I_b \omega + \frac{1}{2} \sum_{i=1}^n \left(\gamma_i \tilde{b}_i^\top \tilde{b}_i + \rho_i (b_i - r_i)^\top (b_i - r_i) \right). \quad (\text{B.40})$$

In light of (4.1) and (4.5), the derivatives of the corresponding rotation matrices are given by $\dot{R} = -S(\omega)R$ and $\dot{\hat{R}} = -S(\beta)\hat{R}$. Therefore, the time-derivative of \mathcal{V} is given by

$$\dot{\mathcal{V}} = \omega^\top u + \sum_{i=1}^n \left(\gamma_i \tilde{b}_i^\top S(\hat{b}_i)(\beta - \omega) + \rho_i (b_i - r_i)^\top S(b_i)\omega \right) \quad (\text{B.41})$$

$$= \omega^\top u + \sum_{i=1}^n \left(\gamma_i \tilde{b}_i^\top S(\hat{b}_i)(\beta - \omega) - \rho_i r_i^\top S(b_i)\omega \right) \quad (\text{B.42})$$

$$= \omega^\top u + z_\gamma^\top (\beta - \omega) + z_\rho^\top \omega. \quad (\text{B.43})$$

Applying the expressions for the estimation and control laws from (4.5),(4.6) and (4.7) we obtain

$$\dot{\mathcal{V}} = -z_\gamma^\top z_\gamma. \quad (\text{B.44})$$

Consequently, \mathcal{V} is non-increasing and bounded, which implies that ω is bounded. Note that Q , \hat{Q} , R and \hat{R} are bounded by definition, which implies that b_i and \hat{b}_i are also bounded a priori. Since $\ddot{\mathcal{V}}$ is bounded, due to the bound of ω , then $\lim_{t \rightarrow \infty} z_\gamma(t) = 0$. At this point we can apply Lemma 4 which implies $\lim_{t \rightarrow \infty} \tilde{Q}(t) = (\pm 1, \mathbf{0})$ or $\lim_{t \rightarrow \infty} \tilde{Q}(t) = (0, \pm v)$ where v is a unit-eigenvector of the matrix W defined by (4.4). Furthermore, one can show that $\ddot{\tilde{Q}}$ is bounded, and therefore

$\lim_{t \rightarrow \infty} \dot{Q} = 0$, which implies $\lim_{t \rightarrow \infty} (\omega(t) - \beta(t)) = 0$. Consequently, $\lim_{t \rightarrow \infty} \omega(t) = 0$ since $\beta = -z_\gamma$ tends to zero. One can also show that $\ddot{\omega}$ is bounded, and therefore, since $\lim_{t \rightarrow \infty} \omega(t) = 0$, this implies that $\lim_{t \rightarrow \infty} \dot{\omega}(t) = 0$. This fact further implies that $\lim_{t \rightarrow \infty} u(t) = \lim_{t \rightarrow \infty} z_\rho(t) = 0$ since z_γ tends to zero.

At this point we wish to write z_ρ in terms of the unit-quaternion scalar q (system attitude). Using (4.3), (2.8), and the properties (2.20) and (2.22) we find

$$z_\rho = 2R \sum_{i=1}^n \rho_i S(r_i) \left(qq^\top + \eta S(q) \right) r_i \quad (\text{B.45})$$

$$= -2R \sum_{i=1}^n \rho_i \left(S(q) r_i r_i^\top q + \eta S(r_i)^2 q \right). \quad (\text{B.46})$$

Using the fact that $r_i r_i^\top = S(r_i)^2 + r_i^\top r_i I$ we obtain

$$z_\rho = 2R(\eta I + S(q))W_c q. \quad (\text{B.47})$$

Note that the matrix W_c , which is defined by (4.4), is positive definite since we assume there are at least two non-collinear vectors. The fact $z_\rho = 0$ therefore implies

$$(\eta I + S(q))W_c q = 0, \quad (\text{B.48})$$

for which an obvious solution is $q = 0$ and therefore $\eta = \pm 1$ (desired solution). To find other equilibria, we pre-multiply by $q^\top \neq 0$ to obtain

$$\eta q^\top W_c q = 0, \quad (\text{B.49})$$

which implies that $\eta = 0$ since W_c is positive definite. When $\eta = 0$, we know from

the unit-norm constraint that $\|q\| = 1$. In this case (B.48) becomes

$$S(q)W_c q = 0 \quad (\text{B.50})$$

Therefore, the equilibrium solutions corresponding to the case $\eta = 0$ is given by $\tilde{Q} = (0, \pm v_c)$ where v_c is a unit eigenvector of the matrix W_c .

We now wish to show that the undesired equilibria (corresponding to $\eta = 0$) are unstable for an appropriate choice of the gains ρ_i using Chetaev arguments. Let us define $\delta := q^\top I_b \omega$ and consider the dynamics of η and δ around the equilibria ($\eta = 0, \omega = 0$)

$$\dot{\eta} = -\frac{1}{2}v_c^\top \omega, \quad (\text{B.51})$$

$$\dot{\delta} = -2\xi_c \eta, \quad (\text{B.52})$$

where $\xi_c = v_c^\top W_c v_c$ is an eigenvalue of the matrix W_c . Let us now consider the following Chetaev function

$$\mathcal{V}_c = -\eta\delta. \quad (\text{B.53})$$

Note that $\mathcal{V}_c = 0$ at the equilibrium points in question, and also note there exists a domain around the equilibrium points such that $\mathcal{V}_c > 0$, which consists of the second and fourth quadrant of the plane (η, δ) . The time-derivative of \mathcal{V}_c in light of (B.51)-(B.52) is given by

$$\dot{\mathcal{V}}_c = 2\xi_c \eta^2 + \frac{1}{2}\delta v_c^\top \omega \geq (2\lambda_{\min}(W_c) - \frac{1}{2}k_b k_q^2)\eta^2, \quad (\text{B.54})$$

where we used the fact that $|\delta| \leq k_b \omega$, with $k_b = \|I_b\|$, and the fact that around the equilibria there exists a positive parameter k_q such that $\|\omega\| \leq k_q |\eta|$. It is clear that

by increasing the gains ρ_i , we can satisfy $\lambda_{\min}(W_c) > \frac{1}{4}k_b k_q^2 := k_c$, which guarantees that $\dot{\mathcal{V}}_c > 0$ for all $\eta \neq 0$. Using Chetaev's arguments, one can conclude that the equilibria characterized by $(\eta = 0, \omega = 0)$ are unstable.

B.4 Proof for Theorem 4.2

(Adaptive Position Tracking)

In the following sections we present the proof of the control law proposed in Section 4.3.2.4. The proof is completed in a number of stages. In Section B.4.1 we focus on the upper and lower bounds for the system thrust as a result of the proposed control law. In Section B.4.2 we analyze the system translational dynamics, the dynamics of the estimation error, and the dynamics of the angular velocity associated with the quaternion Q_d . The parts of the proof contained in Section B.4.1 and B.4.2 are the same for both proposed control laws. Section B.4.3 finalizes the proof for the first proposed control law, where the proof for the second control law can be found in Section B.4.4. Section B.4.5 provides derivatives of a number of functions that are necessary to implement the controller.

B.4.1 Bounded Control

The proposed control laws are based on ensuring that the virtual control law is always contained within the set U defined by (4.22). Fortunately, the singularity can be avoided if the third component of the virtual control law μ_d is bounded such that $\mu_{d3} = e_3^\top \mu_d < g$. Recall the expression for the signal μ_d given by (4.41). Due to Assumption 4.1, the acceleration of the reference trajectory is bounded such that $e_3^\top \ddot{p}_d < \delta_{rz} < g$ and $\|\ddot{p}_d\| < \delta_r$ where the parameters δ_r and δ_{rz} are known *a priori*. Given the projection based estimation law (4.43) and the property (4.40), the

disturbance estimate $\hat{\theta}_1$ is bounded such that $\|\hat{\theta}_1\| < \delta_a + k_\theta + \epsilon_\alpha$. Also, the function $h(\cdot)$, defined by (2.27), is bounded such that $0 \leq \|h(\cdot)\| < 1$. Consequently, the signal μ_d is also bounded by

$$\|\mu_d\| < \bar{\mu}_d = k_p \|\Gamma_v^{-1}\| + \delta_r + \delta_a + 2k_\theta + k_v + \epsilon_\alpha, \quad (\text{B.55})$$

$$|e_3^\top \mu_d| < \bar{\mu}_{d3} = k_p \|e_3^\top \Gamma_v^{-1}\| + \delta_{rz} + \delta_a + 2k_\theta + k_v + \epsilon_\alpha. \quad (\text{B.56})$$

where due to (4.42), the bound on the third component of μ_d is limited to $|e_3^\top \mu_d| = |\mu_{d3}| < \bar{\mu}_{d3} < g$. As a result we find

$$\underline{c}_t = g - \bar{\mu}_{d3} > 0. \quad (\text{B.57})$$

As a result of the bounds (B.55)-(B.57), the system thrust, given by (4.19), is also bounded such that $\underline{c}_t < u_t < \bar{c}_t$ where $\bar{c}_t = \bar{\mu}_d + g$. Therefore, the system thrust never vanishes and μ_d is always contained within the set U given by (4.22).

B.4.2 Translational and Quaternion Dynamics

Recall the expression for the velocity error dynamics defined by (4.32), and let $\tilde{\theta}_1$ denote the following estimation error function

$$\tilde{\theta}_1 = \theta_a - \hat{\theta}_1 - k_\theta h(\tilde{v}). \quad (\text{B.58})$$

Given the virtual control law μ_d defined by (4.41) and the estimation error $\tilde{\theta}_1$, the time derivative of the velocity error can now be written as

$$\dot{\tilde{v}} = \tilde{\mu} - K_1 h(\tilde{p}) - K_2 h(\tilde{v}) - \hat{\theta}_1 + \theta_a = \tilde{\mu} - K_1 h(\tilde{p}) - k_v h(\tilde{v}) + \tilde{\theta}_1, \quad (\text{B.59})$$

where $K_1 = k_p \Gamma_v^{-1}$ and $K_2 = (k_v + k_\theta) I_{3 \times 3}$. Furthermore, in light of assumption (4.3) and the velocity error (B.59) the time-derivative of (B.58) is given by

$$\dot{\tilde{\theta}}_1 = -k_\theta \phi_h(\tilde{v}) \tilde{\theta}_1 + \tau_1 - \dot{\tilde{\theta}}_1, \quad (\text{B.60})$$

$$\tau_1 = -k_\theta \phi_h(\tilde{v}) (\tilde{\mu} - K_1 h(\tilde{p}) - k_v h(\tilde{v})). \quad (\text{B.61})$$

The expressions for $\dot{\tilde{v}}$ and $\dot{\tilde{\theta}}_1$ are dependant on the error function $\tilde{\mu} = \mu - \mu_d$. A more convenient notation is to express the error function $\tilde{\mu}$ in terms of the attitude error $\tilde{Q} = (\tilde{\eta}, \tilde{q}) = Q_d^{-1} \odot Q$, where Q_d is the desired attitude defined by (4.20) and (4.21). This can be achieved if we consider the rotation matrix $\tilde{R} = R R_d^\top$ (which corresponds to the unit quaternion \tilde{Q}) and the fact that $\tilde{R} = I + 2S(\tilde{q})^2 - 2\tilde{\eta}S(\tilde{q})$, to obtain

$$\tilde{\mu} = W_1^\top \tilde{q}, \quad W_1 = -2u_t S(\tilde{q}) R, \quad \tilde{q} = S(e_3) \tilde{q} + \tilde{\eta} e_3. \quad (\text{B.62})$$

Consequently, the expressions for $\dot{\tilde{v}}$ and $\dot{\tilde{\theta}}_1$ can be written as functions of the attitude error \tilde{q} .

At this point we focus our attention on the dynamics of the attitude error in terms of the quaternion scalar $\tilde{\eta}$. From (4.29), we note that the time-derivative of $\tilde{\eta}$ is given by $\dot{\tilde{\eta}} = \frac{1}{2} \tilde{q}^\top (\omega_d - \omega)$, where from (4.25) we recall $\omega_d = M(\mu_d) \dot{\mu}_d$. Differentiating (4.41) in light of (4.43) and (B.59), we find the derivative $\dot{\mu}_d$ to be

given by

$$\dot{\mu}_d = r^{(3)} + w_\beta + W_2 h(\tilde{v}) + W_3 \tilde{q} + W_4 \tilde{v} - (k_\theta + k_v) \phi_h(\tilde{v}) \tilde{\theta}_1, \quad (\text{B.63})$$

$$W_2 = k_v^2 \phi_h(\tilde{v}),$$

$$W_3 = -\gamma_{\theta_1} \gamma_q (k_\theta + k_v) \phi_h(\tilde{v}) M(\mu_d)^\top - k_v \phi_h(\tilde{v}) W_1^\top,$$

$$W_4 = -\gamma_{\theta_1} \Gamma_v - k_p \Gamma_v^{-1} \phi_h(\tilde{p}), \quad (\text{B.64})$$

$$w_\beta = k_v k_p \phi_h(\tilde{v}) \Gamma_v^{-1} h(\tilde{p}) - \gamma_{\theta_1} \alpha(\hat{\theta}_1, \delta_a + k_\theta, \tau_2),$$

from which we obtain the desired attitude dynamics

$$\begin{aligned} \omega_d = & M(\mu_d) \left(p_d^{(3)} + w_\beta + W_2 h(\tilde{v}) + W_3 \tilde{q} + W_4 \tilde{v} \right) \\ & - (k_\theta + k_v) M(\mu_d) \phi_h(\tilde{v}) \tilde{\theta}_1. \end{aligned} \quad (\text{B.65})$$

Since ω_d is not entirely known (due to the presence of the signal $\tilde{\theta}_1$), it is necessary to study the upper bound of the undesired terms in (B.65). For the most part, this analysis is straightforward except for the matrix $M(\mu_d)$. To determine an upper-bound for this matrix defined by (4.26), we first realize that the function $M(\mu_d)$ can also be written as

$$M(\mu_d) = \frac{1}{\|\mu_d - ge_3\|^2 c_1} \cdot \begin{bmatrix} -\mu_{d_1} \mu_{d_2} & -\mu_{d_2}^2 + \|\mu_d - ge_3\| c_1 & \mu_{d_2} c_1 \\ \mu_{d_1}^2 - \|\mu_d - ge_3\| c_1 & \mu_{d_1} \mu_{d_2} & -\mu_{d_1} c_1 \\ \mu_{d_2} \|\mu_d - ge_3\| & -\mu_{d_1} \|\mu_d - ge_3\| & 0 \end{bmatrix} \quad (\text{B.66})$$

where $c_1 = \|\mu_d - ge_3\| + g - \mu_{d_3}$. For convenience we let $\xi = \text{col} [\xi_1, \xi_2, \xi_3] = \mu_d - ge_3$.

Applying the Frobenius norm to this expression for $M(\mu_d)$, we find

$$\|M(\mu_d)\|_F = \sqrt{\frac{2}{\|\xi\|(\|\xi\| + |\xi_3|)} + \frac{1}{\|\xi\|^2}}. \quad (\text{B.67})$$

Due to the bound of μ_d , we find $\inf\{\|\xi\|\} = \inf\{|\xi_3|\} = \underline{c}_t > 0$, and therefore the norm of $M(\mu_d)$ is bounded and given by

$$\|M(\mu_d)\|_F \leq \frac{\sqrt{2}}{\underline{c}_t}. \quad (\text{B.68})$$

We now propose the following function

$$\mathcal{V}_1 = k_p(\sqrt{1 + \tilde{p}^\top \tilde{p}} - 1) + \frac{1}{2}\tilde{v}^\top \Gamma_v \tilde{v} + 2\gamma_q(1 - \tilde{\eta}) + \frac{1}{2\gamma_{\theta_1}}\tilde{\theta}_1^\top \tilde{\theta}_1. \quad (\text{B.69})$$

Given (4.31),(4.33), (B.59)-(B.61), (B.65) and the adaptive estimation law (4.44), we differentiate \mathcal{V}_1 to obtain

$$\begin{aligned} \dot{\mathcal{V}}_1 = & -k_v \tilde{v}^\top \Gamma_v h(\tilde{v}) - \frac{k_\theta}{\gamma_{\theta_1}} \tilde{\theta}_1^\top \phi_h(\tilde{v}) \tilde{\theta}_1 - \tilde{\theta}_1^\top \alpha \left(\hat{\theta}_1, \delta_a + k_\theta, \tau_2 \right) \\ & + \tilde{q}^\top \left(\Phi \tilde{v} + \gamma_q \left(\omega - M(\mu_d) \left(r^{(3)} - M(\mu_d) w_\beta + W_2 h(\tilde{v}) + W_3 \tilde{q} \right) \right) \right), \end{aligned} \quad (\text{B.70})$$

$$\Phi = W_1 \Gamma_v - \gamma_q M(\mu_d) W_4. \quad (\text{B.71})$$

B.4.3 Angular Velocity Error Dynamics - Controller 1

Recall the expression for the angular velocity error is given by $\tilde{\omega} = \omega - \beta_1$. Applying the the virtual control law β_1 , given by (4.46), to $\dot{\mathcal{V}}_1$ defined by (B.70) we obtain

$$\begin{aligned} \dot{\mathcal{V}}_1 = & -k_v \tilde{v}^\top \Gamma_v h(\tilde{v}) - \frac{k_\theta}{\gamma_{\theta_1}} \tilde{\theta}_1^\top \phi_h(\tilde{v}) \tilde{\theta}_1 + \gamma_q \tilde{q}^\top \tilde{\omega} - \tilde{\theta}_1^\top \alpha \left(\hat{\theta}_1, \delta_a + k_\theta, \tau_2 \right) \\ & - \gamma_q \tilde{q}^\top M(\mu_d) W_2 h(\tilde{v}) - \gamma_q \tilde{q}^\top (K_q + M(\mu_d) W_3) \tilde{q}. \end{aligned} \quad (\text{B.72})$$

To further simplify this result, using (2.26) and (B.68) we apply Young's inequality to obtain the following upper-bound

$$|\gamma_q \tilde{q}^\top M(\mu_d) W_2 h(\tilde{v})| \leq \frac{\gamma_q k_v^2}{2\epsilon_1} \tilde{q}^\top \tilde{q} + \frac{\gamma_q k_v^2 \epsilon_1}{\underline{c}_t^2} \tilde{v}^\top h(\tilde{v}), \quad (\text{B.73})$$

where $\epsilon_1 > 0$. Furthermore, due to $\|S(\bar{q})\| \leq 1$ and $u_t < \bar{c}_t = g + \bar{\mu}_d$, we also find

$$\|M(\mu_d) W_3\| \leq \frac{2\sqrt{2}k_v \bar{c}_t}{\underline{c}_t} + \frac{2\gamma_{\theta_1} \gamma_q (k_\theta + k_v)}{\underline{c}_t^2}. \quad (\text{B.74})$$

Due to the bounds (B.73)-(B.74), the time derivative of (B.72) is bounded by

$$\begin{aligned} \dot{\mathcal{V}}_1 &\leq -\tilde{v}^\top \Delta_v h(\tilde{v}) - \gamma_q \tilde{q}^\top \Delta_q \tilde{q} - \frac{k_\theta}{\gamma_{\theta_1}} \tilde{\theta}_1^\top \phi_h(\tilde{v}) \tilde{\theta}_1 \\ &\quad - \tilde{\theta}_1^\top \alpha \left(\hat{\theta}_1, \delta_a + k_\theta, \tau_2 \right) + \gamma_q \tilde{q}^\top \tilde{\omega}, \end{aligned} \quad (\text{B.75})$$

$$\Delta_v = k_v \left(\Gamma_v - \frac{\gamma_q k_v \epsilon_1}{\underline{c}_t^2} I_{3 \times 3} \right), \quad (\text{B.76})$$

$$\Delta_q = K_q - \left(\frac{2\sqrt{2}k_v \bar{c}_t \underline{c}_t + 2\gamma_{\theta_1} \gamma_q (k_\theta + k_v)}{\underline{c}_t^2} + \frac{k_v^2}{2\epsilon_1} \right) I_{3 \times 3}. \quad (\text{B.77})$$

Provided that (4.54) is satisfied, then Δ_v and Δ_q are positive definite matrices. Using the error signals $\tilde{\theta}_2 = \theta_a - \hat{\theta}_2$ and $\tilde{\theta}_3 = \theta_b - \hat{\theta}_3$ we introduce the Lyapunov function candidate

$$\begin{aligned} \mathcal{V}_2 &= \mathcal{V}_1 + \frac{1}{2} \tilde{\omega}^\top I_b \tilde{\omega} + \frac{1}{2\gamma_{\theta_2}} \tilde{\theta}_2^\top \tilde{\theta}_2 + \frac{1}{2\gamma_{\theta_3}} \tilde{\theta}_3^\top \tilde{\theta}_3 \\ &= k_p \left(\sqrt{1 + \tilde{p}^\top \tilde{p}} - 1 \right) + \frac{1}{2} X^\top C X, \end{aligned} \quad (\text{B.78})$$

$$X = \text{col} \left[\tilde{v}, 1 - \tilde{\eta}, \tilde{q}, \tilde{\omega}, \tilde{\theta}_1, \tilde{\theta}_2, \tilde{\theta}_3 \right], \quad (\text{B.79})$$

$$C = \text{diag} \left[\Gamma_v, 4\gamma_q I_{4 \times 4}, I_b, \gamma_{\theta_1}^{-1} I, \gamma_{\theta_2}^{-1} I, \gamma_{\theta_3}^{-1} I \right]. \quad (\text{B.80})$$

where $I = I_{3 \times 3}$ unless otherwise noted. The time-derivative of (B.78) is subsequently found using (B.75), in addition to the control and estimation laws defined by (4.50)-(4.52) to obtain the following result

$$\begin{aligned} \dot{\mathcal{V}}_2 \leq & -\tilde{v}^\top \Delta_v h(\tilde{v}) - \gamma_q \tilde{q}^\top \Delta_q \tilde{q} - \frac{k_\theta}{\gamma_{\theta_1}} \tilde{\theta}_1^\top \phi_h(\tilde{v}) \tilde{\theta}_1 - \tilde{\omega}^\top K_\omega \tilde{\omega} - \tilde{\theta}_1^\top \alpha \left(\hat{\theta}_1, \delta_a + k_\theta, \tau_2 \right) \\ & - \tilde{\theta}_2^\top \alpha \left(\hat{\theta}_2, \delta_a, -\bar{f}_{\beta_1}^\top I_b \tilde{\omega} \right) - \tilde{\theta}_3^\top \alpha \left(\hat{\theta}_3, \delta_b, -R^\top S(e_3) \tilde{\omega} \right). \end{aligned}$$

Due to the property of the projection law given by (4.40) then $\tilde{\theta}_i^\top \alpha > 0$, and the Lyapunov function derivative can be simplified as follows

$$\dot{\mathcal{V}}_2 \leq -\tilde{v}^\top \Delta_v h(\tilde{v}) - \gamma_q \tilde{q}^\top \Delta_q \tilde{q} - \frac{k_\theta}{\gamma_{\theta_1}} \tilde{\theta}_1^\top \phi_h(\tilde{v}) \tilde{\theta}_1 - \tilde{\omega}^\top K_\omega \tilde{\omega}.$$

Therefore, $\dot{\mathcal{V}}_2 \leq 0$ and the states $(\tilde{p}, \tilde{v}, \tilde{\omega})$ are bounded. The attitude error \tilde{Q} is bounded by definition, and the adaptive estimation error $\tilde{\theta}_{1,2,3}$ are bounded due to assumption 2 and due to the property of the projection mechanism (4.40). Applying Barbalat's Lemma, $\ddot{\mathcal{V}}_2$ is bounded due to assumption 1 which shows that $(\tilde{p}, \tilde{v}, \tilde{q}, \tilde{\omega}, \tilde{\theta}_1) \rightarrow 0$ as $t \rightarrow \infty$. Since $\tilde{\theta}_1 \rightarrow 0$ and $\tilde{v} \rightarrow 0$, then $\hat{\theta}_1 \rightarrow \theta_a$. Also, due to the boundedness of \ddot{v} , $\dot{\tilde{v}} \rightarrow 0$, and $\dot{\tilde{v}} = W_1^\top \tilde{q} - K_1 h(\tilde{p}) - (k_v + k_\theta) h(\tilde{v}) - \hat{\theta}_1 + \theta_a = -K_1 h(\tilde{p}) = 0$, then $\tilde{p} \rightarrow 0$ which satisfies the tracking objective.

B.4.4 Proof of Theorem 4.3

The control law considered by Theorem (4.3) is similar to the first control law considered by Theorem (4.2), except for the choice of the virtual control law for the angular

velocity β . Consequently, the sections pertaining to the bounded control and translational and quaternion dynamics are similar to both proofs. Therefore, the reader is referred to sections B.4.1 and B.4.2 before proceeding. Also, Appendix B.4.5 provides derivatives of a number of functions that are necessary to implement the controller.

Using the second control scheme, the angular velocity error is now defined as $\tilde{\omega} = \omega - \beta_2$, where the virtual control law β_2 is given by (4.58). To study the stability of the system using the second controller, we use the same function \mathcal{V}_1 given by (B.69). Using the expression for $\dot{\mathcal{V}}_1$ given by (B.70), in addition to the virtual control law β_2 , the bounds defined by (B.73) and (B.74) and the matrices (B.76) and (B.77), the upper-bound of the $\dot{\mathcal{V}}_1$ is now given by

$$\begin{aligned} \dot{\mathcal{V}}_1 \leq & -\frac{k_\theta}{\gamma_{\theta_1}} \tilde{\theta}_1^\top \phi_h(\tilde{v}) \tilde{\theta}_1 - \tilde{\theta}_1^\top \alpha \left(\hat{\theta}_1, \delta_a + k_\theta, \tau_2 \right) + \tilde{q}^\top \Phi \tilde{v} \\ & - \tilde{v}^\top \Delta_v h(\tilde{v}) - \gamma_q \tilde{q}^\top \Delta_q \tilde{q} + \gamma_q \tilde{q}^\top \tilde{\omega}. \end{aligned}$$

Using (B.71) in addition to (B.62) and (B.64), the expression for Φ can also be written as

$$\Phi = \left(\gamma_{\theta_1} \gamma_q M(\mu_d) - 2u_t S(\bar{q}) R \right) \Gamma_v + \gamma_q k_p M(\mu_d) \Gamma_v^{-1} \phi_h(\tilde{p}).$$

Due to bound of the matrix $M(\mu_d)$ given by (B.68) and the fact $u_t < \bar{c}_t = g + \bar{\mu}_d$, we find the upper bound of the matrix Φ given by

$$\|\Phi\| \leq \left(\frac{\sqrt{2} \gamma_q \gamma_{\theta_1}}{\underline{c}_t} + 2\bar{c}_t \right) \|\Gamma_v\| + \frac{\sqrt{2} \gamma_q k_p}{\underline{c}_t} \|\Gamma_v^{-1}\|.$$

From the definition of δ_1 given by (4.63) we see that $\|\Phi\| \leq \delta_1$, therefore using Young's Inequality we find

$$|\tilde{q}^\top \Phi \tilde{v}| \leq \frac{\delta_1^2}{2\epsilon_2} \tilde{q}^\top \tilde{q} + \frac{\epsilon_2}{2} \tilde{v}^\top \tilde{v},$$

for any $\epsilon_2 > 0$. Therefore, $\dot{\mathcal{V}}_1$ is updated as follows

$$\dot{\mathcal{V}}_1 \leq -\frac{k_\theta}{\gamma_{\theta_1}} \tilde{\theta}_1^\top \phi_h(\tilde{v}) \tilde{\theta}_1 - \tilde{\theta}_1^\top \alpha \left(\hat{\theta}_1, \delta_a, \tau_2 \right) + \gamma_q \tilde{q}^\top \tilde{\omega} - \tilde{q}^\top \bar{\Delta}_q \tilde{q} - \tilde{v}^\top \bar{\Delta}_v \tilde{v}, \quad (\text{B.81})$$

where we define the matrices

$$\begin{aligned} \bar{\Delta}_q &= \gamma_q \Delta_q - \frac{\delta_1^2}{2\epsilon_2} I_{3 \times 3} \\ \bar{\Delta}_v &= \frac{1}{(1 + \tilde{v}^\top \tilde{v})^{1/2}} \Delta_v - \frac{\epsilon_2}{2} I_{3 \times 3}. \end{aligned} \quad (\text{B.82})$$

Using the two estimation error functions $\tilde{\theta}_2 = \theta_a - \hat{\theta}_2$ and $\tilde{\theta}_3 = \theta_b - \hat{\theta}_3$ we introduce the following Lyapunov function

$$\begin{aligned} \mathcal{V}_2 &= \mathcal{V}_1 + \frac{1}{2} \tilde{\omega}^\top I_b \tilde{\omega} + \frac{1}{2\gamma_{\theta_2}} \tilde{\theta}_2^\top \tilde{\theta}_2 + \frac{1}{2\gamma_{\theta_3}} \tilde{\theta}_3^\top \tilde{\theta}_3 \\ &= k_p \left(\sqrt{1 + \tilde{p}^\top \tilde{p}} - 1 \right) + \frac{1}{2} X^\top C X, \end{aligned} \quad (\text{B.83})$$

where X and C are given by (B.79) and (B.80), respectively. In light of (B.81), the estimation laws (4.51)-(4.52) and the control law (4.60), we find the following upper bound for $\dot{\mathcal{V}}_2$

$$\begin{aligned} \dot{\mathcal{V}}_2 &\leq -\tilde{v}^\top \bar{\Delta}_v h(\tilde{v}) - \gamma_q \tilde{q}^\top \bar{\Delta}_q \tilde{q} - \frac{k_\theta}{\gamma_{\theta_1}} \tilde{\theta}_1^\top \phi_h(\tilde{v}) \tilde{\theta}_1 - \tilde{\omega}^\top K_\omega \tilde{\omega} \\ &\quad - \tilde{\theta}_1^\top \alpha \left(\hat{\theta}_1, \delta_a + k_\theta, \tau_2 \right) - \tilde{\theta}_2^\top \alpha \left(\hat{\theta}_2, \delta_a, -\bar{f}_{\beta_2}^\top I_b \tilde{\omega} \right) - \tilde{\theta}_3^\top \alpha \left(\hat{\theta}_3, \delta_b, -R^\top S(e_3) \tilde{\omega} \right). \end{aligned}$$

Due to the property of the projection law (4.40), then $\tilde{\theta}_i^\top \alpha > 0$ and

$$\dot{\mathcal{V}}_2 \leq -\tilde{v}^\top \bar{\Delta}_v h(\tilde{v}) - \gamma_q \tilde{q}^\top \bar{\Delta}_q \tilde{q} - \frac{k_\theta}{\gamma_{\theta_1}} \tilde{\theta}_1^\top \phi_h(\tilde{v}) \tilde{\theta}_1 - \tilde{\omega}^\top K_\omega \tilde{\omega}.$$

Given the requirements (4.61) and (4.62) are satisfied, then $\bar{\Delta}_q > 0$ and $\Delta_v > 0$.

However, in light of (B.82), to ensure that $\bar{\Delta}_v > 0$ we must also satisfy the following inequality

$$\|\tilde{v}\|^2 < \frac{4}{\epsilon_2^2} \|\Delta_v\|^2 - 1.$$

Due to the definition of the Lyapunov function (B.83), the following inequality is always satisfied

$$\frac{1}{2} \lambda_{\min}(\Gamma_v) \|\tilde{v}\|^2 \leq \mathcal{V}_2 \leq k_p \left(\sqrt{1 + \tilde{p}^\top \tilde{p}} - 1 \right) + X^\top \bar{C} X,$$

where \bar{C} is given by (4.68), which we can further simplify to obtain

$$\|\tilde{v}\|^2 \leq 2 \lambda_{\min}(\Gamma_v)^{-1} \left(k_p \left(\sqrt{1 + \tilde{p}^\top \tilde{p}} - 1 \right) + X^\top \bar{C} X \right).$$

Therefore, to ensure $\dot{\mathcal{V}}_2 \leq 0$ it is sufficient to have

$$2 \lambda_{\min}(\Gamma_v)^{-1} \left(k_p \left(\sqrt{1 + \tilde{p}(0)^\top \tilde{p}(0)} - 1 \right) + X(0)^\top \bar{C} X(0) \right) < \frac{4}{\epsilon_2^2} \|\Delta_v\|^2 - 1,$$

which is satisfied due to (4.65), and consequently $\bar{\Delta}_v$ is positive definite. Therefore, $\dot{\mathcal{V}}_2 \leq 0$ and the states $(\tilde{p}, \tilde{v}, \tilde{\omega})$ are bounded. The attitude error \tilde{Q} is bounded by definition, and the adaptive estimation error $\tilde{\theta}_{1,2,3}$ are bounded due to assumption 2 and due to the property of the projection mechanism (4.40). Applying Barbalat's Lemma, $\ddot{\mathcal{V}}_2$ is bounded due to assumption 1 which shows that $(\tilde{p}, \tilde{v}, \tilde{q}, \tilde{\omega}, \tilde{\theta}_1) \rightarrow 0$ as $t \rightarrow \infty$. Since $\tilde{\theta}_1 \rightarrow 0$ and $\tilde{v} \rightarrow 0$, then $\hat{\theta}_1 \rightarrow \theta_a$. Also, the bound of $\ddot{\tilde{v}}$ implies $\dot{\tilde{v}} \rightarrow 0$, and $\dot{\tilde{v}} = W_1^\top \tilde{q} - K_1 h(\tilde{p}) - K_2 h(\tilde{v}) - \hat{\theta}_1 + \theta_a = -K_1 h(\tilde{p}) = 0$, then $\tilde{p} \rightarrow 0$ which satisfies the tracking objective.

B.4.5 Derivatives of Angular Velocity Virtual Control

Laws, β_2 and β_1

In this section we obtain the derivatives of the two virtual control laws for the angular velocity, β_1 and β_2 , which are given by (4.46) and (4.58), respectively. Due to the complexity of the virtual control laws we begin by evaluating the derivatives of several signals before continuing to the derivatives of the virtual control laws. Recall from (4.27) the expression for $Z(\mu_d, v)$, which is the partial derivative of the matrix $M(\mu_d)$. In addition to this function, we also require the partial derivative of the transpose $M(\mu_d)^\top$. Let $\mu_d = \text{col}[\mu_{d1}, \mu_{d2}, \mu_{d3}]$ and $v = \text{col}[v_1, v_2, v_3]$ denote two arbitrary vectors. We define the function $Z_2 : \mathbb{R}^3 \rightarrow \mathbb{R}^3$ such that

$$Z_2(\mu_d, v) := \frac{\partial}{\partial \mu_d} M(\mu_d)^\top v.$$

From the definition of $M(\mu_d)$ given by (4.26), after some straightforward albeit tedious calculations, we evaluate $Z_2(\mu_d, v)$ to be

$$Z_2(\mu_d, v) = \gamma_M^{-1} M(\mu_d)^\top v f_\gamma + \gamma_M \Lambda_2(\mu_d, v),$$

where $f_\gamma = \gamma_M^2 (ge_3 - \mu_d)^\top (3c_1 I_{3 \times 3} + S(e_3)S(ge_3 - \mu_d))$, $\gamma_M = \|\mu_d - ge_3\|^{-2} c_1^{-1}$, $c_1 = \|\mu_d - ge_3\| + g - \mu_{d_3}$ and

$$\begin{aligned} \Lambda_2 &= \begin{pmatrix} 2v_2\mu_{d_1} - \mu_{d_2}v_1 & u_tv_3 - \mu_{d_1}v_1 & 0 \\ \mu_{d_2}v_2 - u_tv_3 & \mu_{d_1}v_2 - 2\mu_{d_2}v_1 & 0 \\ -c_1v_2 & c_1v_2 & 0 \end{pmatrix} \\ &+ \begin{pmatrix} \mu_{d_2}v_3 - c_1v_2 \\ c_1v_1 - \mu_{d_1}v_3 \\ 0 \end{pmatrix} \alpha_1(\mu_d)^\top \\ &+ \begin{pmatrix} -u_tv_2 & u_tv_1 & \mu_{d_2}v_1 - \mu_{d_1}v_2 \end{pmatrix}^\top \alpha_2(\mu_d)^\top, \end{aligned}$$

with $\alpha_1 = (\mu_d - ge_3) / \|\mu_d - ge_3\|$ and $\alpha_2 = \alpha_1 - e_3$.

In order to obtain the derivative of the projection law α , we first focus on obtaining the derivative of the signal τ_2 . Leading up to this goal we first differentiate several signals. Due to the unknown parameter θ_a , in general we group the derivative of an arbitrary signal x into known and unknown components as $\dot{x} = f_x + \bar{f}_x\theta_a$.

Recall the expression for the signal $\dot{\mu}_d$ given by (B.63). This result can also be written as $\dot{\mu}_d = f_{\mu_d} + \bar{f}_{\mu_d}\theta_a$, where the functions f_{μ_d} and \bar{f}_{μ_d} are given by

$$\begin{aligned} f_{\mu_d} &= r^{(3)} + w_\beta + (W_2 + k_\theta K_2 \phi_h(\tilde{v})) h(\tilde{v}) + W_3 \tilde{q} \\ &\quad + W_4 \tilde{v} + K_2 \phi_h(\tilde{v}) \hat{\theta}_1, \\ \bar{f}_{\mu_d} &= -K_2 \phi_h(\tilde{v}), \end{aligned}$$

where $K_2 = (k_\theta + k_v) I_{3 \times 3}$. Similarly, in light of (4.33), the derivative of \tilde{q} can be

written as $\dot{q} = f_{\tilde{q}} + \bar{f}_{\tilde{q}}\theta_a$ using the following expressions

$$\begin{aligned} f_{\tilde{q}} &= \frac{1}{2} (\tilde{\eta}I + S(\tilde{q})) \omega + \frac{1}{2} (S(\tilde{q}) - \tilde{\eta}I) (M(\mu_d) f_{\mu_d}), \\ \bar{f}_{\tilde{q}} &= \frac{1}{2} (S(\tilde{q}) - \tilde{\eta}I) (M(\mu_d) \bar{f}_{\mu_d}). \end{aligned}$$

From the definition of $\tilde{\mu}$ given by (4.18), the derivative $\dot{\tilde{\mu}} = f_{\tilde{\mu}} + \bar{f}_{\tilde{\mu}}\theta_a$ is obtained where

$$\begin{aligned} f_{\tilde{\mu}} &= - \left(I + u_t^{-1} R^\top e_3 (\mu_d - g e_3)^\top \right) f_{\mu_d} - u_t R^\top S(\omega) e_3, \\ \bar{f}_{\tilde{\mu}} &= - \left(I + u_t^{-1} R^\top e_3 (\mu_d - g e_3)^\top \right) \bar{f}_{\mu_d}. \end{aligned}$$

The expression for \dot{v} , previously given by (B.59), can also be given by $\dot{v} = f_{\tilde{v}_1} + \bar{\theta}_1 = f_{\tilde{v}_2} + \theta_a$, where the functions $f_{\tilde{v}_1}$ and $f_{\tilde{v}_2}$ are given by

$$f_{\tilde{v}_1} = -K_1 h(\tilde{p}) - k_v h(\tilde{v}) + \tilde{\mu}, \quad f_{\tilde{v}_2} = -K_1 h(\tilde{p}) - K_2 h(\tilde{v}) + \tilde{\mu} - \hat{\theta}_1.$$

Since we require the derivative of the signal $f_{\tilde{v}_1}$, we also find $\dot{f}_{\tilde{v}_1} = f_{f_{\tilde{v}_1}} + \bar{f}_{f_{\tilde{v}_1}}$ where

$$f_{f_{\tilde{v}_1}} = -K_1 \phi_h(\tilde{p}) \tilde{v} - k_v \phi_h(\tilde{v}) f_{\tilde{v}_2} + f_{\tilde{\mu}}, \quad \bar{f}_{f_{\tilde{v}_1}} = -k_v \phi_h(\tilde{v}) + \bar{f}_{\tilde{\mu}}.$$

At this point we require the derivative of the signal τ_2 , given by (4.44). Using the partial derivative of $\phi(u)$ given by (2.29), we obtain $\dot{\tau}_2 = f_{\tau_2} + \bar{f}_{\tau_2}\theta_a$ where

$$\begin{aligned} f_{\tau_2} &= \Gamma_v f_{\tilde{v}_2} - \frac{k\theta}{\gamma_{\theta_1}} \left(f_{\phi_h}(\tilde{v}, f_{\tilde{v}_1}) f_{\tilde{v}_2} - \phi_h(\tilde{v}) K_1 \phi_h(\tilde{p}) \tilde{v} - k_v \phi_h(\tilde{v})^2 f_{\tilde{v}_2} + \phi_h(\tilde{v}) f_{\tilde{\mu}} \right) \\ &+ \gamma_q \left(f_{\phi_h}(\tilde{v}, K_2 M(\mu_d)^\top \tilde{q}) f_{\tilde{v}_2} + \phi_h(\tilde{v}) K_2 Z_2(\mu_d, \tilde{q}) f_{\mu_d} + \phi_h(\tilde{v}) K_2 M(\mu_d)^\top f_{\tilde{q}} \right), \end{aligned} \quad (\text{B.84})$$

$$\begin{aligned} \bar{f}_{\tau_2} &= \Gamma_v - \frac{k\theta}{\gamma_{\theta_1}} \left(f_{\phi_h}(\tilde{v}, f_{\tilde{v}_1}) - k_v^2 \phi_h(\tilde{v})^2 + \phi_h(\tilde{v}) \bar{f}_{\tilde{\mu}} \right) \\ &+ \gamma_q \left(f_{\phi_h}(\tilde{v}, K_2 M(\mu_d)^\top \tilde{q}) + \phi_h(\tilde{v}) K_2 Z_2(\mu_d, \tilde{q}) \bar{f}_{\mu_d} + \phi_h(\tilde{v}) K_2 M(\mu_d)^\top \bar{f}_{\tilde{q}} \right). \end{aligned} \quad (\text{B.85})$$

In light of the work presented in Cai et al. (2006) and using the above derivatives, we now differentiate the projection law α . Using the projection algorithm defined by (4.36)-(4.39), in addition to the derivative of τ_2 as defined by (B.84) and (B.85) we obtain $\dot{\alpha}(\hat{\theta}_1, \delta_a + k_\theta, \tau_2) = f_\alpha + \bar{f}_\alpha \theta_a$ where the functions f_α and \bar{f}_α are given by

$$\begin{aligned} f_\alpha &= -k_\alpha \dot{\eta}_1 \eta_2 \hat{\theta}_1 - k_\alpha \eta_1 \eta_2 \dot{\hat{\theta}}_1 - k_\alpha \eta_1 \frac{\eta_2}{\eta_2 - \hat{\theta}_1 \tau_2} \left(\tau_2^\top \dot{\hat{\theta}}_1 + \hat{\theta}_1^\top f_{\tau_2} \right) \hat{\theta}_1, \\ \bar{f}_\alpha &= -k_\alpha \eta_1 \frac{\eta_2}{\eta_2 - \hat{\theta}_1^\top \tau_2} \hat{\theta}_1 \hat{\theta}_1^\top \bar{f}_{\tau_2}, \\ \dot{\eta}_1 &= \begin{cases} 4 \left(\hat{\theta}_1^\top \hat{\theta}_1 - \theta_0^2 \right) \hat{\theta}_1^\top \dot{\hat{\theta}}_1 & \text{if } \|\hat{\theta}_1\|^2 > \theta_0^2, \\ 0 & \text{otherwise.} \end{cases} \end{aligned}$$

Having obtained the derivative of α , we differentiate the signal w_β given by (4.47) to obtain $\dot{w}_\beta = f_{w_\beta} + \bar{f}_{w_\beta} \theta_a$ with

$$\begin{aligned} f_{w_\beta} &= k_p k_v f_{\phi_h} \left(\tilde{v}, \Gamma_v^{-1} h(\tilde{p}) \right) f_{\tilde{v}_2} + k_p k_v \phi_h(\tilde{v}) \Gamma_v^{-1} \phi_h(\tilde{p}) \tilde{v} - \gamma_{\theta_1} f_\alpha, \\ \bar{f}_{w_\beta} &= k_p k_v f_{\phi_h} \left(\tilde{v}, \Gamma_v^{-1} h(\tilde{p}) \right) - \gamma_{\theta_1} \bar{f}_\alpha. \end{aligned}$$

Using the expression for \bar{q} given by (4.45), we also find $\dot{\bar{q}} = f_{\bar{q}} + \bar{f}_{\bar{q}} \theta_a$ where

$$\begin{aligned} f_{\bar{q}} &= S(e_3) f_{\tilde{q}} + \frac{1}{2} e_3 \tilde{q}^\top M(\mu_d) f_{\mu_d} - \frac{1}{2} e_3 \tilde{q}^\top \omega, \\ \bar{f}_{\bar{q}} &= S(e_3) \bar{f}_{\tilde{q}} + \frac{1}{2} e_3 \tilde{q}^\top M(\mu_d) \bar{f}_{\mu_d}. \end{aligned}$$

In light of the above results we finally obtain the derivative of the virtual control law for the second controller, $\dot{\beta}_2 = f_{\beta_2} + \bar{f}_{\beta_2} \theta_a$, where

$$f_{\beta_2} = Z_1 \left(\mu_d, p_d^{(3)} + w_\beta \right) f_{\mu_d} + M(\mu_d) \left(p_d^{(4)} + f_{w_\beta} \right) - K_q f_{\tilde{q}} \quad (\text{B.86})$$

$$\bar{f}_{\beta_2} = Z_1 \left(\mu_d, p_d^{(3)} + w_\beta \right) \bar{f}_{\mu_d} + M(\mu_d) \bar{f}_{w_\beta} - K_q \bar{f}_{\bar{q}}, \quad (\text{B.87})$$

which is used to specify the derivative of the virtual control law for the first controller,

$\dot{\beta}_1 = f_{\beta_1} + \bar{f}_{\beta_1} \theta_a$ where

$$\begin{aligned} f_{\beta_1} &= f_{\beta_2} - \gamma_{\theta_1} Z_1(\mu_d, \Gamma_v \tilde{v}) f_{\mu_d} - \gamma_{\theta_1} M(\mu_d) \Gamma_v f_{\tilde{v}_2} - k_p Z_1 \left(\mu_d, \Gamma_v^{-1} \phi_h(\tilde{p}) \tilde{v} \right) f_{\mu_d} \\ &\quad - k_p M(\mu_d) \Gamma_v^{-1} f_{\phi_h(\tilde{p}, \tilde{v})} \tilde{v} - k_p M(\mu_d) \Gamma_v^{-1} \phi_h(\tilde{p}) f_{\tilde{v}_2} - \frac{2u_t}{\gamma_q} S(R\Gamma_v \tilde{v}) f_{\bar{q}} \\ &\quad + \frac{2}{\gamma_q u_t} S(\bar{q}) R\Gamma_v \tilde{v} (\mu_d - g e_3)^\top f_{\mu_d} - \frac{2u_t}{\gamma_q} S(\bar{q}) S(\omega) R\Gamma_v \tilde{v} + \frac{2u_t}{\gamma_q} S(\bar{q}) R\Gamma_v f_{\tilde{v}_2}, \end{aligned} \quad (\text{B.88})$$

$$\begin{aligned} \bar{f}_{\beta_1} &= \bar{f}_{\beta_2} - \gamma_{\theta_1} Z_1(\mu_d, \Gamma_v \tilde{v}) \bar{f}_{\mu_d} - \gamma_{\theta_1} M(\mu_d) \Gamma_v - k_p Z_1 \left(\mu_d, \Gamma_v^{-1} \phi_h(\tilde{p}) \tilde{v} \right) \bar{f}_{\mu_d} \\ &\quad - k_p M(\mu_d) \Gamma_v^{-1} \phi_h(\tilde{p}) + \frac{2}{\gamma_q u_t} S(\bar{q}) R\Gamma_v \tilde{v} (\mu_d - g e_3)^\top \bar{f}_{\mu_d} - \frac{2u_t}{\gamma_q} S(R\Gamma_v \tilde{v}) \bar{f}_{\bar{q}} \\ &\quad + \frac{2u_t}{\gamma_q} S(\bar{q}) R\Gamma_v. \end{aligned} \quad (\text{B.89})$$

B.5 Proof of Theorem 4.4

(Vector Measurement Based Position Control)

Consider the following Lyapunov function candidate

$$\mathcal{V} = k_p \left(\sqrt{1 + \|\tilde{p}\|^2} - 1 \right) + \frac{1}{2} \tilde{v}^\top \Gamma_v^{-1} \tilde{v} + \gamma_q (1 - \tilde{\eta}^2) + \frac{1}{2} \tilde{\omega}^\top I_b \tilde{\omega}. \quad (\text{B.90})$$

From (4.76) and using the properties (2.23) and (2.22) and (2.20) one can obtain the

following time derivative for the attitude error

$$\begin{aligned}
\dot{\tilde{\eta}} &= -\frac{1}{2}\tilde{q}^\top R_d^\top \left(\tilde{\omega} - k_v^2 M(\mu_d) \Gamma_v \phi_h(\tilde{v}) \Gamma_v h(\tilde{v}) + \sum_{i=1}^n \gamma_i S \left(b_i^d \right) b_i + k_v M(\mu_d) \Gamma_v \phi_h(\tilde{v}) \tilde{\mu} \right) \\
&= \tilde{\eta} \tilde{q}^\top W \tilde{q} + \frac{k_v^2}{2} \tilde{q}^\top R_d^\top M(\mu_d) \Gamma_v \phi_h(\tilde{v}) \Gamma_v h(\tilde{v}) - \frac{1}{2} \tilde{q}^\top R_d^\top \tilde{\omega} - \frac{k_v}{2} \tilde{q}^\top R_d^\top M(\mu_d) \Gamma_v \phi_h(\tilde{v}) \tilde{\mu},
\end{aligned} \tag{B.91}$$

where $W = -\sum_{i=1}^n \gamma_i S(r_i)^2$. Note that due to Assumption 4.4, the matrix W is positive definite and the eigenvalues of W can be arbitrarily increased using the gains γ_i . In light of (4.9)-(4.12), (4.72), (4.78), (4.79), (4.80) and (B.91) the time-derivative of (B.90) is given by

$$\begin{aligned}
\dot{V} &= -k_v \tilde{v}^\top h(\tilde{v}) - 2\gamma_q \tilde{\eta}^2 \tilde{q}^\top W \tilde{q} - \tilde{\omega}^\top K_\omega \tilde{\omega} + \tilde{v}^\top \Gamma_v^{-1} \tilde{\mu} - \tilde{\omega}^\top I_b g_{\tilde{\omega}} \tilde{\mu} + \gamma_q \tilde{\eta} \tilde{q}^\top R_d^\top \tilde{\omega} \\
&\quad + \gamma_q k_v \tilde{\eta} \tilde{q}^\top R_d^\top M(\mu_d) \Gamma_v \phi_h(\tilde{v}) \tilde{\mu} - \gamma_q k_v^2 \tilde{\eta} \tilde{q}^\top R_d^\top M(\mu_d) \Gamma_v \phi_h(\tilde{v}) \Gamma_v h(\tilde{v}).
\end{aligned} \tag{B.92}$$

Due to (2.8), (4.16) and (4.17) the error signal $\tilde{\mu} = \mu - \mu_d$ can be expressed in terms of the vector part of the error quaternion, \tilde{q} , since $\tilde{\mu} = 2u_t (\tilde{\eta} I_{3 \times 3} - S(\tilde{q})) S(R^\top e_3) \tilde{q}$. Therefore, due to (4.73) the signal $\tilde{\mu}$ is bounded by

$$\|\tilde{\mu}\| \leq 2\bar{c}_t \|\tilde{q}\|. \tag{B.93}$$

We now focus our attention on the bound of $g_{\tilde{\omega}}$. Due to the bound of the thrust (4.73), and the bound of μ_d due to (4.71) there exists a positive constant c_Z such that the matrix $Z(\mu_d, v)$ is bounded by

$$\|Z(\mu_d, v)\| \leq c_Z \|v\|. \tag{B.94}$$

Consequently, due to Assumption 4.1, (2.26), (4.74), (B.94) and the fact that $\|\tilde{v}\|\|\phi_h(\tilde{v})\| \leq 1$, there exists a positive constant c_g such that

$$\|g_{\bar{\omega}}\| \leq c_g. \quad (\text{B.95})$$

Using this result in addition to (2.26), (4.74), (B.94), and (B.93) one can find $\|\tilde{v}\|^2 \leq 2\lambda_{\min}(\Gamma_v^{-1})^{-1}\mathcal{V}(t)$, in addition to the following inequalities

$$\tilde{v}^T \Gamma_v^{-1} \tilde{\mu} \leq \tilde{v}^T \tilde{v} / (2\epsilon_1) + 2\epsilon_1 \bar{c}_t^2 \|\Gamma_v^{-1}\|^2 \tilde{q}^T \tilde{q}, \quad (\text{B.96})$$

$$\gamma_q \tilde{\eta} \tilde{q}^T R_d^T \tilde{\omega} \leq \gamma_q \epsilon_2 \tilde{\eta}^2 \tilde{q}^T \tilde{q} / 2 + \gamma_q \tilde{\omega}^T \tilde{\omega} / (2\epsilon_2), \quad (\text{B.97})$$

$$\gamma_q k_v^2 \tilde{\eta} \tilde{q}^T R_d^T M(\mu_d) \Gamma_v \phi_h(\tilde{v}) \Gamma_v h(\tilde{v}) \leq \gamma_q k_v^2 \bar{c}_t^4 \epsilon_3 \tilde{\eta}^2 \tilde{q}^T \tilde{q} / \underline{c}_t^2 + \gamma_q k_v^2 \tilde{v}^T h(\tilde{v}) / (2\epsilon_3), \quad (\text{B.98})$$

$$\tilde{\omega}^T I_b g_{\bar{\omega}} \tilde{\mu} \leq 2\bar{c}_g^2 \bar{c}_t^2 \|I_b\|^2 \tilde{\omega}^T \tilde{\omega} / \epsilon_4 + \epsilon_4 \tilde{q}^T \tilde{q} / 2, \quad (\text{B.99})$$

$$\gamma_q k_v \tilde{\eta} \tilde{q}^T R_d^T M(\mu_d) \Gamma_v \phi_h(\tilde{v}) \tilde{\mu} \leq 2\sqrt{2} \gamma_q k_v \bar{c}_t c_\Gamma |\tilde{\eta}| \tilde{q}^T \tilde{q} / \underline{c}_t, \quad (\text{B.100})$$

where $\epsilon_{1,2,3,4} > 0$ and $c_\Gamma = \|\Gamma_v\|$. Consequently, the expression for \dot{V} can be rewritten as

$$\begin{aligned} \dot{\mathcal{V}} \leq & -\tilde{\omega}^T \tilde{\omega} (\lambda_{\min}(K_\omega) - \gamma_q / (2\epsilon_2) - 2\bar{c}_g^2 \bar{c}_t^2 \|I_b\|^2 / \epsilon_4) \\ & - \tilde{v}^T h(\tilde{v}) \left(k_v - \frac{1}{2\epsilon_1} \sqrt{2V(t) / \lambda_{\min}(\Gamma_v^{-1}) + 1} - \frac{\gamma_q k_v^2}{2\epsilon_3} \right) \\ & - 2\gamma_q \tilde{\eta}^2 \tilde{q}^T \tilde{q} \left(\lambda_{\min}(W) - \frac{1}{\tilde{\eta}^2} \frac{\epsilon_1 \bar{c}_t^2}{\gamma_q} \lambda_{\max}(\Gamma_v^{-1})^2 - \frac{\epsilon_2}{4} \right. \\ & \left. - \frac{k_v^2 \bar{c}_t^4 \epsilon_3}{2\bar{c}_t^2} - \frac{1}{|\tilde{\eta}|} \frac{\sqrt{2} k_v \bar{c}_t c_\Gamma}{\underline{c}_t} - \frac{1}{\tilde{\eta}^2} \frac{\epsilon_4}{4\gamma_q} \right), \end{aligned} \quad (\text{B.101})$$

where $\lambda_{\min}(\cdot)$ denotes the smallest eigenvalue of (\cdot) . In order to dominate some of the unwanted terms in (B.101) (and therefore ensure that $\dot{\mathcal{V}} < 0$), we must show that a lower bound $\tilde{\eta}^* := \inf |\tilde{\eta}(t)| > 0$ exists. To further investigate this bound on $\tilde{\eta}$, we

exclude the initial condition $\tilde{\eta}(t_0) = 0$, and consider the function $J = \tilde{\eta}^2/2$. In light of (B.91), the time derivative of J is given by

$$\begin{aligned} \dot{J} = & \frac{\tilde{\eta}^2}{2} \left(2\tilde{q}^\top W \tilde{q} + \frac{k_v^2}{\tilde{\eta}} \tilde{q}^\top R_d^\top M(\mu_d) \Gamma_v \phi_h(\tilde{v}) \Gamma_v h(\tilde{v}) \right. \\ & \left. - \frac{1}{\tilde{\eta}} \tilde{q}^\top R_d^\top \tilde{\omega} - \frac{k_v}{\tilde{\eta}} \tilde{q}^\top R_d^\top M(\mu_d) \Gamma_v \phi_h(\tilde{v}) \tilde{\mu} \right). \end{aligned} \quad (\text{B.102})$$

Using Young's inequality, in addition to the fact that $\tilde{q}^\top \tilde{q} = 1 - \tilde{\eta}^2$ in addition to $\tilde{\omega}^\top \tilde{\omega} \leq 2\bar{V}(t)/\lambda_{\min}(I_b)$ where $\bar{V}(t) = k_p(\sqrt{1 + \|\tilde{p}\|^2} - 1) + \frac{1}{2}\tilde{v}^\top \Gamma_v^{-1} \tilde{v} + \gamma_q + \frac{1}{2}\tilde{\omega}^\top I_b \tilde{\omega}$, we find \dot{J} is bounded by

$$\dot{J} \geq \tilde{\eta}^2 \left(1 - \tilde{\eta}^2 \right) \left(\lambda_w - \rho/\tilde{\eta}^2 - \sigma(t)/(1 - \tilde{\eta}^2) \right), \quad (\text{B.103})$$

$$\rho = \frac{1}{4} + \frac{k_v^2 c_\Gamma^4}{2c_t^2} + \frac{\sqrt{2}k_v \bar{c}_t c_\Gamma}{c_t}, \quad \sigma(t) = \frac{\bar{V}(t)}{2\lambda_{\min}(I_b)} + \frac{k_v^2}{4},$$

where $\lambda_w = \lambda_{\min}(W)$. Using (B.103) we wish to identify the region where $\dot{J} > 0$ and therefore $|\tilde{\eta}|$ is increasing. To find this region we consider setting the right-hand-side of (B.103) to zero, at the time t , to obtain $\lambda_w = \rho/\tilde{\eta}^2 + \sigma(t)/(1 - \tilde{\eta}^2)$. Multiplying this result by $\tilde{\eta}^2$ and $1 - \tilde{\eta}^2$ we obtain

$$-\lambda_w \tilde{\eta}^4 + (\lambda_w + \rho - \sigma(t)) \tilde{\eta}^2 - \rho = 0. \quad (\text{B.104})$$

Let $\alpha(t) = (\lambda_w + \rho - \sigma(t))^2 - 4\rho\lambda_w$. If $\alpha < 0$, (B.104) has complex roots and therefore the lower bound for \dot{J} is negative. Since we can find $\alpha(t) = \lambda_w(\lambda_w - 2(\rho + \sigma(t))) + (\sigma(t) - \rho)^2$, a simple, albeit conservative requirement to force $\alpha(t)$ to be positive is to take $\lambda_w > 2(\rho + \sigma(t))$. As a result the solution to (B.104) has two real positive

roots defined by

$$\tilde{\eta}_u^2(t) = \left(\lambda_w + \rho - \sigma(t) + \sqrt{\alpha(t)} \right) / (2\lambda_w), \quad (\text{B.105})$$

$$\tilde{\eta}_\ell^2(t) = \left(\lambda_w + \rho - \sigma(t) - \sqrt{\alpha(t)} \right) / (2\lambda_w). \quad (\text{B.106})$$

We define the open set $D := (\tilde{\eta}_\ell, \tilde{\eta}_u)$ (where we exclude the negative solutions for $\tilde{\eta}_\ell$ and $\tilde{\eta}_u$). Note that for any $|\tilde{\eta}(t)| \in D$ the value of \dot{J} is positive, and therefore $|\tilde{\eta}(t)|$ is increasing. Note the set D is time varying due to the value of $\sigma(t)$. However, if $\sigma(t)$ is a decreasing function and we choose

$$\lambda_w > 2(\rho + \sigma(t_0)), \quad (\text{B.107})$$

we can show that the lower limit $\tilde{\eta}_\ell$ is decreasing, and the upper limit $\tilde{\eta}_u$ is increasing with respect to t . To prove this fact we consider the following partial derivative

$$\frac{\partial}{\partial \sigma(t)} \tilde{\eta}_u^2 = \left(-1 - \sqrt{(\alpha(t) + 4\rho\lambda_w) / \alpha(t)} \right) / (2\lambda_w). \quad (\text{B.108})$$

If $\sigma(t)$ is decreasing, then $\alpha(t)$ is increasing and therefore (B.108) is well-defined and negative. The partial derivative of the lower limit is given by

$$\frac{\partial}{\partial \sigma(t)} \tilde{\eta}_\ell^2 = \left(-1 + \sqrt{(\alpha(t) + 4\rho\lambda_w) / \alpha(t)} \right) / (2\lambda_w), \quad (\text{B.109})$$

which is always positive. Therefore, if $\sigma(t)$ is decreasing the value of $\tilde{\eta}_\ell^2$ is decreasing, the value of $\tilde{\eta}_u^2$ is increasing and the set D approaches $D \rightarrow (0, 1)$. The gain $\lambda_w = \lambda_{\min}(W) = \lambda_{\min}(-\sum_{i=1}^n \gamma_i S(r_i)^2)$ can be arbitrarily enlarged using the gains γ_i to ensure (B.107) is satisfied and therefore the domain D exists. Therefore, since

$\lim_{\lambda_w \rightarrow \infty} \tilde{\eta}_\ell^2 = 0$, there exists a value \bar{W}_1 such that for all $\lambda_{\min}(W) > \lambda_{\min}(\bar{W}_1)$, $0 < \tilde{\eta}_\ell(t_0) < |\tilde{\eta}(t_0)|$, where we exclude the negative solution for $\tilde{\eta}_\ell(t_0)$. Consequently, if $\sigma(t)$ is a decreasing function the minimum possible value for $\tilde{\eta}^* = \inf |\tilde{\eta}(t)|$ is given by $\tilde{\eta}^* = \min \{|\tilde{\eta}(t_0)|, \tilde{\eta}_u(t_0)\}$, where we exclude the negative solution for $\tilde{\eta}_u(t_0)$. The final step of the proof is to show that $\mathcal{V}(t)$ and therefore $\sigma(t)$ are decreasing functions. If we recall the value of $\dot{\mathcal{V}}$ from (B.101), one can see that there exist values $\bar{\epsilon}_1$ and $\bar{\epsilon}_3$ such that for $\epsilon_1 > \bar{\epsilon}_1$ and $\epsilon_3 > \bar{\epsilon}_3$, the following inequality is satisfied

$$k_v > \sqrt{2\mathcal{V}(t_0)/\lambda_{\min}(\Gamma_v^{-1}) + 1/(2\epsilon_1) + \gamma_q k_v^2/(2\epsilon_3)}, \quad (\text{B.110})$$

for any $k_v > 0$. Furthermore, there exist values $\bar{\epsilon}_2$ and $\bar{\epsilon}_4$ such that for $\epsilon_2 > \bar{\epsilon}_2$, $\epsilon_4 > \bar{\epsilon}_4$

$$\lambda_{\min}(K_\omega) > \gamma_q/(2\epsilon_2) + 2c_g^2 \bar{c}_t^2 \|I_b\|^2/\epsilon_4, \quad (\text{B.111})$$

for any $K_\omega = K_\omega^\top > 0$. Also, there exists a gain \bar{W}_2 such that for $\lambda_{\min}(W) > \lambda_{\min}(\bar{W}_2)$

$$\begin{aligned} \lambda_{\min}(W) > & \frac{1}{(\tilde{\eta}^*)^2} \frac{\epsilon_1 \bar{c}_t^2}{\gamma_q} \lambda_{\max}(\Gamma_v^{-1})^2 + \frac{\epsilon_2}{4} + \frac{k_v^2 c_\Gamma^4 \epsilon_3}{2 \bar{c}_t^2} \\ & + \frac{1}{\tilde{\eta}^*} \frac{\sqrt{2} k_v \bar{c}_t c_\Gamma}{\underline{c}_t} + \frac{1}{(\tilde{\eta}^*)^2} \frac{\epsilon_4}{4 \gamma_q}. \end{aligned} \quad (\text{B.112})$$

There are two conditions for the gain W , where the minimum bound W_1 ensures that $\tilde{\eta}_\ell \leq |\tilde{\eta}(t_0)|$, and the minimum bound W_2 which ensures that (B.112) is satisfied. There exists gains $\bar{\gamma}_i, i = 1, 2, \dots, n$, such that for all $\gamma_i > \bar{\gamma}_i$ $\lambda_{\min}(W) > \max \{ \lambda_{\min}(\bar{W}_1), \lambda_{\min}(\bar{W}_2) \}$, which satisfies both requirements. Therefore, under this condition from (B.101) one can see that $\dot{\mathcal{V}}(t_0) \leq 0$, which implies that for sufficiently small δ , $\mathcal{V}(t_0 + \delta) \leq \mathcal{V}(t_0)$, $\sigma(t_0 + \delta) \leq \sigma(t_0)$ and $|\tilde{\eta}(t_0 + \delta)| \geq \tilde{\eta}^*$. Since

$\mathcal{V}(t_0 + \delta) \leq \mathcal{V}(t_0)$, $\sigma(t_0 + \delta) \leq \sigma(t_0)$ and $\tilde{\eta}(t_0 + \delta) \geq \tilde{\eta}^*$, the inequalities (B.110)-(B.112) remain satisfied, which implies $\dot{\mathcal{V}}(t_0 + \delta) \leq 0$. Therefore, by induction the value of $\dot{\mathcal{V}}$ is guaranteed to be non-positive for all $t > t_0$ and

$$\dot{\mathcal{V}} \leq -\delta_v \tilde{v}^\top h(\tilde{v}) - 2\delta_q \tilde{\eta}^2 \tilde{q}^\top \tilde{q} - \delta_\omega \tilde{\omega}^\top \tilde{\omega}, \quad (\text{B.113})$$

$$\delta_v = k_v - \frac{1}{2\epsilon_1} \sqrt{2\lambda_{\min}(\Gamma_v^{-1})^{-1} V(t_0) + 1} - \frac{\gamma_q k_v^2}{2\epsilon_3}, \quad (\text{B.114})$$

$$\delta_\omega = \lambda_{\min}(K_\omega) - \gamma_q/(2\epsilon_2) - 2c_g^2 \bar{c}_t^2 \|I_b\|^2/\epsilon_4, \quad (\text{B.115})$$

$$\begin{aligned} \delta_q &= \lambda_{\min}(W) - \frac{1}{(\tilde{\eta}^*)^2} \frac{\epsilon_1 \bar{c}_t^2}{\gamma_q} \lambda_{\max}(\Gamma_v^{-1})^2 - \frac{\epsilon_2}{4} \\ &\quad - \frac{k_v^2 c_\Gamma^4 \epsilon_3}{2\bar{c}_t^2} - \frac{1}{|\tilde{\eta}^*|} \frac{\sqrt{2} k_v \bar{c}_t c_\Gamma}{\bar{c}_t} - \frac{1}{(\tilde{\eta}^*)^2} \frac{\epsilon_4}{4\gamma_q}. \end{aligned} \quad (\text{B.116})$$

Since $\ddot{\mathcal{V}}$ is bounded due to Assumption 4.1, Barbalat's Lemma implies that $[\tilde{v}, \tilde{q}, \tilde{\omega}] \rightarrow 0$, and since $\dot{\tilde{v}} \rightarrow 0$, $\tilde{p} \rightarrow 0$.

B.6 Proof for Theorem 4.5

(Position Control Using IMU and GPS Measurements)

We begin by first proving the upper and lower bounds on the thrust control input u_t . Since the function $h(\cdot)$ is bounded by unity, the norm of the virtual control law μ_d is bounded by $\|\mu_d\| < k_p + k_v$. Since the thrust control input is given by $u_t = \|\mu_d - g e_3\|$, and k_p and k_v are chosen such that $k_p + k_v < g$, one easily arrives at the lower and upper bounds for u_t described in the theorem. A nice consequence of the boundedness of u_t , is that the function $M(\mu_d)$ defined by (4.26) is bounded by

$$\|M(\mu_d)\| \leq \sqrt{2}/\bar{c}_t. \quad (\text{B.117})$$

To see more details regarding the derivation of this bound the reader is referred to the proof of Theorem 4.2 given in Appendix B.4. We now focus our attention to the dynamics of the position error $\tilde{p} = p - p_r$ and the system velocity v . In light of the choice for μ_d , the derivatives of the position error and velocity can be written as

$$\dot{\tilde{p}} = v, \quad \dot{v} = -k_ph(\tilde{p}) - k_vh(v) + \tilde{\mu} + \delta_t. \quad (\text{B.118})$$

We also define the *velocity error* function $\tilde{v} = v - \hat{v}$. As previously mentioned, the velocity observer error \tilde{v} is considered as a function of the apparent acceleration vector r_2 . In fact, similar to the design of the observer discussed in Section 3.3.5.1, we define the error function \tilde{r}_2 as

$$\tilde{r}_2 = k_1\tilde{v} - (I - \tilde{R})r_2. \quad (\text{B.119})$$

Another important error function which we will focus on is the attitude error function \tilde{R} , or equivalently $\tilde{Q} = (\tilde{\eta}, \tilde{q})$, which defines the relative orientation between the actual system attitude and the desired attitude. To prove the theorem, we will construct a Lyapunov function in terms of the error functions \tilde{q} , \tilde{r}_2 , v and \tilde{p} , in order to show that all of these states tend to zero. Since the dynamics of \tilde{q} (or equivalently $\tilde{\eta}$), and \tilde{r}_2 are somewhat complicated, we will begin by first simplifying the expressions for their derivatives.

In order to analyze the dynamics of the attitude error, it is sufficient to study the derivative of the quaternion-scalar $\tilde{\eta}$. This is also desired since the derivative of the quaternion scalar can be less complicated than the derivative of the quaternion vector. As a starting point, the derivative of $\tilde{\eta}$ can be found from (4.93) to be $\dot{\tilde{\eta}} = -\tilde{q}^\top \tilde{\omega}/2$ where $\tilde{\omega} = R_d^\top(\omega - \omega_d)$ and $\omega_d = M(\mu_d)\dot{\mu}_d$. To find a result for the desired angular velocity ω_d we first use the results (B.118), in addition to the derivative of the bounded

function $h(\cdot)$, denoted as $\phi(\cdot)$ as defined in section (2.3.2), to differentiate the virtual control law μ_d to obtain $\dot{\mu}_d = -k_p\phi(\tilde{p})v - k_v\phi(v) (-k_ph(\tilde{p}) - k_vh(v) + \tilde{\mu} + \delta_t)$. Simplifying this result, we obtain the following expression for the desired angular velocity

$$\omega_d = M(\mu_d) (f_{\mu_d} - k_v\phi(v)\delta_t - k_v\phi(v)\tilde{\mu}). \quad (\text{B.120})$$

Recall the control input ω uses the function ψ , given by (4.97). Using (B.119), and the properties (2.23)-(2.20), ψ can be rewritten as

$$\begin{aligned} \psi &= \gamma_1 R_d S(r_1) \tilde{R} r_1 + \gamma_2 R_d S(\tilde{r}_2 + (I - \tilde{R})r_2) \tilde{R} r_2 \\ &= R_d (\gamma_1 S(r_1) \tilde{R} r_1 + \gamma_2 S(r_2) \tilde{R} r_2 + \gamma_2 S(\tilde{r}_2) \tilde{R} r_2). \end{aligned} \quad (\text{B.121})$$

Finally, using the expression for the control input ω , the error function \tilde{r}_2 , in addition to (4.25), (B.121) and the fact $b_2 + u_t e_3 = R\delta_t$, we find the derivative of $\tilde{\eta}$ to be

$$\begin{aligned} \dot{\tilde{\eta}} &= -\frac{1}{2} \tilde{q}^\top R_d^\top \left(\gamma_1 R_d S(r_1) \tilde{R} r_1 + \gamma_2 R_d S(r_2) \tilde{R} r_2 + \gamma_2 R_d S(\tilde{r}_2) \tilde{R} r_2 \right. \\ &\quad \left. + k_v M(\mu_d) \phi(v) (I - \tilde{R}) \delta_t + k_v M(\mu_d) \phi(v) \tilde{\mu} \right). \end{aligned} \quad (\text{B.122})$$

To further simplify this result, we first recognize that in light of the definition of the rotation matrix from (2.8) and the property (2.20), one can find $\tilde{q}^\top S(r_i) \tilde{R} r_i = 2\tilde{q}^\top S(r_i) (\tilde{q}\tilde{q}^\top - \tilde{\eta}S(\tilde{q})) r_i = 2\tilde{\eta}\tilde{q}^\top S(r_i) \tilde{q}$. Therefore, using the expression for the matrix W defined by (4.90), we obtain

$$\dot{\tilde{\eta}} = \tilde{\eta}\tilde{q}^\top W\tilde{q} - \frac{\gamma_2}{2} \tilde{q}^\top S(\tilde{r}_2) \tilde{R} r_2 - \frac{k_v}{2} \tilde{q}^\top R_d^\top M(\mu_d) \phi(v) \left((I - \tilde{R}) \delta_t + \tilde{\mu} \right). \quad (\text{B.123})$$

Note that due to Assumption 4.6, the matrix W is positive-definite, and its eigenvalues can be arbitrarily increased using the gains γ_i . We now shift our focus to study

the dynamics of the error function \tilde{r}_2 . In light of the expression for \dot{v} from (4.89), the expression for $\dot{\hat{v}}$ from (4.98), the attitude error dynamics from (4.93)-(4.94), the expressions (4.95), (4.25), and using the fact that $-k_1\tilde{v} + r_2 - \hat{R}^\top b_2 = -\tilde{r}_2$, we obtain

$$\dot{\tilde{r}}_2 = -k_1\tilde{r}_2 - (I - \tilde{R})\dot{r}_2 + k_v R_d^\top S(b_2)M(\mu_d)\phi(v)((I - \tilde{R})\delta_t + \tilde{\mu}). \quad (\text{B.124})$$

A commonality between the dynamic equations for $\dot{\tilde{\eta}}$ and $\dot{\tilde{r}}_2$, is that they both depend on the error functions $(I - \tilde{R})$ and $\tilde{\mu}$. These two error functions can both be expressed in terms of the attitude error using the quaternion vector part \tilde{q} , which will be a useful characteristic later in the Lyapunov analysis. To describe this relationship we define two functions, $f_1(u_t, \tilde{\eta}, \tilde{q}), f_2(x, \tilde{\eta}, \tilde{q}) \in \mathbb{R}^{3 \times 3}$ such that

$$\tilde{\mu} = f_1(u_t, \tilde{\eta}, \tilde{q})\tilde{q}, \quad (I - \tilde{R})x = f_2(x, \tilde{\eta}, \tilde{q})\tilde{q}, \quad (\text{B.125})$$

where $x \in \mathbb{R}^3$. Using the definition of $\tilde{\mu} = \mu - \mu_d$, in addition to the expressions for μ and μ_d from (4.16) and (4.17), respectively, one can find $f_1(u_t, \tilde{\eta}, \tilde{q}) = 2u_t(\tilde{\eta}I - S(\tilde{q}))S(R^\top e_3)$ and $f_2(x, \tilde{\eta}, \tilde{q}) = 2(S(\tilde{q}) - \tilde{\eta}I)S(x)$. Based upon these definitions and the fact that $\|\tilde{\eta}I - S(\tilde{q})\| = 1$, we find the following upper bounds for these two functions

$$\|f_1(u_t, \tilde{\eta}, \tilde{q})\| \leq 2\bar{c}_t, \quad \|f_2(x, \tilde{\eta}, \tilde{q})\| \leq 2\|x\|, \quad (\text{B.126})$$

We now propose the following Lyapunov function candidate:

$$\mathcal{V} = \gamma k_p \left(\sqrt{1 + \tilde{p}^\top \tilde{p}} - 1 \right) + \frac{\gamma}{2} v^\top v + \frac{\gamma k_r}{2} \tilde{r}_2^\top \tilde{r}_2 + \gamma_q \left(1 - \tilde{\eta}^2 \right), \quad (\text{B.127})$$

where γ, γ_q, k_p and k_r are strictly positive constants. In light of (B.118), (B.123),

(B.124), we have

$$\begin{aligned}
\dot{\mathcal{V}} &= \gamma k_p h(\tilde{p})^\top v + \gamma v^\top (-k_p h(\tilde{p}) - k_v h(v) + \tilde{\mu} + \delta_t) \\
&\quad + \gamma k_r \tilde{r}_2^\top \left(-k_1 \tilde{r}_2 - (I - \tilde{R}) \dot{r}_2 + k_v R_d^\top S(b_2) M(\mu_d) \phi(v) (\tilde{\mu} + (I - \tilde{R}) \delta_t) \right) \\
&\quad - 2\gamma_q \tilde{\eta} \left(\tilde{\eta} \tilde{q}^\top W \tilde{q} - \frac{\gamma_2}{2} \tilde{q}^\top S(\tilde{r}_2) \tilde{R} r_2 - \frac{k_v}{2} \tilde{q}^\top R_d^\top M(\mu_d) \phi(v) ((I - \tilde{R}) \delta_t + \tilde{\mu}) \right) \\
&= -\gamma k_v v^\top h(v) + \gamma v^\top \delta_t - \gamma k_r k_1 \tilde{r}_2^\top \tilde{r}_2 - 2\gamma_q \tilde{\eta}^2 \tilde{q}^\top W \tilde{q} \\
&\quad + \gamma k_v k_r \tilde{r}_2^\top R_d^\top S(b_2) M(\mu_d) \phi(v) (f_1(u_t, \tilde{\eta}, \tilde{q}) + f_2(\delta_t, \tilde{\eta}, \tilde{q})) \tilde{q} + \gamma v^\top f_1(u_t, \tilde{\eta}, \tilde{q}) \tilde{q} \\
&\quad - \gamma k_r \tilde{r}_2^\top f_2(\dot{r}_2, \tilde{\eta}, \tilde{q}) \tilde{q} + \gamma_q k_v \tilde{\eta} \tilde{q}^\top R_d^\top M(\mu_d) \phi(v) (f_1(u_t, \tilde{\eta}, \tilde{q}) + f_2(\delta_t, \tilde{\eta}, \tilde{q})) \tilde{q} \\
&\quad + \gamma_2 \gamma_q \tilde{\eta} \tilde{q}^\top S(\tilde{r}_2) \tilde{R} r_2. \tag{B.128}
\end{aligned}$$

Now, we wish to show that for an appropriate choice of the control gains, $\dot{\mathcal{V}}$ is guaranteed to be non-positive. However, this objective is a bit involved, and therefore requires we study the bound of several functions used in the expression of $\dot{\mathcal{V}}$. We begin this analysis by defining the function $\sigma(t) \in \mathbb{R}$ where

$$\sigma(t) := \sqrt{2\mathcal{V}(t)}. \tag{B.129}$$

Based upon the definition of \mathcal{V} from (B.127), the states v and \tilde{r}_2 are bounded by σ as follows $\|v(t)\| \leq \sigma(t)/\sqrt{\gamma}$, $\|\tilde{r}_2(t)\| \leq \sigma(t)/\sqrt{\gamma k_r}$. Therefore, in light of Assumption 4.7(b), one can conclude that

$$\|\delta_t\| \leq c_1 \sigma(t)^2 / \gamma. \tag{B.130}$$

Due to the bounds of the functions $f_1(u_t, \tilde{\eta}, \tilde{q})$ and $f_2(\delta_t, \tilde{\eta}, \tilde{q})$ from (B.126), and the

definition of r_2 from (4.89) we also find

$$\|f_1(u_t, \tilde{\eta}, \tilde{q}) + f_2(\delta_t, \tilde{\eta}, \tilde{q})\| \leq 2 \left(\gamma \bar{c}_t + c_1 \sigma(t)^2 \right) / \gamma \quad (\text{B.131})$$

$$\|b_2\| \leq \left(\gamma \bar{c}_t + c_1 \sigma(t)^2 \right) / \gamma. \quad (\text{B.132})$$

Given these bounds, we now apply Young's inequality to a number of the undesired terms in the expression for $\dot{\mathcal{V}}$:

$$\begin{aligned} \gamma v^\top f_1(u_t, \tilde{\eta}, \tilde{q}) \tilde{q} &\leq \gamma \left(\frac{1}{2} \left(\frac{\epsilon_1}{\sqrt{1+v^\top v}} \right) v^\top v + \frac{1}{2} \left(\frac{\sqrt{1+v^\top v}}{\epsilon_1} \right) 4\bar{c}_t^2 \tilde{q}^\top \tilde{q} \right) \\ &\leq \frac{\gamma \epsilon_1}{2} v^\top h(v) + \frac{2\sqrt{\gamma} \bar{c}_t^2}{\epsilon_1} \sqrt{\gamma + \sigma(t)^2} \tilde{q}^\top \tilde{q}, \end{aligned} \quad (\text{B.133})$$

$$\begin{aligned} &\gamma k_v k_r \tilde{r}_2^\top R_d^\top S(b_2) M(\mu_d) \phi(v) (f_1(u_t, \tilde{\eta}, \tilde{q}) + f_2(\delta_t, \tilde{\eta}, \tilde{q})) \tilde{q} \\ &\leq \frac{\gamma k_v k_r \epsilon_2}{2} \tilde{r}_2^\top \tilde{r}_2 + \frac{\gamma k_v k_r}{2\epsilon_2} \left(\frac{2}{\epsilon_2^2} \right) \left(\frac{4(\gamma \bar{c}_t + c_1 \sigma(t)^2)^4}{\gamma^4} \right) \tilde{q}^\top \tilde{q} \quad (\text{B.134}) \\ &\leq \frac{\gamma k_v k_r \epsilon_2}{2} \tilde{r}_2^\top \tilde{r}_2 + \frac{4k_v k_r}{\epsilon_2 \gamma^3 \epsilon_2^2} \left(\gamma \bar{c}_t + c_1 \sigma(t)^2 \right)^4 \tilde{q}^\top \tilde{q}, \end{aligned}$$

where the norm of $M(\mu_d)$ is given by (B.117). To determine the bound of the term involving the time-derivative of r_2 , we first derive the expression for \dot{r}_2 to be

$$\begin{aligned} \dot{r}_2 &= -\dot{u}_t R^\top e_3 + u_t R^\top S(e_3) \omega + \dot{\delta}_t \\ &= -\frac{1}{u_t} (\mu_d - g e_3)^\top \left(-k_p \phi(e_v) v - k_v \phi(v) f_1(u_t, \tilde{\eta}, \tilde{q}) \tilde{q} + k_v \phi(v) (k_p h(\tilde{p}) + k_v h(v)) \right. \\ &\quad \left. - k_v \phi(v) \delta_t \right) R^\top e_3 + u_t R^\top S(e_3) \left(\gamma_1 S(R_d r_1) b_1 + M(\mu_d) \left(-k_p \phi(e_v) v - k_v \phi(v) \tilde{R} \delta_t \right. \right. \\ &\quad \left. \left. + k_v \phi(v) (k_p h(\tilde{p}) + k_v h(v)) \right) + \gamma_2 R_d S(\tilde{r}_2) \tilde{R} r_2 + \gamma_2 R_d S(r_2) \tilde{R} r_2 \right) + \dot{\delta}_t. \end{aligned} \quad (\text{B.135})$$

Due to the bounds of the functions $h(\cdot)$, $\phi(\cdot)$, the (upper and lower) bounds of the thrust control input u_t , the bound of $\dot{\delta}_t$ from Assumption 4.7(c), the bound of b_2 from

(B.132) (same as the bound of r_2), and the bound of δ_t from (B.130), we find that there exists five positive constants $d_i > 0$, such that the norm of \dot{r}_2 is bounded by $\dot{r}_2 \leq d_1 + d_2\|v\| + d_3\|v\|^2 + d_4\|v\|^3 + d_5\|v\|^4$. However, for the sake of simplicity, from this result we further conclude that there exists positive constants c_3 and c_4 such that $\dot{r}_2 \leq c_3 + c_4\sigma(t)^4$. As a result of this analysis, we again use Young's inequality to establish the following bounds:

$$\gamma k_r \tilde{r}_2^\top f_2(\dot{r}_2, \tilde{\eta}, \tilde{q}) \tilde{q} \leq \frac{\gamma k_r \epsilon_3}{2} \tilde{r}_2^\top \tilde{r}_2 + \frac{2\gamma k_r}{\epsilon_3} \left(c_3 + c_4\sigma(t)^4 \right)^2 \tilde{q}^\top \tilde{q}, \quad (\text{B.136})$$

$$\gamma_2 \gamma_q \tilde{\eta} \tilde{q}^\top S(\tilde{r}_2) \tilde{R} r_2 \leq \frac{\gamma_2^2 \gamma_q \epsilon_4}{2} \tilde{r}_2^\top \tilde{r}_2 + \frac{\gamma_q}{2\gamma^2 \epsilon_4} \left(\bar{c}_t \gamma + c_1 \sigma(t)^2 \right)^2 \tilde{\eta}^2 \tilde{q}^\top \tilde{q}, \quad (\text{B.137})$$

$$\begin{aligned} \gamma_q k_v \tilde{\eta} \tilde{q}^\top R_d^\top M(\mu_d) \phi(v) (f_1(u_t, \tilde{\eta}, \tilde{q}) + f_2(\delta_t, \tilde{\eta}, \tilde{q})) \tilde{q} \\ \leq \gamma_q k_v \left(\frac{\sqrt{2}}{\underline{c}_t} \right) \left(\frac{2(\gamma \bar{c}_t + c_1 \sigma(t)^2)}{\gamma} \right) |\tilde{\eta}| \tilde{q}^\top \tilde{q} \\ \leq \frac{2\sqrt{2} \gamma_q k_v (\gamma \bar{c}_t + c_1 \sigma(t)^2)}{\gamma \underline{c}_t} |\tilde{\eta}| \tilde{q}^\top \tilde{q}, \end{aligned} \quad (\text{B.138})$$

Recall from Assumption 4.6 that the norm of the matrix W has a lower bound which is denoted as c_w . Therefore, in light of the lower bounds defined above, and Assumption 4.7(a) we find the expression $\dot{\mathcal{V}}$ is bounded by

$$\begin{aligned} \dot{\mathcal{V}}(t) \leq & -\gamma v^\top h(v) (k_v - \epsilon_1/2) - \gamma k_r \tilde{r}_2^\top \tilde{r}_2 \left(k_1 - \frac{\epsilon_2 k_v + \epsilon_3}{2} - \frac{\epsilon_4 \gamma_2^2 \gamma_q}{2\gamma k_r} \right) \\ & - \gamma_q \tilde{\eta}^2 \tilde{q}^\top \tilde{q} \left(2c_w - \frac{1}{\tilde{\eta}^2} \left(\frac{\alpha_1(t)}{\epsilon_1} + \frac{\alpha_2(t)}{\epsilon_2} + \frac{\alpha_3(t)}{\epsilon_3} \right) - \frac{\alpha_4(t)}{\epsilon_4} \right. \\ & \left. - \frac{2\sqrt{\gamma} \bar{c}_t^2 (\gamma + \sigma(t)^2)^{1/2}}{\tilde{\eta}^2} - \frac{2\sqrt{2} k_v (\gamma \bar{c}_t + c_1 \sigma(t)^2)}{\gamma \underline{c}_t |\tilde{\eta}|} \right), \end{aligned} \quad (\text{B.139})$$

$$\alpha_1(t) = 2\sqrt{\gamma}\bar{c}_t^2\sqrt{\gamma + \sigma(t)^2}/\gamma_q, \quad (\text{B.140})$$

$$\alpha_2(t) = 4k_vk_r\left(\gamma\bar{c}_t + c_1\sigma(t)^2\right)^4/(\gamma^3\bar{c}_t^2\gamma_q), \quad (\text{B.141})$$

$$\alpha_3(t) = 2\gamma k_r\left(c_3 + c_4\sigma(t)^4\right)^2/\gamma_q, \quad (\text{B.142})$$

$$\alpha_4(t) = \left(\bar{c}_t\gamma + c_1\sigma(t)^2\right)^2/(2\gamma^2). \quad (\text{B.143})$$

Now, let us define a lower bound for $|\tilde{\eta}|$, which based upon some appropriate choices of gains, ensures $\dot{\mathcal{V}} \leq 0$ for all $t \geq t_0$.

Note that when $\tilde{\eta}(t) = 0$ we cannot guarantee stability using (B.139) since in this case $\dot{\mathcal{V}}$ could potentially be positive. To show that $\tilde{\eta}(t)$ is never zero, we first introduce the positive constant ρ which is the desired lower bound for $|\tilde{\eta}(t)|$. Therefore, ρ must be chosen to satisfy $0 < \rho < |\tilde{\eta}(t_0)|$. Subsequently, based upon the definition of the Lyapunov function candidate (B.127), we choose γ as follows

$$\gamma = \bar{\gamma}\left(k_p\left(\sqrt{1 + \|\tilde{p}(t_0)\|^2} - 1\right) + \|v(t_0)\|^2/2 + \|\tilde{r}_2(t_0)\|^2/2 + \xi\right)^{-1}, \quad (\text{B.144})$$

where the parameter ξ is chosen to be strictly positive, and $\bar{\gamma}$ is chosen to satisfy

$$0 < \bar{\gamma} < \gamma_q\left(\tilde{\eta}(t_0)^2 - \rho^2\right), \quad (\text{B.145})$$

where γ_q is chosen to be strictly positive. Recall $k_p > 0$ and $k_v > 0$ are chosen arbitrarily provided that $k_p + k_v < g$. The remaining gains and parameters are chosen to ensure that all terms in (B.139) are guaranteed to be negative at the initial time t_0 , which are chosen as follows: Choose ϵ_1 such that $0 < \epsilon_1 < 2k_v$. Recall from (4.90) that the minimum eigenvalue of W , denoted by $c_w > 0$, can be increased using the gains γ_1 and γ_2 . Therefore, there exists constants $\bar{\gamma}_1, \bar{\gamma}_2$, and $\bar{\epsilon}_i$, $i = 2, 3, 4$, such

that for all $\gamma_1 > \bar{\gamma}_1$, $\gamma_2 > \bar{\gamma}_2$, and $\epsilon_i > \bar{\epsilon}_i$, the following inequality is satisfied

$$2c_w > \frac{1}{\rho^2} \left(\frac{\alpha_1(t_0)}{\epsilon_1} + \frac{\alpha_2(t_0)}{\epsilon_2} + \frac{\alpha_3(t_0)}{\epsilon_3} \right) + \frac{\alpha_4(t_0)}{\epsilon_4} + \frac{2\sqrt{\gamma}\bar{c}_t^2 (\gamma + \sigma(t_0)^2)^{1/2}}{\rho^2} + \frac{2\sqrt{2}k_v (\gamma\bar{c}_t + c_1\sigma(t_0)^2)}{\gamma\mathcal{L}_t\rho}. \quad (\text{B.146})$$

Finally, choosing $k_1 > \kappa_1(\epsilon_2, \epsilon_3, \epsilon_4, \gamma) := (\epsilon_2k_v + \epsilon_3)/2 + (\epsilon_4\gamma_2^2\gamma_q)/(2\gamma k_r)$ we conclude that $\dot{\mathcal{V}}(t_0) \leq 0$ at the initial time t_0 . We now need to show that this is true for all time. Since the functions $\alpha_1(t)$ through $\alpha_4(t)$ are non-increasing if $\dot{\mathcal{V}} \leq 0$, then a sufficient condition for $\dot{\mathcal{V}}(t) \leq 0$ is $|\tilde{\eta}(t)| \geq \rho$. We will now show that indeed $\rho \leq |\tilde{\eta}(t)|$ for all $t > t_0$. Suppose that there exists a time t_1 such that for all $t_0 \leq t < t_1$, $|\tilde{\eta}(t)| \geq \rho$ and $|\tilde{\eta}(t_1)| < \rho$ when $t = t_1$. At the time t_1 from (B.127), it is clear that $\mathcal{V}(t_1) \geq \gamma_q (1 - \tilde{\eta}(t_1)^2) > \gamma_q (1 - \rho^2)$. However, due to the choice of γ and $\bar{\gamma}$, given by (B.144) and (B.145), respectively, the value of the Lyapunov function candidate at the initial time t_0 must satisfy $\mathcal{V}(t_0) < \bar{\gamma} + \gamma_q (1 - \tilde{\eta}(t_0)^2) < \gamma_q (1 - \rho^2)$ and therefore $\mathcal{V}(t_1) > \mathcal{V}(t_0)$. This is a contradiction since $\dot{\mathcal{V}}(t) \leq 0$ for all $t_0 \leq t < t_1$, and the functions $\mathcal{V}(t)$, $\alpha_i(t)$ and $\sigma(t)$ are non-increasing in the interval $t_0 \leq t < t_1$. Therefore, we conclude that $|\tilde{\eta}(t)| \geq \rho$ and $\dot{\mathcal{V}}(t) \leq 0$ for all $t > t_0$, and the states v and \tilde{r}_2 are bounded. Therefore, $\dot{\tilde{r}}_2$, \dot{v} , $\dot{\tilde{\eta}}$, and $\ddot{\mathcal{V}}$ are bounded. Invoking Barbalat's Lemma, one can conclude that $\lim_{t \rightarrow \infty} (v(t), \tilde{r}_2(t), \tilde{q}(t)) = 0$. Furthermore, since $\lim_{t \rightarrow \infty} \dot{v}(t) = 0$, and $\lim_{t \rightarrow \infty} \delta_t(t) = 0$, it follows from the expression of the velocity dynamics $\dot{v} = -k_p h(\tilde{p}) - k_v h(v) - \delta_t = 0$, that $\lim_{t \rightarrow \infty} \tilde{p}(t) = 0$, which ends the proof. \square

Andrew D. Roberts - Curriculum Vitae

Post-secondary Education and Degrees:	2011 Ph.D. Robotics and Control The University of Western Ontario London, Ontario, Canada
	2007 M.E.Sc. Control Engineering Lakehead University Thunder Bay, Ontario, Canada
	2005 B.Sc. Electrical Engineering Lakehead University Thunder Bay, Ontario, Canada

Refereed Journal Publications:

- [1] A. Roberts and A. Tayebi, *Adaptive Position Tracking of VTOL UAVs*. IEEE Transactions on Robotics, vol.10, no.4, pp.1058-1062.

Refereed Conference Publications:

- [1] Andrew Roberts and Abdelhamid Tayebi, "*On the Attitude Estimation of Accelerating Rigid-Bodies Using GPS and IMU Measurements*", Accepted as regular paper the the 50th IEEE Conference on Decision and Control and European Control Conference, December 12-15, 2011, Orlando, FL, USA.
- [2] Andrew Roberts and Abdelhamid Tayebi, "*Position Control of VTOL UAVs Using IMU and GPS Measurements*", Accepted as regular paper the the 50th IEEE Conference on Decision and Control and European Control Conference, December 12-15, 2011, Orlando, FL, USA.

- [3] Abdelhamid Tayebi, Andrew Roberts and Abdelaziz Benallegue, "*Inertial Measurements Based Dynamic Attitude Estimation and Velocity-Free Attitude Stabilization*", In Proc. of American Control Conference, San Francisco, CA, USA, 2011.
- [4] Andrew Roberts and Abdelhamid Tayebi, "*Position Control of VTOL UAVs using Inertial Vector Measurements*", In proc. of the 18th IFAC World Congress, Milan, Italy, 2011.
- [5] Andrew Roberts and Abdelhamid Tayebi, "*Adaptive Position Tracking of VTOL UAVs*", In proc. of the 48th IEEE Conference on Decision and Control, Shanghai, China, 2009, pp. 5233-5238.
- [6] A. Tayebi, S. McGilvray, A. Roberts and M. Moallem, "*Attitude estimation and stabilization of a rigid body using low-cost sensors*", In proc. of the 46th IEEE Conference on Decision and Control, New Orleans, LA, USA, 2007, 6424-6429.

Submissions Under Review:

- [1] Andrew Roberts and Abdelhamid Tayebi, "*Attitude Estimation and Position Control of VTOL UAVs using IMU and GPS Measurements*", Submitted to Automatica (2011), *document can be viewed in arXiv database: <http://arxiv.org/document number:1106.0016>*.

Teaching Assistantships:

- [1] Introduction to C++ Programming Fundamentals
- [2] Advanced Controls I
- [3] Advanced Controls II
- [4] Engineering Analysis B (Ordinary Differential Equations)
- [5] Introduction to Robotics
- [6] Electrostatics and Electromagnetism
- [7] Signals and Systems

Awards:

- [1] Award for Outstanding Presentation in Graduate Symposium, June 2011, Robotics and Control Area, Department of Electrical and Computer Engineering, University of Western Ontario.

-
- [2] Award for Outstanding Presentation in Graduate Symposium, July 2009, Robotics and Control Area, Department of Electrical and Computer Engineering, University of Western Ontario.
 - [3] Ontario Graduate Scholarship (OGS), 2008-2009, University of Western Ontario, (*declined*).
 - [4] National Science and Engineering Research Council Doctoral Postgraduate Scholarship (NSERC PGS-D), 2007-2010,
 - [5] Governor General's Academic Gold Medal, May 2008, Lakehead University.
 - [6] Ontario Graduate Scholarship (OGS), Lakehead University, 2006-2007,
 - [7] Dean Braun Academic Medal, May 2005, Lakehead University, *Highest ranking graduate in B.Sc. Eng. program.*
 - [8] Professional Engineers of Ontario Foundation for Education Medal for Academic Achievement, May 2005, Lakehead University.
 - [9] 1st Place IEEE Canada / Telus Innovation Design Competition, Sept. 2005, \$10,000 (*as part of three-member team*).
 - [10] 1st Place IEEE Canada Student Paper Contest (\$500 Life Member Award), Dec. 2005, Lakehead University, (*as part of three-member team*).